

**Characterization of *Symbiodinium*-associated viruses and
implications for coral health**

By

Scott Anthony Lawrence

**A thesis
submitted to the Victoria University of Wellington
in fulfilment of the requirements for the degree of
Doctor of Philosophy
in Marine Biology**

Victoria University of Wellington

2014

Abstract

Coral reefs are in decline worldwide. Much of this decline is attributable to mass coral bleaching events and disease outbreaks, both of which are linked to anthropogenic climate change. Despite increased research effort, much remains unknown about these phenomena, especially the causative agents of many coral diseases. In particular, coral-associated viruses have received little attention, and their potential roles in coral diseases are largely unknown. This study aimed to address this lack of information by characterising the viruses associated with reef-building corals and *Symbiodinium* (dinoflagellates that can form symbioses with corals).

Symbiodinium virus screening experiments revealed the presence of numerous and varied virus-like particles (VLPs) inside cells. Of the 49 *Symbiodinium* cultures screened, approximately one third contained putative latent viral infections that could be induced to enter their lytic cycle by UV irradiation. Electron microscope examination revealed VLPs closely resembling viruses previously found in dinoflagellates and other microalgae. Three cultures that showed evidence of latent viral infections were chosen for whole transcriptome sequencing, which revealed the presence of viral genes that were expressed in several different types of *Symbiodinium*. The relationship between the detected genes and known viral gene sequences suggested that the cells were infected with double-stranded DNA (dsDNA) viruses.

In order to determine how the host cell responds to stress-induced viral infection, the expression levels of genes associated with stress response and viral infection were measured. The expression levels of many genes were unchanged following UV stress, and expression of genes that were predicted to be upregulated following stress, such as those encoding antioxidant enzymes, in fact showed lower expression levels. Despite this, several groups of genes involved in viral infection and host cell response were upregulated following stress, providing further evidence for stress-induced latent or chronic viral infections.

In addition to the research carried out on *Symbiodinium* cell cultures, viruses associated with three coral diseases were studied using electron microscopy. Virus-like particles were present in coral and *Symbiodinium* cells from all three diseases, but viral abundance was correlated

with disease state in only one: white patch syndrome (WPS) of *Porites australiensis*. The locations and morphologies of the VLPs associated with WPS suggested the presence of dsDNA and single-stranded RNA (ssRNA) viruses infecting both the coral animal and *Symbiodinium* cells. DNA sequences obtained from WPS-affected corals matched closely with sequences obtained from VLP-containing *Symbiodinium* cells. Based on the evidence gathered from *Symbiodinium* cell cultures and coral tissues, I propose a theoretical model of viral infection in WPS. In this model, the coral animal cells are routinely subject to chronic viral infections, and *Symbiodinium* cells harbour two types of chronic or latent infections – a dsDNA and an ssRNA virus – that can be induced *via* stress, resulting in cell lysis or loss of the cells from the coral host.

In addition to detection and rudimentary identification of viruses infecting *Symbiodinium* cells, this study generated the largest dinoflagellate transcriptomic dataset to date. These data will prove valuable for future research into *Symbiodinium*, both in terms of viral infections and more generally.

Acknowledgements

Foremost, I wish to thank my primary supervisor Dr. Simon Davy for giving me the opportunity to undertake this research, and for his help and encouragement during the course of my PhD. I would also like to thank my co-supervisor Dr. Jo Davy, who was a great source of advice and support. Special thanks also go to my international supervisor Dr. Willie Wilson for allowing two fruitful visits to his lab in Maine, USA, and for providing the opportunity to be involved in the Marine Microbial Eukaryote Transcriptome Sequencing Project (MMETSP).

I would like to thank my lab group for their help over the last several years; and Dr. Willie Wilson's lab group – Sheri Floge, Ilana Gilg and Dr. Joaquin Martinez – for welcoming me into their lab and for their help and friendship during my visits. In particular, I would like to thank Sheri for doing RNA extractions on one of my *Symbiodinium* cultures and carrying out electron microscopy on sorted viruses, despite her busy schedule.

I am indebted to numerous other people, without whose help I would not have been able to complete this thesis. Dr. Paul Fisher, Dr. Mareike Sudek, Dr. Gareth Williams and Chris Runyon collected coral samples from Hawaii and the GBR. Thanks also go to Dr. Greta Aeby for helping with collection permits. Dr. Esther Peters and Dr. Patricia Blackwelder aided in identification of virus-like particles and bacteria in coral electron micrographs. Isolation information for several *Symbiodinium* cultures was provided by Dr. Scott Santos. Dr. Olga Pantos generously provided me with virus filtration membranes, despite there being an apparent worldwide shortage at the time.

Special thanks go to St. John Wakefield, Jane Anderson and Robyn Lutzenberger in the Department of Pathology and Molecular Medicine at the University of Otago, Wellington. Without their generosity in allowing me the use of their lab and TEM, none of the electron microscopy in this thesis would have been possible.

I am very grateful to the staff of the National Center for Genome Resources in New Mexico, USA, for sequencing and assembly of *Symbiodinium* transcriptomes, and to the Gordon and Betty Moore Foundation, who provided funding for this work as part of the MMETSP.

I must also thank the excellent technical and administrative staff of the School of Biological Sciences at Victoria University of Wellington (VUW), who ensured that my PhD went as smoothly as possible.

This PhD was made possible by a Top Achiever Doctoral Scholarship from the New Zealand Tertiary Education Commission and a PhD Submission Scholarship from VUW. A VUW Faculty of Science Strategic Research Grant provided funding for a second trip to Dr. Wilson's lab, during which much of the *Symbiodinium* transcriptome work was carried out.

Finally, I wish to thank my parents for their support, and Maria Hook for her encouragement and companionship as we both completed our theses.

Table of Contents

Abstract	i
Acknowledgements	iii
List of Tables	ix
List of Figures	xi
List of Abbreviations	xvii
Chapter 1: General introduction	1
1.1. Rationale	1
1.2. Viruses	2
1.2.1. Marine Viruses	4
1.2.2. Ecological effects of marine viruses	5
1.2.3. Dinoflagellate-infecting viruses	8
1.3. Coral viruses and disease	11
1.3.1. Coral disease	11
1.3.2. Cnidarian-associated viruses	14
1.3.3. Viruses associated with diseased and bleaching corals	15
1.3.4. Biotic and abiotic drivers of coral virus communities	18
1.4. Methods for studying coral- and <i>Symbiodinium</i> -associated viruses	19
1.4.1. Determining viral abundance	19
1.4.2. Identifying viruses	21
1.4.3. Characterising the virus-host interaction	23
1.5. Aim of the study	25
Chapter 2: Viruses associated with <i>Symbiodinium</i>: screening and characterisation	27
2.1. Introduction	27
2.2. Materials and methods	30
2.2.1. Initial screening of <i>Symbiodinium</i> spp. cultures for latent viruses	31
2.2.2. Follow-up virus screening experiments	32
2.2.3. Transmission electron microscopy	33
2.2.4. Molecular analysis of putative latent viruses	34
2.2.5. Single virus sorting and whole genome amplification	38
2.2.6. Virus reinfection experiments	38
2.3. Results	39

2.3.1. Flow cytometry-based virus screening	39
2.3.2. Transmission electron microscopy	40
2.3.3. Molecular analysis of putative latent viruses	59
2.4. Discussion	62
2.4.1. Screening for latent viruses	62
2.4.2. Electron microscopy	64
2.4.3. Molecular analysis	66
2.4.4. Conclusion	68
2.4.5. Future directions and study limitations	69
Chapter 3: Transcriptomic evidence of viral infections in <i>Symbiodinium</i>	71
3.1. Introduction	71
3.2. Materials and methods	73
3.2.1. <i>Symbiodinium</i> spp. culture selection and maintenance	73
3.2.2. Experimental treatments	73
3.2.3. RNA extraction and sequencing	74
3.2.4. Assembly and mapping	75
3.2.5. Sequence homology and phylogenetic analysis	75
3.3. Results	76
3.3.1. Sequencing, assembly and annotation	76
3.3.2. Virus-like gene identification	77
3.3.3. Virus-like genes conserved in <i>Symbiodinium</i> spp.	79
3.4. Discussion	88
Chapter 4: Expression of virus and virus-related genes in response to stress in <i>Symbiodinium</i>	91
4.1. Introduction	91
4.2. Materials and methods	93
4.2.1. <i>Symbiodinium</i> culture selection and experimental treatments	93
4.2.2. Bioinformatic analysis	93
4.3. Results	94
4.3.1. Sequencing, assembly and annotation	94
4.3.2. Differential expression analysis of putative viral genes	96
4.3.3. Differential expression analysis of virus-related genes	102
4.3.4. Functional annotation of transcriptomes	105

4.3.5. Differential expression analysis of host cell stress response	107
4.4. Discussion	110
Chapter 5: <i>Porites</i> white patch syndrome: disease physiology and associated viruses	115
5.1. Introduction	115
5.2. Materials and methods	117
5.2.1. Sample collection	117
5.2.2. Transmission electron microscopy	117
5.2.3. Virus molecular analysis	118
5.3. Results	121
5.3.1. Transmission electron microscopy	121
5.3.2. Virus molecular analysis	125
5.4. Discussion	128
Chapter 6: General discussion	131
6.1. Review of aims	131
6.2. Summary of results	131
6.3. Viruses of <i>Symbiodinium</i> : identities	132
6.4. Viruses of <i>Symbiodinium</i> : latent <i>versus</i> chronic infections	135
6.5. Viruses of <i>Symbiodinium</i> : implications for coral health and disease	136
6.6. Future directions	140
6.7. Conclusion	142
References	143
Appendices	183
Appendix A: Additional data for Chapter 2	183
Appendix B: Single virus sorting and whole genome amplification	207
Appendix C: Virus reinfection experiments	211
Appendix D: Additional data for Chapter 3	237
Appendix E: Additional data for Chapter 4	249
Appendix F: PCR primers used in Chapter 5	259
Appendix G: Viruses associated with the disease <i>Porites</i> tissue loss	261
Appendix H: Viruses associated with <i>Porites</i> growth anomalies	269
Appendix I: Viral communities associated with the coral <i>Montipora capitata</i> in Kaneohe Bay: the influence of local environmental variables	275

List of Tables

Table 1.1	Common diseases of scleractinian corals and putative causative agents	13
Table 2.1	PCR primers used in Chapter 2	36
Table 3.1	Conserved virus-like genes found in <i>Symbiodinium</i> cultures	80
Table 4.1	<i>Symbiodinium</i> transcriptome assembly and annotation statistics	95
Table 4.2	Putative viral genes that showed increased expression in <i>Symbiodinium</i> following UV exposure	101
Table A1	List of <i>Symbiodinium</i> cultures screened for latent viral infections.	183
Table A2	PCR protocols used in Chapter 2	199
Table A3	Results of initial screening for latent viruses in <i>Symbiodinium</i> cultures	200
Table D1	List of unigenes from <i>Symbiodinium</i> cultures which had nearest BLAST matches belonging to the <i>Phycodnaviridae</i>	239
Table D2	List of unigenes from <i>Symbiodinium</i> cultures which had nearest BLAST matches belonging to the <i>Mimiviridae</i> , <i>Megaviridae</i> and <i>Marseilleviridae</i>	242
Table D3	List of unigenes from <i>Symbiodinium</i> cultures which had nearest BLAST matches belonging to assorted viruses	245
Table D4	Putative viral genes found in more than one <i>Symbiodinium</i> culture	246
Table F1	PCR primers used in Chapter 5	259
Table I1	Mean values of environmental variables recorded during virus sampling at Kaneohe Bay, Hawaii	281
Table I2	Morphological diversity and proportions of virus-like particles from the surface microlayer of <i>Montipora capitata</i> and surrounding water	283

List of Figures

Figure 1.1	Diagrams of virus families that potentially infect corals and associated microbes	3
Figure 1.2	Genome types and transcription strategies of different viruses	5
Figure 1.3	Viral replication mechanisms	11
Figure 1.4	Components of the coral holobiont	17
Figure 1.5	Comparison of methods for enumerating viruses	20
Figure 2.1	Overview of the methods used to identify viral infections in <i>Symbiodinium</i> cell cultures	30
Figure 2.2	Transmission electron micrographs of <i>Symbiodinium</i> culture CCMP421 before and after UV exposure	41
Figure 2.3	Transmission electron micrographs of <i>Symbiodinium</i> culture CCMP828 before and after UV exposure	43
Figure 2.4.	Transmission electron micrographs of <i>Symbiodinium</i> culture CCMP2430 before and after UV exposure	45
Figure 2.5	Transmission electron micrographs of <i>Symbiodinium</i> culture CCMP2465 before and after UV exposure	47
Figure 2.6	Transmission electron micrographs of <i>Symbiodinium</i> culture CCMP2469 before and after UV exposure	50
Figure 2.7	Transmission electron micrographs of <i>Symbiodinium</i> culture Ap1 before and after UV exposure	51
Figure 2.8	Transmission electron micrographs of <i>Symbiodinium</i> culture FLAp1 before and after UV exposure	53
Figure 2.9	Transmission electron micrographs of <i>Symbiodinium</i> culture Mf13.14 before and after UV exposure	54
Figure 2.10	Transmission electron micrographs of <i>Symbiodinium</i> culture Mp before and after UV exposure	55
Figure 2.11	Transmission electron micrographs of <i>Symbiodinium</i> culture PK13 before and after UV exposure	57
Figure 2.12	Transmission electron micrographs of <i>Symbiodinium</i> culture Sin before and after UV exposure	58

Figure 2.13	Gel electrophoresis photo showing ribonucleotide reductase small subunit PCR products from <i>Symbiodinium</i> cultures	59
Figure 2.14	Gel electrophoresis photo showing restriction digests of plasmids containing ribonucleotide reductase small subunit sequences	59
Figure 2.15	Amino acid sequence alignment of partial ribonucleotide reductase small subunit genes from <i>Symbiodinium</i> cultures and diseased <i>Porites australiensis</i> corals	60
Figure 2.16	Phylogenetic tree of ribonucleotide reductase small subunit amino acid sequences from <i>Symbiodinium</i> cultures and diseased <i>Porites australiensis</i> corals	61
Figure 3.1	Numbers of unigenes with nearest BLAST matches belonging to viruses in the combined transcriptomes of three <i>Symbiodinium</i> cultures	78
Figure 3.2	Phylogenetic tree of putative viral helicase genes from three <i>Symbiodinium</i> cultures	81
Figure 3.3	Phylogenetic tree of <i>Phycodnaviridae</i> -like genes from three <i>Symbiodinium</i> cultures	82
Figure 3.4	Phylogenetic tree of putative viral aminotransferase/dehydratase-like genes from four <i>Symbiodinium</i> cultures	83
Figure 3.5	Phylogenetic tree of <i>Mimiviridae</i> -like genes from three <i>Symbiodinium</i> cultures	84
Figure 3.6	Phylogenetic tree of <i>Phycodnaviridae</i> -like genes from three <i>Symbiodinium</i> cultures	85
Figure 3.7	Phylogenetic tree of putative viral protein kinase genes from three <i>Symbiodinium</i> cultures	87
Figure 4.1	Numbers of unigenes with nearest BLAST matches belonging to viruses in the transcriptomes of two <i>Symbiodinium</i> cultures	97
Figure 4.2	Putative viral unigenes upregulated after UV exposure in <i>Symbiodinium</i> cultures CCMP2430 and Mp	98
Figure 4.3	Differential expression of virus-related GO terms containing transcripts from <i>Symbiodinium</i> cultures CCMP2430 and Mp	104

Figure 4.4	KOG annotation of unigenes from <i>Symbiodinium</i> cultures CCMP2430 and Mp	106
Figure 4.5	Expression levels of GO terms associated with viral infection and replication in <i>Symbiodinium</i> cultures CCMP2430 and Mp	108
Figure 4.6	Expression levels of GO terms associated with antioxidant enzyme activity in <i>Symbiodinium</i> cultures CCMP2430 and Mp	109
Figure 5.1	Macroscopic signs of white patch syndrome	116
Figure 5.2	Transmission electron micrographs of tissue sections from healthy and white patch syndrome-affected <i>Porites australiensis</i> colonies	122
Figure 5.3	Transmission electron micrographs of virus-like particles in <i>Porites australiensis</i> colonies	123
Figure 5.4	Abundance of virus-like particles in healthy and white patch syndrome-affected <i>Porites australiensis</i> colonies	124
Figure 5.5	Representative transmission electron micrograph of <i>Porites australiensis</i> sucrose gradient fraction	125
Figure 5.6	Phylogenetic tree of ribonucleotide reductase small subunit amino acid sequences from white patch syndrome-affected <i>Porites australiensis</i> colonies	127
Figure 6.1	Proposed infection strategies of <i>Symbiodinium</i> viruses, and their role in white patch syndrome of <i>Porites</i> spp. corals	139
Figures A1 – A12	Responses of <i>Symbiodinium</i> cultures and associated virus-like particles to 302 nm wavelength UV irradiation	185
Figures A13 – A25	Responses of <i>Symbiodinium</i> cultures and associated virus-like particles to thermal stress	189
Figure A26	<i>Symbiodinium</i> cell densities following exposure to three levels of 254 nm wavelength UV radiation	194
Figure A27	Virus-like particle densities following exposure of <i>Symbiodinium</i> cultures to three levels of 254 nm wavelength UV radiation	195
Figure A28	Flow cytograms of <i>Symbiodinium</i> cultures before and after UV exposure, showing virus-like particle populations	196

Figures A29 – A40	Responses of <i>Symbiodinium</i> cultures and associated virus-like particles to 254 nm wavelength UV irradiation	202
Figure B1	Representation of 384 well plate containing virus-like particles sorted for whole genome amplification	209
Figures C1 – C10	Responses of <i>Symbiodinium</i> cultures and associated virus-like particles to 254 nm wavelength UV irradiation, and to addition of filtered (0.2 µm pore size) lysate from UV-irradiated cultures	213
Figures C11 – C20	Responses of <i>Symbiodinium</i> cultures and associated virus-like particles to 254 nm wavelength UV irradiation, and to addition of filtered (0.8 µm pore size) lysate from UV-irradiated cultures	224
Figure D1	Phylogenetic positions of the <i>Symbiodinium</i> cultures used in Chapter 3	237
Figure D2	<i>Symbiodinium</i> cell and virus-like particle densities in UV-irradiated and control samples of <i>Symbiodinium</i> culture CCMP2430	238
Figure D3	<i>Symbiodinium</i> cell and virus-like particle densities in UV-irradiated and control samples of <i>Symbiodinium</i> culture Mp	238
Figure D4	Phylogenetic tree of chromalveolate species that were searched for the presence of conserved viral genes in Chapter 3	248
Figure E1	Contig length <i>versus</i> number of mapped reads for the transcriptomes obtained from <i>Symbiodinium</i> cultures CCMP2430 and Mp	241
Figure E2	Expression levels of dinoflagellate viral nucleoprotein unigenes detected in <i>Symbiodinium</i> culture CCMP2430	242
Figure E3	Expression levels of dinoflagellate viral nucleoprotein unigenes detected in <i>Symbiodinium</i> culture Mp	242
Figure E4	Expression levels of <i>Phycodnaviridae</i> -like unigenes detected in transcriptomes of <i>Symbiodinium</i> culture CCMP2430	243
Figure E5	Expression levels of <i>Phycodnaviridae</i> -like unigenes detected in transcriptomes of <i>Symbiodinium</i> culture Mp	244
Figure E6	Expression levels of <i>Mimiviridae</i> -like unigenes detected in transcriptomes of <i>Symbiodinium</i> culture CCMP2430	245

Figure E7	Expression levels of <i>Mimiviridae</i> -like unigenes detected in transcriptomes of <i>Symbiodinium</i> culture Mp	246
Figure E8	Expression levels of dsDNA virus-like unigenes detected in transcriptomes of <i>Symbiodinium</i> culture CCMP2430	247
Figure E9	Expression levels of dsDNA virus-like unigenes detected in transcriptomes of <i>Symbiodinium</i> culture Mp	248
Figure E10	Expression levels of antioxidant unigenes detected in transcriptomes of <i>Symbiodinium</i> culture CCMP2430	249
Figure E11	Expression levels of antioxidant unigenes detected in transcriptomes of <i>Symbiodinium</i> culture Mp	250
Figure G1	Transmission electron micrographs of tissue sections from healthy and <i>Porites</i> tissue loss-affected colonies of <i>Porites compressa</i>	254
Figure G2	Transmission electron micrographs of virus-like particles in tissue sections from <i>Porites compressa</i> colonies suffering from <i>Porites</i> tissue loss	256
Figure G3	Transmission electron micrographs of virus-like particles in tissue sections from healthy <i>Porites compressa</i> colonies	257
Figure G4	Abundances of virus-like particle size classes in tissues of healthy and <i>Porites</i> tissue loss-affected <i>Porites compressa</i> colonies	258
Figure H1	Abundances of virus-like particle size classes in tissues of healthy and <i>Porites</i> growth anomaly-affected <i>Porites compressa</i> colonies	262
Figure H2	Transmission electron micrographs of virus-like particles in tissue sections from healthy and <i>Porites</i> growth anomaly-affected <i>Porites compressa</i> colonies	263
Figure H3	Transmission electron micrographs of <i>Symbiodinium</i> cells in healthy and <i>Porites</i> growth anomaly-affected <i>Porites compressa</i> colonies	264
Figure I1	Transmission electron micrographs of virus-like particles isolated from the surface microlayer of <i>Montipora capitata</i> and surrounding seawater	273

Figure I2

Ordination diagrams of the virus-like particle communities of seawater and the surface microlayer of *Montipora capitata*

277

List of abbreviations

AA	Amino acid
bp	Base pairs
BLAST	Basic local alignment search tool
cDNA	Complementary DNA
CDS	Coding sequence
cm	Centimetre
CSM	Coral surface microlayer
DNA	Deoxyribonucleic acid
dNTP	Deoxyribonucleotide triphosphate
dsDNA	Double-stranded DNA
EDTA	Ethylenediaminetetraacetic acid
EST	Expressed sequence tag
FISH	Fluorescence <i>in situ</i> hybridisation
FVLP	Filamentous virus-like particle
GBR	Great Barrier Reef
GFL	Green fluorescence
GO	Gene ontology
HGT	Horizontal gene transfer
IPTG	Isopropyl β -D-1-thiogalactopyranoside
KOG	Eukaryotic orthologous groups
L	Litre
LB	Lysogeny broth
m	Metre
mL	Millilitre
mm	Millimetre
mM	Millimolar
MANOVA	Multivariate analysis of variance
mRNA	Messenger RNA
NCBI	National Center for Biotechnology Information
NCGR	National Center for Genome Resources
NCMA	National Center for Marine Algae and Microbiota

nm	Nanometre
nMDS	Non-metric multidimensional scaling
PCR	Polymerase chain reaction
PEG	Polyethylene glycol
PES	Polyethersulfone
PBTL	<i>Porites</i> bleaching with tissue loss
pmol	Picomole
PorGA	<i>Porites</i> growth anomaly
PorTL	<i>Porites</i> tissue loss
ppt	Parts per thousand
qPCR	Quantitative real time PCR
RFL	Red fluorescence
RNA	Ribonucleic acid
RNA-Seq	Whole transcriptome shotgun sequencing
ROS	Reactive oxygen species
RR	Ribonucleotide reductase small subunit
rRNA	Ribosomal RNA
RT	Room temperature
SOC	Super Optimal broth with Catabolite repression
SSC	Side scatter
ssDNA	Single-stranded DNA
ssRNA	Single-stranded RNA
TAE	Tris-acetate-EDTA
TE	Tris-EDTA
TEM	Transmission electron microscopy
TNE	Tris-NaCl-EDTA
TPM	Transcripts per million
UV	Ultraviolet
VLP	Virus-like particle
WPS	White patch syndrome
X-gal	5-bromo-4-chloro-3-indolyl- β -D-galactopyranoside
μ L	Microlitre
μ m	Micrometre
μ M	Micromolar

Chapter 1: General introduction

1.1. Rationale

Coral reefs are in decline worldwide, particularly due to the growing incidence of climate change-related bleaching events, and are predicted to suffer increasing mortality due to rising seawater temperatures and ocean acidification (Hoegh-Guldberg *et al.*, 2007; Veron, 2011). In addition to these threats, corals are increasingly at risk of disease (Harvell *et al.*, 2007). The causative agents of many coral diseases are unknown. This lack of knowledge is due in part to the fact that corals are associated with an incredibly diverse range of microbes, including bacteria, viruses, fungi, archaea and algae (Wegley *et al.*, 2007), making the distinction between mutualistic and pathogenic microbes difficult. Largely, however, the lack of knowledge arises from a paucity of research in this area.

One particular area that has only recently begun to receive interest is the role of viruses in the health and functioning of corals and their dinoflagellate symbionts. Even with the scarcity of research into this interaction, there is already evidence that viruses may cause coral disease and dysfunction of cnidarian-dinoflagellate symbioses (Wilson *et al.*, 2001; Davy *et al.*, 2006; Davy, 2007; Lohr *et al.*, 2007). Research into coral-associated viruses is still in its infancy, and a great many questions remain unanswered. For example, the identity of most of these viruses is unknown, as few studies to date have utilised molecular methods to characterise them. More research is also needed in order to determine the relative importance of different stressors in triggering the lytic cycle where latent viral infections are present. Equally important is a better understanding of the interaction between host and virus at the cellular level, as this is fundamental to determining the mode of infection and the effects on the physiology of the host. The research described in this thesis attempted to address several of these questions through field studies and laboratory-based work, using a range of conventional and molecular virological techniques.

The following introduction provides an overview of the current state of knowledge of marine viruses, particularly those that have the potential to infect scleractinian corals or their associated microbes. Methodological approaches to studying these viruses are presented, as are descriptions of the aim and objectives of the present research.

1.2. Viruses

Viruses are ubiquitous biological entities that infect every type of organism studied thus far (Koonin *et al.*, 2006). Indeed, viral abundance is estimated to be at least an order of magnitude higher than that of cellular organisms (Edwards and Rohwer, 2005; Suttle, 2005). Essentially, a virus is a piece of nucleic acid wrapped in a protein coat, though there are many structural variations on this theme (Fig. 1.1). Similarly, while viruses can contain different genome types (Fig. 1.2) and use different reproductive strategies (Fig. 1.3), all rely on host cell machinery for reproduction, and are therefore obligate parasites. Viral genomes are generally very small, often consisting of only a few genes and relying heavily on host genes for transcription and reproduction (Fauquet *et al.*, 2005); however several viruses, for example the microbe-mimicking mimiviruses, contain large genomes, approaching the level of complexity seen in cellular organisms (La Scola *et al.*, 2003; Claverie *et al.*, 2006). Unlike cellular organisms, viruses can have single- or double-stranded DNA or RNA genomes, and can therefore be classified by either the classical Linnaean system (from Order to Species) or by the Baltimore system (Baltimore, 1971; Temin, 1985), which distinguishes viral groups based on the nature of their genome (Fig. 1.2). Due to their high abundance, often high virulence, and ability to facilitate horizontal gene transfer, viruses are both ecologically and evolutionarily important (Sano *et al.*, 2004; Koonin *et al.*, 2006).

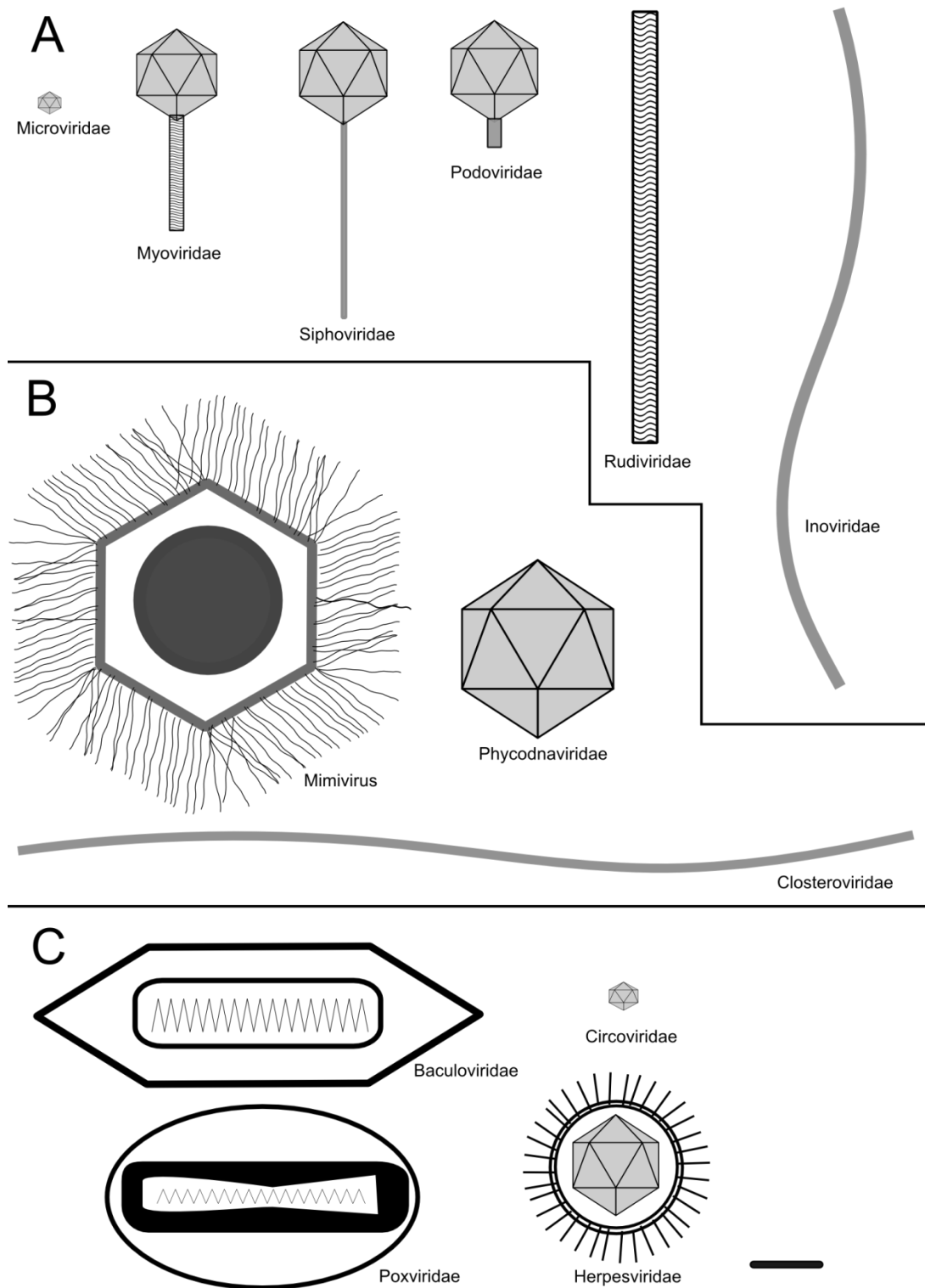


Figure 1.1. Diagrams of some common virus families that potentially infect corals and associated microbes. (A) Viruses of bacteria. (B) Viruses of algae. (C) Viruses of invertebrates. Adapted from Fauquet *et al.* (2005). Scale bar represents 100 nm.

1.2.1. Marine viruses

Viruses are the most abundant and diverse biological entities in the oceans, with up to 10^7 viral particles per mL (Suttle, 2005) and more than 5,000 viral genotypes found in just 100 L of seawater (Rohwer and Vega Thurber, 2009). Generally speaking, viral abundance is highest in shallow near-shore waters and sediments, and in areas of high productivity, owing to an increase in host organisms (Suttle, 2005). Recent molecular work, particularly analyses of marine viromes (viral metagenomes) has shown that, while particular viral genotypes can be endemic to a relatively small oceanographic region (Bench *et al.*, 2007), many viruses with extremely similar genotypes are found in distant geographic locations (Short and Suttle, 2005). For example, T7-like podophages isolated from different oceans, as well as terrestrial and freshwater sources, showed greater than 99% sequence similarity in their DNA *pol* genes (Breitbart *et al.*, 2004).

Despite knowledge of their existence for at least 57 years (Spencer, 1955), marine viruses and the ecological and biogeochemical roles they play were largely overlooked until recently. This was due in large part to the difficulties involved with working with viruses, particularly their cultivation, meaning viral research was restricted to microscopic examination of environmental samples (Wommack and Colwell, 2000). In the last 10 – 20 years the development of culture-independent techniques such as PCR and flow cytometry, and enhanced nucleic acid stains, have led to a better understanding of the abundance and diversity of viruses in the oceans, but much remains unknown. Indeed, the application of such techniques is beginning to show how little of the viral community has been characterised. Recent molecular analyses of marine viruses revealed that 60 – 80% of sequenced viral genomes and 65 – 95% of marine viromes show no similarity to existing DNA sequences (Sandaa, 2008). In addition to revealing some of the diversity of marine viruses, recent work, including whole-genome sequencing, proteomics and transcriptomics, has shed light on the infection strategies of these viruses, and their potential ecological effects (Wilson *et al.*, 2005b; Kegel *et al.*, 2007; Allen *et al.*, 2008; Allen and Wilson, 2008). Some of the more common ecological effects of viruses in the ocean are discussed below.

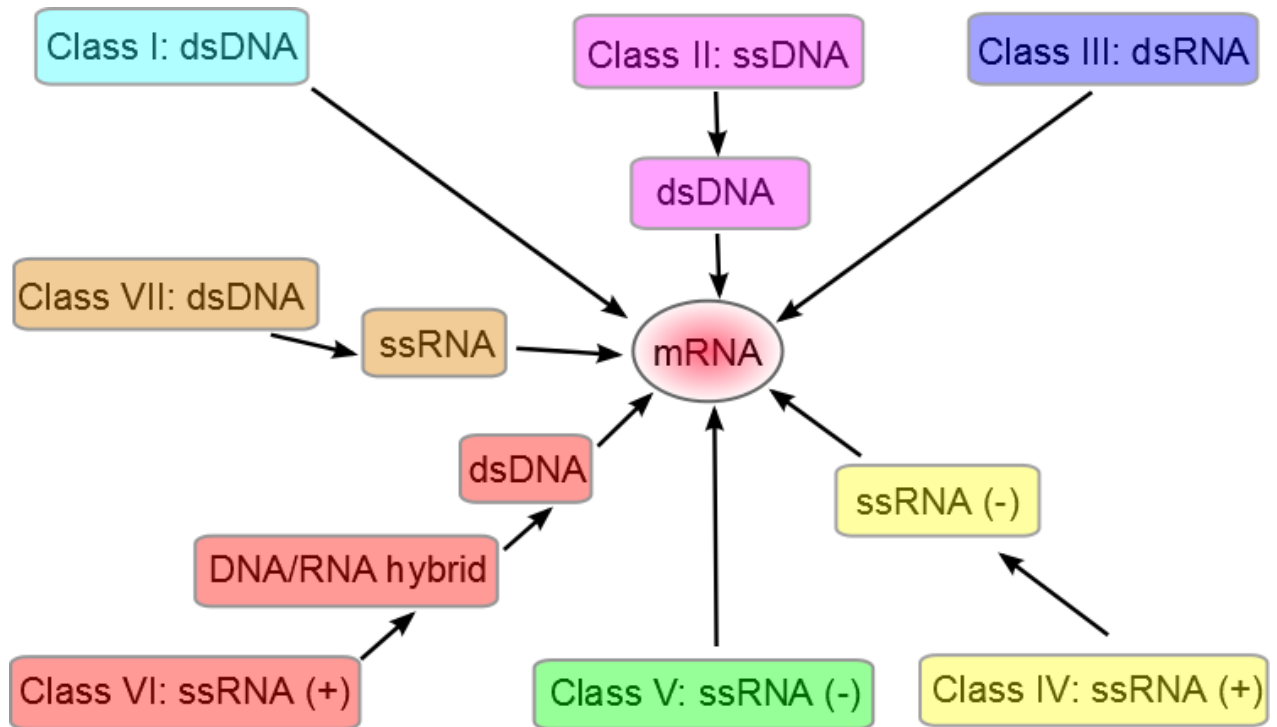


Figure 1.2. The genome types and transcription strategies of the seven classes of viruses recognised by the Baltimore classification system.

1.2.2. Ecological effects of marine viruses

Perhaps the most significant ecological role played by marine viruses is the control of phytoplankton populations. It has been suggested that viruses may be partially responsible for Hutchinson's "paradox of the plankton" (i.e. the presence of many phytoplankton species despite limited resources and the principle of competitive exclusion; Hutchinson, 1961). As viruses passively move about the marine environment, the likelihood of contact with a susceptible host increases with host abundance; thus numerically (competitively) dominant phytoplankton species are more likely to become infected (Fuhrman, 1999; Sandaa, 2008; Bourne *et al.*, 2009). In this "kill the winner" scenario, phytoplankton diversity is maintained as viral lysis prevents the dominant species from completely out-competing other species. While this hypothesis remains to be proven on a large scale, mesocosm experiments have shown that viruses can account for 25 – 100% of the net mortality of the phytoplankter *Emiliania huxleyi* during blooms where the species is numerically dominant (Bratbak *et al.*, 1993; Jacquet *et al.*, 2002). Furthermore, studies of natural phytoplankton populations have

demonstrated that viral infection can result in up to a 78% reduction in primary production (Suttle, 2005).

While the importance of viral infection in structuring natural phytoplankton communities remains equivocal, considerable research has shown that viruses are often responsible for the termination of algal blooms (Rhodes *et al.*, 2008). Algal blooms occur when one or a few phytoplankton species rapidly increase in number. Blooms can occur naturally, as happens with spring blooms in temperate regions, or as a result of eutrophication or other anthropogenic impacts, the latter often leading to harmful algal blooms which can cause ecological and economic harm (Sunda *et al.*, 2006). Viral infection of bloom-forming phytoplankton has been demonstrated in many groups, such as dinoflagellates (Nagasaki *et al.*, 2003; Nagasaki *et al.*, 2006; Tomaru *et al.*, 2009), coccolithophores (Wilson *et al.*, 2002) and cyanobacteria (Wilson *et al.*, 1998). One of the best-studied bloom-forming species is the coccolithophore *E. huxleyi*. Several workers have determined that infection by *E. huxleyi*-specific viruses plays a large role in termination of blooms (Brussaard *et al.*, 1996; Schroeder *et al.*, 2003; Frada *et al.*, 2008). The viruses involved have been identified as large (up to 200 nm diameter), icosahedral viruses with large double-stranded DNA genomes ~410 kb in size, belonging to the family *Phycodnaviridae* (the most common alga-infecting viruses) (Schroeder *et al.*, 2002). It appears that *E. huxleyi* viruses act by disrupting the electron transport chain in photosystem II (Evans *et al.*, 2006; Llewellyn *et al.*, 2007). Only the diploid stage of the *E. huxleyi* lifecycle is susceptible to viral infection, possibly due to alterations of the cell wall or receptor molecules in the cell membrane, meaning that at least some of the population survives the large-scale viral infection (Frada *et al.*, 2008). Understanding the virus – *E. huxleyi* interaction is important, as *E. huxleyi* can form blooms exceeding 100,000 square kilometres that have significant ecological and biogeochemical effects, including oxygen and dimethyl sulphide production.

Viral lysis of marine prokaryotes is theorised to have a major impact on the availability of carbon and nutrients to higher trophic levels (Proctor and Fuhrman, 1990). In coastal sediments, viruses can be responsible for over 50% of prokaryotic mortality (Mei and Danovaro, 2004). This high rate of virus-induced mortality results in accelerated transformation of nutrients from particulate to dissolved forms, meaning that there is less microbial biomass available for higher organisms to feed on (Danovaro *et al.*, 2008b; Danovaro *et al.*, 2008c). Conversely, high rates of viral lysis may stimulate increased

microbial respiration and reproduction through nutrient release, so the overall microbial biomass may not always be significantly reduced by virus infection (Danovaro *et al.*, 2008c).

Viruses also play an important ecological role by acting as vectors for gene transfer between organisms. Viruses can promote genetic exchange *via* two routes. The first is transduction, where a virus picks up DNA from one host and transfers it to another. Given that viruses use the hosts' cellular machinery for replication it is likely that this is a fairly common occurrence. Clokie *et al.* (2003) tested this experimentally by using a molecular marker to determine whether a cyanophage incorporated DNA from its *Synechococcus* sp. host during replication. Their results showed that approximately 1 in 100,000 phage particles did in fact incorporate the marker into their capsids. An interesting example of such gene transfer comes from certain cyanophages, which have acquired photosynthesis genes from cyanobacteria. These genes are expressed during infection, and act to repair damage to the host photosystem II, so ensuring sufficient energy for viral replication (Mann *et al.*, 2003; Lindell *et al.*, 2005; Sharon *et al.*, 2009). The second route of genetic exchange occurs less directly: viral lysis causes release of host DNA, which can then be transferred to another organism through natural transformation. Even though this is a relatively rare occurrence, the huge number of viruses and the vast size of the ocean suggest that this could be happening as often as a million times per day (Fuhrman, 1999).

It has been proposed that in some cases viral infection may be advantageous to marine microorganisms (Fuhrman, 1999). One potential benefit of viral infection is the superinfection immunity conferred by latent infections. In a latent infection, the virus nucleic acid is incorporated into the host genome, where it can remain dormant for extended periods of time, or it forms an episome, separate from the host genome. Latency is very common in the marine environment; for example, up to 50% of viral infections of bacterioplankton have been shown to be latent (Jiang and Paul, 1998). Latent infections often result in immunity from further infection by related viruses (Weinbauer, 2004). If such a latent virus merely passes along its genome as the host cell replicates and has minimal effect on the cell, clearly the infection is beneficial. Viruses can also provide a nutritional benefit to cellular organisms. On average, only one out of every 20 – 50 viruses released during host cell lysis will meet a compatible host. Many of the remaining > 95% will come into contact with 'incompatible' hosts, i.e. cells which the virus particles can enter, but cannot successfully infect due to genetic incompatibilities or destruction by restriction enzymes in the cytoplasm. These virus

particles are therefore available for digestion by the cell (Fuhrman, 1999). While this may seem an unimportant source of energy, the sheer number of viruses in the ocean suggests that this could be happening often enough to be of benefit to the host cells. In reality, there is likely a trade-off between costs and benefits of resistance to viruses. It is thought that resistance to viruses often comes at too high a cost to host cells, as it frequently involves the loss of cell receptors (used as attachment points by viruses) which may confer a competitive disadvantage (Fuhrman, 1999).

Finally, and perhaps most obviously, marine viruses have ecological effects as agents of disease. Coral disease and the role viruses may play will be discussed in detail in section 1.3., however many other marine organisms are also susceptible to viral diseases. To describe the full range of viral diseases in the marine environment is beyond the scope of this review; however a few examples are presented from the excellent review by Munn (2006). An economically important virus is White Spot Syndrome Virus, a DNA virus with some similarity to herpes viruses. This virus infects shrimps and can cause 100% mortality of farmed shrimp populations in the space of a few days. Infectious Salmon Anaemia Virus is another virus which has had severe impacts in the aquaculture industry. This is an RNA virus that causes anaemia and ultimately death in farmed salmon, with outbreaks having occurred in Norway, Scotland, Canada and the USA. Marine mammals are also prone to viral disease. For example, Phocine Distemper Virus, an RNA virus infecting seals, caused mass mortalities of European seals between 1988 and 2002, with over 60% population losses in some areas (Munn, 2006).

1.2.3. Dinoflagellate-infecting viruses

Dinoflagellates are eukaryotic microalgae, most often unicellular and possessing two flagella. They are ecologically important because they are abundant in the ocean, and second only to diatoms in terms of species diversity (Guiry, 2012). Several species form harmful blooms and some form vital symbioses with invertebrates, for example the *Symbiodinium*-cnidarian symbiosis. It is this symbiosis that allows the persistence of coral reefs, as the symbionts provide the coral hosts with the energy required for reef building (Davy *et al.*, 2012). The well-known phenomenon of coral bleaching is a result of loss of, or loss of pigment from, these dinoflagellate symbionts (Weis, 2008).

One of the earliest reports of viruses infecting dinoflagellates was published in 1979 (Sicko-Goad and Walker, 1979). These authors used transmission electron microscopy (TEM) to examine infected *Gymnodinium uberrimum* cells, and found icosahedral viruses, approximately 385 nm in diameter, inside viroplasms (virus inclusion bodies). Associated with these viroplasms were abundant Golgi bodies, which likely provide precursor material and participate in viral assembly. Since this study, only two dinoflagellate-infecting viruses have been successfully isolated and cultured: *Heterocapsa circularisquama* virus (HcV) (Tarutani *et al.*, 2001) and *Heterocapsa circularisquama* RNA virus (HcRNAV) (Tomaru *et al.*, 2004). HcV is an icosahedral, dsDNA virus, with a diameter of about 200 nm. HcRNAV is a small (30 nm diameter), icosahedral ssRNA virus, with a genome size of 4.4 kb. Both of these viruses infect *H. circularisquama*, a red-tide-forming dinoflagellate that can cause mass mortality of shellfish (Horiguchi, 1995). Despite the lack of successfully isolated viruses, some additional information has been obtained about dinoflagellate-infecting viruses *in situ*. In particular, several viruses of dinoflagellates have received attention as their hosts form harmful blooms or have other undesirable ecological/economic effects. For example, Onji *et al.* (2003) found two types of virus-like particles (VLPs) in the red-tide-forming dinoflagellate *Gymnodinium mikimotoi*. These VLPs had DNA genomes, and were around 100 nm in diameter and icosahedral in shape. These characteristics suggest that the VLPs belong to the family *Phycodnaviridae*. The *Phycodnaviridae* are large icosahedral viruses with large double-stranded DNA genomes (100 – 560 kb) that infect marine and freshwater algae (Fauquet *et al.*, 2005).

The effects of viral infection on the physiology of dinoflagellate hosts are poorly understood. However, in other algal groups it appears that viral infection leads to the production of reactive oxygen species (ROS) by interrupting the electron transport chain in photosystem II, resulting in cell damage (Evans *et al.*, 2006; Llewellyn *et al.*, 2007). Whatever the physiological response to viral infection, some cells within host populations seem to be resistant to viral infection. For example, Nagasaki *et al.* (2003) reported that when infected with HcV, a proportion of *H. circularisquama* cells, which resembled temporary cysts, did not lyse. When such cells were regrown in fresh culture medium they were sensitive to the virus, so their survival appeared to be due to their physiological state rather than any acquired resistance.

It is likely that most dinoflagellates are susceptible to viral infection, although such infections may not always be obvious. As with many other organisms, dinoflagellates can harbour latent viral infections. In its latent state, either as a provirus or an episome, the virus is effectively hidden from view, and the viral replication rate is matched with the division rate of the host (Prescott *et al.*, 1993; see also Fig. 1.3). In some circumstances, the latent infection can be induced to enter the lytic cycle (i.e. the virus begins replication, ultimately resulting in lysis of the host cell); this is often caused by environmental stressors. Two studies have shown that symbiotic dinoflagellates harbour latent viral infections which can be induced by such stressors. In the first, Wilson *et al.* (2001) isolated *Symbiodinium* cells from the anemone *Anemonia viridis* and exposed them to heat stress for 24 hours. This thermal stress resulted in lysis of the cells, with significantly more dead cells in the treatment than in the control cell culture. TEM analysis of the heat-stressed dinoflagellates revealed abundant VLPs, which were spherical or icosahedral in shape and 40 – 50 nm in diameter. The *Symbiodinium* used in this study are closely related to those found in reef corals (Bythell *et al.*, 1997); therefore latent viral infections may play a role in coral bleaching, which is linked to elevated seawater temperatures (Harvell *et al.*, 2002).

The second study of latent infections in symbiotic dinoflagellates was carried out by Lohr *et al.* (2007). These authors subjected *Symbiodinium* cells taken from a tridacnid clam to stress in the form of UV irradiation. Using TEM and flow cytometry, they found that UV stress induces a latent infection consisting of filamentous VLPs 2 – 3 μm long and ~30 nm wide. The morphology of these VLPs suggests that they may be RNA viruses. If correct, this would be the second report of RNA viruses infecting dinoflagellates. More recent work by Correa *et al.* (2012), analysing the viromes of the coral *Montastraea cavernosa*, also revealed the presence of a ssRNA virus and a large dsDNA virus in *Symbiodinium* cells.

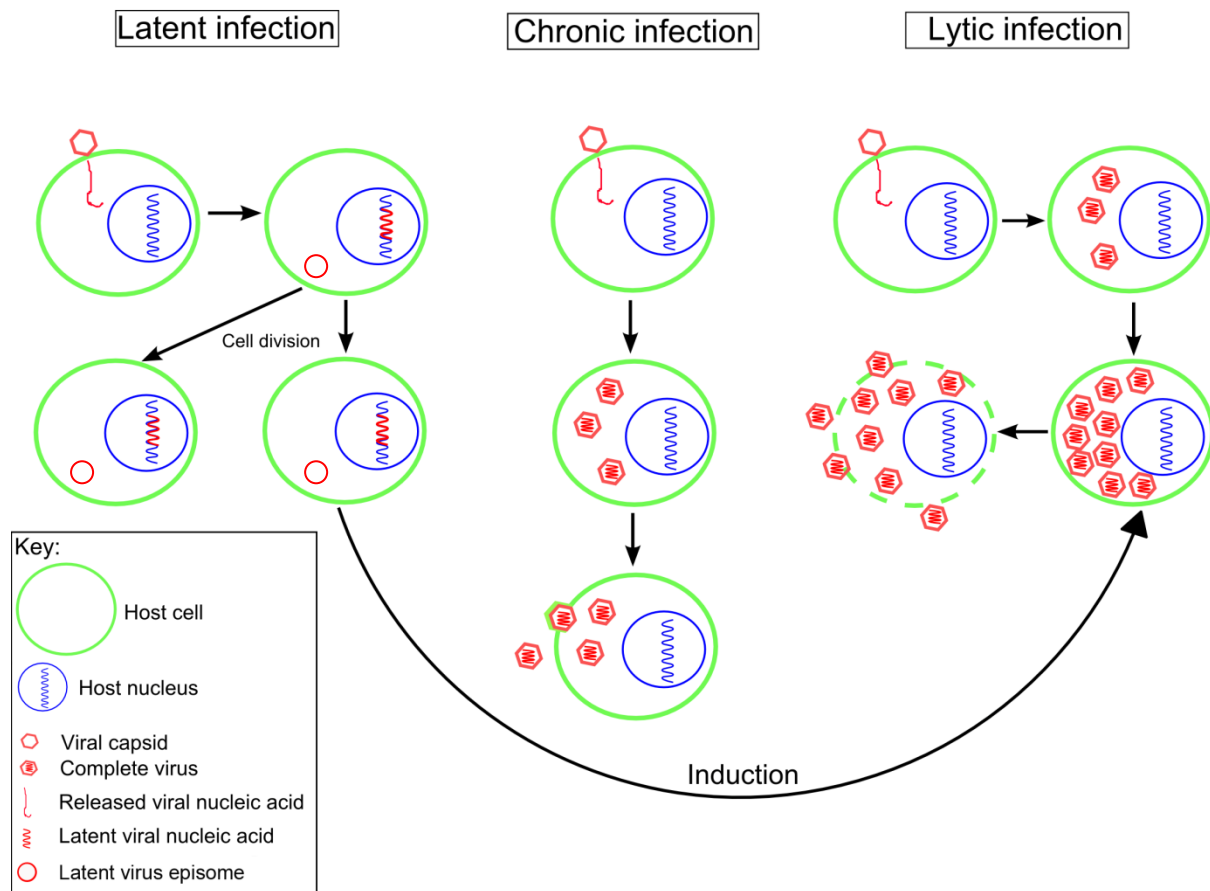


Figure 1.3. A comparison of viral replication mechanisms. In a latent infection, attachment to and penetration of the host cell is followed by incorporation of the viral genome into the genome of the host, or formation of a viral episome (where the viral genome remains independent of the host genome). In this way, the virus is able to reproduce each time the host cell divides, without causing cell lysis. If the latent infection is induced (for example, through environmental stress) it may enter the lytic cycle. In a chronic, or persistent infection, viral nucleic acid is not incorporated into the host genome. The infective virus replicates itself at a lower rate than seen in a lytic infection, periodically releasing newly-formed virions, but not causing cell lysis. In a lytic infection, viruses replicate rapidly before bursting from the cell, causing cell lysis.

1.3. Coral viruses and disease

1.3.1. Coral disease

Coral disease is one of the biggest threats to coral reefs, and in conjunction with phenomena such as coral bleaching and ocean acidification is causing massive declines in coral reefs worldwide (Harvell *et al.*, 1999; Hoegh-Guldberg *et al.*, 2007). Sutherland *et al.* (2004)

described disease as “any impairment (interruption, cessation, proliferation, or other disorder) of vital body functions, systems or organs”, after the medical definition. This definition would include bleaching, however for the purpose of this review coral bleaching is considered a separate phenomenon to coral disease. In certain regions, such as the Caribbean, disease is now the most important factor in coral reef decline (Weil *et al.*, 2006). In the 1980s, an outbreak of white band disease resulted in a 95% reduction in colonies of two *Acropora* species in this region (Sutherland *et al.*, 2004). This was followed in the 1990s by an outbreak of white pox disease that further reduced the cover of one of these species by 70% (Patterson *et al.*, 2002). Although such species-specific disease outbreaks may not decimate entire reefs, the elimination of important coral species alters the biodiversity of these ecosystems and creates space for opportunistic organisms such as macroalgae. Furthermore, disease outbreaks are not always so species-specific. For example, following a mass bleaching event in 2005, simultaneous outbreaks of at least five diseases, affecting 19 coral species, resulted in a 51% decrease in coral cover over 12 months. These coral colonies did not recover from this outbreak; in fact two years after the outbreak the reduction in coral cover was 61% (Miller *et al.*, 2009).

Although Caribbean reefs have been the most affected, coral diseases are by no means restricted to this region. It appears also that coral disease prevalence is increasing, with many new diseases reported since the early 1990s (Richardson, 1998). While some of this may be due to increased monitoring, the extensive and obvious symptoms of many of the diseases suggest that they would have been recorded earlier had they been occurring. Furthermore, the fossil record shows no evidence of the rapid coral community shifts that are signatures of disease epidemics (Harvell *et al.*, 1999). It is likely that many of these new coral diseases are not new microorganisms, but represent a host-shift. For example, aspergillosis of soft corals is caused by a fungus which is usually soil-borne and infects terrestrial animals (Harvell *et al.*, 1999). It is probable that there will be more emerging diseases and large-scale outbreaks in the future, as several coral pathogens grow best at temperatures higher than those optimal for their hosts (Bruno *et al.*, 2007; Arotsker *et al.*, 2009; Dalton *et al.*, 2010) and will likely thrive at temperatures predicted in models of global climate change (Harvell *et al.*, 2002).

Table 1.1 lists some of the more common coral diseases, along with the putative causative agents. It should be noted that there are several more coral diseases for which causative agents have not been established, and of those listed in the table only three have had Koch's

postulates fulfilled (white band II, white plague II and white pox). Many coral diseases have only been described based on gross morphology, and this is reflected in the disease names seen in Table 1.1 (e.g. black band, yellow blotch, dark spots).

Table 1.1. Common diseases of scleractinian corals and putative causative agents. Adapted from Harvell *et al.* (2007).

Disease	Pathogen	No. of species infected
Caribbean		
Black band	Cyanobacterial consortium	19
White band I	Gram negative bacterium	2
White band II	<i>Vibrio carchariae</i>	2
White plague I	Gram negative bacterium	12
White plague II	<i>Aurantimonas coralicida</i>	41
White pox	<i>Serratia marcescens</i>	1
Growth anomalies	Algal and other causes	7
Red band	<i>Oscillatoria</i> sp. and other cyanobacteria	13
Yellow blotch	Possibly <i>Vibrio</i> sp.	11
Dark spots I	Possibly <i>Vibrio</i> sp.	10
Dark bands	Unknown	8
Indo-Pacific and Mediterranean		
<i>Porites</i> trematodiasis	<i>Podocotyloides stenometra</i> (Trematode)	4
Skeletal eroding band	<i>Halofolliculina corallasia</i> (Ciliate)	2
Brown band	Undescribed ciliate	2
<i>Porites</i> ulcerative white spots	<i>Vibrio</i> sp.	3
White plague	<i>Thalassomonas loyona</i>	5

As noted above, the causative agents of many coral diseases are yet to be definitively established. With the increasing use of culture-independent microbiological methods, vast amounts of information are now becoming available about the microbes associated with

corals. One thing that is becoming clear is that coral microbial communities are incredibly diverse. For example, Rohwer *et al.* (2001) found 75 different bacterial 16S gene sequences associated with the coral *Montastrea franksi*. The following year, the same authors carried out a similar study on three coral species, finding 430 distinct bacterial sequences and estimating that there may in fact be up to 6,000 different bacterial types associated with the three corals (Rohwer *et al.*, 2002). Such studies highlight the difficulties in assigning a disease to a particular microbe - without isolation of the suspected pathogen and fulfilment of Koch's postulates, it is very difficult to distinguish true pathogens from other co-occurring microbes. The situation is similar, if not even more complicated, with viruses, as they are generally more abundant and diverse than bacteria and other microbes that may be associated with corals.

1.3.2. Cnidarian-associated viruses

Aside from one early examination of *Symbiodinium* from the anemone *Anthopleura xanthogrammica*, which failed to find virus-like particles (O'Brien *et al.*, 1984), research into viruses associated with anemones and corals has only taken place since the turn of this century. In the first of these more recent studies, Wilson and Chapman (2001) found VLPs in the non-symbiotic anemone *Metridium senile*. These VLPs were icosahedral and ~60 nm in diameter, and were found in the amoebocytes and spiroblasts of the animal. The same year, *Symbiodinium* cells from the anemone *Anemonia viridis* were found to harbour latent viral infections (Wilson *et al.*, 2001). By exposing the symbionts to thermal stress, the authors were able to induce the latent virus to enter the lytic cycle, producing icosahedral viruses 40 – 50 nm in diameter. Moreover, the authors were able to infect and cause lysis in healthy, unstressed *Symbiodinium*, thus fulfilling Koch's postulates. The presence of a temperature-induced viral infection in symbiotic anemones led the authors to speculate that such a mechanism could play a role in bleaching if it also exists in corals. This was tested in 2005 by exposing the coral *Pavona danai* to heat stress and looking for the presence of VLPs using TEM (Wilson *et al.*, 2005a). Icosahedral VLPs, 40 – 50 nm in diameter, were found in both stressed and control corals, however their abundance increased in the heat-stressed corals. Furthermore, larger viruses (50 – 60 nm) were seen in stressed samples but not in controls. The results suggested that stress brings the larger viruses out of latency, and the smaller viruses present in controls are either a chronic and relatively harmless infection, or were induced as a result of the stress of laboratory maintenance. In the interim, Cervino *et al.*

(2004) had discovered large, phycodnavirus-like VLPs in the *Symbiodinium* cells of the coral *Montastrea* sp. subjected to elevated temperatures and bacterial pathogens. This work was followed by Davy *et al.* (2006), who used TEM to examine the tissues, *Symbiodinium* cells and surrounding seawater of the corals *Pavona danai* and *Acropora formosa*, and the zoanthid *Zoanthus* sp. after heat stress. In all samples except for one *Symbiodinium* preparation, icosahedral VLPs 40 – 50 nm in diameter were abundant after heat stress, while various other VLPs of assorted shapes and sizes were seen in smaller numbers. The abundance of VLPs released from the corals after heat stress was quantified using flow cytometry, and it was found that virus numbers were much higher after stress. The authors tested the infectivity of the released viruses by exposing healthy *Symbiodinium* cells to culture medium from heat-stressed *Symbiodinium* cells; while no VLPs were subsequently observed in the exposed cells, the medium did cause the cells to lyse, suggesting that the released viruses were responsible.

Stresses other than increased temperature have also been shown to induce latent viral infections in corals. Vega Thurber *et al.* (2008) subjected the coral *Porites compressa* to temperature, nutrient and pH stresses, and then analysed the viromes associated with the coral tissues. A diverse array of viruses from several families was found in all corals, however in stressed corals the majority of viral sequences were most closely related to the *Herpesviridae*. TEM examination confirmed these findings, with large, icosahedral, enveloped VLPs resembling the *Herpesviridae* seen in the tissues of stressed corals.

1.3.3. Viruses associated with diseased and bleaching corals

Several studies have investigated the possible roles of viruses in naturally-occurring coral diseases (i.e. without the use of artificial stressors). Patten *et al.* (2008) used TEM to examine tissues from healthy colonies of *Acropora muricata* and those suffering from white syndrome. Virus-like particles were found in epidermal and gastrodermal tissues from both healthy and diseased corals; thus a causative link between viruses and white syndrome could not be established. Of interest, however, was the diversity of VLPs seen within coral tissues. In most samples, ~90% of observed VLPs were icosahedral with diameters of 100 – 200 nm, resembling large dsDNA viruses of the families *Phycodnaviridae*, *Iridoviridae* and *Herpesviridae*, but long (1 – 2 µm) filamentous VLPs, hook-shaped VLPs and bacteriophages were occasionally seen in the coral tissue. Members of the *Phycodnaviridae*,

in addition to infecting algae, can cause tumours in reef fish (Panek, 2005), and members of the *Iridoviridae* and *Herpesviridae* can cause harmful infections in bivalves and fish (Elston, 1997; Essbauer and Ahne, 2001).

The diversity of viruses associated with healthy and bleached corals in the Caribbean was examined by Marhaver *et al.* (2008). These authors used metagenomics to analyse the viral communities associated with the coral *Diploria strigosa*. Of the eukaryote-infecting viruses found in the viromes, most were herpes-like viruses (69% in the healthy coral, 84% in the bleached coral), a finding that appears to be unique to corals (viromes from previous studies of seawater and marine sediment had significantly lower herpes-virus counts). Less than 10% of viral sequences in both healthy and bleached corals belonged to the *Phycodnaviridae*, but their presence suggests that at least some of the coral-associated viruses may have been infecting the *Symbiodinium* cells within the corals. The majority of sequences belonged to cyanophages (viruses infecting cyanobacteria); these made up 29% and 44% of phage sequences in healthy and bleached corals, respectively. Although not yet observed in *D. strigosa*, endosymbiotic, nitrogen-fixing cyanobacteria are found in some corals (Lesser *et al.*, 2004), and it is possible the cyanophages may have been infecting such microbes. Vibriophages (viruses infecting bacteria of the genus *Vibrio*) were also present in substantial numbers, making up ~4% and 6% of phage sequences in healthy and bleached corals, respectively. Vibriophages may be beneficial to corals by infecting coral pathogens, or they may be harmful if lysis of the bacteria releases toxins or creates space for more virulent bacterial strains. This scenario is typical of the problem facing those working on coral-associated viruses: the coral holobiont (Rowan, 1998; Rohwer *et al.*, 2002; Wegley *et al.*, 2004) is so complex that it is difficult to fully understand the interactions between its members (see Fig. 1.4 for a depiction of the holobiont, including potential viral members). Davy and Patten (2007) were able to distinguish at least 17 morphological/size classes of VLPs within the mucus layer of *Acropora muricata* and *Porites* spp. corals, suggesting a wide range of hosts within this microhabitat. Wegley *et al.* (2007) conducted a metagenomic analysis of the coral *Porites astreoides*, and also found a diverse array of viruses, including bacteriophages, cyanophages, iridoviruses and lymphocystis viruses (pathogens of fish). Marhaver *et al.* (2008) predict, based on their virome data, that *D. strigosa* harbours nearly 29,000 distinct virus types. It is entirely possible that many of these viruses, rather than being harmful to the coral, may be important for the stability of the coral holobiont (van Oppen *et al.*, 2009).

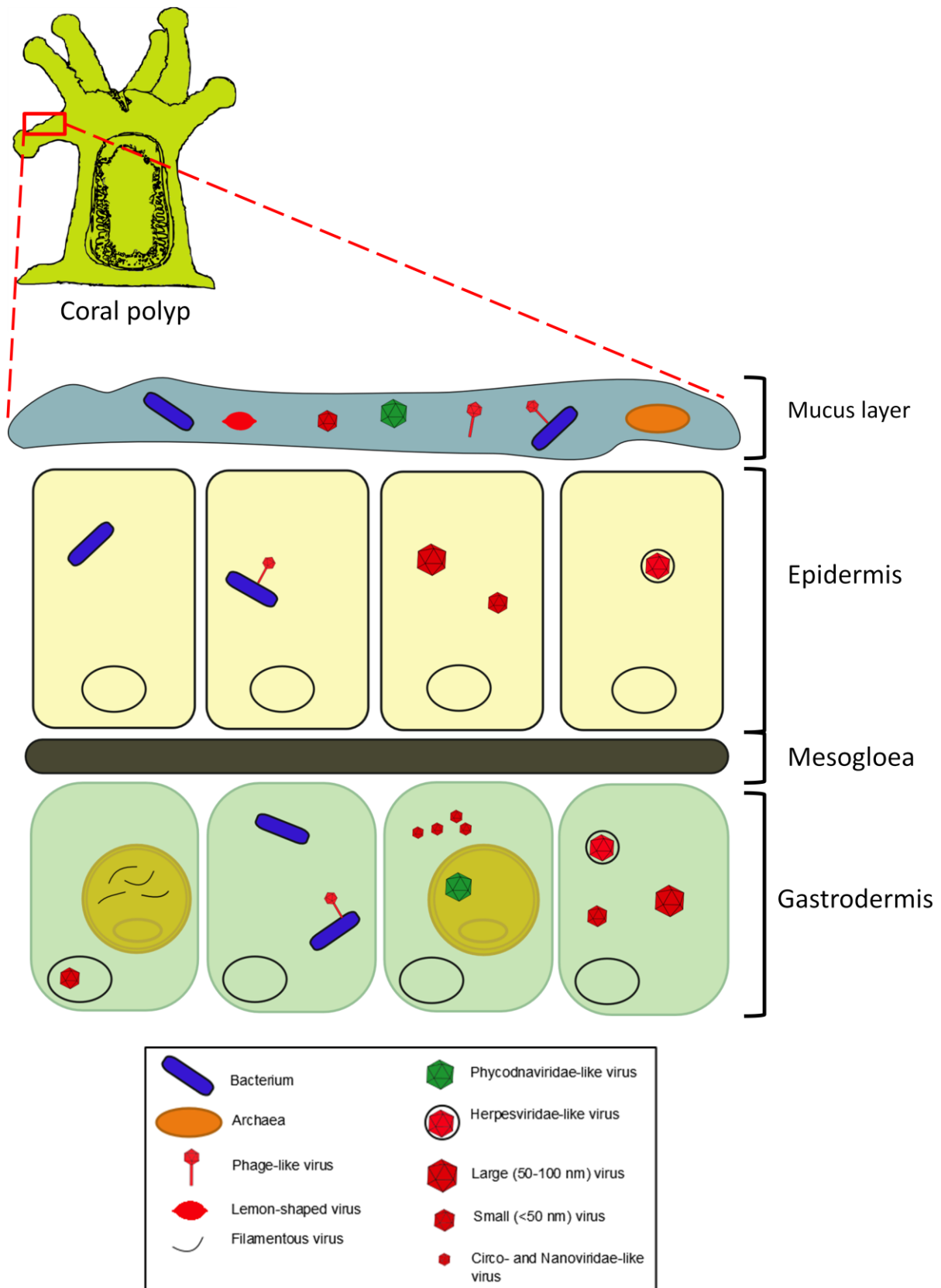


Figure 1.4. Tissue layers of a coral polyp, showing known members of the holobiont. Figure adapted from Kellogg (2004), Rosenberg *et al.* (2007) and Vega Thurber and Correa (2011). Figure is not to scale.

1.3.4. Biotic and abiotic drivers of coral virus communities

One aspect of the coral-virus association which has only received attention in the last five years is the role of environmental conditions and anthropogenic impacts in driving viral community composition. Dinsdale *et al.* (2008) used metagenomics and epifluorescence microscopy to characterise and quantify the microbial and viral communities associated with corals around the Northern Line Islands in the Central Pacific. This study site is useful because it provides an environmental gradient, ranging from the heavily-populated Kiritimati to the uninhabited and relatively pristine Kingman Reef. Clear differences were seen in the metagenomes of these two sites, with waters from Kingman having ten times as many bacteria and viruses as those from Kiritimati. Sampling sites between these two extremes showed correspondingly intermediate viral and bacterial abundances. Furthermore, the microbial and viral community compositions at Kingman Reef were characteristic of those found in open-ocean ecosystems, while those at Kiritimati were characteristic of those from near-shore environments. These differences are likely attributable to anthropogenic impacts at Kiritimati, such as fishing, and agricultural and sewage runoff which increase nutrient concentrations around the reef. This is supported by the fact that historic surveys at Kingman and Kiritimati showed little difference in benthic community structure, whereas there is now much less coral cover and a higher incidence of coral disease at Kiritimati. Similarly, Garren *et al.* (2009) found, using epifluorescence microscopy, that proximity to fish farm effluent had an effect on virus abundance in the coral *Porites cylindrica*. Viral abundance was positively correlated with bacterial abundance and levels of dissolved organic carbon and chlorophyll *a*. Although their methods did not reveal what types of viruses were most abundant, the relationship with bacterial abundance and chlorophyll *a* concentration suggests that they were predominantly bacteriophages and algal viruses or cyanophages.

These studies, and those of latent viruses (Wilson *et al.*, 2001; Wilson *et al.*, 2005a; Davy *et al.*, 2006; Danovaro *et al.*, 2008a), show that environmental conditions or anthropogenic impacts can affect coral virus communities in two ways. First, certain environmental stressors can induce latent viral infections or provide favourable growth conditions for existing viruses, resulting in increased abundance of those particular viruses at the expense of the coral or microbial host. Second, changes in environmental conditions, such as increased nutrient levels, can provide optimal growth conditions for microbes associated with the coral, increasing their abundance. This in turn leads to greater contact with viruses and therefore

regulation of their populations. The former scenario is clearly detrimental to the coral, while the latter may in fact be beneficial if the viruses keep the coral-associated microbiota in balance and prevent potentially harmful microbes from dominating the community. The latter scenario was tested experimentally by Efrony and co-workers (Efrony *et al.*, 2007; Efrony *et al.*, 2009), who used naturally-occurring marine bacteriophages to control the bacteria *Thalassomonas loyaeana* (causes white plague-like disease in the coral *Favia fava*) and *Vibrio corallilyticus* (thought to cause coral bleaching in *Pocillopora damicornis*). By adding the phages to aquaria containing the corals prior to, or within 24 hours of, bacteria addition, infection was prevented. It remains to be seen if such results can be repeated in the field, but these studies do prove that viruses can provide a net benefit to corals.

Clearly, despite an increase in research interest over the last ten years, much remains unknown about coral-virus interactions. Questions that still need to be answered include: How does the viral community vary among different species of corals and different reef locations? How specific is the coral-associated viral community compared to normal seawater viral communities? Are latent viral infections common in corals and/or their symbionts? Are viruses the causative agents for any of the coral diseases with unknown etiologies? And, if so, what is the physiological nature of the virus-host interaction that causes the disease state?

1.4. Methods for studying coral- and *Symbiodinium*-associated viruses

1.4.1. Determining viral abundance

The presence of abundant viruses in aquatic environments has been known for over 40 years (Anderson *et al.*, 1967), but effective quantification of these viruses only began 20 years later, using TEM (Bergh *et al.*, 1989; Proctor and Fuhrman, 1990). Transmission electron microscopy remains a useful tool for enumeration of viruses, particularly viruses within cells. Newer methods, including epifluorescence microscopy and flow cytometry, have become very useful for enumerating ‘free’ viruses (such as those in coral mucus or seawater), but are inferior to TEM for determining the abundance of viruses inside coral or *Symbiodinium* cells, and provide limited information about the size or morphology of the viruses under study.

While TEM is more time-consuming than other methods and requires access to specialised equipment, a well prepared sample can yield valuable information about viral identity, as well as abundance (Ackermann and Haldal, 2010; Fig. 1.5). Disadvantages of using TEM to quantify viruses include the presence of staining artefacts (Hennes and Suttle, 1995; Weinbauer and Suttle, 1997), and the potential operator error inherent in visual counts. That said, TEM remains an invaluable tool for viral ecology research, especially when used in conjunction with other methods.

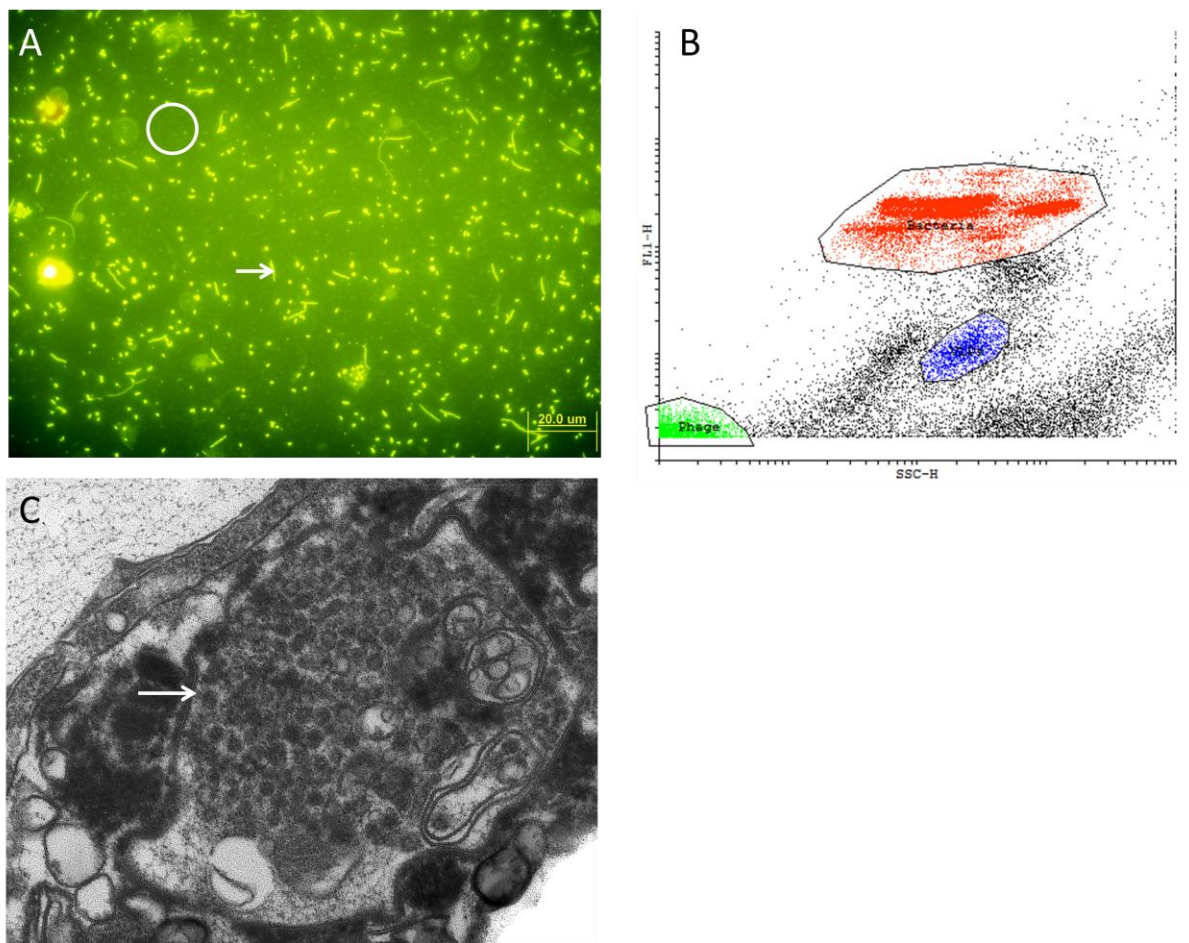


Figure 1.5. Comparison of methods for enumerating coral- and *Symbiodinium*-associated viruses. (A) Epifluorescence micrograph of a *Symbiodinium* culture after UV stress. Numerous bacteria are present (arrow), and small VLPs can be faintly seen (circle). (B) Flow cytogram of a *Symbiodinium* culture after UV stress. The cytogram shows side-scatter vs. green fluorescence (sample was stained with SYBR Green). The VLP, bacterial and phage populations are coloured blue, red and green, respectively. (C) Transmission electron micrograph of small icosahedral VLPs (arrow) inside a coral cell.

Epifluorescence microscopy of VLPs involves filtering viruses and prokaryotes out of a liquid sample, staining with a nucleic acid stain such as SYBR Green or Gold, and viewing with a standard epifluorescence microscope (Patel *et al.*, 2007). It has the advantages of relatively quick processing and analysis times, allowing the user to enumerate viruses in a sample more rapidly than when using TEM. While the method does not provide information on size or morphology of the viruses, it has been shown to provide accurate count data (Suttle and Fuhrman, 2010). The reliability of the technique does depend on appropriate sample preparation, and in some sample types, for example coral mucus, autofluorescence can interfere with the fluorescent signal of the target VLPs (Arlidge, 2011; Leruste *et al.*, 2012). Also, depending on the stain used and the sample type, very small viruses or those with RNA genomes may be missed. This method has, however, been used successfully to enumerate VLPs associated with coral mucus and surrounding seawater (Leruste *et al.*, 2012)

As with epifluorescence microscopy, flow cytometry is a very rapid way to enumerate VLPs and prokaryotes in liquid samples, such as coral mucus, seawater and *Symbiodinium* cell cultures (Marie *et al.*, 1999). The method suffers from some of the same limitations as epifluorescence microscopy, namely that it is restricted to ‘free’ viruses in liquid samples; small viruses and RNA viruses may be overlooked; and only limited information is obtained regarding VLP size and morphology. Unlike epifluorescence microscopy, however, counting is automated, reducing potential user error. Additionally, through the use of appropriate fluorescent stains and instrument settings, different VLP types, prokaryotes and eukaryotes can be easily distinguished from one another (Brussaard, 2004a; Fig. 1.5). Several studies have used flow cytometry to enumerate VLPs associated with corals (Seymour *et al.*, 2005; Davy *et al.*, 2006; Patten *et al.*, 2006) and *Symbiodinium* (Lohr *et al.*, 2007).

All three of the above approaches are useful in their own right for enumerating coral- and *Symbiodinium*-associated viruses, but their use in combination – for example, flow cytometry enumeration followed by TEM examination to confirm the presence of VLPs and determine their morphology – will often be much more informative than following just one approach.

1.4.2. Identifying viruses

Identification of marine viruses is challenging for several reasons: isolation and cultivation are difficult, many viruses are morphologically similar, and the overwhelming majority of

marine viruses are yet to be identified, meaning few characterised viruses are available for comparison.

As noted in the previous section, TEM is an effective way to determine the size and morphology of VLPs inside cells or in aquatic samples. However, when accurate identification of viruses is required, TEM by itself may not be sufficient. The morphological similarity of many viruses means that even the highest quality TEM will be unable to distinguish them. When higher resolution identification is required, several molecular methods can be used.

Shotgun sequencing of environmental samples (metagenomics) has been used to identify viral communities associated with corals (Wegley *et al.*, 2007; Marhaver *et al.*, 2008). The advantages of this method are the coverage provided (whole viral or microbial communities can be profiled at once) and the fact that marker sequences are not required as in other methods (e.g. PCR). This latter feature is particularly helpful when working with viruses, as they lack conserved genes – as opposed to cellular organisms that contain conserved genes such as the 16S and 18S rRNA genes. Disadvantages include sequencing costs, and often a lack of sequence matches in databases, meaning that many viruses remain unidentified; though the latter is not actually a fault of the method itself, rather a consequence of the difficulty involved with characterising environmental viruses.

When identification of one or a few virus types, for example those associated with *Symbiodinium* cells in culture or *in hospite* inside coral cells, is needed, a conventional PCR-based approach can be taken. The lack of conserved viral genes means that PCR primers must be selected/designed carefully to target the viruses of interest. Electron microscopy of the target viruses may provide clues to their identity and guide primer selection. Despite a lack of universal target genes, certain taxa (e.g. some viral families) do share common genes, so appropriate primers can be chosen if their approximate identity is already known. The PCR-based approach has been used successfully in many studies to identify marine viruses (Fuller *et al.*, 1998; Breitbart *et al.*, 2004) and algal viruses (Chen *et al.*, 1996; Martínez *et al.*, 2007; Larsen *et al.*, 2008), including viruses of dinoflagellates (Ogata *et al.*, 2009). When an RNA virus is suspected, reverse transcription (RT)-PCR can be used (Donaldson *et al.*, 2002).

With the decreasing cost of DNA sequencing, whole genome analysis of viruses is increasingly becoming an option in place of PCR and sequencing of single genes. Viral genomes can be obtained by conventional shotgun sequencing of numerous virus particles (of one or more types) at once (e.g. Culley *et al.*, 2003; Culley *et al.*, 2007; Wilson and Schroeder, 2010), or of single virus particles (Allen *et al.*, 2011; Yoon *et al.*, 2011). Starting with large numbers of viruses means that more nucleic acid is available, thus increasing the chance of successful genome sequencing. This approach has been used successfully on viruses of marine algae (Chen and Lu, 2002; Wilson *et al.*, 2005b; Weynberg *et al.*, 2009), including viruses infecting a dinoflagellate (Nagasaki *et al.*, 2005) and a symbiotic *Chlorella* (Van Etten and Meints, 1999). Single-particle genomics, on the other hand, offers several advantages, especially for uncharacterised viruses such as those associated with corals and *Symbiodinium* cells, despite a reduction in the amount of starting nucleic acid. First, by using flow cytometer-based cell sorting to isolate a single virus particle, contaminating nucleic acid is eliminated. Second, the ability to isolate single viruses from an environmental sample or cell culture removes the need for isolation and cultivation of the virus of interest. This is particularly useful for coral- and *Symbiodinium*-associated viruses, as none have yet been successfully cultivated. Finally, by using the nucleic acid of a single virus as starting material, genetic variation among individual viruses is removed (viruses have high mutation rates), leading to more reliable genome sequences. The reduction in starting material when starting with a single viral particle can be overcome by techniques such as multiple displacement amplification (MDA), which has been used to successfully amplify DNA from single viruses (Allen *et al.*, 2011).

1.4.3. Characterising the virus-host interaction

Perhaps the most important pieces of information that can be obtained about a virus are the effects it has on host health and functioning, and how the virus itself functions (e.g. infection and replication strategies). Attempting to obtain such information using traditional virological methods usually requires that virus-host cultures be available (Nagasaki and Bratbak, 2010). This is problematic for viruses associated with corals and *Symbiodinium* cells: no virus-host laboratory system exists for either, and *Symbiodinium* cells appear to contain latent infections (Lohr *et al.*, 2007), which are difficult to isolate (Nagasaki and Bratbak, 2010). Despite these limitations, methods are available to at least partially characterise these viruses and their effects on their hosts.

Electron microscopy can be used, for example, to determine whether the virus of interest replicates in the nucleus or cytoplasm, and how the processes of attachment and penetration occur (Meints *et al.*, 1984). In the case of *Symbiodinium*, where laboratory cultures may be available, TEM can also be used in conjunction with treatments such as experimental stress to determine how this affects viral production and host cell health (Lohr *et al.*, 2007)

TEM analysis of viruses in environmental samples, such as corals, can be confounded by the presence of several virus types, which may be playing different roles. For this reason, and for the greater volume of information they can provide, molecular methods may be preferable.

A basic PCR-based study can be used to search for the presence of viral genes of a particular function (Sharon *et al.*, 2009), however a genomic or transcriptomic approach can provide much more information about the ecology of the virus and effects on the host cell. Sequencing the genomes of algal viruses has yielded valuable information about viral adsorption and release (Allen *et al.*, 2006), induction of host apoptosis (Wilson *et al.*, 2005b), and viral replication and transcription (Allen *et al.*, 2006). Analysis of gene expression using microarrays or whole transcriptome analysis (RNA-seq) can provide even more information about the processes going on in the host during infection. Gene expression analysis has been used previously to elucidate the cellular mechanisms of cnidarian stress responses (Edge *et al.*, 2005; Richier *et al.*, 2008) and stress-induced bleaching (DeSalvo *et al.*, 2008). *Symbiodinium* gene expression has also been analysed in several studies (Leggat *et al.*, 2007; Leggat *et al.*, 2011; Bayer *et al.*, 2012), as have the combined transcriptomes of cnidarian-*Symbiodinium* symbioses (Rodriguez-Lanetty *et al.*, 2006; Sunagawa *et al.*, 2009). These studies have yielded interesting insights into the cellular mechanisms underlying the symbiosis. As yet, however, no transcriptomic studies have been carried out to determine changes in gene expression in virus-infected corals or *Symbiodinium* cells (though Correa *et al.* (2012) did find viral sequences in EST libraries of *Symbiodinium*). With the advent of next generation sequencing it is now possible to simultaneously compare expression levels of numerous genes in infected and uninfected hosts without pre-existing knowledge of the genome (Woodhouse *et al.*, 2010; Yang *et al.*, 2010), and look for the presence of latent viral genes in the host (Sun *et al.*, 1998; Chandriani *et al.*, 2010). The ability to detect latent viral genes is particularly useful for *Symbiodinium*, given the evidence of latent viruses in these organisms (Lohr *et al.*, 2007).

1.5. Aim of the study

The aim of this study was to characterise the viruses associated with reef-building corals and dinoflagellates of the genus *Symbiodinium*. Although definitive identification of such viruses is difficult, this study, using a combination of environmental samples and laboratory cultures, aimed to provide evidence for the presence of these viruses, and preliminary identification. By examining putative viruses associated with diseased corals and experimentally-stressed *Symbiodinium* cells, this study also aimed to shed light on the roles such viruses play in host health, and elucidate the host response to viral infection.

The specific objectives were as follows:

1. Screen laboratory cultures of *Symbiodinium* for the presence of latent viral infections.

Based on previous studies of *Symbiodinium* and other marine algae, it was hypothesised that some *Symbiodinium* cultures would harbour latent infections that could be induced to enter the lytic cycle through environmental stress.

This objective was achieved by experimentally stressing a range of *Symbiodinium* cultures, and monitoring population decline and VLP production using flow cytometry. Transmission electron microscopy was used to further examine VLPs when found using flow cytometry, and VLPs of two *Symbiodinium* cultures were characterised through the use of PCR and sequence analysis.

2. Analyse *Symbiodinium* transcriptomes to identify viral genes common to different types of *Symbiodinium*.

Given the evidence from this and previous studies suggesting that viral infections of *Symbiodinium* are common and may be latent in nature, it was hypothesised that *Symbiodinium* cells would commonly express viral genes.

To test this hypothesis, transcriptomes from three *Symbiodinium* cultures were sequenced and searched for the presence of virus-like genes.

3. Elucidate the response of *Symbiodinium* cells to induction of latent viruses, through transcriptome analysis.

It was hypothesised that transcripts associated with latent viral infection and induction would be found in *Symbiodinium* after stress, and that host genes involved in stress-response and response to viral-infection would be upregulated.

To achieve this objective, two *Symbiodinium* cultures were experimentally stressed using short-wave ultraviolet radiation, and RNA was extracted at various time points. Following RNA-seq, various bioinformatics tools were used to search for virus-related genes and determine the transcriptional response of the *Symbiodinium* cells.

4. Determine whether or not viruses play a role in several diseases of scleractinian corals.

Given the lack of identified causative agents for many coral diseases, and previous evidence for viral infection of scleractinian corals, it was hypothesised that increases in particular viral morphotypes/genotypes would be observed in tissues of diseased corals relative to healthy coral colonies.

Three coral diseases were examined using TEM: white patch syndrome, affecting *Porites* spp. corals on the Great Barrier Reef (GBR); *Porites* tissue loss, affecting *Porites* spp. corals at Kaneohe Bay, Hawaii; and *Porites* growth anomaly, also affecting *Porites* spp. at Kaneohe Bay. PCR and sequencing were carried out to identify viruses associated with white patch syndrome.

The four data chapters in this thesis (Chapters 2 – 5) are written as independent manuscripts. There is therefore some overlap, particularly in the introductions to chapters.

Chapter 2: Viruses associated with *Symbiodinium*: screening and characterisation

2.1. Introduction

The study of dinoflagellate-infecting viruses has largely been restricted to host species which cause toxic blooms, such as *Gymnodinium mikimotoi* (Onji *et al.*, 2003) and *Heterocapsa circularisquama* (e.g. Nagasaki *et al.*, 2003; Nagasaki *et al.*, 2006; Ogata *et al.*, 2009). *Heterocapsa circularisquama* is known to be infected by two viruses: a small (~30 nm diameter) RNA virus and a larger (~200 nm diameter) DNA virus (Nagasaki *et al.*, 2006). Large virus-like particles (VLPs; ~400 nm diameter) have also been found in the freshwater dinoflagellate *Gymnodinium uberrimum* (Sicko-Goad and Walker, 1979). These studies showed that the viruses of dinoflagellates vary considerably between hosts. Viruses of symbiotic dinoflagellates such as *Symbiodinium* have not been studied as extensively, however several studies have suggested that *Symbiodinium* are also infected by potentially harmful viruses. Wilson *et al.* (2001) isolated *Symbiodinium* cells from an anemone, and found that heat stress caused production of icosahedral VLPs of ~40 – 50 nm diameter in these cells. These VLPs were also present in freshly isolated *Symbiodinium* cells exposed to a filtrate obtained from the infected cells, proving that the observed VLPs were infectious viruses. Lohr *et al.* (2007) provided evidence of a latent viral infection in *Symbiodinium* spp. by inducing production of filamentous VLPs in cells through UV stress. These VLPs were 200 nm – 2 µm in length, and resembled viruses belonging to the family *Closteroviridae*. Small icosahedral VLPs have also been seen in *Symbiodinium* cells *in hospite* in corals (Wilson *et al.*, 2005a), while larger VLPs were observed in *Symbiodinium* cells in diseased *Montastrea* spp. corals by Cervino *et al.* (2004). These latter VLPs were icosahedral and ~100 – 150 nm in diameter, resembling members of the family *Phycodnaviridae*, which commonly infect algae (see Van Etten *et al.* (2002) for a review of this viral family). Indirect evidence for viral infection of *Symbiodinium* has also come from the study of coral-associated viruses. Davy and Patten (2007), using electron microscopy, found VLPs which were morphologically similar to the *Phycodnaviridae* and filamentous algal viruses in the surface microlayer of scleractinian corals. Particularly interesting was the recent study by Correa *et al.* (2012), which analysed metatranscriptomes obtained from the coral *Montastrea cavernosa* and compared them with cDNA libraries obtained from *Symbiodinium* cultures.

These authors found evidence of two *Symbiodinium*-infecting viruses: a nucleocytoplasmic large DNA virus (NCLDV) and a single-stranded (ss) RNA virus similar to the virus HcRNAV that infects the dinoflagellate *Heterocapsa circularisquama*.

The study of *Symbiodinium*-infecting viruses is particularly important given the threats to survival of coral reefs worldwide from disease (Lesser *et al.*, 2007; Bourne *et al.*, 2009) and large-scale bleaching events (Baker *et al.*, 2008). There are currently at least 18 commonly-seen coral diseases (Harvell *et al.*, 2007; Bourne *et al.*, 2009), some highly specific, and some affecting a range of coral species. Causative agents have so far been identified for approximately half of these diseases (Rosenberg *et al.*, 2007; Bourne *et al.*, 2009), and in some cases there is debate over whether disease-associated microorganisms are in fact causative agents or opportunistic infections following environmental stress (Lesser *et al.*, 2007; Muller and van Woesik, 2012). Causative agents so far identified include fungi (Rosenberg *et al.*, 2007), trematodes (Aeby, 2007) and, most commonly, bacteria (Rosenberg and Ben-Haim, 2002; Rosenberg *et al.*, 2007; Bourne *et al.*, 2009). Given the number of diseases with unknown causes, and the paucity of studies on coral-associated viruses until recently, viruses may be causing, or playing a role in, some coral diseases.

Most of the described coral diseases appear to affect the coral animal, however there are several diseases in which *Symbiodinium* cells are involved. For example, *Porites* bleaching with tissue loss (PBTL) manifests as necrosis of coral tissue and loss of *Symbiodinium* cells (Sudek *et al.*, 2012b), and white patch syndrome (WPS) of *Porites* spp. similarly involves *Symbiodinium* loss (Davy, 2007). As the causative agents of these diseases have not yet been determined, it is unknown if *Symbiodinium* cells are a primary site of infection or are lost secondarily following infection of the animal host.

Coral bleaching, in comparison, is known to involve *Symbiodinium* cells. Bleaching is the loss of, or loss of pigmentation from, *Symbiodinium* cells, resulting in the characteristic white colouration of bleached corals (Falkowski and Dubinsky, 1981; Hoegh-Guldberg and Smith, 1989). The primary cause of coral bleaching is thermal stress (Lesser, 2011), though it can be exacerbated by other factors such as elevated UV radiation and pollution (Hoegh-Guldberg, 2004; Lesser, 2004, 2006). Current knowledge of the bleaching response suggests that the *Symbiodinium*-coral symbiosis breaks down due to damage to photosynthetic and mitochondrial membranes in the algae (predominantly due to thermal stress), and production

of reactive oxygen species (ROS), which cause the symbiotic relationship to become unsustainable (Venn *et al.*, 2008; Weis, 2008). In at least one species of coral, however, bleaching is known to be caused by a bacterial infection. During periods of elevated seawater temperature, the coral *Oculina patagonica* is infected by *Vibrio shiloi*, a bacterium that produces toxins causing photosynthetic impairment and ultimately *Symbiodinium* cell lysis and bleaching (Kushmaro *et al.*, 1996; Kushmaro *et al.*, 1998; Rosenberg and Ben-Haim, 2002). Viruses have not been implicated in bleaching, but their ability to lyse *Symbiodinium* cells following thermal (Wilson *et al.*, 2001; Davy *et al.*, 2006) or UV stress (Lohr *et al.*, 2007) certainly shows parallels with the bacterium-induced bleaching of *O. patagonica*.

Several studies of *Symbiodinium*-infecting viruses or VLPs have provided evidence of latent infections (Wilson *et al.*, 2001; Wilson *et al.*, 2005a; Lohr *et al.*, 2007), or chronic infections with low levels of productivity that can be increased by stress (Wilson *et al.*, 2005a; Davy *et al.*, 2006). The presence of latent or chronic infections that can be induced *via* environmental stress has important implications for coral health and disease. In particular, these findings provide evidence that viruses may be directly responsible for disease or bleaching, rather than being opportunistic infections arising externally to the cell following stress-induced cellular disruption. Of course, latent or chronic infections may also simply increase viral production in response to cellular disruption, rather than actually causing the disruption. In either case, key cellular machinery must still be intact for the viruses to replicate, so the presence of these latent or chronic infections presumably leads to more cellular damage than would be achieved *via* environmental stress alone.

In the present study, I screened a range of *Symbiodinium* cultures for the presence of latent viral infections and, when found, identified the viruses morphologically. Phylogenetic analysis was also carried out on putative viral DNA sequences from two *Symbiodinium* cultures, in an attempt to better characterise the viruses infecting these cells.

2.2. Materials and methods

In order to identify viruses associated with *Symbiodinium*, a range of methods were employed. An overview of the approach taken is illustrated in the flowchart below, and the individual methods are described in more detail in the following sections.

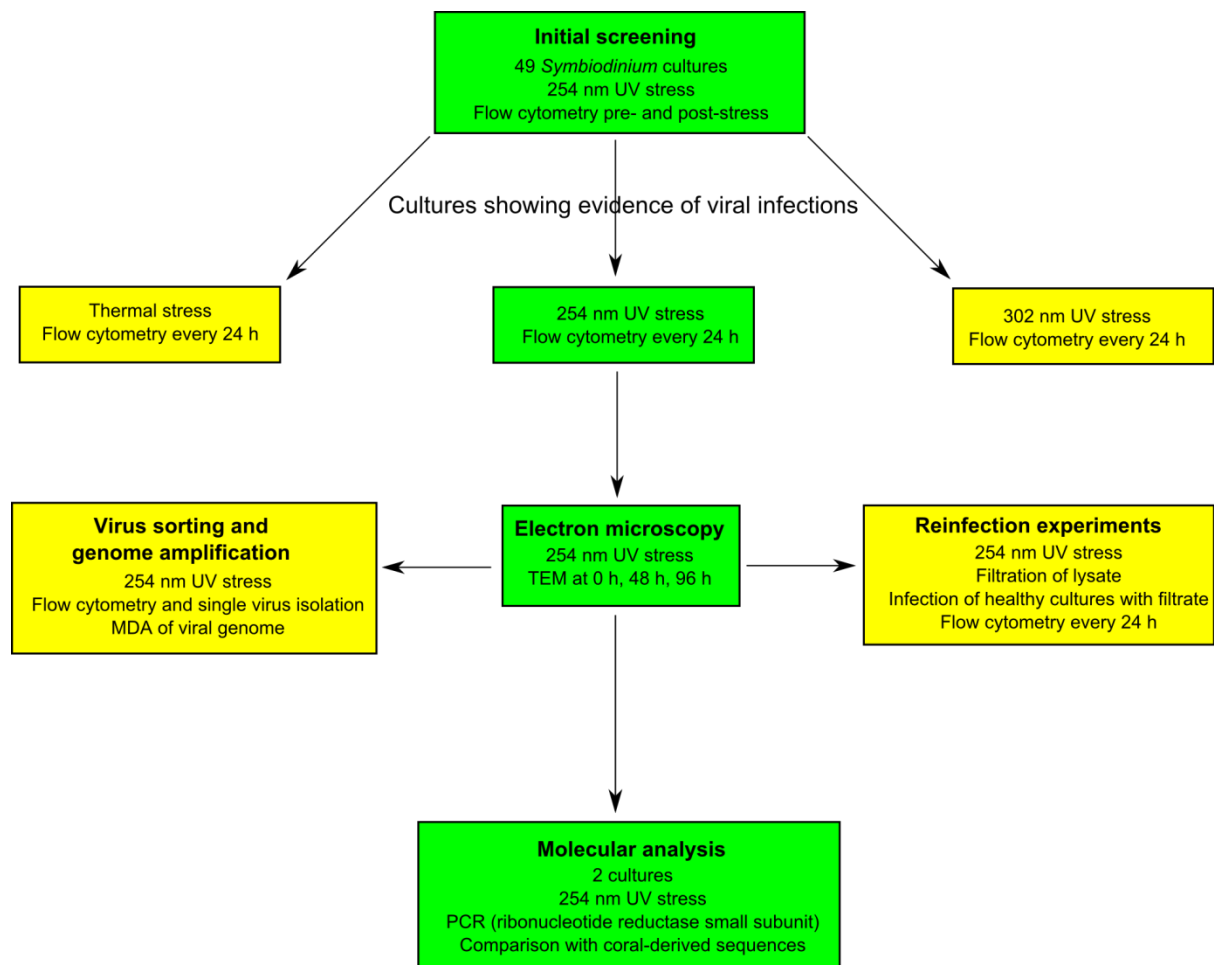


Figure 2.1. Overview of the methods used to identify viral infections in *Symbiodinium* cell cultures. Green boxes indicate the steps that provided evidence of viral infections and/or preliminary identification of viruses. Yellow boxes indicate methods that were less effective or did not produce results. See text for a more detailed description of these methods.

2.2.1. Initial screening of *Symbiodinium* spp. cultures for latent viruses

Symbiodinium cultures

Cultures of *Symbiodinium* were obtained from the National Center for Marine Algae and Microbiota (NCMA, East Boothbay, ME, USA) and the Davy Lab (Victoria University of Wellington, New Zealand). Two clonal cultures from the anemone *Aiptasia pulchella* (SLClone1 and 2) were also isolated and cultured for use in these experiments. In total, 49 cultures were used (see Appendix A, Table A1). All cultures were grown in f/2 medium (Guillard, 1975) without addition of silica, and were maintained at 25 °C on a 12 h light: 12 h dark cycle at 80 $\mu\text{mol quanta m}^{-2} \text{ s}^{-1}$ (supplied by Duro-Test Vita-Lite full spectrum fluorescent tubes).

Experimental treatments

A 50 mL sample was taken from each *Symbiodinium* culture during exponential growth phase ($\sim 10^3 - 10^5 \text{ cells mL}^{-1}$ depending on the culture) and placed into a sterile plastic Petri dish. Each sample was exposed for 2 min to 254 nm UV radiation from an inverted Apollo Instrumentation transilluminator placed 12 cm away ($\sim 1500 \text{ J m}^{-2}$ total radiation). Following UV exposure, samples were transferred to sterile culture flasks and returned to normal growth conditions (as above). Control samples were also taken and subjected to all steps except UV irradiation.

Enumeration of Symbiodinium cells, virus-like particles and bacteria

Duplicate 1 mL samples were collected from each culture flask at Time 0 (prior to UV exposure) and at 24, 48, 96 and 192 h post-exposure for *Symbiodinium* enumeration. A further sample (1 mL) was also collected from each flask at T0 and T96 and/or T192 for VLP and bacterium enumeration. The post-exposure sampling time was chosen based on *Symbiodinium* growth curves to increase the chance of detecting putative viruses, with samples collected at times corresponding to initial *Symbiodinium* population decline. All samples were enumerated using a FACScan flow cytometer (Becton Dickinson, Franklin Lakes, NJ, USA) fitted with an air-cooled 15 mW 488 nm argon-ion laser, operated with Cellquest Pro software. *Symbiodinium* cells were analysed using undiluted samples, run for 1

min at high flow rate ($\sim 80 - 90 \mu\text{L min}^{-1}$) with the trigger set on red fluorescence (RFL). Readings were collected in logarithmic mode and cytograms plotting RFL *versus* side scatter (SSC) were produced. Cytograms were exported to the program Cyflogic (CyFlo Ltd, Turku, Finland), where *Symbiodinium* populations were gated and cells were enumerated. Virus-like particle and bacterium samples were fixed in glutaraldehyde (0.5% final concentration), flash frozen in liquid nitrogen, and then stored at -80°C until analysis. Thawed samples were diluted 1:10 to 1:1,000 with sterile $0.2 \mu\text{m}$ -filtered TE buffer in order to attain a flow cytometer event rate between 100 and 1,000 events per second. The nucleic acid stain SYBR Green was added to each dilution ($0.5 \times$ final concentration) and incubated in the dark for 10 min at 80°C . Following staining, samples were cooled at room temperature for 3 min, then analysed using the flow cytometer. Samples were run for 1 min at high flow rate, with the trigger set on green fluorescence (GFL). Readings were collected in logarithmic mode and cytograms plotting GFL *versus* SSC were produced. Blanks containing $0.2 \mu\text{m}$ -filtered TE buffer were also stained and run as above and used to compensate for instrument and buffer noise. Cytograms were exported to the program Cyflogic, where bacterium, VLP and phage populations were gated and enumerated. The presence and location of these populations were determined following the methods of Brussaard (2004a) and Lohr *et al.* (2007). All counts were collated in Excel (Microsoft, Redmond, WA, USA) and graphs of *Symbiodinium* cell, VLP and bacterium counts *versus* time were produced using the software QtiPlot (<http://soft.proindependent.com/qtiplot.html>).

2.2.2. Follow-up virus screening experiments

Following initial screening, cultures showing putative latent viral groups on cytograms were again subjected to stress in order to monitor putative virus population progression. In addition to 254 nm wavelength UV irradiation, the more ecologically-relevant 302 nm wavelength UV light and thermal stress were tested; however, despite often causing cell lysis, these were considerably less effective at causing VLP production (see Appendix A, Figs. A1 – A12 (302 nm UV stress) and A13 – A25 (thermal stress)). The remainder of this chapter therefore refers to stress experiments using 254 nm wavelength UV light.

The following *Symbiodinium* cultures were used for this experiment: CCMP421 (clade E), CCMP828 (unknown clade), CCMP2430 (clade A), CCMP2431 (unknown clade), CCMP2467 (clade A), Ap1 (clade B), FLAp1 (clade A), Mf13.14 (clade A), Mp (clade C),

Pd (clade B), PK13 (clade B) and Sin (clade C). Cultures were grown as described previously. Experimental treatments were as used in the earlier screening experiments, however for all cultures used in these experiments except CCMP2431, Mf13.14 and Sin, the UV light source used was a 30 W linear lamp (model G30W T8, Sylvania, Danvers, MA, USA) placed 55 cm above the upper surface of the Petri dishes. To determine the appropriate irradiation level using this lamp, *Symbiodinium* cultures were exposed to levels of 803, 1606 and 2,408 J m⁻² (see Figs. A26 and A27 in Appendix A). The higher irradiation level of 2,408 J m⁻² was found to most consistently cause *Symbiodinium* population decline and VLP production, and this was therefore used for subsequent experiments. Samples (1 mL) were taken from each treatment and control flask prior to UV exposure, then every 24 h for 4 days, and prepared as previously described for *Symbiodinium*, VLP and bacterium enumeration. CCMP2431, Mf13.14 and Sin were exposed to UV irradiation from an inverted Apollo transilluminator as described for earlier experiments, and sampled at Time 0, and again after 24, 48, 96 and 192 h. Flow cytometry and data analysis were as previously described.

2.2.3. Transmission electron microscopy

Transmission electron microscopy (TEM) was used to determine whether the putative viral groups seen in cytograms were in fact viruses. The following cultures were selected for TEM examination: CCMP421, CCMP828, CCMP2430, CCMP2465, CCMP2469, Ap1, FLAp1, Mf13.14, Mp, PK13 and Sin. Samples (50 mL) were taken from each culture and placed in sterile Petri dishes, then exposed to 254 nm wavelength UV light (2,408 J m⁻² total irradiation). Following irradiation, samples were returned to culture flasks and maintained under normal growth conditions (see above). Control samples were subjected to all steps except UV irradiation. Aliquots (10 mL) were removed from irradiated samples 48 h and 96 h after irradiation and from control samples 96 h after the start of the experiment. Samples were pelleted by centrifugation at 4,000 × *g* for 5 min. The cell pellet was then washed and re-pelleted twice in sterile f/2 medium, before fixation in glutaraldehyde (2% final concentration) in sterile f/2 medium for 4 h at 4 °C. Following fixation, cells were again pelleted and the solution was replaced with sterile f/2 medium, which was left for 2 h at 4 °C. Cells were then pelleted once more, and molten agar (2%, ~60 °C), was added to the cells. Cells were resuspended in the agar, then centrifuged at full speed for 1 min. After cooling the centrifuge tubes in water to set the agar, the agar was removed from the tube. The tip of the agar plug containing the pelleted cells was removed, and this was cut into ~2 mm cubes. The

agar cubes were post-fixed in a 1:1 solution of 4% osmium tetroxide and f/2 medium for 2 h at room temperature. Following post-fixation, samples were pelleted and washed twice in sterile f/2 medium, then dehydrated through an ethanol series (30%, 50%, 70%, 80%, 90%, 95%, $2 \times 100\%$; 15 min each). Ethanol was then removed and replaced with two changes of 100% propylene oxide, which were left for 20 min each. Propylene oxide was replaced with 50% propylene oxide and 50% Procure 812 resin (ProSciTech, Thuringowa, Australia) and left for 1 h. Samples were then removed and placed in 100% resin (three changes, 1 h each). Finally, samples were transferred to BEEM capsules containing 100% resin, left for 20 min, and placed into a 65 °C oven for 2 days to polymerise. Thick sections ($\sim 1 \mu\text{m}$) were cut on an Ultracut T ultramicrotome (Leica Microsystems, Vienna, Austria) fitted with a glass knife, stained with toluidine blue, and viewed under a light microscope to determine appropriate sections for TEM examination. Ultra-thin sections were cut on the same microtome, using an Ultra 45° diamond knife (DiATOME, Biel, Switzerland). Sections were mounted on 200 μm mesh copper grids (ProSciTech, Thuringowa, Australia) and were stained with 2% aqueous uranyl acetate and Reynold's lead citrate before viewing on a Philips CM-100 TEM operated at 80 kV. Micrographs were captured using the inbuilt camera of the TEM; negatives were scanned using an Epson Perfection V700 Photo scanner, and were converted to positive images using Photoshop CS4 (Adobe Systems, San Jose, CA, USA).

2.2.4. Molecular analysis of putative latent viruses

In order to further determine whether putative VLPs seen in cytograms and electron micrographs were viruses, two *Symbiodinium* cultures (CCMP421 and PK13) were selected for viral DNA extraction and PCR analysis. A 150 mL sample of each culture was placed into a sterile Petri dish and exposed to 254 nm UV radiation for 2 min from an inverted Apollo Instrumentation transilluminator placed 12 cm above the dish. Samples were then returned to normal growth conditions (see above) for 48 h. Control samples were subjected to all steps except UV irradiation. After 48 h, samples were centrifuged at $200 \times g$ for 7 min to pellet cells. Cells were then resuspended in sterile f/2 medium and incubated for 48 h under normal growth conditions. Following incubation, cultures were centrifuged at $30,000 \times g$ for 15 min to pellet cells. The supernatant was removed and mixed with polyethylene glycol (PEG, MW: 10,000), at a ratio of 1 volume PEG: 4 volumes supernatant, then refrigerated at 4 °C overnight. The following day, the solution was centrifuged at $1,000 \times g$ for 45 min and the supernatant removed. The virus-containing pellet was resuspended in $\sim 2 \text{ mL}$ of the

supernatant and stored at -80 °C until DNA extraction. A 500 µL aliquot was taken from each sample and mixed with Proteinase K to a final concentration of 0.2 mg mL⁻¹, and then incubated at 45 °C for 2 h. Sodium dodecyl sulfate (SDS) was added to a final concentration of 0.5% and the mixture was incubated at 45 °C for a further 1 h. Phenol:chloroform:isoamyl alcohol (500 µL, 25:24:1) was added and thoroughly mixed before centrifugation at 5,000 × *g* for 5 min. The aqueous layer was transferred to a fresh microcentrifuge tube and mixed with an equal volume of chloroform, before being centrifuged at 5,000 × *g* for 5 min. The aqueous layer was again transferred to a fresh microcentrifuge tube, and 1/10 volume of 3 M sodium acetate (pH 5.5), 2 volumes 100% ethanol, and Ambion GlycoBlue™ co-precipitant (50 µg mL⁻¹ final concentration; Life Technologies, Carlsbad, CA, USA) were added and gently mixed. The tubes were stored at -20 °C for 20 min, and then centrifuged at 5,000 × *g* at 4 °C for 10 min. The supernatant was removed and the pellet was washed with 70% ethanol by low-speed centrifugation at 4 °C for 2 min. Ethanol was removed, and the pellet left to dry at room temperature, before being dissolved in 100 µL TE buffer at 4 °C overnight. Several pairs of existing and newly-designed PCR primers were used in an attempt to amplify viral DNA (see Table 2.1 for primer details, and Table A2 in Appendix A for PCR protocols). Primers were chosen based on previous work on viruses of *Symbiodinium* (Davy 2007) and other algae (Chen and Suttle 1995, Vega Thurber et al 2008), as well as hypothesised viral groups based on VLP morphologies seen in micrographs in the present study. Amplification was only successful with the RR2 primer pair, and the following methods refer to this primer pair.

Table 2.1. PCR primer pairs used in this study.

Primer pair	Sequence	Target group	Target gene
RR2 F/R	GAYGARGGIYTICAY YTCRAARAARTTIGTYTT	Viruses, prokaryotes, eukaryotes	Ribonucleotide reductase small sub-unit
CircoRep F1/R1 (this study)	ACICCICAYYTICARGGI CCAICCRTARAARTCRTC	<i>Circoviridae</i>	Replication- associated (<i>rep</i>) gene
<i>Nanoviridae</i> F1/R1 (this study)	MGIATHATHTGGGTITAYGGICC RTAYTTICCISWYTG DATDATICC	<i>Nanoviridae</i>	Replication- associated (<i>rep</i>) gene
Nanovirus F1/R1 (this study)	CARGTIATHTGYTGGTGYTTYAC SWRAACATICCISWICKIGG	Nanovirus	Replication- associated (<i>rep</i>) gene
Herpes F/R (Vega Thurber <i>et al.</i> , 2008)	AAAATAAGATTGGGAGATCTAGGC TGCCATTTTAGGTAAATCAGAAAC	Herpes-like viruses	Thymidylate synthase gene
AVS1/AVS2 (Chen and Suttle, 1995)	GARGGIGCIACIGTIYTIGAYGC GCIGCRTAICKYTTYTTISWRTA	Green algae viruses	DNA polymerase

A two-stage PCR was carried out, with the product from the first round used as template for the second round. The initial reaction mixture contained 3 μ L DNA, $1.7 \times$ PCR buffer, 5 mM $MgCl_2$, 0.17 mM each deoxynucleoside triphosphate (dNTP), 100 pmol forward primer, 100 pmol reverse primer and 1 unit GoTaq DNA polymerase (Promega, Fitchburg, WI, USA) in a total volume of 30 μ L per reaction. PCR was performed on an iCycler thermal cycler (Bio

Rad, Hercules, CA, USA) using the following conditions: 95 °C for 3 min; 33 cycles of 95 °C for 45 s, 49 °C for 45s, 72 °C for 45 s; and a final extension step of 72 °C for 10 min. Negative controls contained all reagents except template DNA. PCR products were visualised on a 2% (w/v) agarose gel in TAE buffer run at 100 V for 30 min. The second round of PCR used 5 µL of PCR product as the DNA template, but otherwise used the same conditions and controls as above. PCR products were again checked on a 2% agarose gel, and were then cloned using the pGEM-T Easy Vector System (Promega, Fitchburg, WI, USA), following the manufacturer's instructions. For the transformation step, 2 µL of ligate were added to 20 µL of JM109 High Efficiency competent *E. coli* cells (Promega, Fitchburg, WI, USA), placed on ice for 20 min, and then heat shocked at 42 °C for 30 s before being placed back on ice. SOC medium (500 µL, Promega, Fitchburg, WI, USA) was added to each transformation reaction and incubated at 37 °C in a shaking incubator for 2 h. An aliquot (300 µL) of each sample was spread onto LB/ampicillin/X-Gal/IPTG plates and incubated at 37 °C overnight. White colonies were screened for inserts by PCR using M13F and M13R primers in 10 µL reactions containing 1 × PCR buffer, 1.25 mM MgCl₂, 0.05 mM each dNTP, 10 pmol forward primer, 10 pmol reverse primer, 0.2 units GoTaq DNA Polymerase, and 2 µL DNA. PCR was performed on an iCycler thermal cycler (Bio Rad, Hercules, CA, USA) using the following conditions: 94 °C for 10 min; 30 cycles of 95 °C for 30 s, 50 °C for 30 s, 72 °C for 45 s; and a final extension of 72 °C for 10 min. Negative controls contained all reagents except template DNA. PCR products were run on a 2% (w/v) agarose gel in TAE buffer at 80 V for 20 min to check for inserts. Clones containing inserts were grown overnight in a 37 °C shaking incubator, in 15 mL centrifuge tubes containing 5 mL LB broth and 50 µg mL⁻¹ ampicillin (Sigma-Aldrich, St. Louis, MO, USA). Plasmids containing inserts were isolated using a QIAprep Spin Miniprep kit (Qiagen, Gaithersburg, MD, USA) following the manufacturer's instructions. Plasmid preps were checked by digestion with the enzyme *SacI* (New England Biolabs, Ipswich, MA, USA) and visualisation on a 2% agarose gel in TAE buffer. Restriction digests were performed using the enzymes *HaeIII* and *MspI*. Digest reactions consisted of 10 µL colony PCR product, 1 × digestion buffer and 10 units of each enzyme, and were run at 37 °C for 3 hours, followed by visualisation on a 4% agarose gel in TAE buffer. Plasmids with unique restriction patterns were sequenced at the University of Illinois Core Sequencing Facility (Urbana, IL, USA). Forward and reverse sequences were assembled using the program Geneious (version 5.6.5, Biomatters, Auckland, New Zealand). Amino acid sequences were aligned with BLAST (Altschul *et al.*, 1997) matches and five putative viral partial RR sequences obtained from *Porites australiensis* coral samples (see Chapter 5),

using CLUSTALW (Thompson *et al.*, 1994) within the program Geneious. Maximum likelihood analysis was performed using PHYML (Guindon and Gascuel, 2003) in the program Geneious, with bootstrap analysis of 100 replicates.

The following ribonucleotide reductase small subunit sequences from Genbank were used for alignment and phylogenetic analysis: *Aureococcus anophagefferens*, EGB06310; *Bergeyella zoohelcum*, EKB61170; *Caenorhabditis remanei*, EFO94473; *Candidatus Amoebohilus asiaticus*, ACE05936; *Candidatus Protochlamydia amoebophila*, CAF24073; *Capnocytophaga* sp., EGJ58079; *Cardinium endosymbiont*, YP006705556 ; *Cecembia lonarensis*, EKB47525; *Chitinophaga pinensis*, ACU59471; *Chlamydomonas reinhardtii*, EDP05574; *Cytophaga hutchinsonii*, ABG57741; *Danio rerio*, AEO79844; *Ectocarpus siliculosus*, CBJ30029; *Fibrisoma limi*, ZP10335168; *Flexibacter litoralis*, AFM04620; *Fluviicola taffensis*, AEA43795; *Indibacter alkaliphilus*, EJZ24719; *Leishmania mexicana*, XP003875583; *Marivirga tractuosa*, ADR21803; *Microscilla marina*, EAY24093; *Mucilaginibacter paludis*, ZP09487567; *Nematostella vectensis*, EDO42116; *Niastella koreensis*, AEW01725; *Pedobacter heparinus*, ACU02912; *Pontibacter* sp., EJF09607; *Populus tremula*, ACE96785; *Saprospira grandis*, EJF54108; *Solitalea canadensis*, AFD05853; *Sphingobacterium* sp., ADZ76922; *Trichinella spiralis*, EFV55552.

The nucleotide sequence accession numbers for the PCR products in the Genbank database are: KC540767 – KC540772 (*Symbiodinium* spp.) and KC540773 – KC540777 (*Porites australiensis*).

2.2.5. Single virus sorting and whole genome amplification

In an attempt to better characterise the putative latent viruses associated with *Symbiodinium* cells, FLAp1 and Mf13.14 were selected for single virus sorting and viral genome amplification. Amplification of these viral genomes was unsuccessful; see Appendix B for a description and discussion of the experiment.

2.2.6. Virus reinfection experiments

Cultures that showed declines in population densities and development of a VLP population following stress were selected for viral reinfection experiments, in an attempt to prove that

viruses could cause *Symbiodinium* cell lysis in the absence of stress, thus fulfilling Koch's postulates. Ten cultures were chosen for these experiments, but none showed evidence of *Symbiodinium* population decline or production of VLPs after reinfection attempts. A brief description of the methods and results/discussion can be found in Appendix C.

2.3. Results

2.3.1. Flow cytometry-based virus screening

Of the 49 *Symbiodinium* cultures initially screened, 42 showed a lower cell density relative to control samples after UV irradiation (Appendix A, Table A3). Not all of these cultures showed declines over time, however, suggesting that in some cultures UV irradiation was inhibiting population growth relative to control cultures but not necessarily causing cell lysis. Fifteen cultures had putative VLP groups in cytograms following UV irradiation, and one of these (PK13) also had a putative VLP group in the control sample (see Fig. A28 in Appendix A). Twelve cultures were chosen for follow-up experiments involving more regular sampling of *Symbiodinium* and VLP populations post-stress. In each of these 12 cultures, exposure to 254 nm irradiation at a total irradiance of 2,408 J m⁻² resulted in an initial decline in *Symbiodinium* population density, or retardation of growth relative to the control culture. The *Symbiodinium* populations followed one of three general trajectories following irradiation: a) an absolute decline, tending towards zero (CCMP421, CCMP2430, Ap1, FLAp1, Mp, Sin); b) maintenance of a relatively stable population density, while control samples increased in density (CCMP828, CCMP2431, CCMP2467, Pd, PK13); or c) initial population decline, followed by recovery (Mf13.14) (see Appendix A, Figs. A29 – A40). An increase in VLP density was seen in eight of the twelve cultures. Of the four remaining cultures, three (CCMP421, Mp and Pd) had no VLP group, and one (CCMP2431) had a VLP group present in cytograms of both control and UV-irradiated samples, that followed the same trajectory in both samples.

Increases in VLP density following irradiation were generally rapid, with populations tripling within the first 24 h. Population increases were usually followed by a plateau or decline several days after UV exposure (Appendix A, Figs. A29 – A40). It should be noted that, apart

from CCMP2431, where control cytograms contained a reasonably well-defined VLP group, the VLP numbers reported for control samples (Appendix A, Figs. A29 – A40) represent background noise within the VLP-gated area rather than a defined VLP group. As such, the control VLP lines in the graphs can be considered a baseline or ‘zero’ for the corresponding +UV VLP lines.

Bacteria showed a relative decrease in density following irradiation in all cultures except CCMP421. In most cases, this decrease was followed by a gradual increase in density towards initial levels. The putative phage group showed more variation, although in the majority of cultures this group showed a decrease in density following UV exposure (Appendix A, Figs. A29 – A40).

2.3.2. Transmission electron microscopy

Ten of the eleven *Symbiodinium* cultures examined here showed evidence of VLPs within cells after 254 nm UV irradiation (numerous filamentous VLPs were seen in control and irradiated cultures of CCMP2430, but these were always seen surrounding the cells rather than within them). In some cases, VLPs were also seen in various stages of expulsion from damaged cells following irradiation. Cells of seven cultures (CCMP421, CCMP2430, CCMP2465 Ap1, FLAp1, Mf13.14 and Mp) also contained VLPs in control samples. Virus-like particles varied in size and morphology: CCMP421 and PK13 contained crystalline arrays of icosahedral VLPs ~20 nm in diameter; icosahedral VLPs ranging in size from ~50 nm to ~500 nm diameter were seen in Ap1, FLAp1 and Mf13.14; and all other cultures contained rod-shaped and filamentous VLPs ~100 – 200 nm in length (Figs. 2.2 – 2.12). In some cases filamentous VLPs resembled host cell membranes, however they were smaller (usually several nm thinner) than surrounding membranes, and often were a uniform length, unlike fragmented cell membranes. In Ap1 and FLAp1, large, enveloped VLPs were present outside cells in both control and irradiated samples (Fig. 2.7I and 2.8D), though these were seen much more frequently in UV-exposed samples. Bacteria and other organisms were never seen within the cells.

Various stages of cell death were observed in both control and irradiated samples, but dying cells were in the minority in control samples, unlike irradiated samples where compromised cells were found in similar numbers to viable cells by 96 h post-UV exposure (observational

only; this was not quantified). This is in agreement with the preceding flow cytometric analysis, where substantial reductions in cell density were observed post-stress. Apoptotic and necrotic cells were defined based on the characterisations of *Symbiodinium* cell death in Dunn *et al.* (2004) and Strychar *et al.* (2004) where possible, though apoptosis and necrosis can be difficult to distinguish in *Symbiodinium* (Franklin *et al.*, 2004) so modes of cell death are not always defined here. Descriptions of observed VLPs and cell death mechanisms for each culture are found in Figs. 2.2 – 2.12 below.

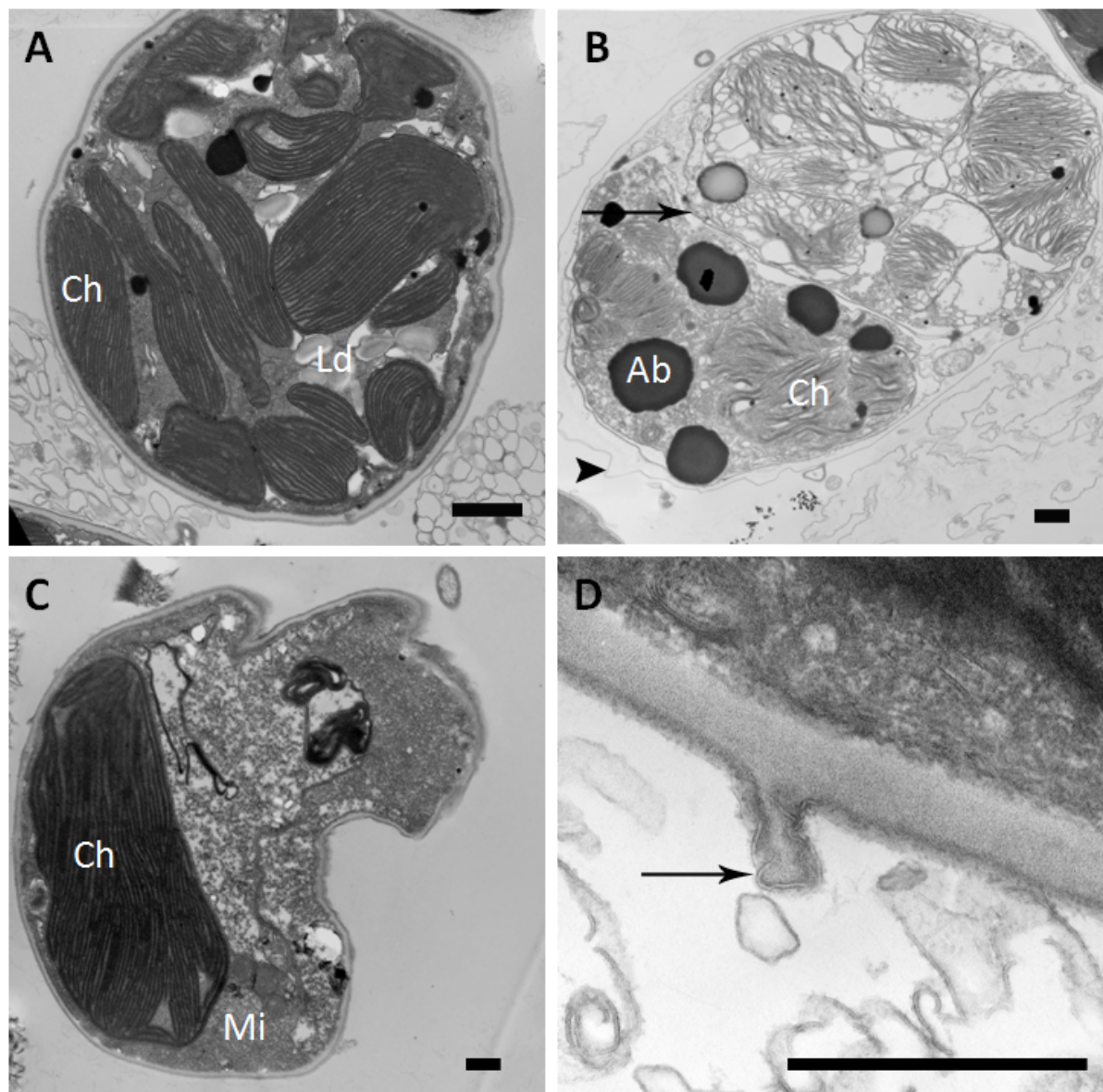


Figure 2.2. Description on page 42.

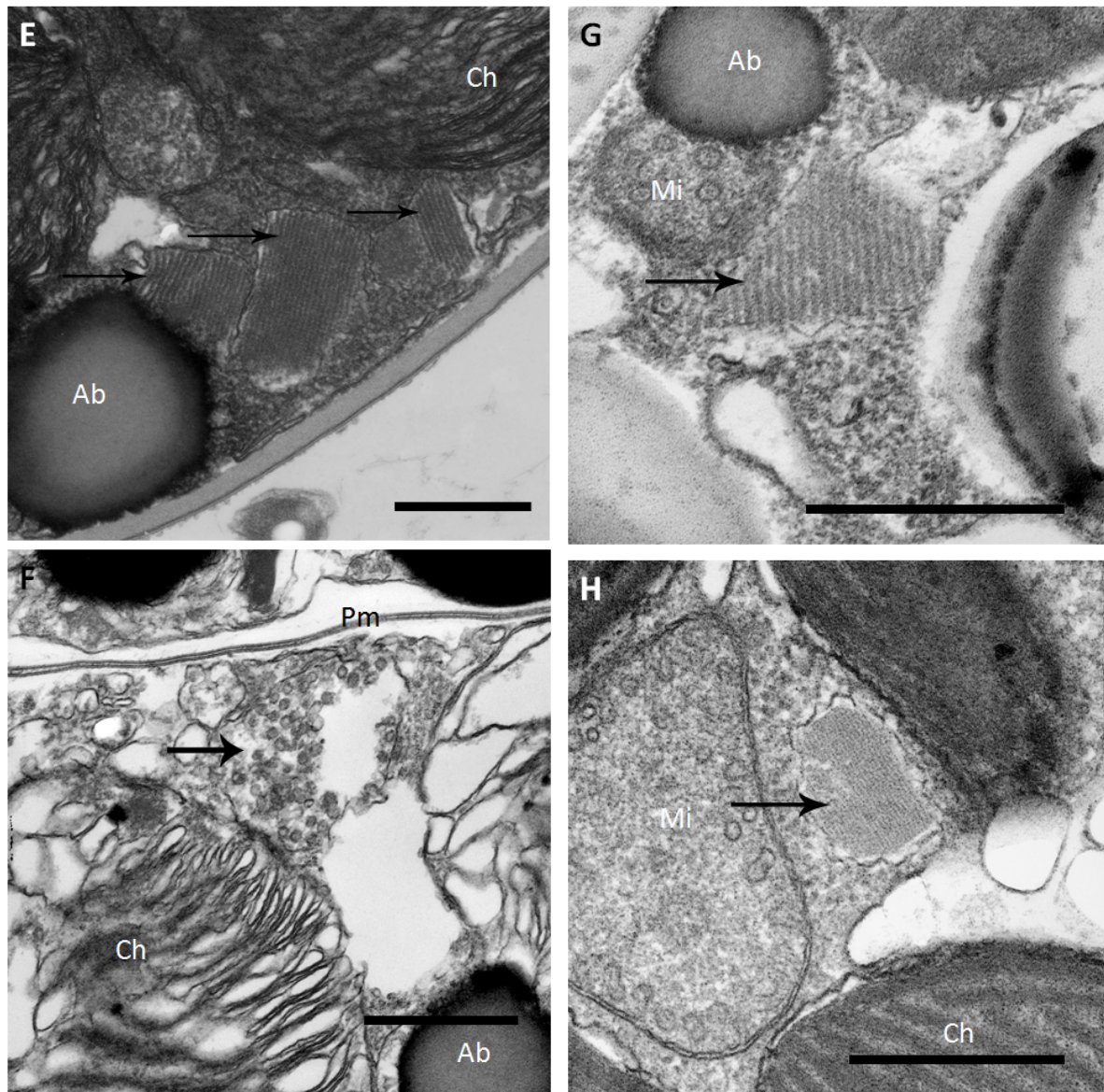


Figure 2.2 (above and previous page). Transmission electron micrographs of *Symbiodinium* culture CCMP421. (A) Viable cell, not exposed to UV irradiation. (B) Dividing cell (doublet; arrow indicates fissure between daughter cells) in intermediate stage of cell death, 96 h after UV exposure. Cell shows symptoms of both necrosis (disintegration of chloroplasts) and apoptosis (accumulation bodies, intact cell membrane and cell shrinkage: note the arrowhead marking the cell wall). (C) Cell in early stage of apoptosis 48 h post-exposure: note cell shrinkage and membrane blebbing. (D) Filamentous virus-like particles (VLPs) being ejected from cell 96 h post-exposure. (E) Crystalline arrays of VLPs 96 h post-exposure (arrows). (F) VLPs in a dying cell, 96 h post-exposure. (G) and (H) Crystalline arrays of VLPs in control cells not exposed to UV irradiation. Key: Ab – accumulation body, Ch – chloroplast, Ld – lipid droplet, Mi – mitochondrion, Pm – plasma membrane. Scale bars represent 500 nm.

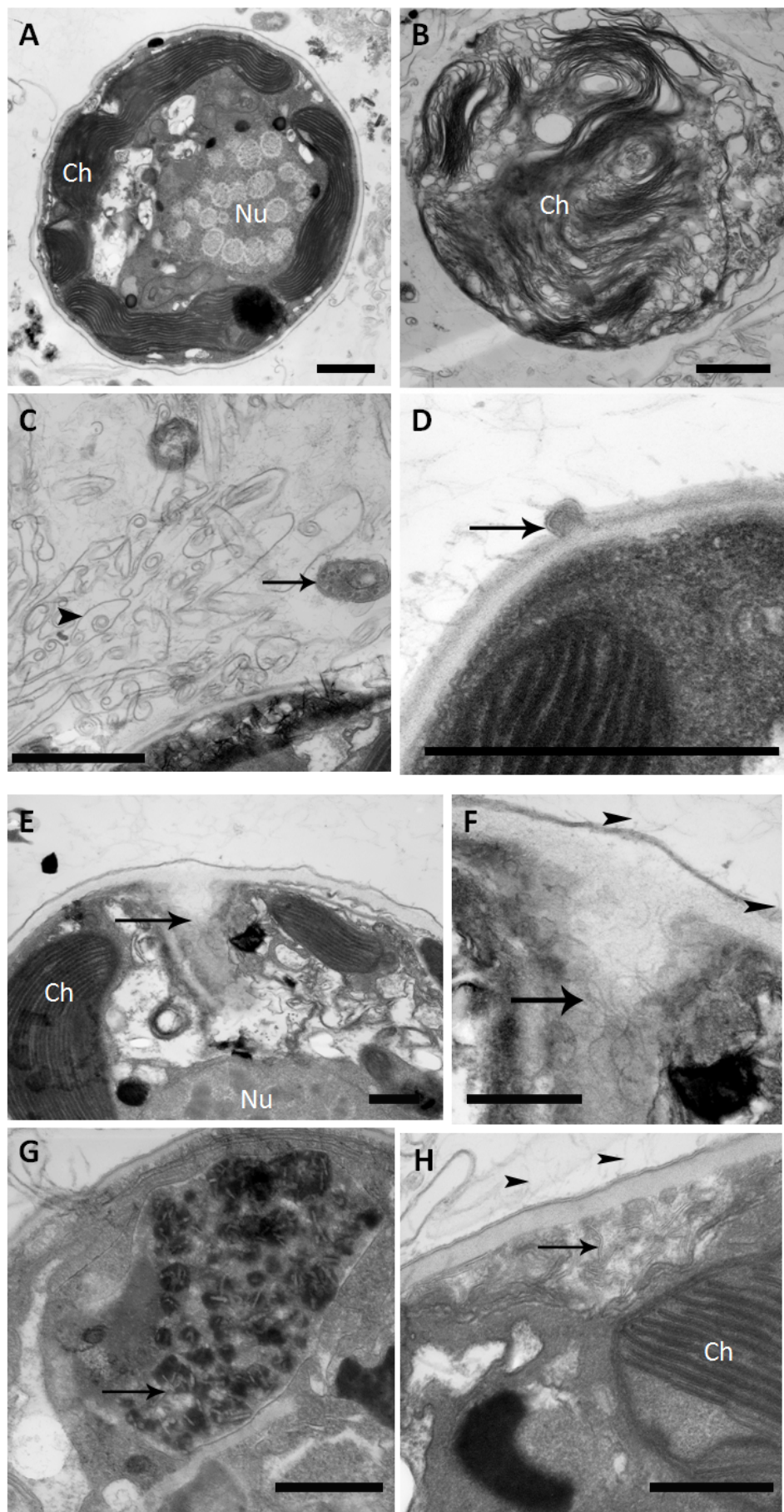


Figure 2.3. Description on page 44.

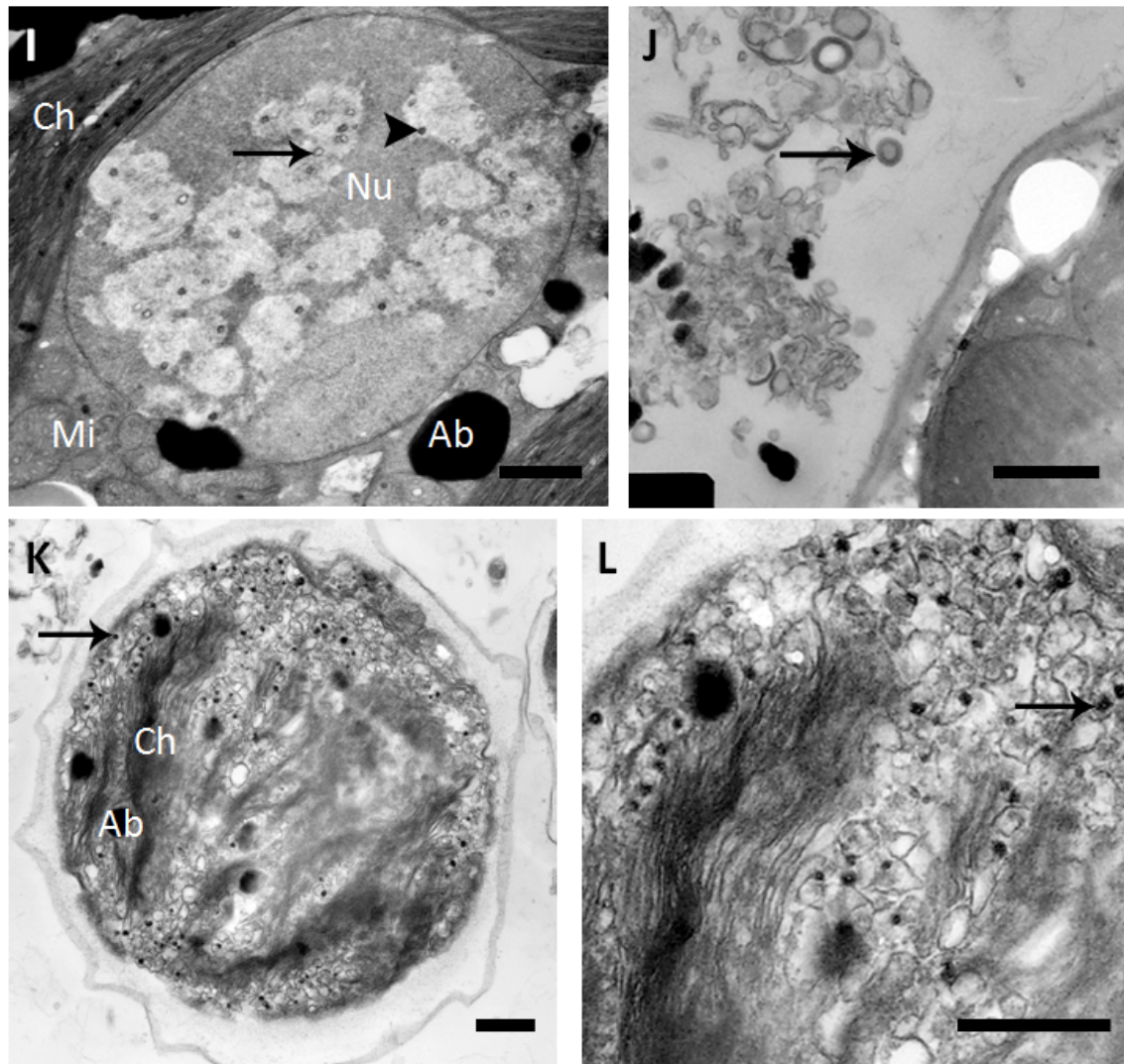


Figure 2.3 (above and previous page). Transmission electron micrographs of cells of *Symbiodinium* culture CCMP828. (A) Viable cell not exposed to UV irradiation. (B) Necrotic cell 96 h post-UV exposure. Chloroplasts show signs of disintegration, including loosened thylakoid membranes, and plasma membrane shows signs of rupturing. (C) Filaments, presumed to be shed cell membranes (arrow head), in *Symbiodinium* culture medium 96 h post-exposure. Note also the vesicle containing virus-like particles (VLPs; arrow). (D) Possible VLP being ejected from cell (arrow), 48 h after UV exposure. (E) Filamentous VLPs (arrow) being released from the host cell 48 h after UV exposure. (F) Higher magnification image of filamentous VLP release. Note also the filamentous VLPs just outside of the cell (arrow heads). (G) Numerous filamentous/rod-shaped VLPs (arrow) in a vacuole inside a *Symbiodinium* cell 96 h after UV exposure. (H) Filamentous VLPs just inside the plasma membrane of a cell 96 h after UV exposure. (I) Putative viral capsids (arrow) and nucleocapsids (arrow head) in the nucleus of a cell 96 h post-exposure. (J) A large icosahedral VLP (arrow) associated with debris from a disintegrated *Symbiodinium* cell, 96 h post-exposure. (K) Apoptotic cell (note cell shrinkage, presence of accumulation bodies and fusion of organelles such as chloroplasts) 96 h after UV exposure. Arrow indicates one of the numerous VLPs seen in the dying cell. (L) A higher magnification image showing the VLPs in (K) (arrow). Key: Ab – accumulation body, Ch – chloroplast, Mi – mitochondrion, Nu – nucleus. Scale bars represent 1 μm (A – D) and 500 nm (E – L).

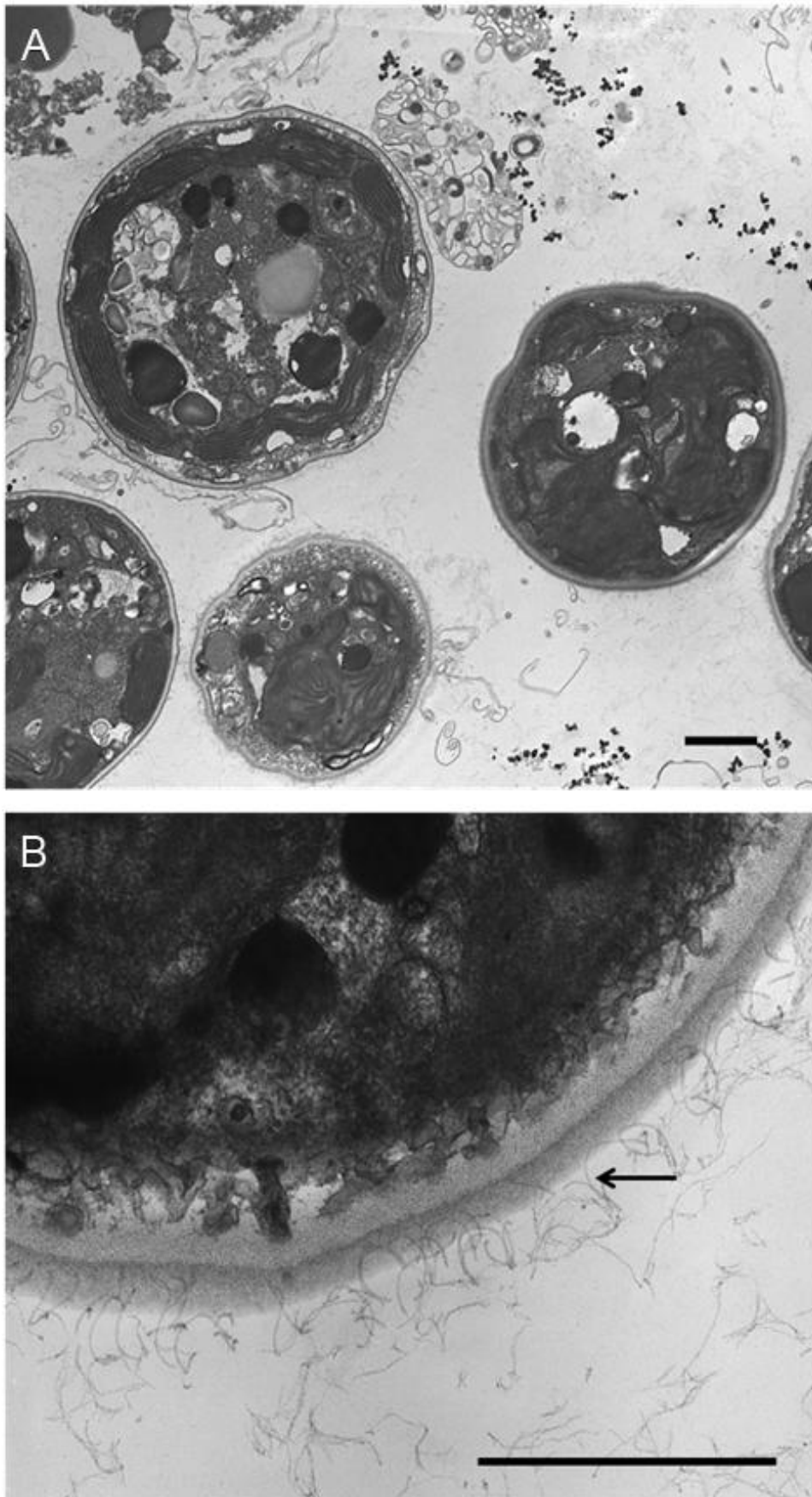


Figure 2.4. Description on page 46.

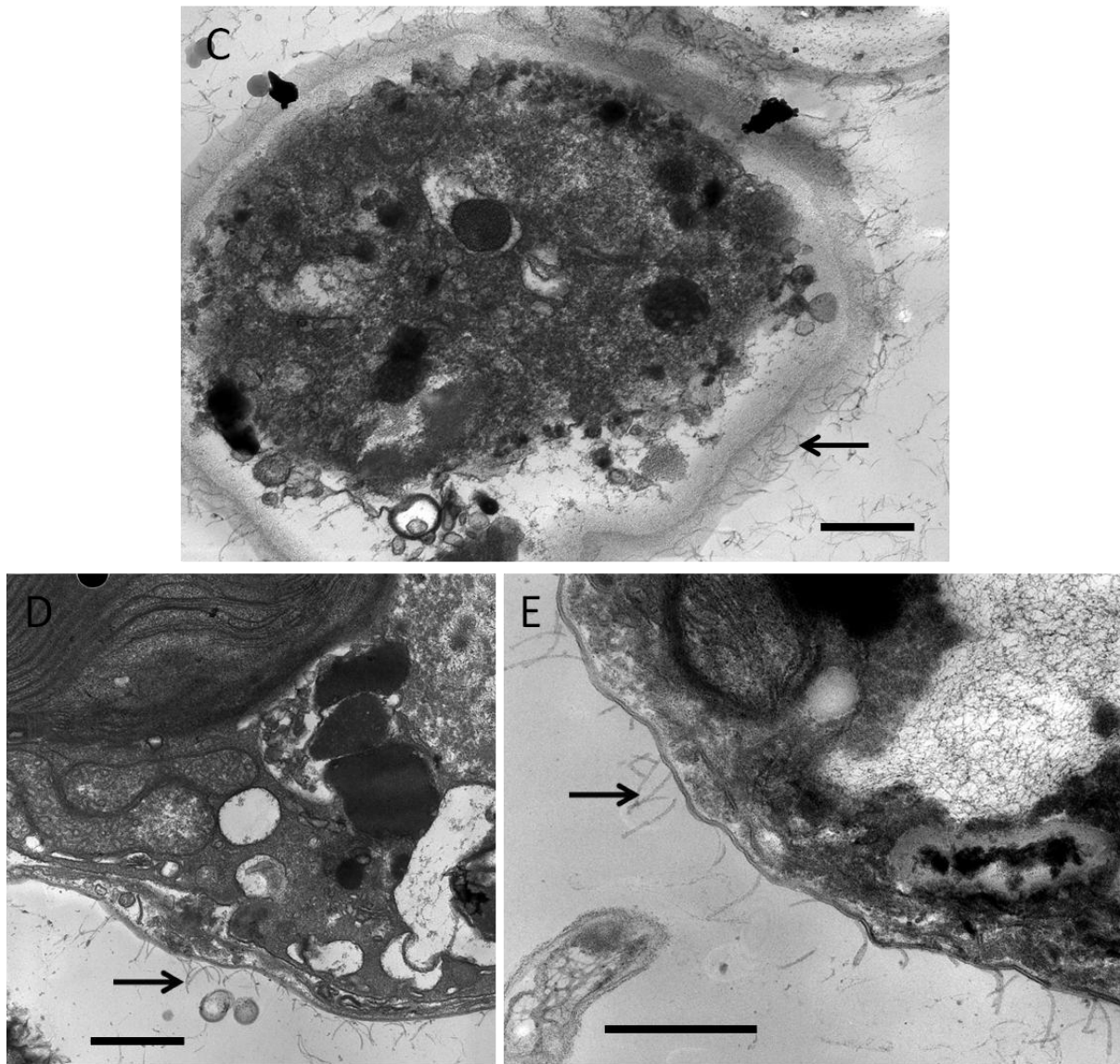


Figure 2.4 (above and previous page). Transmission electron micrographs of cells of *Symbiodinium* culture CCMP2430. (A) Viable cells not exposed to UV radiation. (B) Filamentous VLPs (arrow) surrounding a cell in a non-irradiated sample. (C) Apoptotic cell surrounded by filamentous VLPs (arrow) 48 h after UV exposure. (D) Cell in early stage of apoptosis with surrounding filamentous VLPs (arrow), 96 h after UV exposure. (E) Higher magnification image of filamentous VLPs (arrow). Scale bars represent 1 μm (A, B) and 500 nm (C – E).

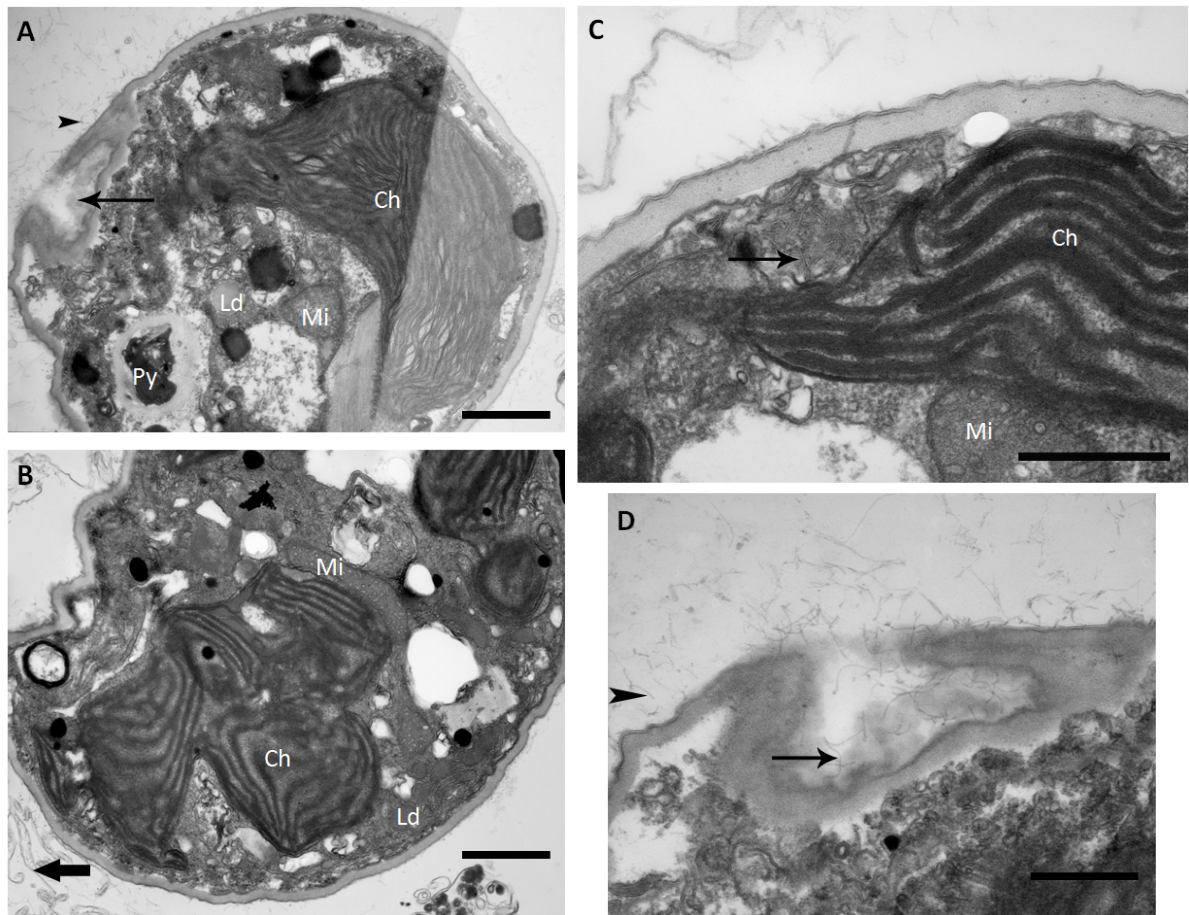


Figure 2.5. Description on page 49.

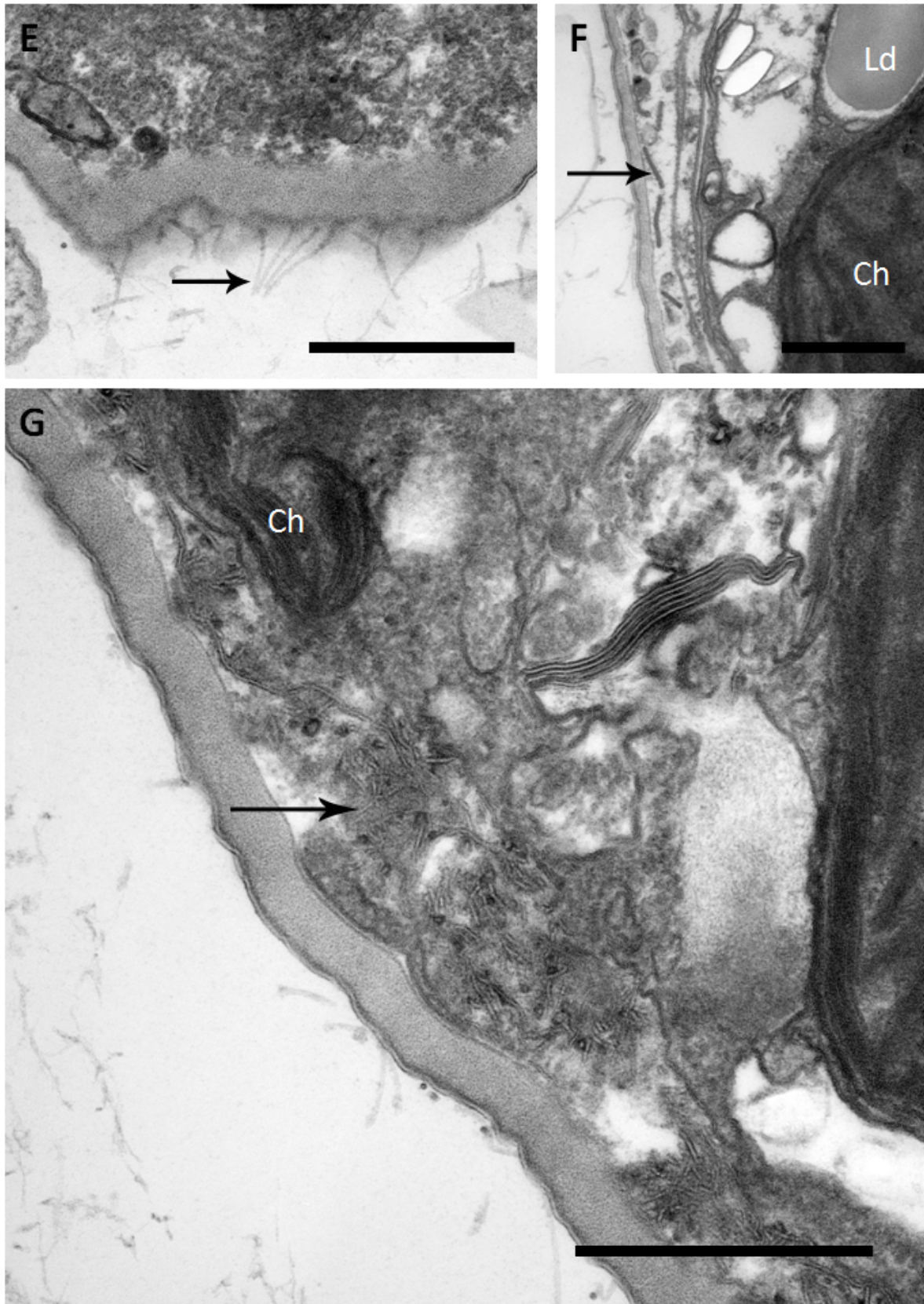


Figure 2.5 continued. Description overleaf.

Figure 2.5 (previous pages). Transmission electron micrographs of cells of *Symbiodinium* culture CCMP2465. (A) A *Symbiodinium* cell in early stage of cell death (possibly necrotic, given the dissociation of thylakoid membranes that appears to be beginning in the chloroplasts), examined 96 h after UV exposure. Filamentous virus-like particles (VLPs) appear to be leaving the cell (arrow), and similar VLPs are seen around the outside of the cell (arrow head). (B) A cell in mid-stage apoptosis, 96 h after UV exposure. Chloroplasts are fusing and there is apparent cell shrinkage. Shed cell membranes can also be seen outside of the cell (arrow). (C) A visibly healthy cell from a non-irradiated culture, containing filamentous VLPs (arrow) between the chloroplast and plasma membrane. (D) Higher magnification image of filamentous VLPs seen in (A). Arrow indicates VLPs being released from cell and arrow head indicates similar VLPs found outside of the cell. (E) Filamentous VLPs near the outside of a cell (arrow), 96 h after UV exposure. (F) Filamentous VLPs (arrow) located near the plasma membrane of a cell 96 h after UV exposure. (G) Numerous filamentous VLPs (arrow) located near the plasma membrane of a cell 96 h after UV exposure. Key: Ab – accumulation body, Ch – chloroplast, Ld – lipid droplet, Mi – mitochondrion, Nu – nucleus, Py – pyrenoid. Scale bars represent 1 μm (A – B) and 500 nm (C – G).

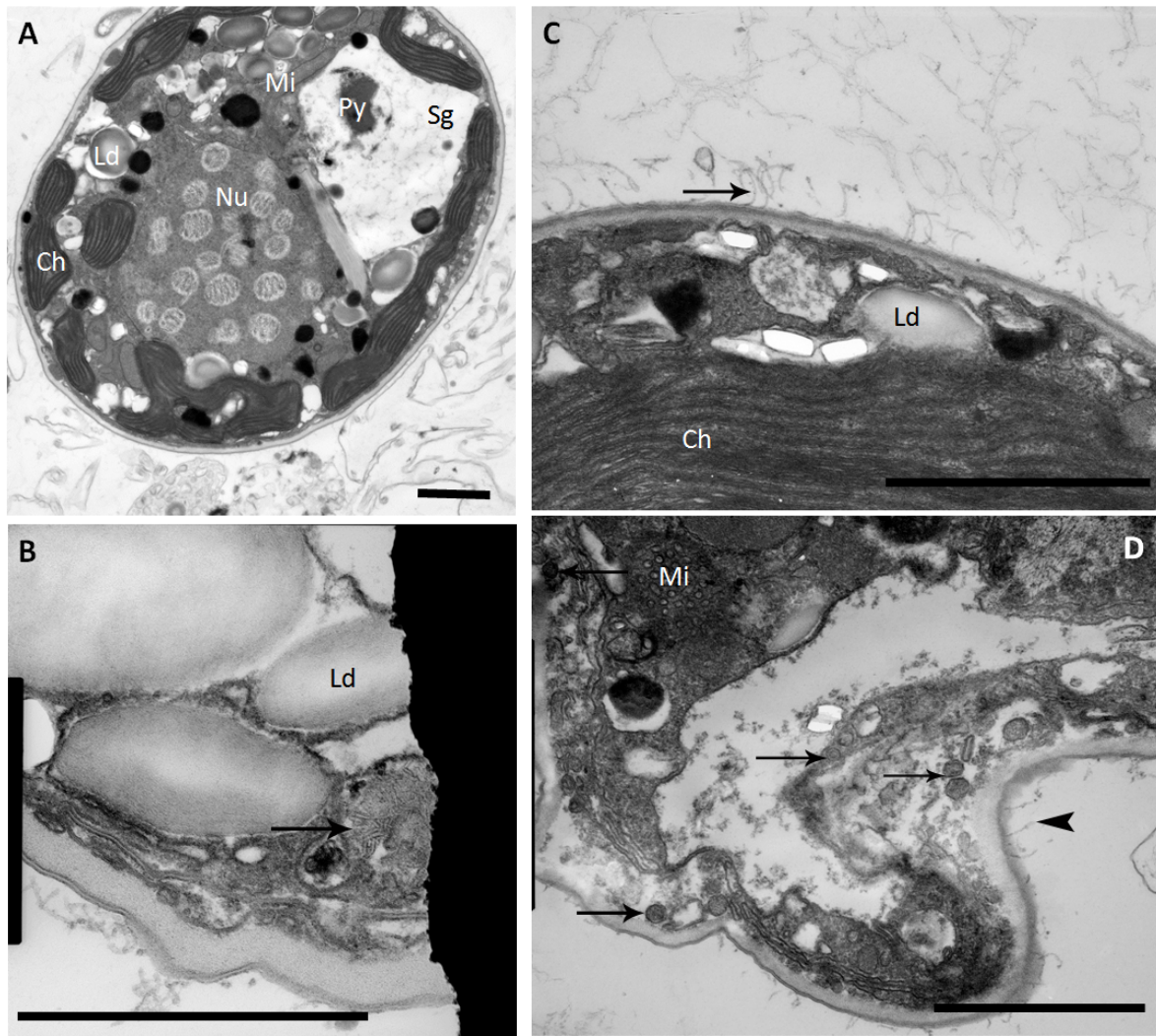


Figure 2.6. Transmission electron micrographs of cells of *Symbiodinium* culture CCMP2469. (A) Viable cell not exposed to UV irradiation. (B) A degraded cell 48 h after UV exposure, possibly undergoing necrosis, given the apparent plasma membrane rupture and presence of numerous lipid droplets. A cluster of filamentous VLPs can be seen within a vacuole in the cell (arrow). (C) Filamentous VLPs (arrow) surrounding a cell 48 h after UV exposure. (D) Icosahedral VLPs (arrows) inside a cell, and filamentous VLPs outside of the cell (arrow head), 96 h after UV exposure. Key: Ab – accumulation body, Ch – chloroplast, Ld – lipid droplet, Mi – mitochondrion, Nu – nucleus, Py – pyrenoid, Sg – starch grains. Scale bars represent 1 μm .

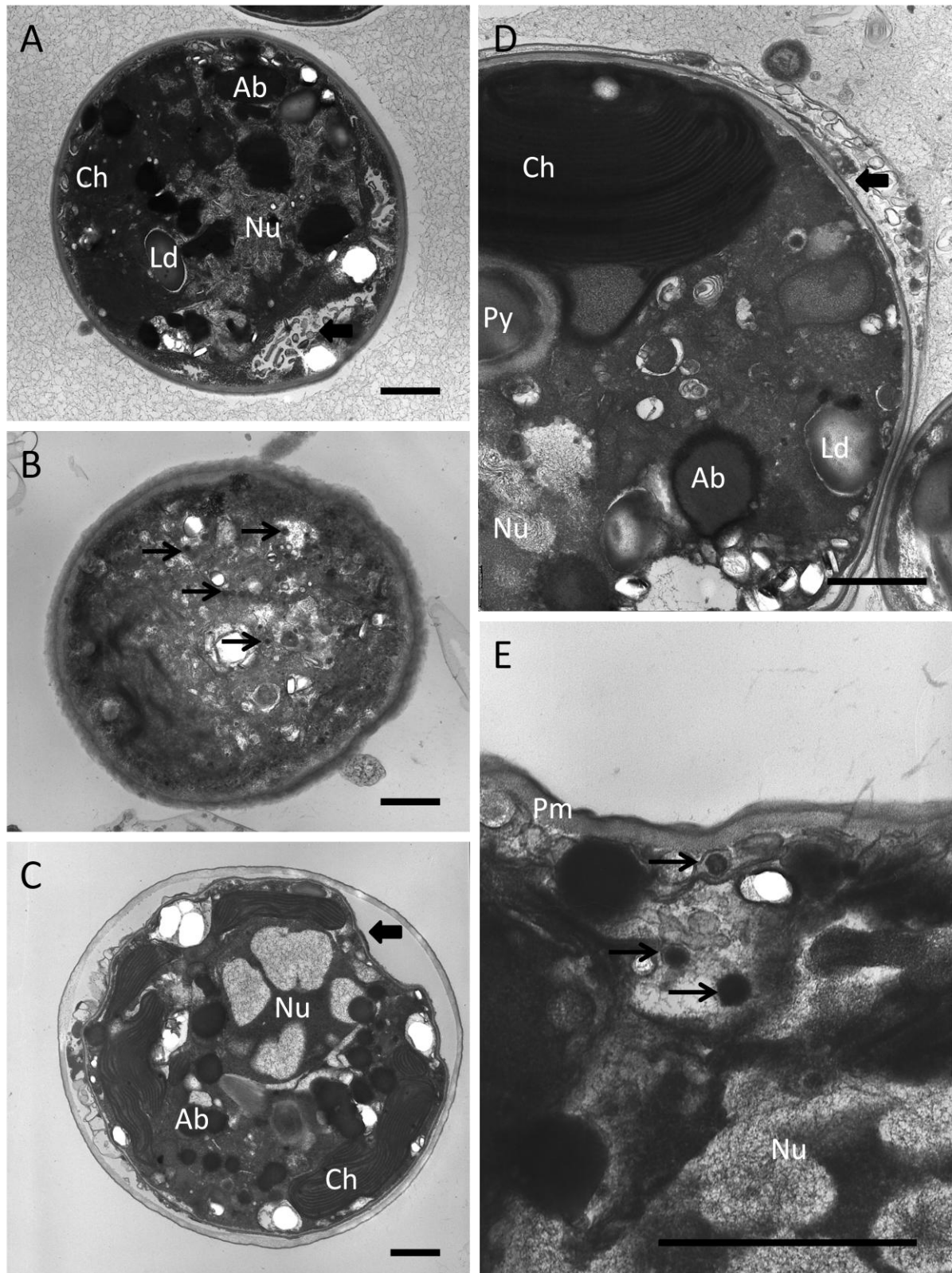


Figure 2.7. Description overleaf.

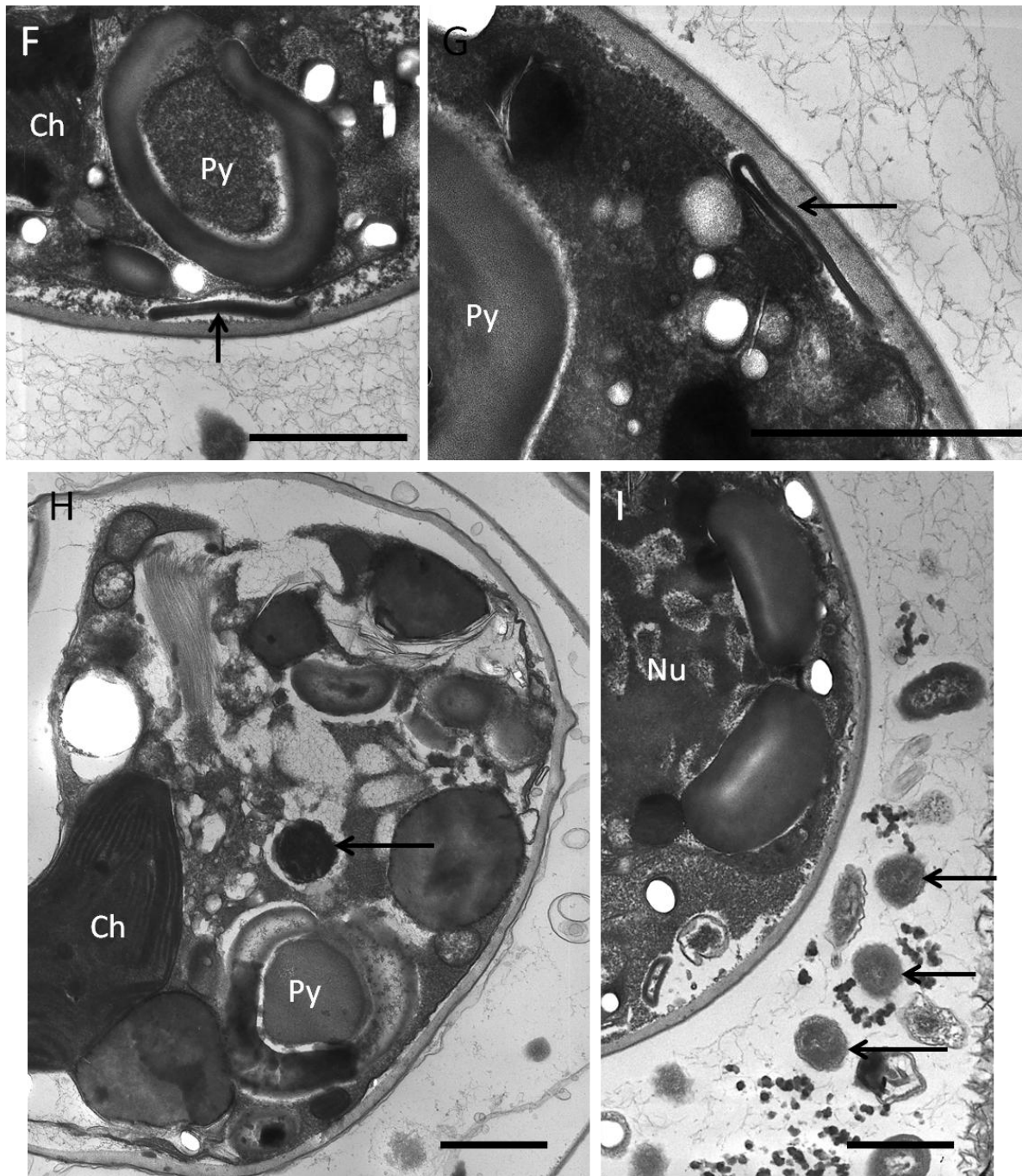


Figure 2.7 (above and previous page). Transmission electron micrographs of cells of *Symbiodinium* culture Ap1. (A) Necrotic cell 48 h after UV exposure; note disintegrated organelles (block arrow). (B) Necrotic cell 96 h after UV exposure, with small (~50 nm diameter) icosahedral VLPs present (arrows). (C) Apoptotic cell in non-irradiated culture. Block arrow indicates an area of cell shrinkage. (D) Apoptotic cell 96 h after UV exposure; note cell shrinkage (block arrow). (E) ~100 nm diameter icosahedral VLPs (arrows) in a cell from a non-irradiated culture. (F, G) Large (~1 μm length) filamentous VLPs (arrows) immediately beneath the plasma membrane in cells 48 h after UV exposure. (H) Large (~500 nm diameter), enveloped icosahedral VLP in a cell 96 h after UV exposure (I) Similar VLPs to that seen in (H), observed outside a cell 96 h after UV exposure. Key: Ab – accumulation body, Ch – chloroplast, Ld – lipid droplet, Nu – nucleus, Pm – plasma membrane, Py – pyrenoid. Scale bars represent 1 μm .

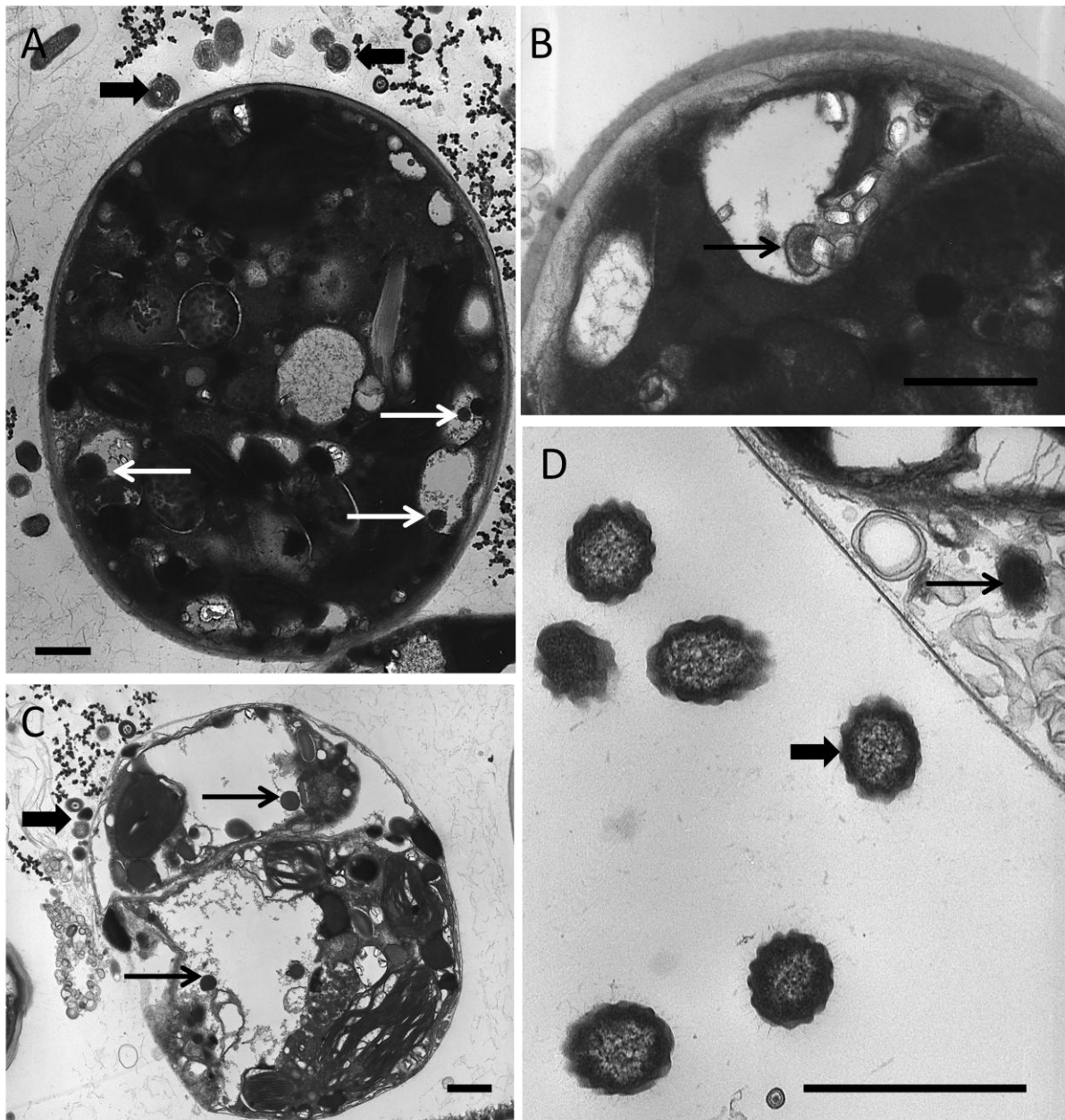


Figure 2.8. Transmission electron micrographs of cells of *Symbiodinium* culture FLAp1. (A) *Symbiodinium* cell 96 h after UV exposure, showing giant (~200 – 500 nm diameter) icosahedral VLPs within the cell (arrows) and ~500 nm diameter VLPs outside of the cell (block arrows). (B) ~250 nm diameter enveloped, icosahedral VLP inside a cell from a culture not exposed to UV radiation. (C) Large enveloped icosahedral VLPs inside (arrows) and outside (block arrow) a cell 48 h after UV exposure. (D) Icosahedral VLP inside a cell (arrow), and large, enveloped VLPs outside the cell (block arrow) 48 h after UV exposure. Scale bars represent 1 μm.

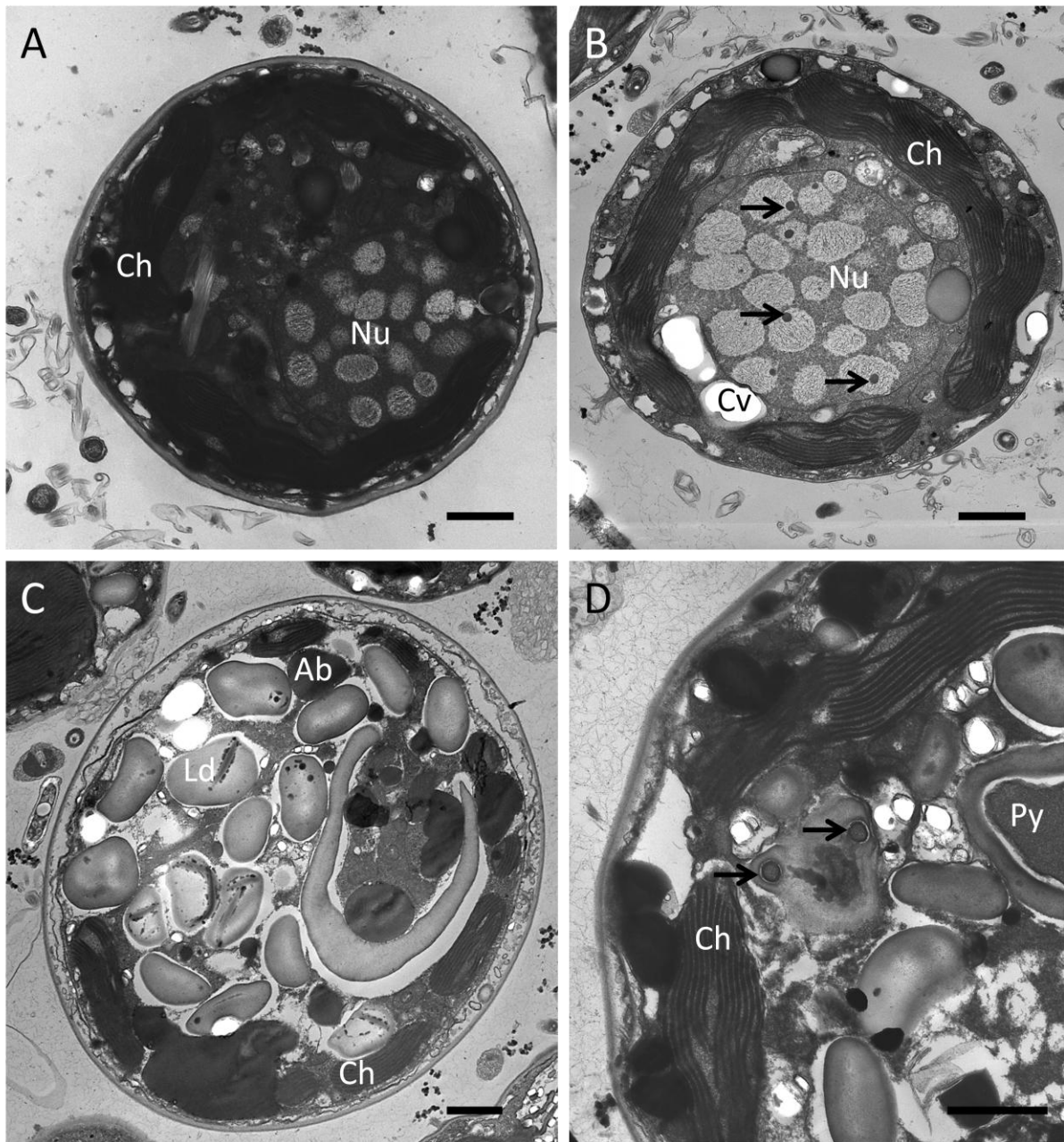


Figure 2.9. Transmission electron micrographs of cells of *Symbiodinium* culture Mf13.14. (A) Viable cell in a non-irradiated culture. (B) Cell in early stage of apoptosis, 48 h after UV exposure. Arrows indicate icosahedral VLPs ~150 nm in diameter in the nucleus. (C) Apoptotic cell 96 h after UV exposure. (D) Icosahedral VLPs (~200 nm diameter, arrows) inside a cell 96 h after UV exposure. Key: Ab – accumulation body, Ch – chloroplast, Cv – cytoplasm vacuole, Ld – lipid droplet, Nu – nucleus, Py – pyrenoid. Scale bars represent 1 μ m.

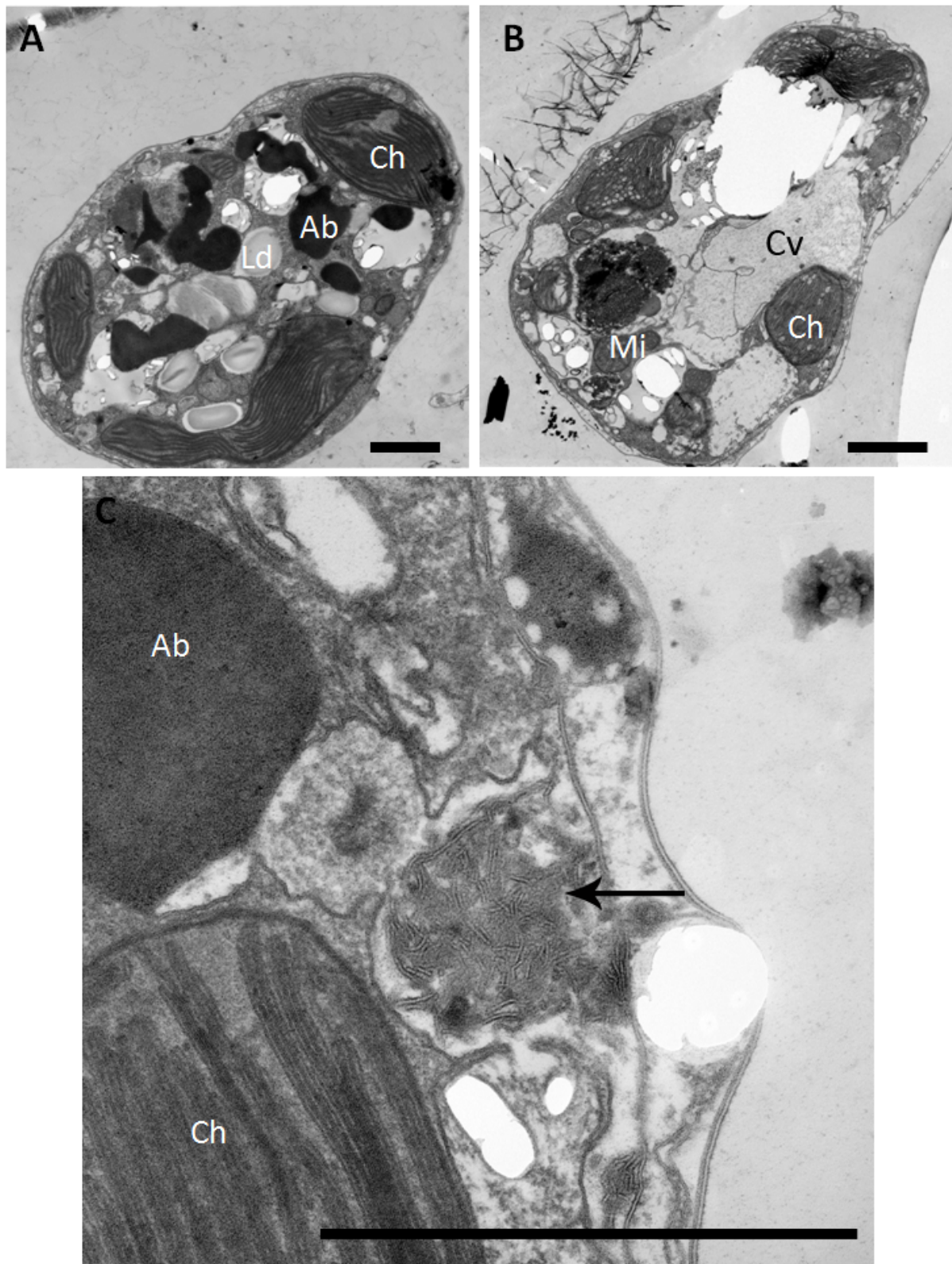


Figure 2.10. Description on page 56.

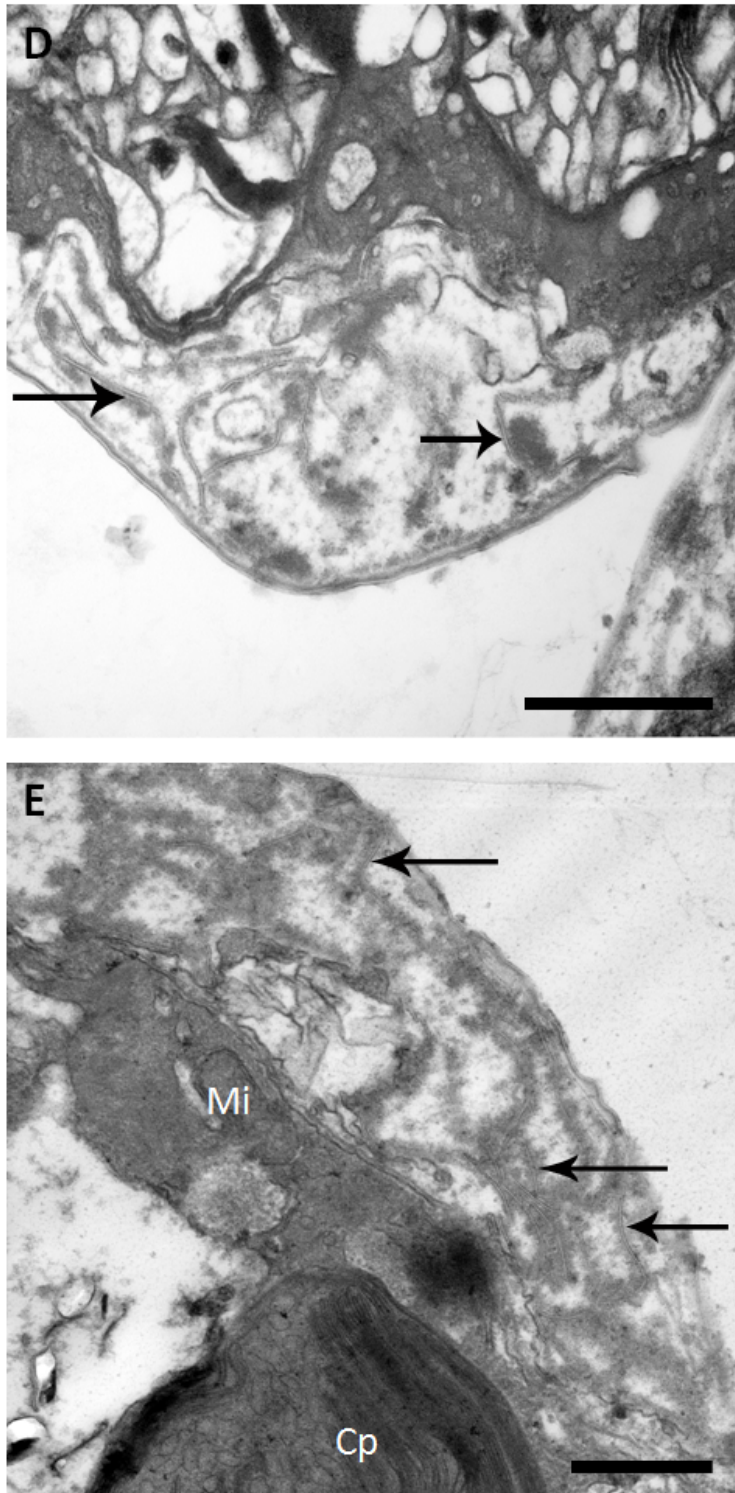


Figure 2.10 (above and previous page). Transmission electron micrographs of cells of *Symbiodinium* culture Mp. (A) Viable cell not exposed to UV irradiation. (B) Necrotic cell 96 h after UV exposure. The cytoplasm is vacuolated, and chloroplasts are disintegrating and contain numerous vesicles. (C) Filamentous VLPs (arrow) in a cell not exposed to UV radiation. (D) Filamentous VLPs (arrows) in a degraded cell 48 h after UV exposure. (E) Filamentous VLPs (arrows) in a degraded cell 96 h after UV exposure. Key: Ab – accumulation body, Ch/Cp – chloroplast, Cv – cytoplasm vacuole, Ld – lipid droplet, Mi – mitochondrion. Scale bars represent 1 μm (A – C) and 500 nm (D – E).

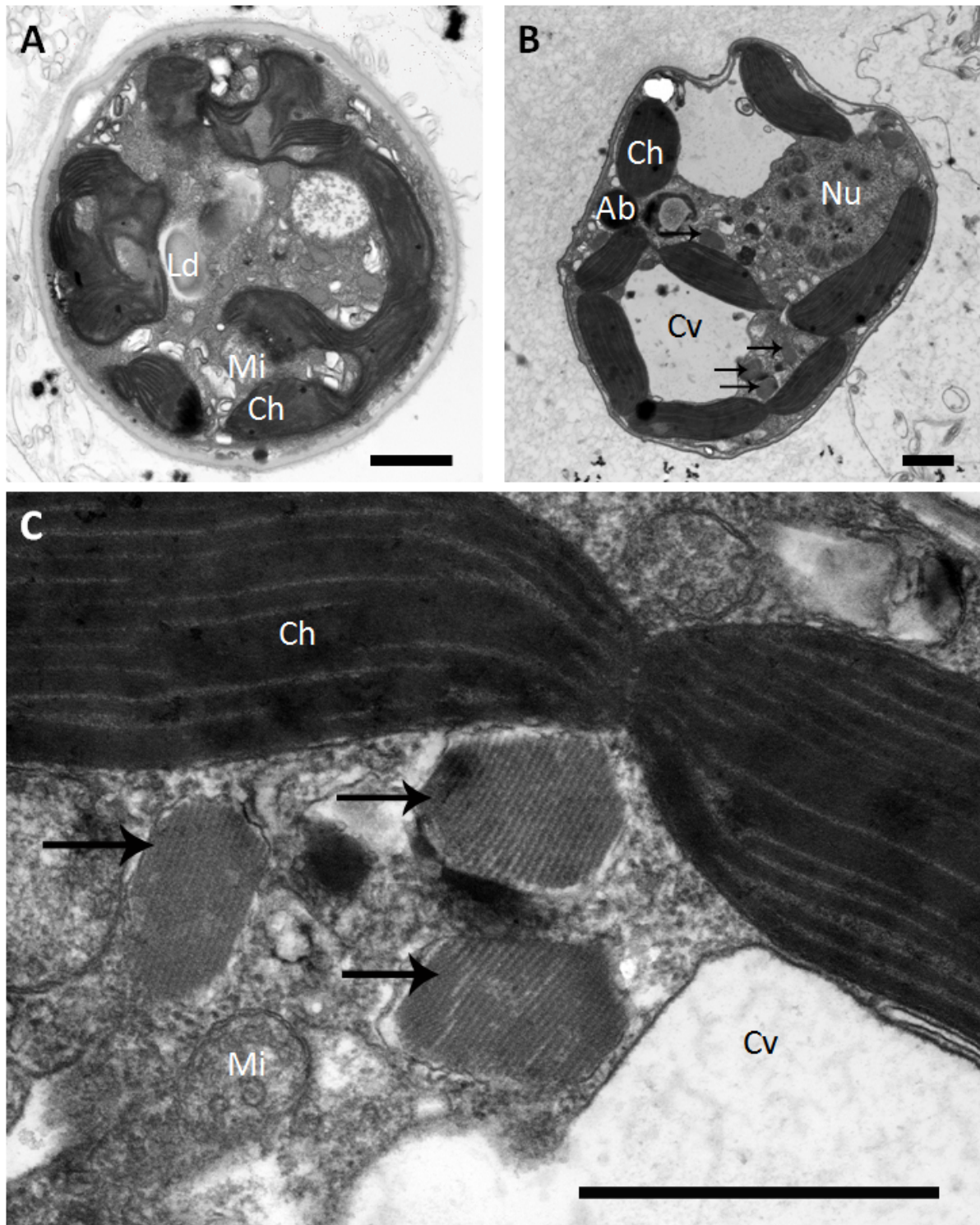


Figure 2.11. Transmission electron micrographs of cells of *Symbiodinium* culture PK13. (A) Viable cell not exposed to UV irradiation. (B) Cell undergoing necrosis or apoptosis 48 h after UV exposure. Cytoplasmic vacuoles are present, as would be expected with necrotic cell death, but an accumulation body can be seen and cell shrinkage is apparent, suggesting apoptosis. Arrows indicate crystalline arrays of VLPs. (C) Higher magnification of crystalline arrays of VLPs (arrows) seen in (B). Key: Ab – accumulation body, Ch – chloroplast, Cv – cytoplasm vacuole, Ld – lipid droplet, Mi – mitochondrion, Nu – nucleus. Scale bars represent 1 μm.

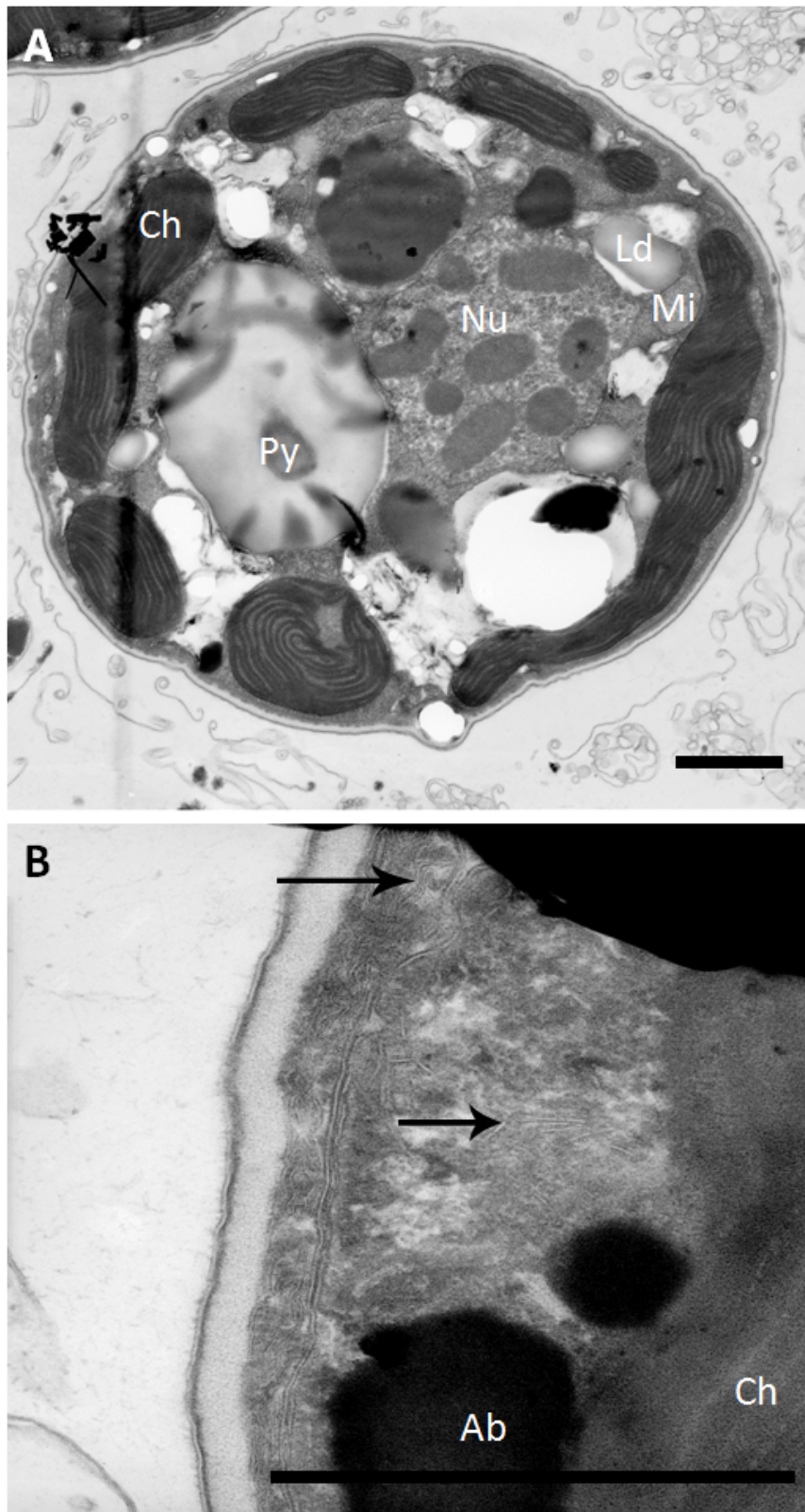


Figure 2.12. Transmission electron micrographs of cells of *Symbiodinium* culture Sin. (A) Viable cell not exposed to UV irradiation. (B) Filamentous VLPs (arrows) in a degraded cell 96 h after UV exposure. Key: Ab – accumulation body, Ch – chloroplast, Ld – lipid droplet, Mi – mitochondrion, Nu – nucleus, Py – pyrenoid. Scale bars represent 1 μm (A) and 500 nm (B).

2.3.3. Molecular analysis of putative latent viruses

DNA was successfully extracted from UV-irradiated and control samples of *Symbiodinium* culture CCMP421 and from the UV-irradiated sample of PK13. PCR was successful using the RR2 forward and reverse primers, and resulting PCR products were ~270 bp in length (Fig. 2.13). Digests with the enzymes *Hae*III and *Msp*I revealed two restriction patterns in each of CCMP421 +UV and CCMP421 Control, and three in PK13 +UV (one of which was not sequenced due to low DNA concentration) (Fig. 2.14). Sequencing was successful on all six RFLP types, resulting in six unique sequences varying in length from 284 – 291 bp.

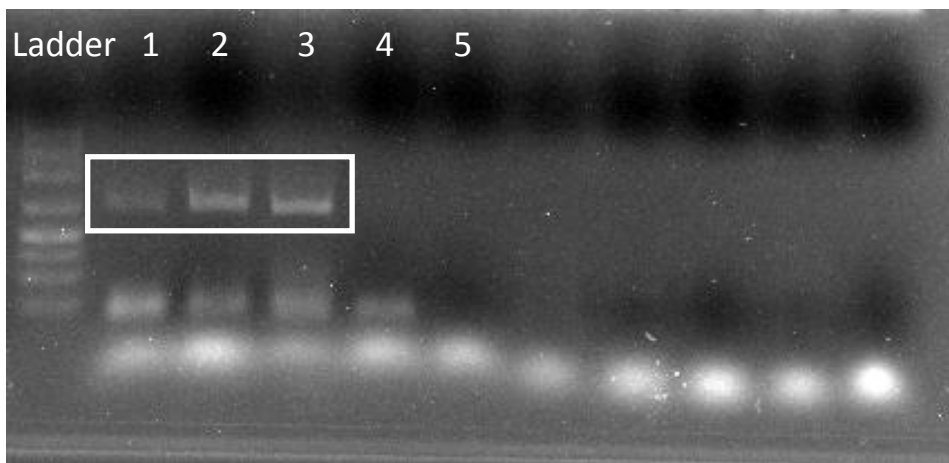


Figure 2.13. RR2 PCR products obtained from *Symbiodinium* cultures. (1) CCMP421, UV-irradiated. (2) CCMP421, control. (3) PK13, UV-irradiated. (4) PK13, control. (5) Negative control (no DNA template). Ladder is a 50-1500 bp molecular marker; RR2 bands correspond approximately with the 250 bp marker.

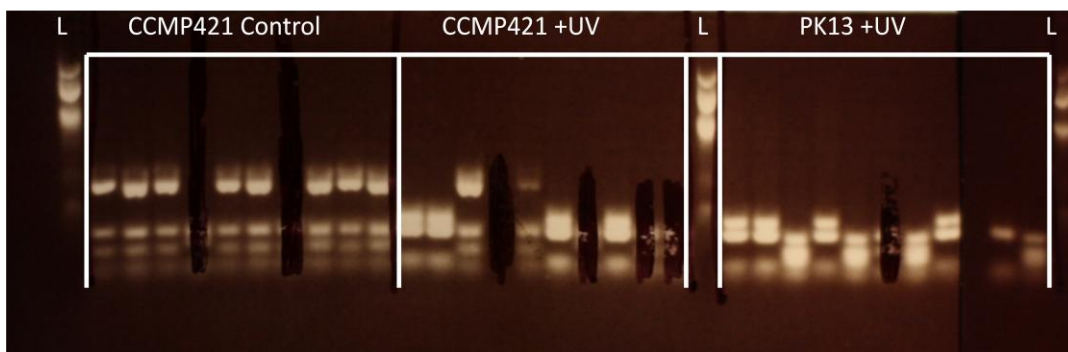


Figure 2.14. Restriction digests of plasmids containing putative viral RR2 sequences. L = 100 bp ladder (New England Biolabs, Ipswich, MA, USA). Blacked-out lanes are samples that showed no insert in colony PCR screening.

Alignment of the translated amino acid sequences with nearest matches in the NCBI non-redundant protein database confirmed that the PCR products were partial ribonucleotide reductase genes. The nearest matches varied, and included bacteria, algae, plants and animals (Fig. 2.16). Also included in the alignment were five putative viral ribonucleotide reductase sequences obtained from *Porites australiensis* corals (see Chapter 5). Similarity between sequences obtained here and the NCBI database matches was low (65 – 85% pairwise identity), making identification of their origin difficult. Of interest, however, was the fact that the three sequences obtained from UV-irradiated *Symbiodinium* samples showed very high identity (up to 97%) to the three putative viral sequences obtained from coral tissue bordering disease lesions (Fig. 2.15). Although the diverse nature of these sequences and their small size (92 – 97 AA length) resulted in low bootstrap values for many branches on the resulting phylogenetic tree, the branches on which these putative viral sequences cluster are well-supported (> 90%). In total there were two clusters of sequences from each *Symbiodinium* culture, with one of the clusters containing a sequence from both cultures (Fig. 2.16).



Figure 2.15. Amino acid sequence alignment of putative viral partial ribonucleotide reductase small subunit gene from *Symbiodinium* cultures CCMP421 and PK13 and *Porites australiensis* corals suffering from white patch syndrome (WPS). WPS lesion: sequence obtained from sample taken directly from white patch lesion. WPS1cm: sequence obtained from sample taken 1 cm away from white patch lesion. Coloured letters represent the amino acid most commonly shared at each position in the sequence. Coloured bars above alignment indicate level of identity among sequences, from red (few sequences sharing the same amino acid at a given position) to green (all sequences sharing the same amino acid at a given position).

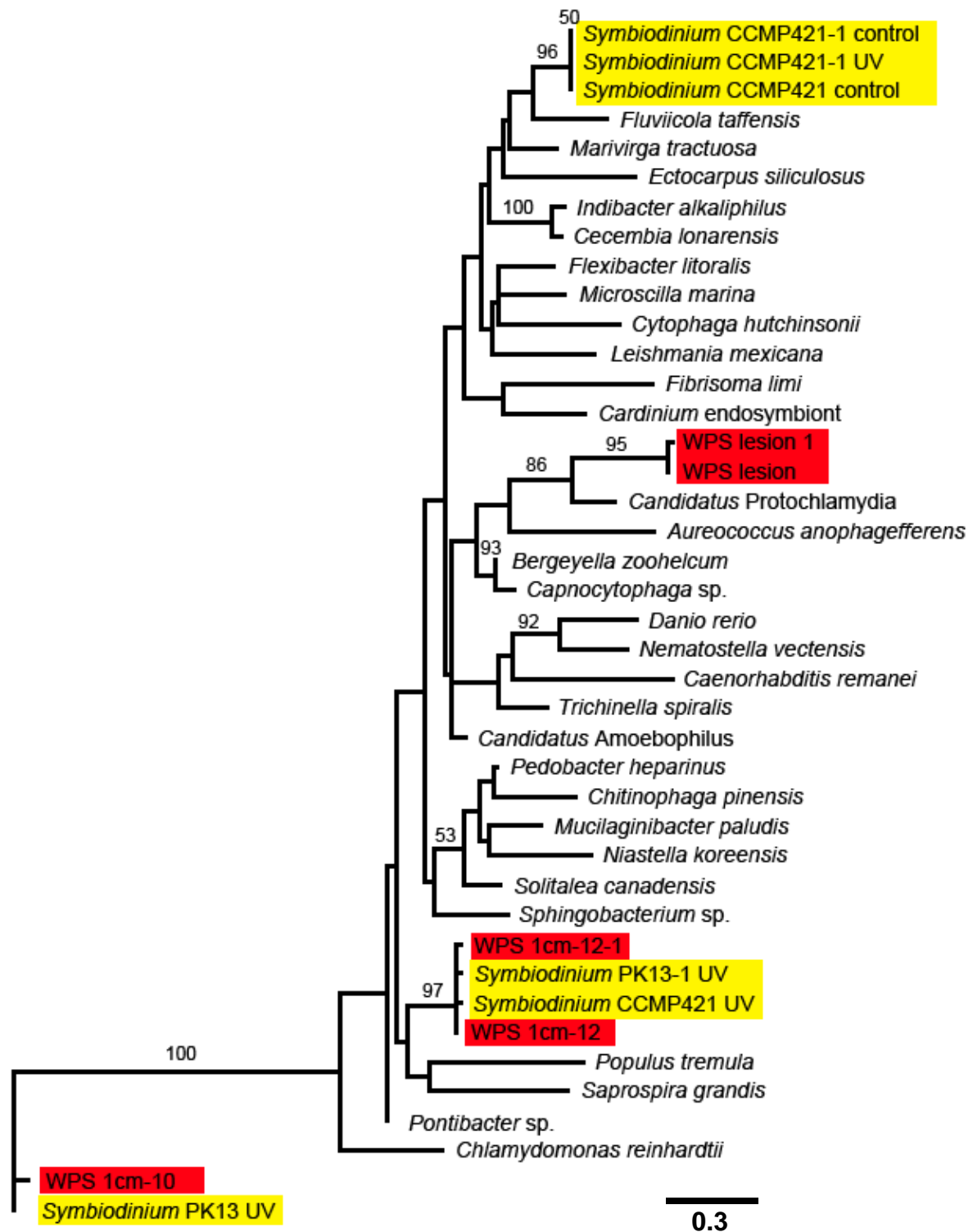


Figure 2.16. Maximum likelihood tree of ribonucleotide reductase small subunit amino acid sequences obtained from control and UV-irradiated *Symbiodinium* cultures (yellow boxes) and from *Porites australiensis* corals suffering from white patch syndrome (WPS; red boxes). WPS lesion: tissue sample taken directly from disease lesion by Davy (2007); WPS 1cm: tissue sample taken 1cm away from the disease lesion. Branch labels show bootstrap support (100 iterations) and the scale bar represents the number of nucleotide substitutions per site. Tree was constructed using the LG substitution model. Bootstrap values < 50 are not shown.

2.4. Discussion

The aims of this chapter were to determine whether or not a range of *Symbiodinium* cultures contained latent viral infections that could be induced to cause cell lysis *via* stress, and to take steps towards identification of these viruses when they were found. To this end, UV and thermal stress were used in an attempt to induce lytic infections, and flow cytometry, electron microscopy and PCR analysis were used to detect viruses and perform initial characterisation when they were found to be present.

2.4.1. Screening for latent viruses

Forty-nine cultures of *Symbiodinium* were initially screened for latent viral infections using 254 nm wavelength UV radiation as a source of stress, and 15 of these showed putative VLP groups in cytograms. The VLP groups generally had high side scatter and green fluorescence signals, suggesting that the putative viruses were either large icosahedral or filamentous viruses. This is in line with the work of Lohr *et al.* (2007), who found filamentous VLPs in *Symbiodinium* culture CCMP2465, and with previous reports of algal viruses, which often belong to the family *Phycodnaviridae*, members of which are large (100 – 200 nm diameter) icosahedral viruses (Van Etten *et al.*, 2002; Dunigan *et al.*, 2006). Interestingly, the *Symbiodinium* culture in which Lohr *et al.* (2007) found VLPs did not show a VLP group in cytograms in the present study, suggesting that variation in viral infections occurs among samples of the same culture. Subsequent TEM examination did reveal filamentous VLPs in this culture, though their absence from cytograms suggests they may be different viruses to those found by Lohr and co-workers. The presence of different, co-occurring viruses has been noted previously in the dinoflagellate *Heterocapsa circularisquama* (Tomaru and Nagasaki 2004, Tomaru *et al.* 2009), and the same phenomenon may be occurring here.

Of note, 42 of the 49 cultures showed declines in *Symbiodinium* population densities, while only 15 contained VLP groups in cytograms, suggesting that 27 of the cultures were undergoing cell lysis directly as a result of UV damage rather than induced viral infections. This result may in fact obscure the true number of virus-induced declines, as the nucleic acid stain used for flow cytometry (SYBR Green) preferentially stains large DNA-containing viruses (Brussaard *et al.*, 2000), meaning that RNA viruses may have been present but not

detected. Additionally, small viruses (such as those forming the crystalline arrays seen in electron micrographs of CCMP421 and PK13) may not have been detected by flow cytometry due to their small size and presumably low nucleic acid content. Therefore, the finding that ~30% of *Symbiodinium* cultures harboured potential latent viral infections may be an underestimate. Nevertheless, this is the first study to screen such a large number of *Symbiodinium* cultures, and the results suggest that many types harbour latent viral infections that can be induced to enter their lytic cycle by physiological stress to the host cell.

In addition to 254 nm wavelength irradiation, the more environmentally-relevant stressors of 302 nm wavelength radiation and increased temperature were used following initial latent virus screening. Thermal stress, while causing *Symbiodinium* population decline, failed to produce VLPs. This was somewhat surprising, as increased temperature has previously been shown to increase virus production in *Symbiodinium* cells (Wilson *et al.*, 2005a; Lohr *et al.*, 2007). In the current study only two levels of temperature stress were tested, and it may be that there is a fine line between the temperature required for viral induction and the temperature at which the *Symbiodinium* cell breaks down directly as a result of excess heat energy. The 302 nm wavelength UV radiation was more effective than elevated temperature, but less effective than 254 nm wavelength radiation at causing VLP production, with 50% (6 of 12) of cultures showing an increase in VLP abundance following UV exposure.

The putative viruses induced by UV stress (both 254 nm and 302 nm wavelength) generally followed a pattern of rapid increase over the first 24 – 48 h after UV exposure, followed by a) a continued increase over the study period; b) a plateau; or c) a reduction in density towards starting levels. These VLP population dynamics, and the corresponding population dynamics of the host *Symbiodinium* cells, closely resemble those seen in other algal viruses, such as *Emiliania huxleyi* virus 86 (Jacquet *et al.*, 2002; Evans *et al.*, 2007) and *Phaeocystis pouchetti* virus 1 (Malin *et al.*, 1998; Marie *et al.*, 1999), except for the lack of initial penetration and eclipse periods where few viruses are seen. This makes sense, as a latent viral infection can bypass the steps of adsorption, penetration and uncoating normally required before synthesis of new virions.

2.4.2. Electron microscopy

Transmission electron microscopy revealed the presence of VLPs inside cells of all but one of the *Symbiodinium* cultures examined. The observed VLPs were either icosahedral or filamentous/rod-shaped. In six of the cultures examined (CCMP421, CCMP828, CCMP2469, Ap1, FLAp1 and Mf13.14), more than one size or morphological type of VLP was seen inside cells. In CCMP421 and CCMP2469, icosahedral and filamentous VLPs were seen, while in CCMP828 there were at least two types of filamentous VLPs present in addition to icosahedral VLPs.

The filamentous VLPs, which made up the majority of VLPs seen here, resembled those previously seen in *Symbiodinium* cells (Lohr *et al.*, 2007). These authors noted that the putative viruses resembled members of the family *Closteroviridae*. Other viral families resembling the filamentous VLPs seen here include the *Flexiviridae* and *Potyviridae* (Fauquet *et al.*, 2005), both of which are comprised of plant-infecting RNA viruses. The shorter, more rod-like filamentous VLPs seen in CCMP828 resemble viruses of the genera *Tobamovirus*, *Tobravirus*, *Pecluvirus*, *Pomovirus* (all in the family *Virgaviridae*) and *Benyvirus* (unassigned family) (Fauquet *et al.*, 2005). All members of these genera are RNA viruses that infect plants.

The icosahedral VLPs seen in electron micrographs consisted of several size groups: ‘giant’ (200 – 500 nm diameter; seen in Ap1 and FLAp1), large (100 - 200 nm diameter; seen in CCMP2469, Ap1 and Mf13.14), small (50 - 100 nm diameter; seen in CCMP421, CCMP828 and Ap1) and crystalline arrays made up of hundreds of small VLPs (17 – 18 nm diameter, seen in CCMP421 and PK13). The giant viruses seen here appeared to be enveloped, and structurally resembled members of the *Paramyxoviridae* (Fauquet *et al.*, 2005), though they were more similar to the *Mimiviridae* in size (Claverie *et al.*, 2009). The large icosahedral VLPs resemble a range of viruses, including phycodnaviruses, which are common viruses of single-celled algae (Van Etten *et al.*, 2002; Kang *et al.*, 2005). The ~30 nm diameter VLPs seen in CCMP421 and CCMP828 are difficult to classify based on their appearance in the electron micrographs, as similar viruses are found in genera infecting plants, animals and prokaryotes. They do quite closely resemble *Heterosigma akashiwo* RNA virus, which infects a single-celled marine alga (Tai *et al.*, 2003; Lang *et al.*, 2004), however these tend to be seen in large numbers throughout the cell cytoplasm, not in small groups as seen here.

The crystalline arrays of small VLPs seen in CCMP421 and PK13 were particularly interesting. Many viruses form crystalline arrays, but based on their size, the particles seen here most closely resemble viruses in the families *Circoviridae* and *Nanoviridae*, DNA viruses that infect animals and plants, respectively (Fauquet *et al.*, 2005). Although circoviruses and nanoviruses have never been isolated from algae or marine organisms, recent studies have found *Circoviridae*- and *Nanoviridae*-like DNA sequences associated with *Symbiodinium* (Correa *et al.*, 2012) and corals (Vega Thurber *et al.*, 2008; Vega Thurber and Correa, 2011). Polymerase chain reaction primers targeting the *Circoviridae* and *Nanoviridae* were designed in the present study, but these failed to amplify DNA, despite extensive testing of different PCR protocols. This does not necessarily mean that the crystalline VLP arrays were not made up of circoviruses or nanoviruses; the very small genomes found in these viruses made designing effective PCR primers difficult, and it may be that the failure to amplify was due to unsuitable primers rather than a lack of target viruses.

Of the eleven cultures examined by TEM, four contained visible VLPs only after UV exposure (CCMP828, CCMP249, PK13 and Sin), while seven (CCMP421, CCMP2430, CCMP2465, Ap1, FLAp1, Mf13.14 and Mp) contained VLPs in both control and irradiated cells. Interestingly, several samples showed VLPs in electron micrographs, despite not producing VLP groups in cytograms during initial screening experiments. This is not entirely unexpected given that flow cytometry may miss some virus groups, as mentioned earlier. In the case of CCMP421 for example, VLPs were seen in micrographs of pre- and post-stress samples, but were only seen in cytograms of post-stress samples. The electron micrographs revealed the presence of very different VLPs pre- and post-stress, however, with the former only containing crystalline arrays of very small VLPs that may have been missed by the flow cytometry protocol used here. Similarly, in Ap1 and Mf13.14 the VLPs seen in samples post-exposure differed morphologically from those seen in control samples. While there was not such an obvious difference in VLP morphology or size in CCMP2465, FLAp1 or Mp, a similar phenomenon may be occurring with these cells (i.e. the putative viruses in control samples may be RNA viruses, or contain less nucleic acid than those seen in UV-irradiated samples). Furthermore, the fact that control samples were not undergoing cell lysis, and therefore not releasing large numbers of viruses, may explain the lack of a VLP group in

cytograms. It may be that many *Symbiodinium* cultures contain chronic productive viral infections, in addition to latent infections that can be induced by stress.

The lack of VLPs inside cells of CCMP2430 was surprising; however, the numerous VLPs seen outside of these cells may have produced the VLP population seen in cytograms. The presence of these VLPs in close proximity to cells suggests that the *Symbiodinium* cells were the hosts, but without observing them inside of cells it is not possible to confirm this.

More unusual was the fact that PK13 and Sin, which contained VLP groups in cytograms of control samples, did not show any VLPs in electron micrographs of non-UV exposed cells. These cultures, along with many others examined here, did show varying responses in terms of VLP and *Symbiodinium* population dynamics across the different sets of flow cytometry-based experiments, however. For example, PK13 contained a VLP population in both control and UV-irradiated samples in the initial screening experiments, but follow-up screening experiments and reinfection experiments produced a VLP group only in irradiated samples. As noted in section 2.4.1., there may be temporal variation in viral infection/production among samples of the same *Symbiodinium* culture, which may explain the inconsistency among experiments. The absence of these VLPs from electron micrographs may have also been a result of the TEM preparation process, which involved washing the cells, meaning most of the surrounding culture medium was removed. Thus, most VLPs that were released from cells (and that would have appeared in flow cytograms) would not have been observed in electron micrographs.

2.4.3. Molecular analysis

Several approaches were taken to confirm that the VLPs seen in cytograms and electron micrographs were viruses: single-virus isolation and whole genome amplification, PCR amplification and sequencing of putative viral DNA, and infection of healthy *Symbiodinium* cultures with filtrates containing the putative viruses.

Despite successful virus sorting, multiple displacement amplification (MDA) of a viral genome was unsuccessful. Multiple displacement amplification is a very sensitive technique, capable of amplifying genomic DNA from single eukaryotic and prokaryotic cells (Raghunathan *et al.*, 2005; Lasken, 2007; Yoon *et al.*, 2011; Stepanauskas, 2012). The

method has also been used successfully on single sorted viruses (Allen *et al.*, 2011), although it has more commonly been used with larger starting amounts of viral DNA (Kim *et al.*, 2008; Wang *et al.*, 2008; Ekström *et al.*, 2010). The failure to amplify viral DNA here was likely caused by one of two factors: an insufficient amount of starting DNA, or a lack of DNA entirely because the sorted particles were RNA viruses. Both are feasible, as the VLP group seen in cytograms suggested a small particle size and electron micrographs revealed VLPs that resembled RNA viruses.

Sequencing of partial ribonucleotide reductase genes isolated from CCMP421 and PK13 was successful. The sequences that were obtained fell among sequences from a range of other organisms, including bacteria, plants and animals, but showed low levels of identity to these sequences. The low levels of identity with nearest matches from the database suggest that the sequences obtained here were not derived from plants, animals or bacteria themselves, leaving open the possibility that they are instead viral in origin. There is a paucity of viral ribonucleotide reductase sequences in the Genbank database, which may explain why no close matches to viral sequences were seen.

Despite not providing identification of the putative viruses present in the *Symbiodinium* cultures as was hoped, the phylogenetic analysis provided some interesting results. Sequences obtained from both *Symbiodinium* cultures formed two branches each on the phylogenetic tree. For CCMP421, one branch contained closely-related sequences from control and UV-irradiated samples, and the other branch contained a sequence obtained from the UV-irradiated sample. These results agreed with the findings of the TEM examination, where crystalline VLP arrays were seen in both control and irradiated cells, but morphologically different VLPs were seen post-UV exposure. Combined with the results of flow cytometry analysis, these findings suggest that CCMP421 harbours a productive chronic viral infection that does not affect host population growth, but also contains a latent viral infection that, through environmental stress, can be induced to enter the lytic cycle and cause host cell death. An alternative interpretation of the results is that UV stress itself is causing cell death, and the induction of the latent infection is a by-product of this, with the latent virus utilising the host's cell machinery for virion production prior to complete cell breakdown. The latter interpretation still assumes the presence of an induced latent viral infection, however, which by its very nature would be capable of causing cell lysis if the UV stress had not done so directly.

Putative viral RR2 sequences from PK13 were only obtained following UV exposure. Again, this agreed with TEM examination, which only showed VLPs in cells following UV exposure, and suggests the presence of a latent infection. Sequences obtained from PK13 fell on two distinct branches. One sequence clustered closely with the sequence obtained from the irradiated CCMP421 sample, suggesting that very similar viruses were present in both cultures post-UV exposure. The other sequence was apparently not closely related to either the nearest BLAST matches or the other *Symbiodinium*-derived sequences. These results suggest that PK13 may harbour two latent infections, which can be induced *via* stress. Interestingly, only one morphological type of VLP was seen in cells of PK13, although the limited resolution of the electron microscope may have disguised the presence of two viruses with similar morphologies.

Perhaps most interestingly, the three sequences derived only from UV-irradiated samples all clustered with putative viral sequences obtained from tissues of *Porites australiensis* suffering from white patch syndrome, with sequence identities of up to 97%. This suggests that the sequences may be viral in origin, and also that *Symbiodinium* viruses may play a role in this coral disease. Whether the putative virus is the causative agent or is merely induced following the onset of disease remains to be determined (Chapter 5).

2.4.4. Conclusion

In this chapter it has been shown that a range of *Symbiodinium* types harbour what appear to be latent and chronic viral infections. In most cases the latent infections could be induced to enter the lytic cycle by exposure to UV radiation. Electron microscopy revealed the presence of VLPs inside cells, and several different morphologies were seen; the most common being filamentous VLPs, in agreement with a previous report of an inducible viral infection in *Symbiodinium* (Lohr *et al.*, 2007). Results of molecular analysis were ambiguous, though the similarity to sequences obtained from diseased corals, their low level of identity to the nearest database matches and their correspondence with the electron micrographs certainly suggest a viral origin. Unfortunately, infection of healthy cultures with the putative viruses was unsuccessful, and therefore it cannot be proven beyond doubt that the VLPs seen here do represent viruses. On balance, however, this does seem the most likely explanation for the observed results.

This is the first study to screen such a wide range of *Symbiodinium* cultures for latent viral infections, and the finding that many appear to contain such infections is interesting. Based on the results of this study alone, it is not possible to say whether the putative induced viral infections are responsible for cell death, or merely a by-product. Proving that these putative viruses are responsible would require infection of otherwise healthy host cells, which, as noted earlier, is often difficult to carry out successfully. Additionally, the wavelength of the UV light used here to induce putative viral infections does not represent conditions that *Symbiodinium* cells would experience in nature, as UV-C radiation does not reach the Earth's surface. Nevertheless, it has been shown here that these cells most likely harbour a latent viral infection, and such infections are generally inducible *via* some type of environmental stress, so their mere presence likely has biological and ecological consequences.

At a time when *Symbiodinium* and their coral hosts are increasingly threatened by disease (Bruno *et al.*, 2007; Lesser *et al.*, 2007; Bourne *et al.*, 2009) and bleaching events (Baker *et al.*, 2008; Miller *et al.*, 2009), the presence of inducible latent viruses in *Symbiodinium* cells presents another potential threat to consider. At the same time, however, these viruses may provide an explanation for some of the numerous coral diseases that currently have no causative agent assigned to them.

2.4.5. Future directions and study limitations

As noted above, infection of healthy cultures with UV-induced viruses was unsuccessful. This is an important step if it is to be proven that *Symbiodinium* cells do in fact harbour an inducible latent infection. Future work should include the use of different filter types, to avoid any loss of infectivity, and electron microscopic examination to determine whether or not infective viruses are being excluded from successful infection. A more detailed molecular analysis of these putative viruses would also be desirable. While the sequences presented here provide preliminary evidence of viral presence, the use of other, virus-specific PCR primers (for example, those targeting the DNA polymerase gene of phycodnaviruses (Short and Suttle 2002)) might allow more precise identification of the viruses and their potential roles in the health of their hosts. Whole genome amplification of single viruses would provide the most definitive answers to these questions, however this is an expensive procedure with a high risk of failure when used with such small target genomes, as was discovered in this study. Given

the potential importance of latent viral infections to *Symbiodinium* and coral health, further research is certainly warranted on this little-understood system.

Chapter 3: Transcriptomic evidence of viral infections in *Symbiodinium*

3.1. Introduction

The mutualism between scleractinian corals and their algal endosymbionts (dinoflagellates of the genus *Symbiodinium*) is one of the most important symbioses in the marine environment. By translocating the products of photosynthesis to their host, *Symbiodinium* cells, which can be present at densities of several million cells per square centimetre (Stimson *et al.*, 2002), provide the energy necessary for coral reef building and sustenance. This symbiosis, and the coral reef ecosystems it supports, are increasingly under threat, largely due to the increasing frequency and severity of coral bleaching events caused by the warming of the world's oceans (Hoegh-Guldberg *et al.*, 2007). In addition to the danger posed by temperature-induced bleaching, the coral-*Symbiodinium* symbiosis is under threat from an array of stressors including ocean acidification (Veron, 2011), sedimentation (Fabricius, 2005) and disease (Bourne *et al.*, 2009). The net effect of these various stressors will likely be less diverse coral ecosystems and loss of the calcium carbonate reef structures provided by scleractinian corals (Hoegh-Guldberg *et al.*, 2007).

Given the importance of coral reefs economically (Moberg and Folke, 1999) and ecologically (Knowlton, 2001), and their uncertain future, it is not surprising that substantial research has been conducted on corals and their various microbial associates (the most well-known being the aforementioned *Symbiodinium*, but also including numerous other eukaryotes and prokaryotes – the so-called coral holobiont (Rohwer *et al.*, 2002)). Two areas of research that have received considerable attention recently are the cellular mechanisms involved in establishment, maintenance and dysfunction (including bleaching) of the coral-*Symbiodinium* symbiosis (Davy *et al.*, 2012), and coral disease ecology, including the possible roles played by microbial associates of corals (Knowlton and Rohwer, 2003; Bourne *et al.*, 2009). Research into the coral-*Symbiodinium* symbiosis has already revealed a wealth of information, and has led to a better understanding of coral bleaching mechanisms (e.g. Weis (2008)). Similarly, our understanding of coral disease outbreaks has increased rapidly in recent years, with the causative agents of several coral diseases now known (e.g. Cooney *et al.* (2002); Patterson *et al.* (2002); Sussman *et al.* (2008)).

Despite the advances made thus far, research into coral diseases has been hindered somewhat by the sheer complexity of the coral holobiont, which makes identification of causative agents and processes difficult. One area in particular that has been largely overlooked until recently is the role that coral- and *Symbiodinium*-associated viruses may play in coral disease or dysfunction of the symbiosis. Several studies have provided evidence that viruses infect corals and *Symbiodinium* (reviewed in Vega Thurber and Correa, 2011). Whether or not these viruses play a role in coral disease remains to be proven; however a few studies have shown that *Symbiodinium* cells can harbour latent viral infections that are induced *via* stress (Wilson *et al.*, 2001; Wilson *et al.*, 2005a; Lohr *et al.*, 2007). The induction of viruses *via* heat or UV stress, as seen in these studies, suggests that viruses could play a role in coral disease, as these stressors have also been shown to influence coral disease outbreaks (Bruno *et al.*, 2007; Williams *et al.*, 2010) and bleaching events (Lesser and Farrell, 2004).

While metagenomics has been used to identify viruses associated with the coral holobiont (Vega Thurber *et al.*, 2008), identification of viruses specifically infecting *Symbiodinium* cells has mostly been limited to electron microscope analysis (with the notable exception of Correa *et al.* (2012), who identified two *Symbiodinium*-associated viruses using a metagenomics approach). Here I took a different approach, examining the newly-generated transcriptomes of three *Symbiodinium* cultures for the presence of virus-like sequences. This approach allows for the detection of latent viral genes without the need for specific gene markers or a sequenced *Symbiodinium* genome. The effect of stress on the expression levels of virus-like sequences in the transcriptomes of two of these *Symbiodinium* cultures is examined elsewhere (see Chapter 4). Here, transcriptomes from stressed and healthy cultures were combined to search for virus-like genes, and attempts were made to distinguish latent viral genes (i.e. those belonging to viruses currently infecting the algae) from virus-like genes resulting from ancient horizontal gene transfer events (i.e. genes which have been incorporated into the algal genome and are no longer active infections). This is a first step towards molecular identification of viruses in these cells, which is expanded upon in Chapter 4, where expression levels of virus-like and virus-related genes in control and stressed samples of these cultures are compared.

3.2. Materials and methods

3.2.1. *Symbiodinium* spp. culture selection and maintenance

Three *Symbiodinium* cultures were selected for transcriptomic analysis: CCMP421 (clade E, free-living), CCMP2430 (clade A, *Tridacna maxima* symbiont) and Mp (clade C, *Mastigias papua* symbiont). These cultures were chosen instead of coral-derived *Symbiodinium* cultures as they showed the strongest evidence of latent viral infections (see Chapter 2). The phylogenetic positions of these cultures can be found in Appendix D, Fig. D1. CCMP421 and CCMP2430 were obtained from the National Center for Marine algae and Microbiota (NCMA, East Boothbay, ME, USA), and Mp was obtained from the Davy Lab (Victoria University of Wellington, New Zealand). Cultures were grown in 1 L volumes of f/2 medium (Guillard, 1975) without addition of silica, and were maintained at 25 °C on a 12 h light: 12 h dark cycle at 80 $\mu\text{mol quanta m}^{-2} \text{ s}^{-1}$ (supplied by Duro-Test Vita-Lite full spectrum fluorescent tubes).

3.2.2. Experimental treatments

For CCMP2430 and Mp, 1 L of exponentially-growing cells from each culture was split among 5 sterile 200 mL Petri dishes and exposed for 2 min to 254 nm wavelength UV radiation from an inverted Apollo Instrumentation transilluminator placed 12 cm away. Approximately 200 mL ($\sim 10^7 - 10^8$ cells) were collected from each culture for immediate RNA extraction, and the remaining ~ 800 mL of each culture were transferred to a sterile culture flask and returned to normal growth conditions (see above). Control samples (also 1 L volume) were subjected to all steps except UV exposure, and a 200 mL control sample was collected from each culture for immediate RNA extraction. Further 200 mL samples were collected for RNA extractions from UV-exposed samples at time points corresponding to immediately before *Symbiodinium* population crash, and mid-crash (based on flow cytometry of UV-exposed samples; see Appendix D, Figs. D2 – D3). This corresponded to 24 h and 54 h post-exposure for CCMP2430, and 24 h and 66 h post-exposure for Mp. A control sample (i.e. not exposed to UV radiation) was also collected for RNA extraction 66 h post-treatment for Mp.

Because of difficulties with isolating sufficient high-quality RNA, *Symbiodinium* culture CCMP421 did not undergo stress experiments as above. For this culture, RNA was extracted as above from apparently healthy (unstressed), exponentially-growing cells only.

3.2.3. RNA extraction and sequencing

Prior to RNA extraction, all working areas were thoroughly cleaned and treated with RNaseZAP (Sigma-Aldrich, St. Louis, MO, USA) to prevent RNA degradation. *Symbiodinium* cells were pelleted by centrifugation at $10,000 \times g$ for 5 min at 4 °C, then resuspended in 1.5 mL sterile f/2 medium. Cells were again pelleted at $10,000 \times g$ for 5 min, supernatant was removed, and the pellet was resuspended in 500 μ L Trizol (Life Technologies, Carlsbad, CA, USA). Approximately 400 μ L of acid-washed 0.5 mm glass beads were added to the suspension, and cells were homogenised in a Vortex Genie 2 vortex mixer (Scientific Industries, Bohemia, NY, USA) for 8 min at 4 °C. Supernatant was then transferred to a fresh microcentrifuge tube, and a further 300 μ L Trizol were added to the bead/cell mix and vortexed for 30 s. Supernatant was again transferred to the second tube, and the process was repeated once more with 200 μ L Trizol. Bromochloropropane (100 μ L) was added to the Trizol/cell suspension and mixed by shaking for 15 s. The solution was then incubated for 3 min at RT, before centrifugation at $10,000 \times g$ for 15 min at RT. Supernatant was transferred to a fresh microcentrifuge tube and an equal volume of 100% ethanol was added and mixed, before transferring to an Absolutely RNA Microprep spin column (Agilent Technologies, Santa Clara, CA, USA). The remainder of the RNA preparation was carried out according to the manufacturer's instructions, except that twice the recommended volume of DNase solution was used, and RNA was eluted twice, with 100 μ L elution buffer used each time. Extracted RNA was quantified using a Qubit 2.0 fluorometer (Life Technologies, Carlsbad, CA, USA), and RNA quality was assessed using an Experion automated electrophoresis system (Bio-Rad, Hercules, CA, USA). RNA samples were again assessed for quality and quantity at the National Center for Genome Resources (NCGR, Santa Fe, NM, USA) using an Agilent 2100 Bioanalyzer (Agilent Technologies, Santa Clara, CA, USA) and a Qubit fluorometer. Complementary DNA (cDNA) libraries were made from 2 μ g RNA using a TruSeq™ RNA sample preparation kit (Illumina, San Diego, CA, USA). The average insert size ranged from 250 to 350 bp. Libraries were sequenced using an Illumina HiSeq 2000 sequencer to obtain 2×50 bp (paired-end) reads.

3.2.4. Assembly and mapping

Transcriptome assembly was carried out using NCGR's internal pipeline, Batch Parallel Assembly (BPA) version 1.0. SGA preprocess (Simpson and Durbin, 2012) was used to prepare reads for assembly. Reads with Q-scores < 15 or that were < 25 nucleotides long after trimming were discarded. Sequence reads were assembled into contigs and paired-end scaffolds using ABySS v1.3.0 (Simpson *et al.*, 2009). Gaps created during the scaffolding process were closed using Gap Closer version 1.10, part of the SOAPdenovo sequence assembly package (Li *et al.*, 2008). Contigs were combined, and miraEST (Chevreux *et al.*, 2004) was used to identify overlaps (minimum 100 bp) between the contigs and assemble larger contigs, while collapsing redundancies. Sequence reads were aligned to the contigs using BWA (Li and Durbin, 2009). Alignments were processed by SAMtools mpileup (<http://samtools.sourceforge.net>) to generate consensus nucleotide calls at positions where bases were introduced by miraEST. In an attempt to remove incomplete sequences, only contigs > 150 nt in length were included in the final contig set. Coding sequences (CDSs) were predicted using ESTScan (Iseli *et al.*, 1999; Lottaz *et al.*, 2003) with a Bacillariophyta scoring matrix, and sequence reads were aligned back to the predicted coding sequences using BWA (Li and Durbin, 2009).

Transcriptome sequences, assemblies and annotations will be made publicly available through the Community Cyberinfrastructure for Advanced Microbial Ecology Research and Analysis (CAMERA; <http://camera.calit2.net>) in the near future.

3.2.5. Sequence homology and phylogenetic analyses

Transcriptomes that came from the same *Symbiodinium* culture were pooled, in order to maximise the number of expressed genes per culture. Predicted CDSs from the three *Symbiodinium* cultures were searched against the NCBI non-redundant protein database with a maximum e-value of 10^{-6} , and were annotated using the program Blast2GO (Conesa and Götz, 2008; Götz *et al.*, 2008). Sequences with nearest BLAST matches belonging to viruses were clustered into groups of unigenes with a minimum sequence identity of 90% using CDHIT (Li *et al.*, 2001, 2002). BLAST searches were then carried out using these putative viral unigenes as query sequences, and three *Symbiodinium* EST libraries as reference

databases. Two of the EST libraries, consisting of *Symbiodinium* cultures CassKb8 (clade A) and Mf1.05b (clade B) (Bayer *et al.*, 2012) were downloaded from <http://medinalab.org/zoox/> and used for local BLAST searches with the software Geneious version 6.1.5 (Biomatters, Auckland, New Zealand). Searches against the third EST library (*Symbiodinium* type C3; available through the SymBioSys database at <http://sequoia.ucmerced.edu/SymBioSys/>) were conducted using virus-like sequences that were found in at least two other *Symbiodinium* cultures as query sequences, utilising the BLAST search function provided with the Systems Biology of Symbiosis database (<http://sequoia.ucmerced.edu/SymBioSys/>). Sequences from the EST libraries that showed > 90% pair-wise identity to the putative viral unigenes from the transcriptomes were then searched against the NCBI non-redundant protein database to ensure that they shared the same nearest BLAST match as the putative viral sequences. Open reading frames (ORFs) in the putative viral sequences from CassKb8 and Mf1.05b were translated using BioEdit version 7.2.0 (Hall, 1999), and were aligned with the protein sequences of the viral unigenes from the three *Symbiodinium* transcriptomes and their significant BLAST matches using ClustalW with a BLOSUM cost matrix. Phylogenetic trees were created using PHYL, within the software package Geneious version 6.1.5 (Biomatters, Auckland, New Zealand), with the LG substitution model and bootstrap analysis of 100 replicates.

3.3. Results

3.3.1. Sequencing, assembly and annotation

Illumina sequencing was successful for all samples, resulting in over 2 Gb (2×10^9 base pairs) of sequence data for each sample. Contiguous sequences were assembled using ABySS (Simpson *et al.*, 2009), with 39,000 – 78,000 contigs identified in each sample. Coding sequence prediction using ESTScan (Iseli *et al.*, 1999) led to the designation of 30,000 – 72,000 CDSs per sample. Pooling and clustering of predicted protein sequences using CDHIT (Li *et al.*, 2001, 2002) led to the identification of 64,101 unigenes in CCMP421, 58,094 in CCMP2430, and 63,727 in Mp. Approximately 40 – 46% of CDSs had significant (e-value < 10^{-6}) BLAST hits in each sample, and 30 – 35% could be assigned gene ontology (GO) annotations (The Gene Ontology Consortium, 2000).

3.3.2. Virus-like gene identification

With the exception of one sequence, with a nearest BLAST match from a single-stranded RNA (ssRNA) virus, all of the nearest viral BLAST matches belonged to the double-stranded DNA (dsDNA) viruses. Sequences obtained in this study that matched most closely with dinoflagellate viral nucleoproteins (DVNPs), which are found in dinoflagellates and phycodnaviruses (Gornik *et al.*, 2012) were excluded from analysis. Dinoflagellate viral nucleoproteins are a normal component of dinoflagellate genomes, and it was not possible to distinguish these from true viral sequences. The majority of the remaining viral BLAST matches belonged to the *Phycodnaviridae* and *Mimiviridae* families (Fig. 3.1). The number of unigenes corresponding to each viral family was similar in CCMP421 and CCMP2430, while in Mp there was a notable increase in sequences with nearest BLAST matches belonging to the *Mimiviridae* (73 unigenes, compared to 20 in both CCMP421 and CCMP2430). The number of unigenes in each transcriptome corresponding to each viral BLAST hit can be found in Appendix D, Tables D1 – D3. Despite significant e-values, BLAST hits generally showed low levels of sequence identity and query sequence coverage. There was little overlap of putative viral genes among samples; only 26 putative viral unigenes were found in more than one transcriptome or EST library (Appendix D, Table D4).

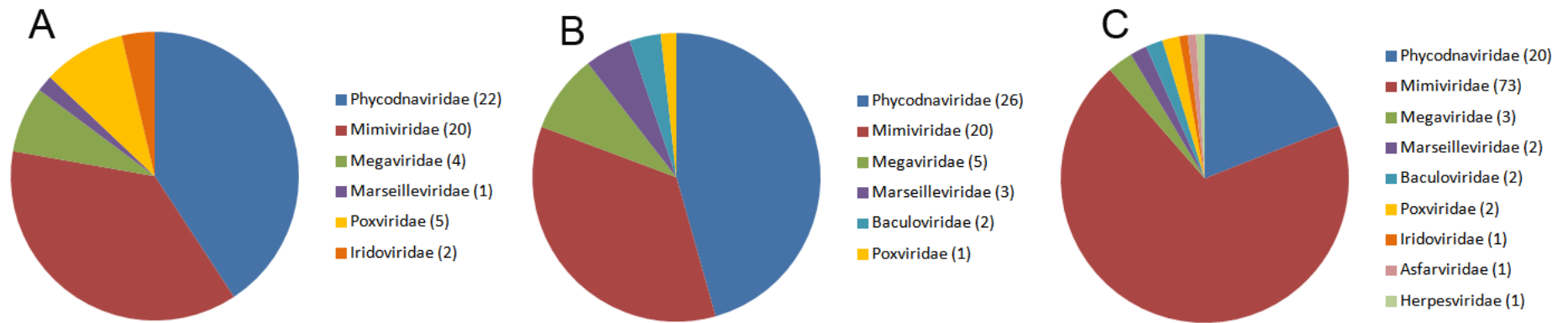


Figure 3.1. Total numbers of unigenes with nearest BLAST matches belonging to dsDNA viruses in each transcriptome. A: CCMP421, B: CCMP2430, C: Mp. Unique CDSs were determined using a cutoff of < 99% pairwise sequence identity.

3.3.3. Virus-like genes conserved in *Symbiodinium* spp.

Putative viral genes found in three or more *Symbiodinium* cultures (referred to hereafter as ‘conserved genes’) are shown in Table 3.1. Four of these conserved genes appear to belong to the *Phycodnaviridae* (a family of dsDNA viruses infecting microalgae), one appears to be a member of the *Mimiviridae* (large dsDNA viruses which generally infect amoebae), and one matched most closely with a gene from a Megavirus (large, amoeba-infecting viruses, similar to the *Mimiviridae*). The nearest BLAST matches encode helicases, aminotransferases, protein kinases and membrane- and plastid-associated proteins. Interestingly, none of the conserved viral genes were found in either of the clade C *Symbiodinium* cultures (though several putative viral genes were shared between Mp (clade C) and one other culture – see Appendix D, Table D4). All six conserved genes were present in the two clade A cultures (CCMP2430 and CassKB8), and five were also present in the clade E culture (CCMP421). Phylogenetic relationships of the six conserved genes to the nearest BLAST matches are shown in Figs. 3.2 – 3.7. The putative viral sequences clustered together in all trees, forming distinct sister groups to other taxa. In all cases, the sister groups of the putative *Symbiodinium* viral sequences contained prokaryotic and/or eukaryotic sequences in addition to viral sequences, preventing definitive confirmation of the sequences’ viral origin. The sister groups of two of the putative viral genes, however, were dominated by viral sequences (Figs. 3.4 and 3.5).

To examine the possibility that the conserved genes represented ancient horizontal gene transfer events rather than latent viral infections, the conserved genes were searched against 13 genomes and transcriptomes of chromalveolates ancestral to *Symbiodinium*. Given that the genes were expressed, and therefore presumably functional, one might expect to find very similar genes in ancestors of *Symbiodinium* if the genes were the result of ancient transfer events. Using a minimum pair-wise identity value of 90% and a maximum e-value of 10^{-6} , no sequences matching the conserved viral genes were found. Chromalveolate species used are found in Appendix D, Fig. D4.

Table 3.1. Virus-like genes present in 3 or more *Symbiodinium* cultures. BLAST matches and accession numbers belong to the most significant hit (i.e. the lowest e-value).

Predicted gene	BLAST match	BLAST accession number	CCMP421 (Clade E)	CCMP2430 (Clade A)	Mp (Clade C)	CassKB8 (Clade A)	Mf1.05b (Clade B)
helicase	<i>Emiliana huxleyi</i> virus 202	AET42504	✓	✓		✓	
putative membrane protein	<i>Emiliana huxleyi</i> virus 86	YP_002296197	✓	✓		✓	
aminotransferase/ dehydratase	<i>Ostreococcus tauri</i> virus RT-2011	AFC34947	✓	✓		✓	✓
mimivirus encoded protein	<i>Acanthamoeba castellanii</i> str. Neff	ELR14641	✓	✓		✓	
hypothetical protein	<i>Micromonas pusilla</i> virus 12T	YP_007676259		✓		✓	✓
serine/threonine protein kinase	Megavirus Courdo11	AFX93119	✓	✓		✓	

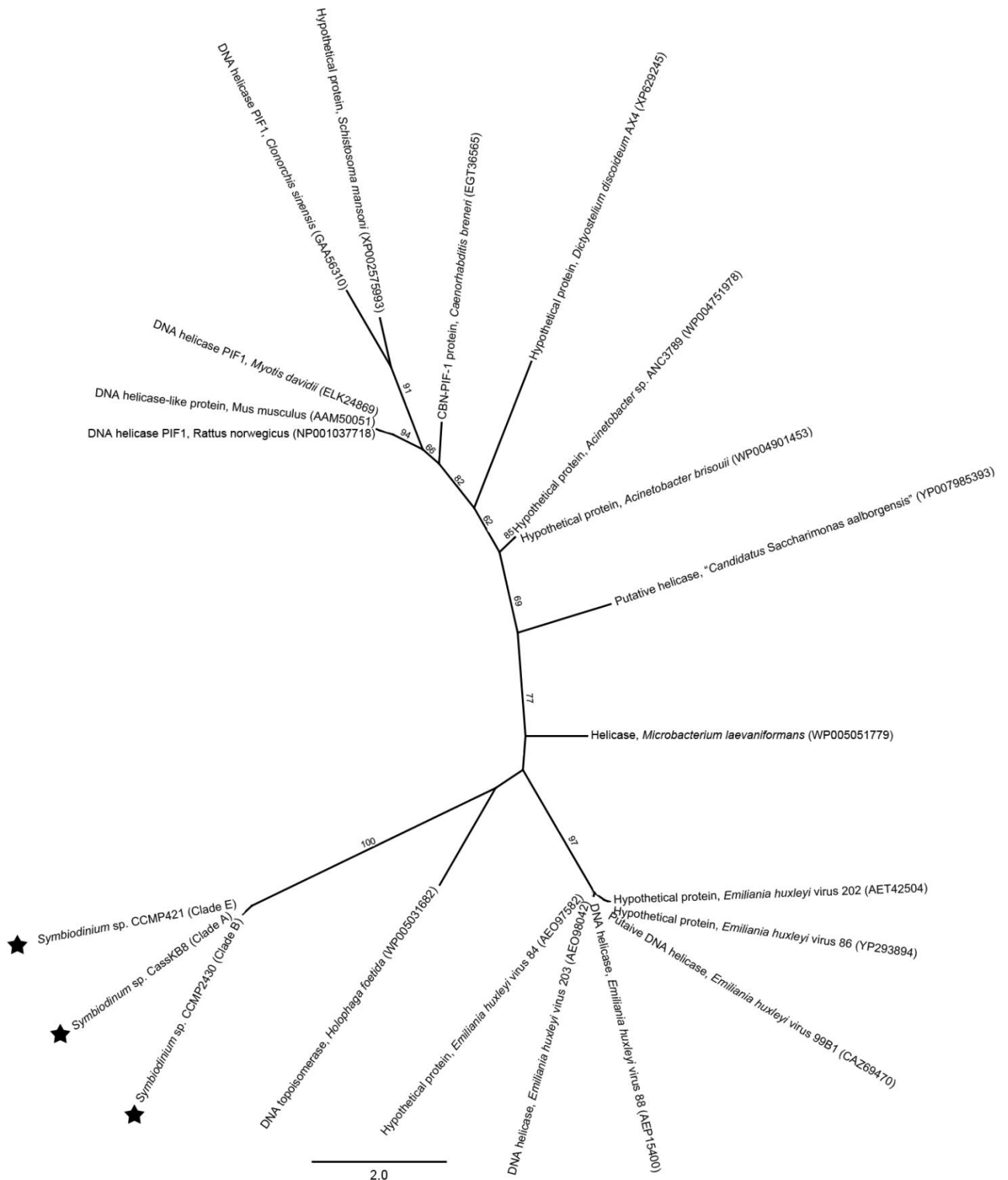


Figure 3.2. Unrooted maximum likelihood tree of helicase-like protein sequences from three *Symbiodinium* cultures and nearest BLAST matches. Branch numbers represent bootstrap support (100 replicates); bootstrap values < 50 are not shown. Stars indicate protein sequences obtained in the present study. Scale bar represents number of nucleotide substitutions per site.

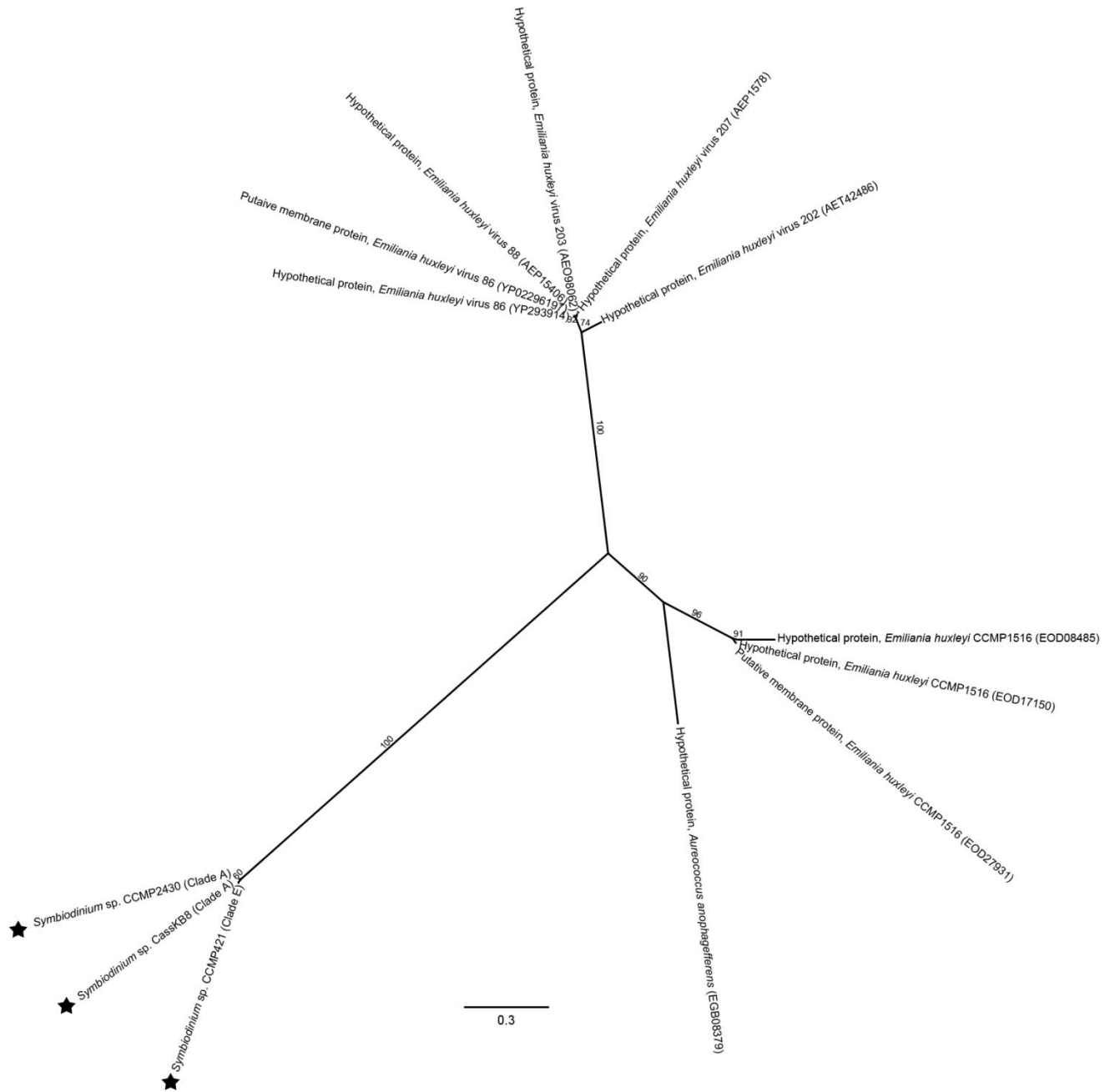


Figure 3.3. Unrooted maximum likelihood tree of *Phycodnaviridae*-like protein sequences from three *Symbiodinium* cultures and nearest BLAST matches. Branch numbers represent bootstrap support (100 replicates); bootstrap values < 50 are not shown. Stars indicate protein sequences obtained in the present study. Scale bar represents number of nucleotide substitutions per site.

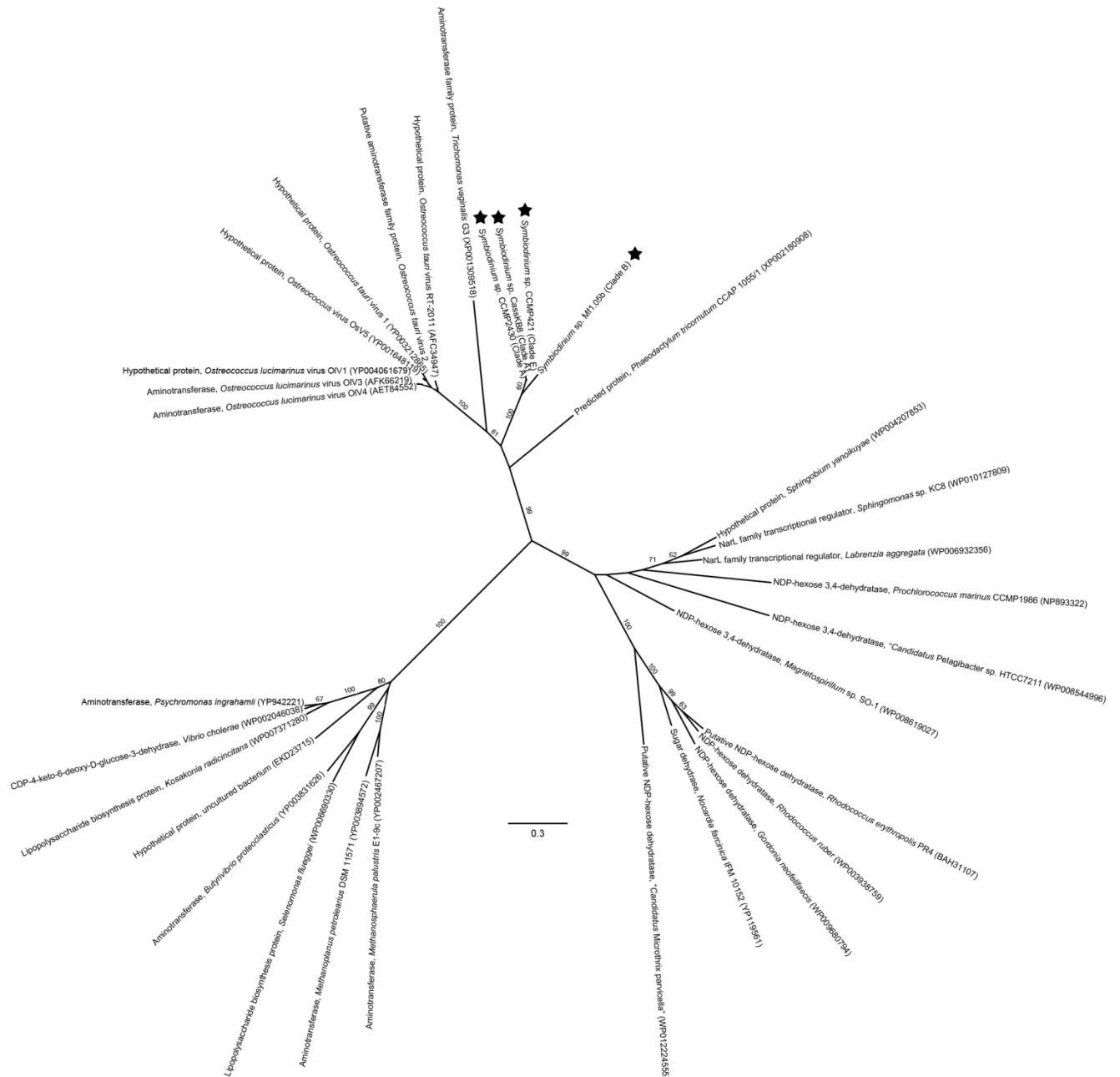


Figure 3.4. Unrooted maximum likelihood tree of aminotransferase/dehydratase-like protein sequences from four *Symbiodinium* cultures and nearest BLAST matches. Branch numbers represent bootstrap support (100 replicates); bootstrap values < 50 are not shown. Stars indicate protein sequences obtained in the present study. Scale bar represents number of nucleotide substitutions per site.

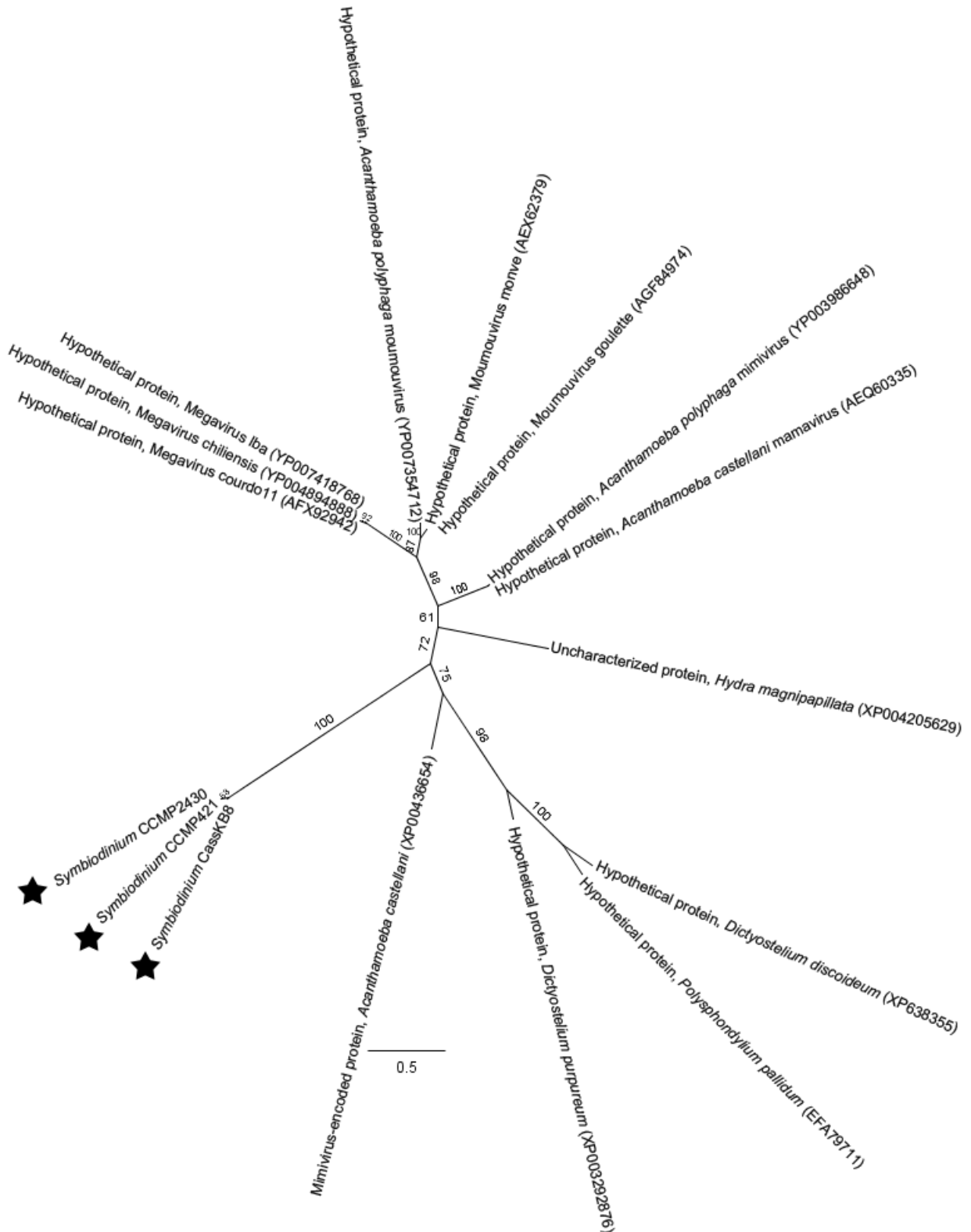


Figure 3.5. Unrooted maximum likelihood tree of *Mimiviridae*-like protein sequences from three *Symbiodinium* cultures and nearest BLAST matches. Branch numbers represent bootstrap support (100 replicates); bootstrap values < 50 are not shown. Stars indicate protein sequences obtained in the present study. Scale bar represents number of nucleotide substitutions per site.

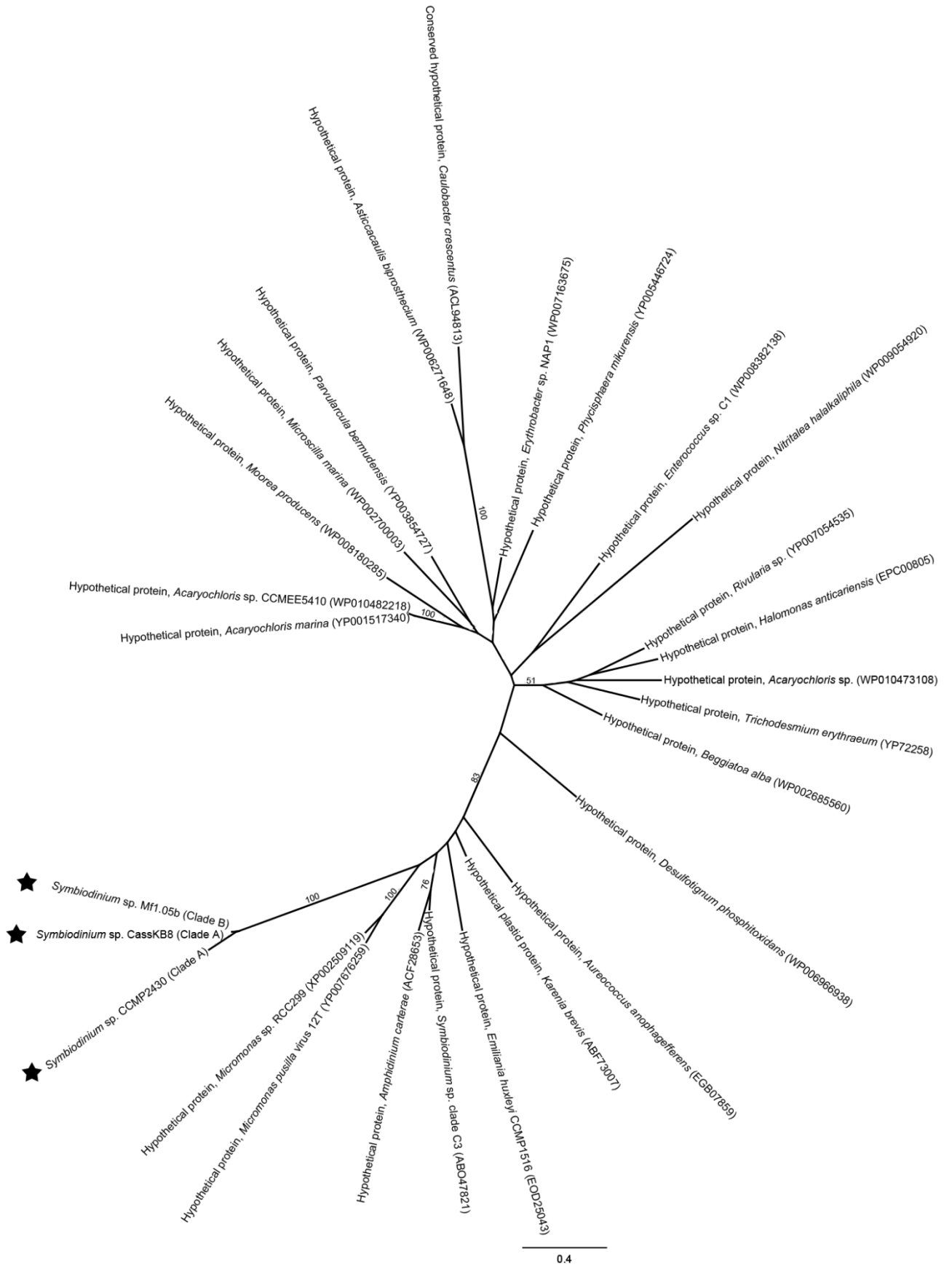


Figure 3.6 (previous page). Unrooted maximum likelihood tree of *Phycodnaviridae*/alga-like protein sequences from three *Symbiodinium* cultures and nearest BLAST matches. Branch numbers represent bootstrap support (100 replicates); bootstrap values < 50 are not shown. Stars indicate protein sequences obtained in the present study. Scale bar represents number of nucleotide substitutions per site.

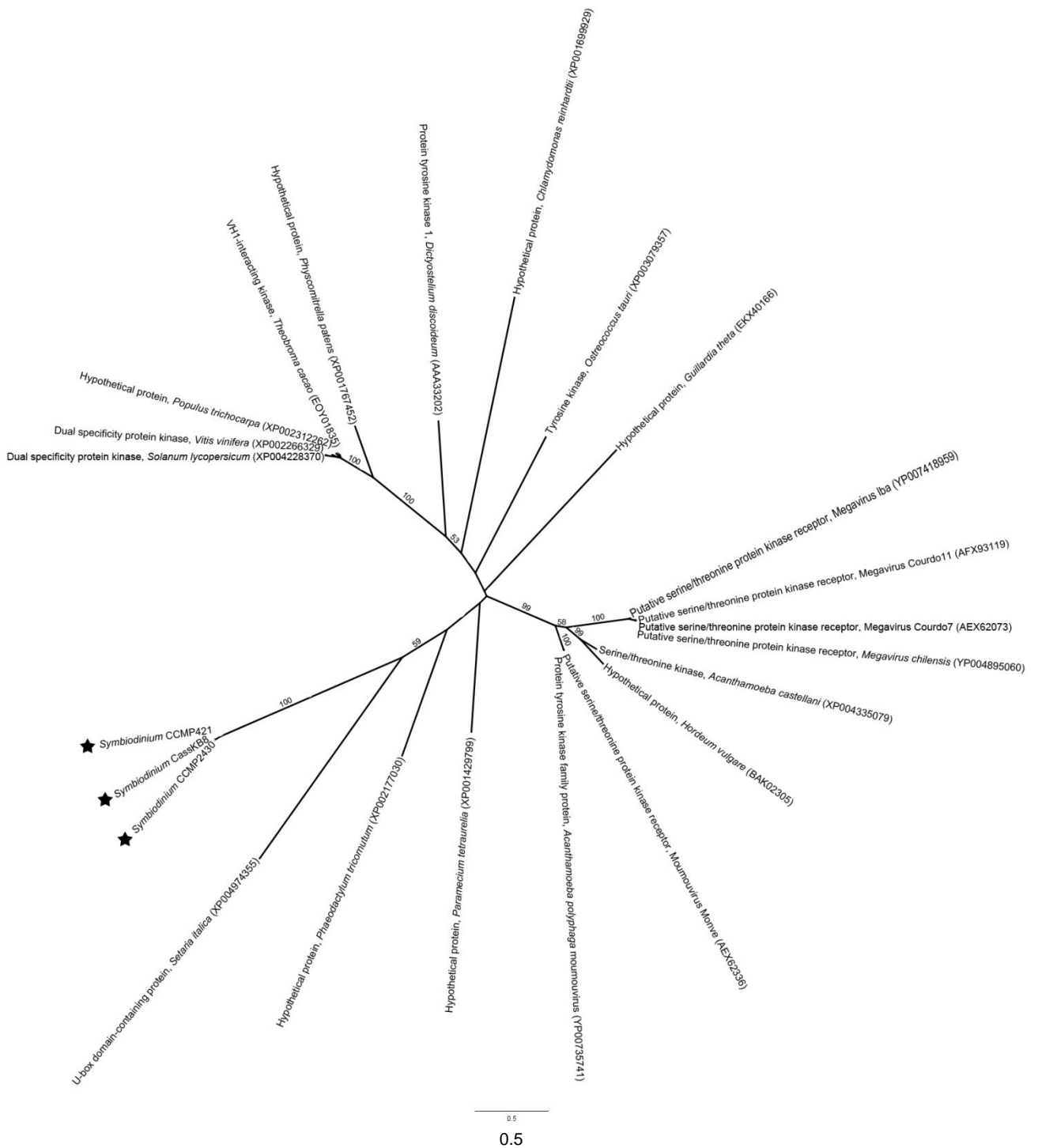


Figure 3.7. Unrooted maximum likelihood tree of protein kinase-like protein sequences from three *Symbiodinium* cultures and nearest BLAST matches. Branch numbers represent bootstrap support (100 replicates); bootstrap values < 50 are not shown. Stars indicate protein sequences obtained in the present study. . Scale bar represents number of nucleotide substitutions per site.

3.4. Discussion

This study utilised transcriptome sequencing to identify viral genes in several cultures of *Symbiodinium*. All of the *Symbiodinium* cultures examined contained virus-like gene sequences, and, with a single exception, these sequences appeared to belong to dsDNA viruses. Comparisons with existing *Symbiodinium* EST libraries and chromalveolate genomes revealed that six of the putative viral genes were present in three or more *Symbiodinium* cultures, yet none were found in the closely-related chromalveolates. Together, these results suggest the presence of common, closely-related viruses which infect *Symbiodinium*. Whether or not these viruses infect other dinoflagellates is unknown – currently no dinoflagellate genome exists, and while searches of a dinoflagellate (*Alexandrium tamarense*) transcriptome returned no matching sequences, this may have simply reflected a lack of genome coverage in the transcriptome. The lack of similar sequences in any of the eleven genomes and two transcriptomes of chromalveolates that were searched does lend support, however, to the notion that these putative viral genes represent current viral infections of *Symbiodinium* rather than ancient horizontal gene transfer (HGT) events. Furthermore, the fact that these genes were being transcribed into mRNA implies that they are functional.

It is highly unlikely that the conserved viral genes came from free viruses in the *Symbiodinium* cultures, as the RNA preparation method used for Illumina sequencing included a poly-A selection step that removed non-polyadenylated transcripts. The sequences obtained here therefore belong to *Symbiodinium* or to viruses infecting the *Symbiodinium* cell and using its transcriptional machinery. Combined with the fact that all of the conserved viral genes were found in at least one non-stressed, apparently healthy *Symbiodinium* sample, these results suggest the presence of latent or chronic viral infections, rather than new infections from free viruses.

In a chronic infection, viruses replicate at a steady rate within the cell, and are periodically released without host cell death (Fuhrman, 1999). Latent infections can take two forms: proviral and episomal. In a proviral infection, virus DNA is incorporated into the host genome and replicated along with the genome during cell division. Episomal latency, on the other hand, refers to infections where the viral genome does not enter the host genome;

rather, it forms an episome – a circular DNA molecule – in the nucleus or cytoplasm, as seen in the herpesviruses (Minarovits, 2006).

Based solely on the evidence of the present study, it is not possible to state which type of replication strategy these viruses are employing, but given that the viral genes were expressed in apparently healthy cells, proviral latency seems unlikely. Episomal latency, on the other hand, is a possibility. The Epstein-Barr virus (EBV) – a member of the *Herpesviridae* that forms episomal latent infections – for example, expresses several genes during its latent phase (Calderwood *et al.*, 2007), including several membrane proteins (Longnecker and Kieff, 1990). Furthermore, as episomal viral genomes are not automatically replicated by the host, as in proviral infections, virus replication-associated genes (such as the helicase found here) are expressed during host cell division. Latency has not often been observed in members of the *Phycodnaviridae* or *Mimiviridae*, the two virus groups most closely related to the conserved viral genes. There is, however, at least one report of a member of the *Phycodnaviridae* forming a provirus in the genome of a brown alga (Delaroque *et al.*, 1999). Similarly, while not observed often, probable chronic viral infections of the phycodnaviruses *Ostreococcus tauri* virus 5 (OtV-5) (Thomas *et al.*, 2011a) and *Micromonas pusilla* virus (MpV) (Waters and Chan, 1982) have been documented. These putative chronic infections are particularly interesting, as the nearest BLAST matches of two of the conserved viral genes found in the present study belonged to an OtV and an MpV.

The low levels of sequence identity seen between the conserved viral genes and their nearest BLAST matches make precise identification difficult. The results do agree, however, with previous reports of viruses infecting *Symbiodinium* (Correa *et al.*, 2012) and other dinoflagellates (Tarutani *et al.*, 2001), both of which found dsDNA viruses infecting these algae.

It is likely that the number of conserved viral genes in *Symbiodinium* was underestimated in the present study, for several reasons. First, genes that were not being expressed at the time of sampling are not represented in the transcriptomes. Second, less than half of the predicted coding regions in the transcriptomes had significant BLAST matches, meaning that more than half were unidentifiable. Finally, horizontal gene transfer from host to virus may occur frequently in algal viruses (Derelle *et al.*, 2008), potentially leading to viral genes that closely resembled algal genes and were therefore overlooked. Nonetheless, this study has identified

several putatively conserved viral genes in *Symbiodinium*, providing further evidence that these algae are commonly infected with dsDNA viruses similar to those seen in other marine algae

Chapter 4: Expression of virus and virus-related genes in response to stress in *Symbiodinium*

4.1. Introduction

Dinoflagellates of the genus *Symbiodinium* form symbioses with a range of animals and protists, including sponges (Carlos *et al.*, 1999), molluscs (Belda-Baillie *et al.*, 1999; Ishikura *et al.*, 1999; Baillie *et al.*, 2000), flatworms (Trench and Winsor, 1987), foraminiferans (Langer and Lipps, 1995; Pochon and Pawlowski, 2006; Pochon *et al.*, 2007) and ciliates (Lobban, 2002; Lobban *et al.*, 2002). The most well known of these symbioses, however, are those involving cnidarian hosts (corals, anemones and jellyfish). In the case of scleractinian corals, this symbiotic relationship is the cornerstone upon which the entire coral reef ecosystem is built.

The relationship between *Symbiodinium* and their hosts is a mutualism, where the hosts receive translocated photosynthate (e.g. glycerol and sugars) from the algal cells (Muscatine, 1967; Muscatine *et al.*, 1984; Streamer *et al.*, 1988; McCloskey *et al.*, 1994), which in return receive inorganic nutrients, such as nitrogen and phosphorus, from host cells (Muscatine and Pool, 1979; Trench, 1987; Belda *et al.*, 1993). In addition, the symbionts are provided with a relatively safe and stable position in the photic zone of the ocean (Davy *et al.*, 2012). In many cases, the algal symbionts have the potential to satisfy most or all of the host's daily carbon demand (Davies, 1984; McCloskey *et al.*, 1994; Venn *et al.*, 2008). Accordingly, the loss of *Symbiodinium* cells from the host, as occurs in the well-known phenomenon of coral bleaching, can have severely detrimental effects; in cases of coral bleaching the host may die if the symbiosis is not re-established sufficiently quickly (Hoegh-Guldberg, 1999; Weis, 2008). Similar bleaching-induced death has been observed in jellyfish (Dawson *et al.*, 2001) and anemones (Hill and Scott, 2012).

The primary driver of bleaching is thermal stress, which causes production of reactive oxygen species (ROS) in symbiont and host cells (Lesser, 2006; Weis *et al.*, 2008), leading to damage of photosynthetic and mitochondrial membranes and subsequent breakdown of the symbiosis (Weis *et al.*, 2008). With mean global sea surface temperatures predicted to rise by

~0.6 – 4 °C by the end of the century (IPCC, 2007b), bleaching events are expected to increase in frequency, especially for scleractinian corals, many of which already live at temperatures very near the upper threshold beyond which bleaching occurs (Baker *et al.*, 2008). In addition to thermal stress, other environmental stresses, including ultra-violet (UV) radiation (Banaszak and Lesser, 2009) and bacterial infection (Kushmaro *et al.*, 1996; Kushmaro *et al.*, 1998) can cause or exacerbate coral bleaching.

Climate change also plays a role in coral disease prevalence, with higher seawater temperatures linked to disease outbreaks, either in conjunction with, or independent of bleaching events (Harvell *et al.*, 2002; Rosenberg *et al.*, 2007). There are currently at least 20 recognised coral diseases, affecting both coral and *Symbiodinium* cells (Bourne *et al.*, 2009; Aeby *et al.*, 2010; Sudek *et al.*, 2012b), many of which do not have positively identified causative agents. Known causative agents include bacteria (Rosenberg *et al.*, 2007; Bourne *et al.*, 2009), ciliates (Antonius and Lipscomb, 2001), trematodes (Aeby, 2007) and fungi (Rosenberg *et al.*, 2007). Preliminary evidence suggests that viruses may also play a role in coral disease (Davy *et al.*, 2006). Virus-like particles (VLPs) have also been observed in isolated *Symbiodinium* cells, and there is evidence that *Symbiodinium* cells harbour latent viral infections that can be induced, *via* stress, to enter the lytic cycle (Wilson *et al.*, 2001; Lohr *et al.*, 2007). Electron microscopy has revealed VLPs with varying morphologies in *Symbiodinium* cells (Wilson *et al.*, 2001; Davy *et al.*, 2006; Lohr *et al.*, 2007), but their identities remain unknown. Likewise, whether or not these putative viral infections can lead to dysfunction of the host-*Symbiodinium* relationship, or to disease in the host, remains to be seen.

In the current study, transcriptomes obtained from healthy and stressed *Symbiodinium* cells were used to search for evidence of viral infection. *Symbiodinium* have large genomes, though they are thought to be among the smallest of the dinoflagellates, which have estimated genome sizes of 2 – 200 gigabases (Gb) (LaJeunesse *et al.*, 2005) and 40,000 – 90,000 protein-coding genes (Hou and Lin, 2009). For comparison, the human genome is ~2.9 Gb in size and contains around 20,000 protein-coding genes (International Human Genome Sequencing Consortium, 2004; Pennisi, 2012). Despite their ecological importance, no complete genome sequence exists for *Symbiodinium* or any other dinoflagellate. The use of RNA-seq to generate complete transcriptomes can therefore provide useful insights into *Symbiodinium* genome composition, and show the response of the cells to stimuli such as

environmental stress or infection. Here I used this approach to determine the response of *Symbiodinium* cells to stress and to search for evidence of latent viral infections induced by this stress. The presence of latent or induced viral infections can be detected either through direct identification of viral sequences within the transcriptome (Schuster *et al.*, 1986; Chandriani *et al.*, 2010; Liu *et al.*, 2011), or through expression of host genes in response to viral infection and replication (Ortmann *et al.*, 2008; Yang *et al.*, 2010; Lu *et al.*, 2012). This marker-free approach is particularly useful when working with viruses, which lack conserved genetic elements and can therefore be difficult to detect by more conventional molecular means. This chapter builds on the results of Chapter 3, where virus-like genes were identified and analysed phylogenetically. The current study examines the expression levels of virus-like genes and *Symbiodinium* genes associated with viral infection, in an attempt to characterise latent viral infections in these algae.

4.2. Materials and methods

4.2.1. *Symbiodinium* culture selection and experimental treatments

Two *Symbiodinium* cultures that had already undergone transcriptome sequencing (see Chapter 3) were selected for this study: CCMP2430 (Clade A) and Mp (Clade C). Experimental treatments are described in Chapter 3. Briefly, exponentially-growing cells were subjected to stress in the form of 254 nm wavelength UV radiation, and RNA was extracted from control cells (pre-stress), cells harvested 24 h post-stress, and cells harvested either 54 h (CCMP2430) or 66 h (Mp) post-stress. For Mp, an additional control (unstressed) sample was collected 66 h after collection of the pre-stress control sample.

RNA extraction, sequencing and assembly methods are described in Chapter 3.

4.2.2. Bioinformatic analysis

Protein sequences were searched against the NCBI non-redundant protein database using the program Blast2GO (Conesa and Götz, 2008; Götz *et al.*, 2008), with a maximum e-value of 10^{-6} . Blast2GO was also used to obtain Gene Ontology (GO; The Gene Ontology

Consortium, 2000) and InterPro (Hunter *et al.*, 2012) annotations. Gene Ontology groupings were obtained using WEGO (Ye *et al.*, 2006). Redundant sequences were removed from the set of predicted protein sequences using CD-HIT (Li *et al.*, 2001, 2002), with a sequence similarity threshold of 95%. Eukaryotic Orthologous Groups (KOG) annotations of the resulting unigenes were acquired using WebMGA (Wu *et al.*, 2011). Differential expression of unigenes and GO terms among samples was assessed by comparing transcript per million (TPM; Wagner *et al.*, 2012) values of unique reads, with a detection limit of > 1 TPM. Identification of unigenes in the transcriptomes was based on the results of BLASTP searches of the NCBI non-redundant protein sequence database using Blast2GO. Putative viral genes were identified based on their most significant BLAST matches. In each transcriptome, putative viral sequences showing $> 90\%$ similarity were clustered into unigenes, using CDHIT (Li *et al.*, 2001, 2002).

4.3. Results

4.3.1. Sequencing, assembly and annotation

Illumina sequencing was successfully carried out on all samples, resulting in over 2 Gb (2×10^9 base pairs) of sequence data for each sample. Contiguous sequences were assembled using ABySS (Simpson *et al.*, 2009), with 35,000 – 48,000 contigs identified for each sample (Table 4.1). Comparison of contig length with number of mapped reads revealed no apparent bias toward longer sequences in read mapping (Appendix E, Fig. E1). Contig lengths ranged from 150 bp (the cutoff value used here) to $> 25,000$ bp, while the number of mapped reads in some cases was $> 200,000$ per contig (Appendix E, Fig. E1). Coding sequence prediction using ESTScan (Iseli *et al.*, 1999) led to the designation of 30,000 – 44,000 coding sequences (CDSs) in each sample. Peptide prediction based on the assembled contigs led to similar numbers of defined proteins. Approximately 40 – 46% of protein sequences from each sample had significant ($e\text{-value} < 10^{-6}$) BLAST matches in the NCBI non-redundant protein database. Around 30% of all proteins could be annotated with GO (The Gene Ontology Consortium, 2000) and Interpro (Hunter *et al.*, 2012) terms, and $\sim 10\%$ could be assigned to Kyoto Encyclopedia of Genes and Genomes (KEGG) pathways (Kanehisa *et al.*, 2006).

(Table 4.1). Clustering of predicted protein sequences resulted in ~27,000 – 39,000 non-redundant unigenes per sample.

Table 4.1. Sequence assembly and annotation statistics. ^a 50% of the assembly is made up of contigs \geq this length. ^b Percentage of contigs $> 1,000$ bp in length. ^c Percentage of contigs $> 2,000$ bp in length. * The data in these rows were derived from all transcripts (not only the non-redundant unigene set). ** The data in this row were derived from the non-redundant unigene set (sequences were clustered at a threshold of 95% similarity).

	CCMP2430 T0	CCMP2430 T24	CCMP2430 T54	Mp T0	Mp T24	Mp T66	Mp T66 Control
ASSEMBLY							
No. of contigs	47,752	40,140	39,104	47,710	37,758	35,273	40,531
Mean contig length (bp)	1,123	894	868	1,129	777	805	1,009
N50 (bp) ^a	1,551	1,187	1,163	1,551	1,129	1,123	1,355
B1000 ^b	74.2%	61.9%	60.2%	73.5%	57.0%	58.3%	70.5%
B2000 ^c	33.2%	14.4%	13.6%	32.2%	15.2%	11.4%	20.2%
ANNOTATION							
No. of predicted CDSs	43,410	35,883	34,654	43,608	30,732	29,544	36,476
No. of predicted proteins	44,145	36,618	33,345	44,283	31,591	30,274	37,041
No. of non- redundant unigenes	39,188	33,315	32,212	38,981	28,518	27,494	33,438
Protein sequences with BLASTP matches*	20,395 (46.2%)	15,782 (43.1%)	15,084 (42.7%)	20,292 (45.8%)	12,639 (40%)	12,634 (41.7%)	16,979 (45.8%)
Protein sequences with GO/Interpro annotations*	15,009 (34.0%)	11,388 (31.1%)	10,997 (31.1%)	14,903 (33.7%)	9,379 (29.7%)	9,635 (31.8%)	12,426 (33.5%)
Total KOG annotations**	19,182	14,029	13,317	19,712	10,719	10,786	16,319

4.3.2. Differential expression analysis of putative viral genes

BLAST searches revealed the presence, in all samples, of unigenes that were most similar to viral gene sequences (< 0.2% of unigenes in each sample). In each sample, > 88% of these sequences could be assigned to three groups: phycodnaviruses, mimiviruses (including the megaviruses and marseilleviruses) and dinoflagellate viral nucleoproteins (DVNPs; genes shared by phycodnaviruses and dinoflagellates (Gornik *et al.*, 2012)) (Fig. 4.1). The BLAST matches of the remaining < 12% all belonged to the double-stranded DNA (dsDNA) virus group, to which the three classes defined above also belong. Several DVNP unigenes showed significant increases in expression following UV exposure (Appendix E, Figs. E2 and E3), however the nearest BLAST matches included several dinoflagellates, and due to the ambiguity of their origin these were not considered as candidate viral genes. Of the remaining putative viral genes, 25% (16 unigenes) and 17% (20 unigenes) showed significantly (> 2-fold) higher expression levels or were only expressed after UV exposure in CCMP2430 and Mp, respectively (Fig. 4.2).

In Mp a temporal change in expression levels was observed for several putative viral genes, with the T66 control sample showing a significant change in expression relative to the T0 control sample. To prevent overestimation of differentially-expressed genes here and in all subsequent expression analyses of this culture, treatment samples were only considered differentially expressed if they showed a > 2-fold change in the same direction, relative to both control samples. In order to take a conservative approach to viral gene discovery, virus-like genes that were downregulated or did not change significantly in treatment samples – and may therefore represent algal host genes, possibly resulting from horizontal gene transfer – were not considered candidate viral genes. As shown for several of these genes in Chapter 3, this is not necessarily the case; however further characterisation of these genes would be necessary to determine this. Expression levels of all virus-like genes are shown in Appendix E, Figs. E2 – E9.

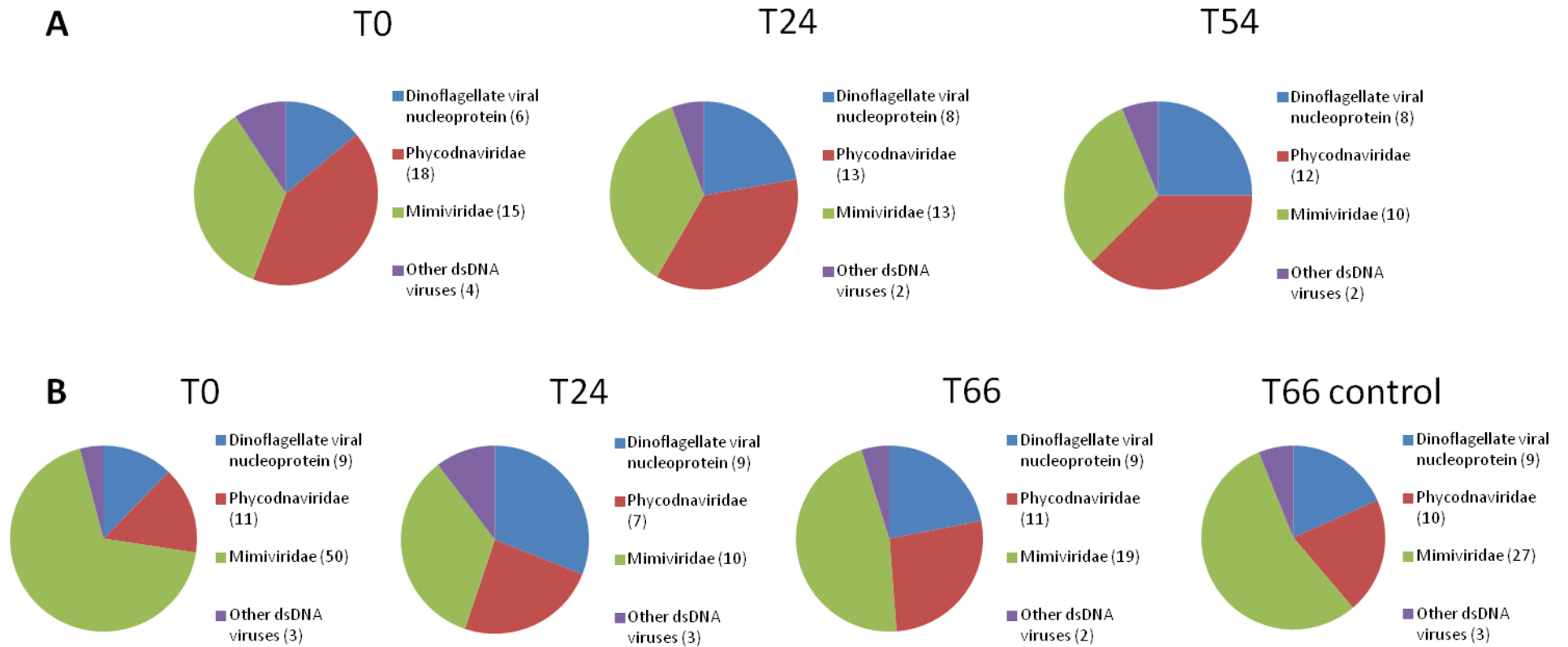


Figure 4.1. Total numbers of unigenes with nearest BLAST matches of viral origin in each transcriptome. A: *Symbiodinium* culture CCMP2430, B: *Symbiodinium* culture Mp. BLAST matches were grouped into four viral categories: dinoflagellate viral nucleoproteins, phycodnaviruses, mimiviruses and other dsDNA viruses.

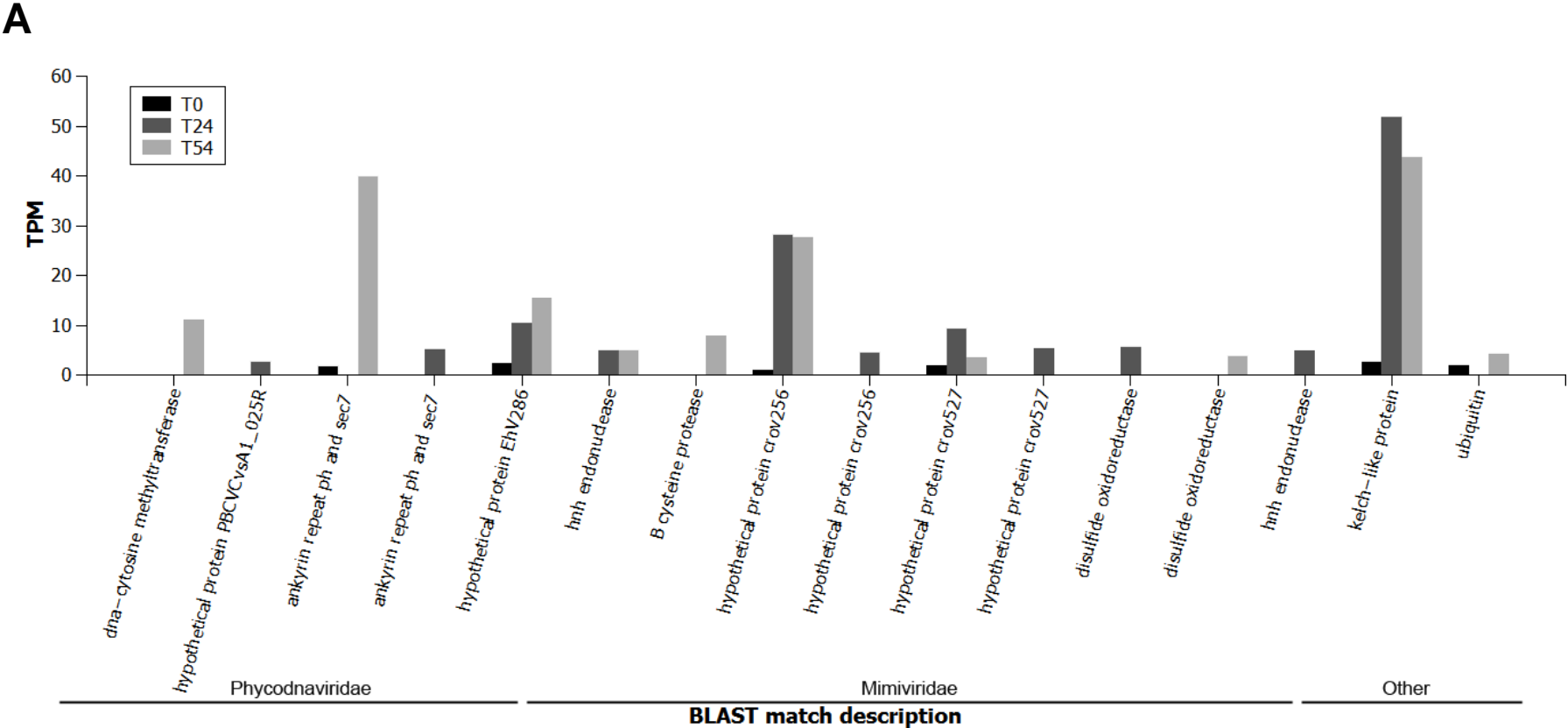


Figure 4.2. See overleaf for continuation of figure.

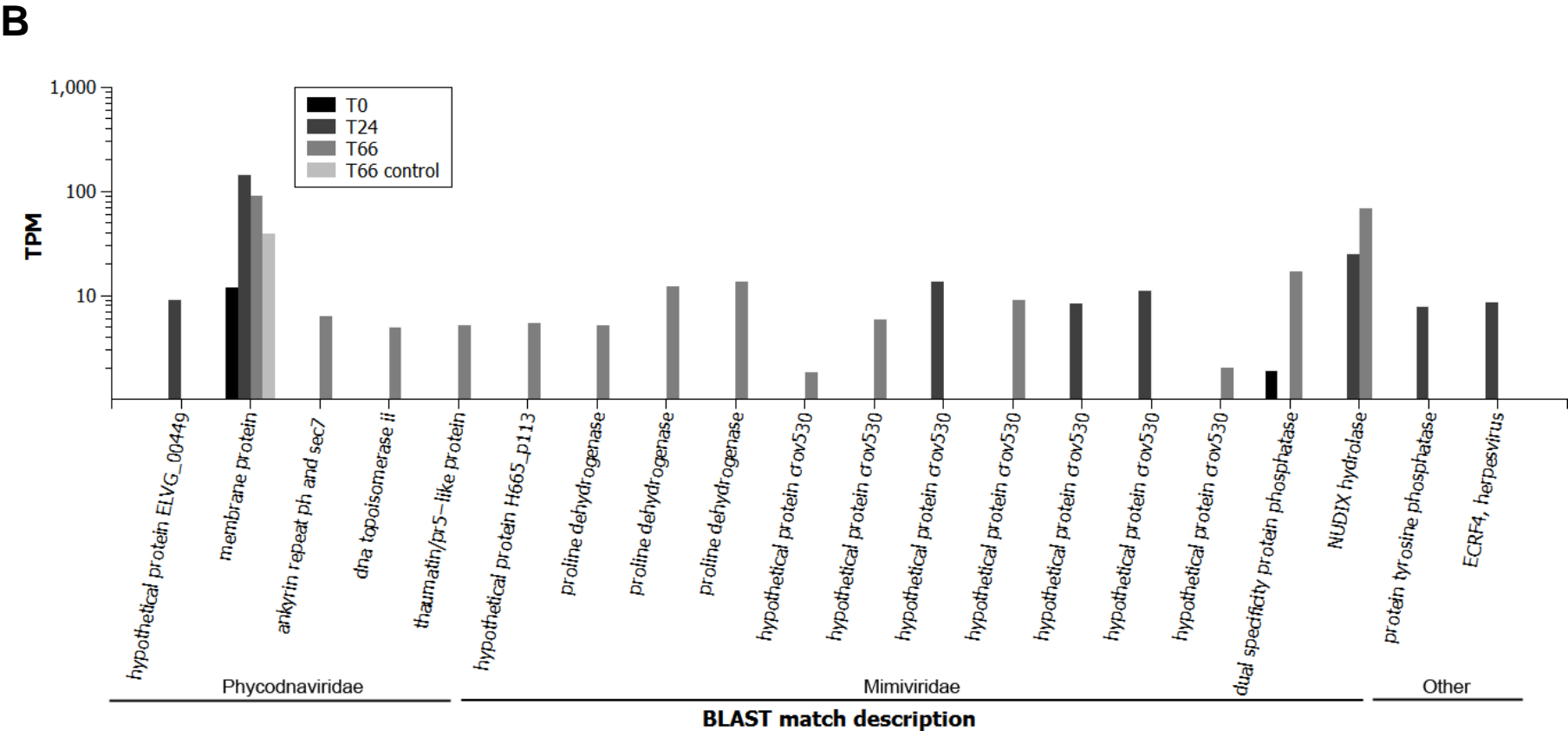


Figure 4.2. Putative viral unigenes from *Symbiodinium* cultures CCMP2430 (A) and Mp (B) that showed a > 2-fold increase in expression, or were only detected, following UV exposure.

Expression levels of viral unigenes varied, ranging from ~2 TPM to > 100 TPM. The identities of the genes, based on GO annotation and nearest BLAST matches, were consistent with latent viral replication (Table 4.2). In CCMP2430 in particular, many were early genes associated with viral genome replication and protein production. These included: a ubiquitin-encoding gene, which may play a role in viral replication through ubiquitination of viral polymerases (Si *et al.*, 2008); two homing endonucleases (excision of the integrated viral genome and/or first stages of DNA replication); a methyltransferase (protection of DNA from host nucleases); a cysteine protease and two disulfide oxidoreductases (protein processing); and two ankyrin repeat, PH and sec7 domain-containing proteins (ANK/PH/SEC7; protein folding). The most highly-expressed putative viral unigenes in CCMP2430 encoded a kelch-like protein, which may be involved in virulence and host cell degradation (Balinsky *et al.*, 2007), an ANK/PH/SEC7 protein, and a protein of unknown function.

The putative viral unigenes that were upregulated in Mp also included early genes, such as a DNA topoisomerase (DNA replication) and an ANK/PH/SEC7 protein. Also present were genes encoding proteins that affect the host, and hence facilitate viral replication, including two protein phosphatases that can suppress host antiviral responses in other systems (Guan *et al.*, 1991; Peters *et al.*, 2002), and a NUDIX hydrolase-like protein (NUDIX proteins are involved in mRNA decapping, and may facilitate viral protein synthesis at the expense of host protein production (Parrish *et al.*, 2007)). The genes showing the highest expression levels in Mp encoded a NUDIX hydrolase and a putative membrane protein.

These results were partially consistent with the virus-related GO term differential expression analysis (section 4.3.3.), which showed marked upregulation of the terms “viral transcription” (both cultures), “viral envelope” (both cultures), “intracellular transport of viral proteins” (CCMP2430) and “viral assembly” (Mp), and with changes in the expression levels of terms associated with viral genome replication in CCMP2430.

Chapter 4: Virus-related gene expression in *Symbiodinium*

Table 4.2. Putative viral genes that showed increased expression following UV exposure.

<i>Symbiodinium</i> culture ID	Sequence description (Blast2GO)	Most significant BLASTP match	Accession number	e-value*	Sequence similarity (%)**
CCMP2430	DNA-cytosine methyltransferase	<i>Emiliana huxleyi</i> virus PS401	AET73407	2.25E-19	42
CCMP2430	hypothetical protein	<i>Paramecium bursaria Chlorella</i> virus CvsA1	AGE52380	1.86E-29	52
CCMP2430	ankyrin repeat PH and SEC7 domain containing protein	<i>Paramecium bursaria Chlorella</i> virus 1	NP048353	2.33E-08	50
CCMP2430	HNH endonuclease	<i>Acanthamoeba polyphaga</i> moulouovirus	YP007354246	1.01E-16	48
CCMP2430	HNH endonuclease	Megavirus Courdo7	AEX61451	1.74E-11	45
CCMP2430	hypothetical protein	<i>Cafeteria roenbergensis</i> virus BV-PW1	YP003969888	5.38E-15	52
CCMP2430	hypothetical protein	<i>Cafeteria roenbergensis</i> virus BV-PW1	YP003969888	1.91E-14	49
CCMP2430	B cysteine protease family protein	Moumouvirus Goulette	AGF85419	5.03E-19	74
CCMP2430	disulfide oxidoreductase	Lausannevirus	YP004347288	1.42E-13	59
CCMP2430	disulfide oxidoreductase	Lausannevirus	YP004347288	1.14E-10	58
CCMP2430	kelch-like protein	Deerpox virus W-1170-84	YP002302501	3.37E-08	59
CCMP2430	ankyrin repeat PH and SEC7 domain containing protein	<i>Paramecium bursaria Chlorella</i> virus 1	NP049038	4.56E-25	55
CCMP2430	hypothetical protein	<i>Emiliana huxleyi</i> virus 86	YP294043	1.58E-08	63
CCMP2430	hypothetical protein	<i>Cafeteria roenbergensis</i> virus BV-PW1	YP003970160	1.39E-130	56
CCMP2430	hypothetical protein	<i>Cafeteria roenbergensis</i> virus BV-PW1	YP003970163	1.34E-36	62
CCMP2430	ubiquitin	<i>Ectropis obliqua</i> nucleopolyhedrovirus	YP874214	2.58E-10	75
Mp	ankyrin repeat PH and SEC7 domain containing protein	<i>Paramecium bursaria Chlorella</i> virus CVR-1	AGE52194	6.44E-07	56
Mp	hypothetical protein	<i>Emiliana huxleyi</i> virus 203	AEO98022	3.95E-09	45
Mp	hypothetical protein	<i>Ostreococcus tauri</i> virus 1	YP003212936	6.18E-14	47
Mp	membrane protein	<i>Emiliana huxleyi</i> virus 201	AET98250	2.92E-10	49
Mp	thaumatin pr5-like protein	<i>Feldmannia</i> sp. virus	YP002154632	3.82E-07	67
Mp	dual specificity protein phosphatase	Lausannevirus	YP004347041	2.75E-11	53
Mp	NUDIX hydrolase-like protein	<i>Megavirus chiliensis</i>	YP004894702	5.43E-07	45
Mp	ECRF-4	Macacine herpesvirus 4	YP068008	2.24E-09	48
Mp	protein tyrosine phosphatase	<i>Thysanoplusia orichalcea</i> nucleopolyhedrovirus	YP007250413	1.91E-12	69
Mp	DNA topoisomerase II	<i>Cafeteria roenbergensis</i> virus NYs1	AGE58893	2.26E-24	87
Mp	proline dehydrogenase	<i>Cafeteria roenbergensis</i> virus BV-PW1	YP003970160	5.80E-13	61
Mp	proline dehydrogenase	<i>Cafeteria roenbergensis</i> virus BV-PW1	YP003970160	8.97E-11	61
Mp	proline dehydrogenase	<i>Cafeteria roenbergensis</i> virus BV-PW1	YP003970160	4.36E-13	65
Mp	hypothetical protein	<i>Cafeteria roenbergensis</i> virus BV-PW1	YP003970163	2.22E-48	62
Mp	hypothetical protein	<i>Cafeteria roenbergensis</i> virus BV-PW1	YP003970163	1.37E-26	58
Mp	hypothetical protein	<i>Cafeteria roenbergensis</i> virus BV-PW1	YP003970163	4.88E-28	65
Mp	hypothetical protein	<i>Cafeteria roenbergensis</i> virus BV-PW1	YP003970163	1.76E-28	61
Mp	hypothetical protein	<i>Cafeteria roenbergensis</i> virus BV-PW1	YP003970163	2.41E-15	62
Mp	hypothetical protein	<i>Cafeteria roenbergensis</i> virus BV-PW1	YP003970163	2.72E-12	63
Mp	hypothetical protein	<i>Cafeteria roenbergensis</i> virus BV-PW1	YP003970163	5.87E-08	56

* Where a gene was present in more than one sample, the highest (least significant) e-value is reported. **Where a gene was present in more than one sample, the lowest level of sequence similarity is reported (sequences never differed by more than 2% for any gene).

4.3.3. Differential expression analysis of virus-related genes

Enrichment of virus-related GO terms (see Box 1) was assessed in both *Symbiodinium* cultures by comparing the summed TPM values of the transcripts assigned to each term (Fig. 4.3). The minimum threshold value for transcript detection was set at 1.0 TPM and a fold change of > 2.0 in either direction was considered to represent a significant difference in expression level. As mentioned previously, because of temporal expression changes in Mp, genes were only considered differentially expressed in this culture if there was a > 2 -fold change in TPM values relative to both T0 and T66 control samples.

The two cultures showed similar responses in terms of virus-related gene expression. In CCMP2430, changes in expression were largely consistent with the onset of viral infection: increases in expression were seen in GO terms associated with virion components, viral replication and transcription, while expression levels decreased for genes associated with regulation of the host response to viral infection (Fig. 4.3A). Similarly, Mp showed an increase in expression of genes related to viral transcription and assembly following UV exposure, though this culture did not show evidence for the downregulation of host-defence response genes that was seen in CCMP2430 (Fig. 4.3B). Unlike in CCMP2430, the majority of differentially expressed GO terms in Mp did not sustain their levels of differential expression across both treatment time points (as seen in the reduced number of double triangles in Fig. 4.3B compared to Fig. 4.3A), though this was due in part to the conservative approach adopted to accommodate the temporal changes in expression seen in this culture.

Box 1. Virus-related GO terms associated with transcripts found in this study.

GO Term	Description	GO term	Description
0009615	Response to virus	0045070	Positive regulation of viral genome replication
0009616	Virus-induced gene silencing	0045071	Negative regulation of viral genome replication
0016032	Viral reproduction	0045870	Positive regulation of retroviral genome replication
0019028	Viral capsid	0046740	Spread of virus in host, cell to cell
0019031	Viral envelope	0046778	Modification by virus of host mRNA processing
0019048	Virus-host interaction	0046784	Intronless viral mRNA export from host nucleus
0019058	Viral infectious cycle	0046788	Egress of virus within host cell
0019059	Initiation of viral infection	0046790	Virion binding
0019060	Intracellular transport of viral proteins in host cell	0046826	Negative regulation of protein export from nucleus
0019061	Uncoating of virus	0050434	Positive regulation of viral transcription
0019064	Viral entry via fusion with the plasma membrane	0050687	Negative regulation of defence response to virus
0019067	Viral assembly, maturation, egress and release	0050688	Regulation of defence response to virus
0019083	Viral transcription	0050690	Regulation of defence response to virus by virus
0019089	Transmission of virus	0051534	Negative regulation of NFAT protein import into nucleus
0045069	Regulation of viral genome replication	0051607	Defence response to virus

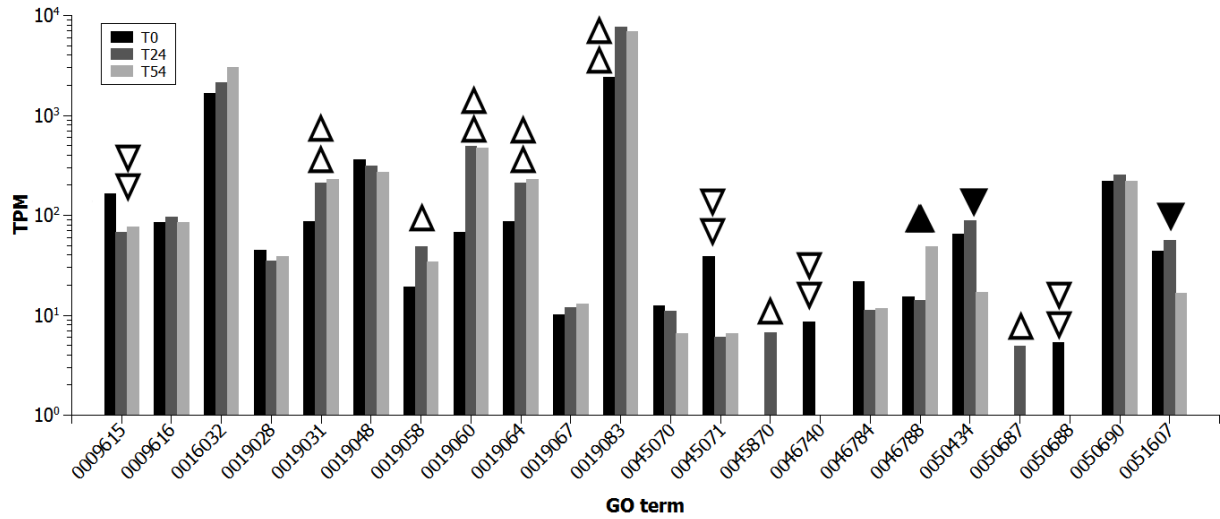
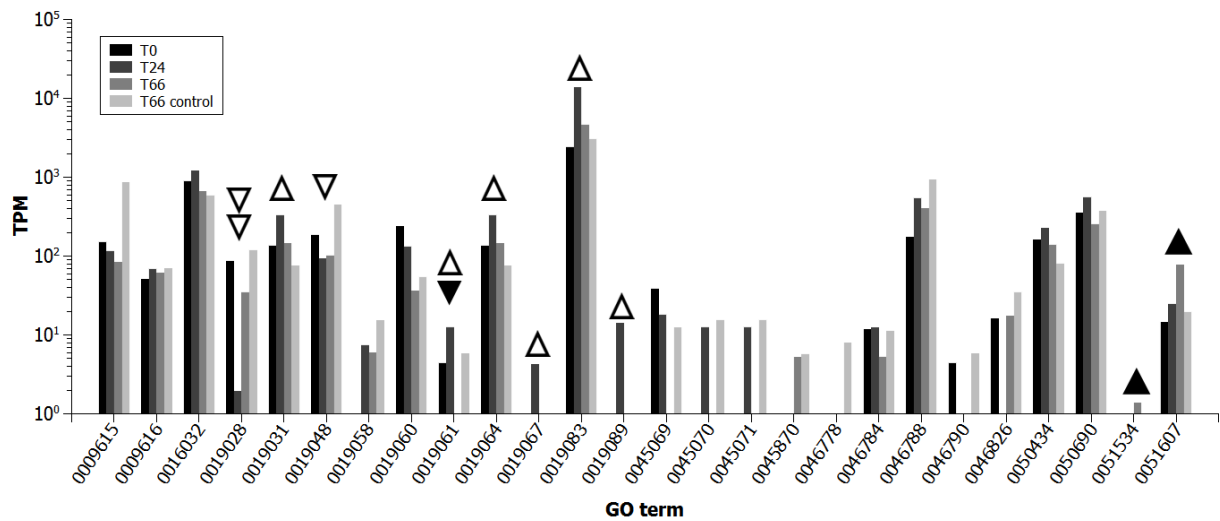
A**B**

Figure 4.3. Differential expression analysis of virus-related GO terms containing transcripts from CCMP2430 (A) and Mp (B). TPM values were summed from all transcripts associated with a given GO term. Single triangles indicate a significant (> 2 -fold) change in expression level at T24 (empty triangles) or T54 (CCMP2430)/T66 (Mp) (filled triangles), relative to T0. Double triangles indicate a significant change in expression level at both T24 and T54/T66, relative to controls. Upward-pointing triangles indicate an increase in expression, downward-pointing triangles indicate a decrease in expression.

4.3.4. Functional annotation of transcriptomes

Unigenes were annotated using the Eukaryotic Orthologous Groups (KOG) database, resulting in ~11,000 – 20,000 functional annotations for each transcriptome (Table 4.1; note that these numbers include unigenes assigned to more than one functional annotation). The five largest KOG classes in both cultures, and in both control and treatment samples, were “signal transduction mechanisms”, “general function prediction only”, “posttranslational modification, protein turnover, chaperones”, “inorganic ion transport and metabolism” and “cytoskeleton” (Fig. 4.4). Generally there was a decrease in the number of genes associated with each KOG class following UV exposure, with the sole exception being the class “defence mechanisms” in CCMP2430, which remained stable throughout the experiment. Control samples collected at T66 in Mp showed a temporal decrease in expressed gene numbers; however this decrease was not as pronounced as in the treatment samples (Fig. 4.4B).

Box 2. KOG classes.

KOG Class	Description	KOG Class	Description
A	RNA processing and modification	O	Posttranslational modification, protein turnover, chaperones
B	Chromatin structure and dynamics	P	Inorganic ion transport and metabolism
C	Energy production and conversion	Q	Secondary metabolites biosynthesis, transport and catabolism
D	Cell cycle control, cell division, chromosome partitioning	R	General function prediction only
E	Amino acid transport and metabolism	S	Function unknown
F	Nucleotide transport and metabolism	T	Signal transduction mechanisms
G	Carbohydrate transport and metabolism	U	Intracellular trafficking, secretion, and vesicular transport
H	Coenzyme transport and metabolism	V	Defence mechanisms
I	Lipid transport and metabolism	W	Extracellular structures
J	Translation, ribosomal structure and biogenesis	X	Multiple functions
K	Transcription	Y	Nuclear structure
L	Replication, recombination and repair	Z	Cytoskeleton
M	Cell wall/membrane/envelope biogenesis		
N	Cell motility		

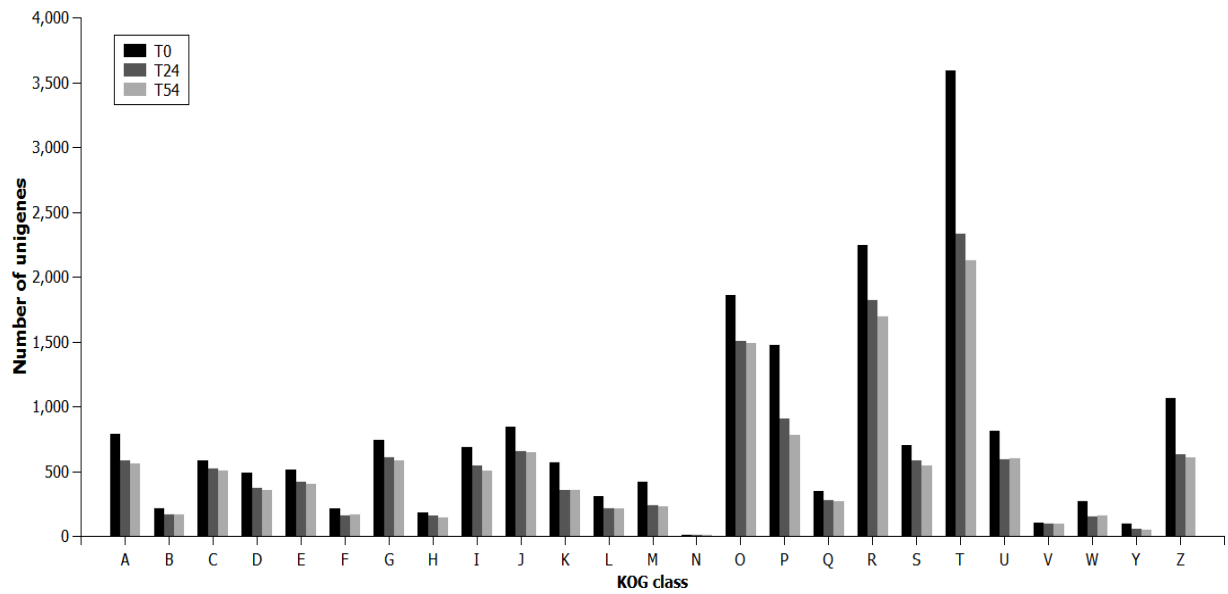
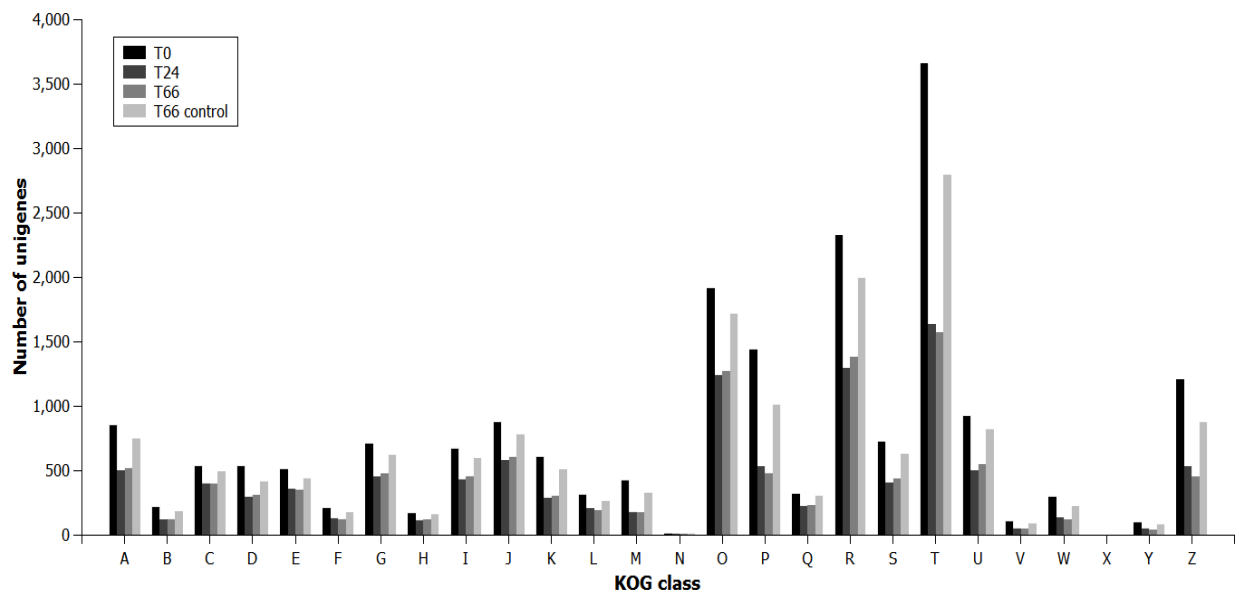
A**B**

Figure 4.4. Eukaryote orthologous groups (KOG) annotation of unigenes from *Symbiodinium* cultures CCMP2430 (A) and Mp (B). See Box 2 for a description of KOG classes.

4.3.5. Differential expression analysis of host cell stress response

Differential expression analysis was carried out on GO gene groups associated with cellular components and biological processes previously shown to play a role in viral infection and replication (Fig. 4.5). In both *Symbiodinium* cultures, most virus-associated GO terms showed no difference in expression levels in response to UV exposure. The exceptions to this were genes encoding ribosomal proteins, which showed a > 2-fold increase in transcript per million (TPM) values in both cultures following UV stress. In Mp, RNA polymerase-associated genes were also upregulated after UV exposure, though there was also a significant upregulation in the non-irradiated control sample.

As reactive oxygen species (ROS) and antioxidant activity have previously been shown to play a role in viral infection response (Riedle-Bauer, 2000; Clarke *et al.*, 2002), the expression levels of several common antioxidant enzymes (catalase/peroxidase, ascorbate peroxidase, glutathione peroxidase, peroxiredoxin and superoxide dismutase) were analysed in each of the *Symbiodinium* samples. Thirty-one and 38 antioxidant unigenes were identified in CCMP2430 and Mp, respectively. Expression levels of many of the antioxidant unigenes were unchanged after UV irradiation; 20 genes in CCMP2430, and five in Mp, showed > 2-fold changes in expression levels in the treatment samples, though these were not consistently in one direction (Appendix E, Figs. E10 and E11). Comparing the antioxidant genes at the GO term level, 3/5 and 2/5 terms showed decreased expression in at least one treatment time point in CCMP2430 and Mp, respectively, while the remainder were unchanged (Fig. 4.6). Genes that showed decreased expression were associated with ascorbate peroxidase activity (CCMP2430), glutathione peroxidase activity (CCMP2430), peroxidase activity (Mp) and peroxiredoxin activity (both cultures).

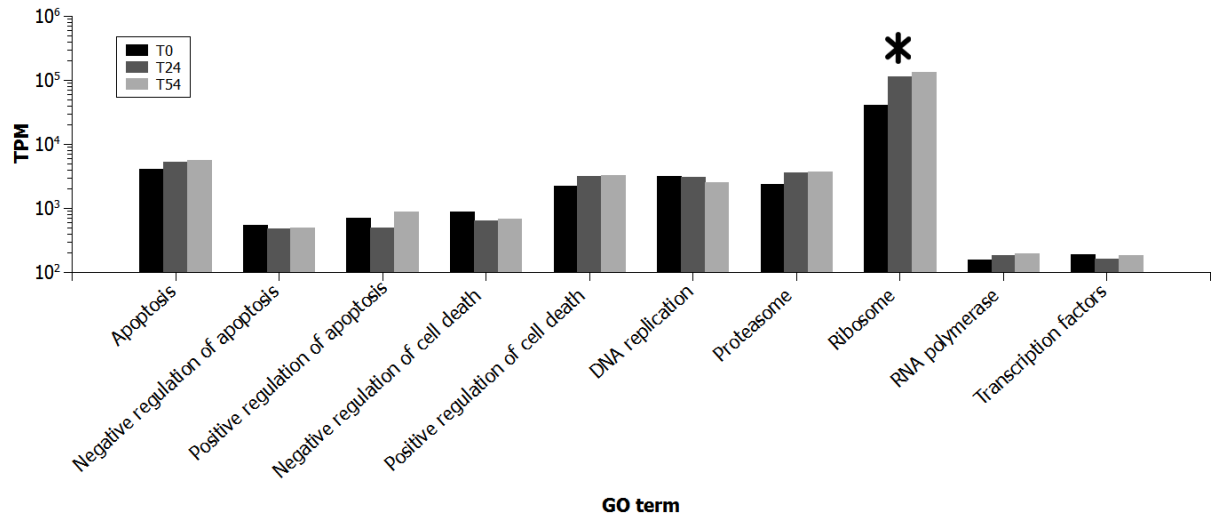
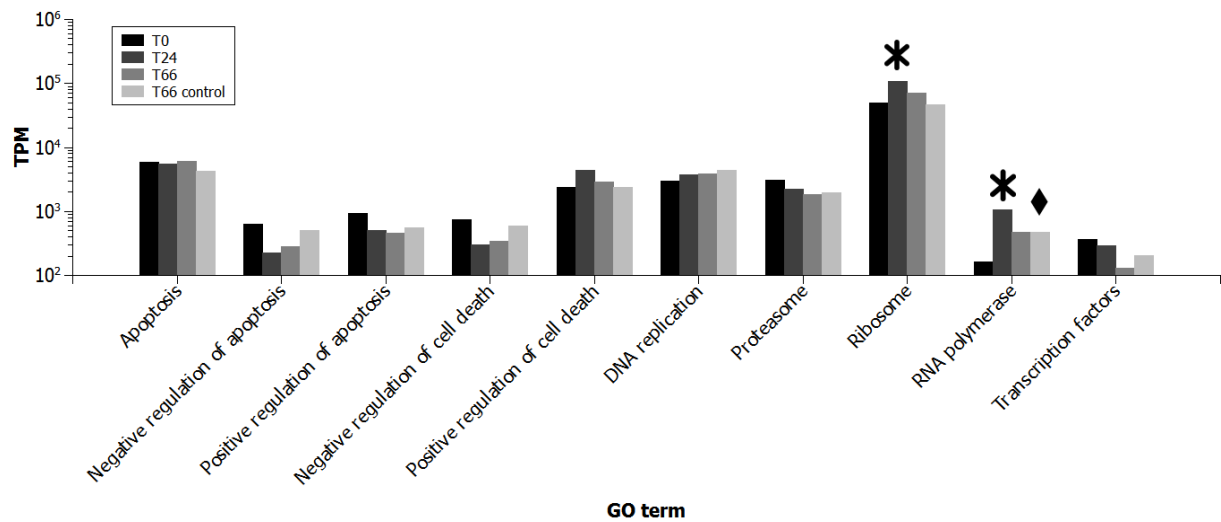
A**B**

Figure 4.5. Expression levels (transcripts per million) of selected GO terms associated with viral infection and replication in *Symbiodinium* cultures CCMP2430 (A) and Mp (B). Asterisks represents a significant (> 2-fold) increase in expression following UV exposure; diamond indicates a significant difference in expression levels between the T0 and T66 control samples in Mp.

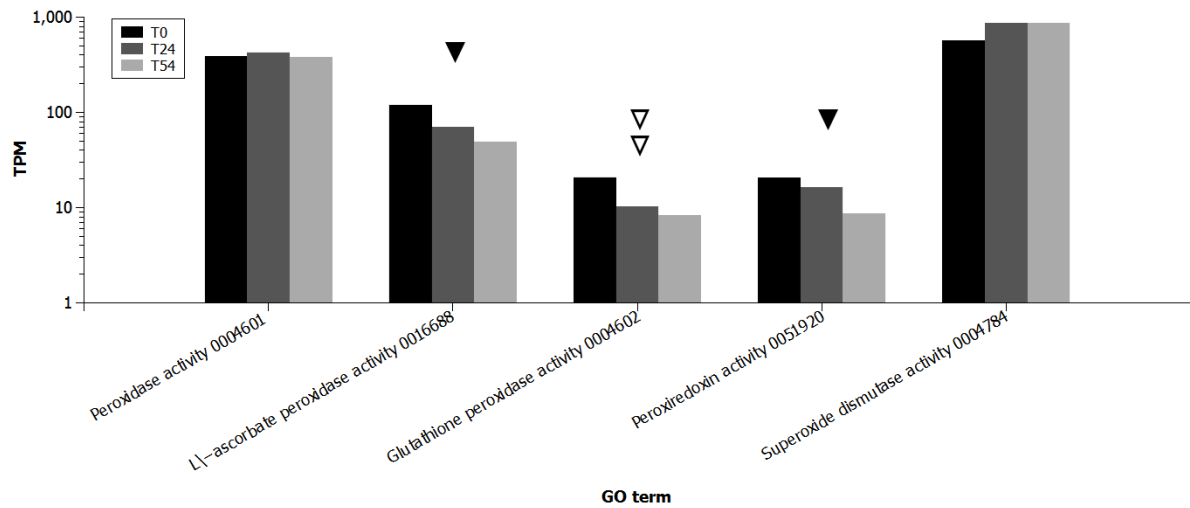
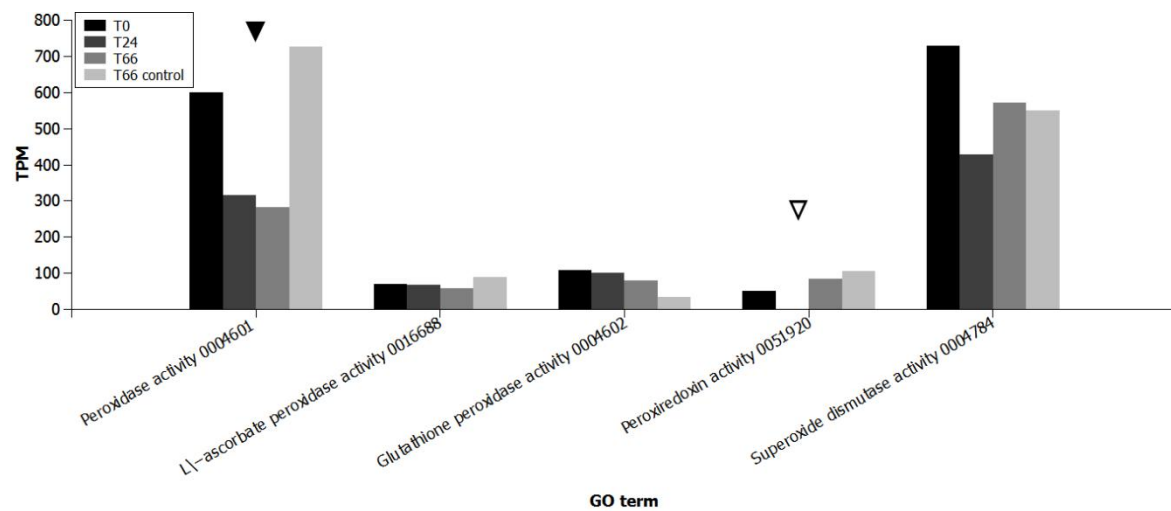
A**B**

Figure 4.6. Expression levels (transcripts per million) of GO terms associated with antioxidant enzyme activity in CCMP2430 (A) and Mp (B). Single triangles indicate a significant (> 2-fold) decrease in expression level at T24 (empty triangles) or T54 (CCMP2430)/T66 (Mp) (filled triangles), relative to T0. Double triangles indicate a significant decrease in expression level at both T24 and T54/T66, relative to T0.

4.4. Discussion

In this study, the transcriptomic responses of two *Symbiodinium* cultures to stress were analysed, and transcriptomes were searched for the presence of latent viruses. The two cultures studied here were from different clades (CCMP2430: clade A; Mp: clade C), and showed both similarities and differences in their responses to the experimental stress, both in terms of host gene response and expression of putative viral genes.

Numerous putative viral genes were discovered in the two *Symbiodinium* cultures, and BLAST searches suggested that they almost exclusively belonged to the double-stranded DNA (dsDNA) viruses, with most of the BLAST matches coming from nucleocytoplasmic large DNA viruses (NCLDVs). Of note, most of these viruses are large icosahedral or ovoid particles, unlike the filamentous VLPs seen in electron micrographs of these *Symbiodinium* cultures (Chapter 2). This may be a consequence of inadequate sampling in Chapter 2, meaning viruses were missed during electron microscopy, or, as noted below, the sequences may in fact belong to non-NCLDV viruses which do not currently have sequences in the Genbank database.

Sequence similarities between the putative viral genes and BLAST matches were generally low, meaning that accurate identification of the viruses was not possible; however the viral families represented in the BLAST matches were the *Phycodnaviridae*, *Mimiviridae*, *Megaviridae*, *Poxviridae*, *Herpesviridae*, *Baculoviridae* and the as yet unclassified Lausannevirus (similar to the *Mimiviridae* (Thomas *et al.*, 2011b)). The presence of phycodnaviruses in these algae would not be surprising, as these viruses are known to infect marine algae, including dinoflagellates (Nagasaki *et al.*, 2006; Tomaru *et al.*, 2008). The potential presence of other dsDNA viruses not typically associated with algae was an interesting result. Although the hosts of these groups are typically terrestrial animals (for *Herpesviridae*, *Poxviridae* and *Baculoviridae*) and amoebae (for *Mimiviridae*, *Megaviridae* and Lausannevirus), there is increasing evidence that viruses related to these groups infect corals and/or their dinoflagellate symbionts. For example, Vega Thurber *et al.* (2008) found an increase in *Herpesviridae*-like sequences in the metagenomes of stressed scleractinian corals. Recently, Correa *et al.* (2012) also found evidence of poxviruses and mimiviruses associated with a scleractinian coral and two types of *Symbiodinium*. Given the low level of

sequence similarity between the detected genes and BLAST matches seen in the present study, it would be imprudent to conclude that these *Symbiodinium* cultures are infected with members of these viral families, as the similarity may be merely an artefact arising from the lack of viral sequences in the database. Nevertheless, this finding does provide further evidence of viral infection in these cells, and highlights the potential diversity of currently unidentified viruses infecting marine algae.

It is worth noting that the genes identified here as being viral in origin differ from the putative conserved viral genes identified in Chapter 3. This is a reflection of the different approaches taken in the two chapters; in Chapter 3, a phylogenetic approach was taken, whereas in the present chapter putative viral genes were identified based on relative expression levels. Because they were not upregulated following stress, the viral genes identified in Chapter 3 were not among the putative viral genes identified here. These results, rather than contradicting each other, simply highlight the fact that the conservative approach taken in this chapter may have led to an underestimation of the true number of viral genes present.

Although a conservative approach was taken when identifying transcripts as putative viral genes, there remains the possibility that these genes were in fact endogenous viral genes rather than latent viral genes. While horizontal gene transfer (HGT) usually occurs from host to virus (Iyer *et al.*, 2001), examples of HGT occurring in the other direction are manifold (Hensel and Schmidt, 2008; Liu *et al.*, 2010) and include phycodnaviruses (Villareal and DeFilippis, 2000) and megaviruses (Hingamp *et al.*, 2013). Likewise, it is probable that the approach taken here resulted in some viral genes being overlooked. This was due in part to the desire to act conservatively when identifying genes as ‘viral’, and in part to the sampling regime; in order to capture all viral genes that were being expressed, more sampling time points would be necessary.

The relative expression levels of virus-related GO terms supported the hypothesis of UV-induction of latent viruses in the two *Symbiodinium* cultures. In both cultures, numerous terms associated with viral reproduction were more highly expressed following UV irradiation, however there were differences between the two cultures. In CCMP2430, terms associated with viral entry into the cell and genome replication were upregulated, in addition to terms associated with transcription and virion component production. Additionally, genes

involved in regulation of defence responses to viral infection were downregulated following irradiation. Taken together, these results suggest that the samples were collected during the relatively early stages of viral induction and replication. In Mp, on the other hand, GO terms associated with viral assembly and transmission were upregulated, while genome replication-associated terms showed no changes in expression relative to controls, suggesting that the hypothetical induced viruses were generally in a later stage of the replication cycle. These findings were partially supported by the identity of the putative viral genes that were upregulated following stress. In CCMP2430, viral genes encoded several proteins involved with the early stages of replication, such as DNA replication and protection, and protein production. The unigenes upregulated in Mp, however, did not include genes associated with virion production as predicted by the GO term analysis. Three of the upregulated viral unigenes were of unknown function, however, and the possibility that any of these may have been associated with virion assembly cannot be discounted.

The number of genes associated with common cellular components and processes was highly similar in control samples of both cultures, as were the expression levels of genes thought to play roles in infection-related cellular processes, such as cell death, DNA replication, transcription and antioxidant activity. Somewhat unexpectedly, the expression levels of many of these gene groups were unchanged following UV irradiation, though in both cultures, ribosome-associated genes were upregulated following irradiation.

The overall response of antioxidant enzyme genes was also surprising: in both cultures, antioxidant gene expression either remained at pre-treatment levels or declined following irradiation, though at the individual unigene level some antioxidant genes did show increases in expression. This finding appears to contrast with previous studies that have found that viral infection causes an increase in ROS (Schwarz, 1996; Beck *et al.*, 2000). Evans *et al.* (2006) found elevated levels of ROS following viral infection of the coccolithophore *Emiliania huxleyi*, which they hypothesised were due to the breakdown of photosystem II following infection, or may have been a requirement for viral replication. Despite the evidence for virus-induced ROS production, several studies have demonstrated downregulation (Clarke *et al.*, 2002; Mohankumar and Ramasamy, 2006) or rapidly transient changes in expression (Gómez-Anduro *et al.*, 2006) of antioxidant genes. In the latter study, for example, the authors found an increase in manganese-containing superoxide dismutase 1 h after infection of shrimp with white spot syndrome virus, followed by a decrease to levels

significantly lower than in control samples by 12 h post-infection. While an increase in antioxidant levels has been shown to mitigate ROS-induced damage in *Symbiodinium* (Lesser, 1996), increased ROS production following stress with no corresponding increase in antioxidant production has also been demonstrated (McGinty *et al.*, 2012). The results presented here may therefore be due to downregulation following the initial viral induction and early replication stages, or they may be indicative of *Symbiodinium* response to ROS production, which may not involve upregulation of antioxidant genes.

In addition to a more extensive sampling regime, future work would ideally include replicate samples. Although the Illumina sequencing technology has a low error rate (Minoche *et al.*, 2011; Luo *et al.*, 2012), the inclusion of biological replicates would allow a more robust statistical analysis of gene expression. Similarly, qPCR would be useful for validation of expression levels derived from the RNA-seq data. Despite the potential limitations, this study is the first to examine the expression levels of putative virus genes in *Symbiodinium*, and provides evidence that these algae contain latent dsDNA viral infections that may be induced *via* stress. Furthermore, as an initial exploratory study of latent viral infections of *Symbiodinium* spp., this work provides a list of candidate latent and/or endogenous viral genes for further study.

Chapter 5: *Porites* white patch syndrome: disease physiology and associated viruses

5.1. Introduction

Coral reefs worldwide are increasingly under threat from climate change-induced bleaching events (Hoegh-Guldberg, 1999; Baker *et al.*, 2008), ocean acidification (Hoegh-Guldberg *et al.*, 2007), predator outbreaks (Kayal *et al.*, 2012) and disease (Harvell *et al.*, 1999; Harvell *et al.*, 2007). While we are beginning to better understand the mechanisms involved in bleaching (Douglas, 2003; Weis, 2008), the causative agents of many coral diseases remain unknown. Given that coral diseases are often opportunistic infections arising after stress to the host (Lesser *et al.*, 2007), it is likely that disease prevalence will increase in the future in response to climate change and other anthropogenic impacts. Already, disease following bleaching has resulted in drastic declines in coral cover in the Caribbean (Miller *et al.*, 2009). Clearly a better understanding of the numerous identified coral diseases is critical if we are to mitigate at least some of the degradation of reefs that is predicted to occur.

Corals of the genus *Porites* are important members of many reefs in the Indo-Pacific, and are commonly affected by disease (Raymundo *et al.*, 2005). Documented diseases of poritid corals in this region include growth anomalies (tumours) (Domart-Coulon *et al.*, 2006; Kaczmarzky, 2006; Kaczmarzky and Richardson, 2007), *Porites* ulcerative white spot disease (PUWS) (Raymundo *et al.*, 2003), *Porites* bleaching with tissue loss (Sudek *et al.*, 2012b) and trematodiasis (Aeby, 2006). The disease under study here, white patch syndrome (WPS) was first described in the literature in 2008 (Roff *et al.*, 2008). These authors found that WPS manifested as patches of discolouration (with no associated tissue loss) on colonies of *Porites lobata* on the Great Barrier Reef. Patches were 20 – 100 mm in diameter, circular to oblong in shape and had distinct edges (Fig. 5.1). Measurements of photosynthetic health suggested that *Symbiodinium* within the patches were either damaged or expelled. Davy (2007), who studied WPS prior to publication of the above research, also provided evidence that WPS affects *Symbiodinium* cells rather than host tissue: lesion tissue was found to have decreased *Symbiodinium* cell density and photosynthetic health, while host protein content analysis suggested that coral tissue was unaffected. The causative agent of WPS is currently unknown.

Roff *et al.* (2008) noted that the macroscopically similar disease PUWS may be caused by *Vibrio* sp., however the relationship between these two diseases is unknown.



Figure 5.1. Macroscopic signs of WPS on *Porites australiensis* colonies.

In the current study I set out to further characterise WPS through microscopic analysis and to identify the causative agent of this disease. A particular focus of this study was to determine whether viruses play a role in WPS. Virus-like particles (VLPs) have previously been found in tissues of thermally-stressed corals (Wilson *et al.*, 2005a; Davy *et al.*, 2006) and stressed *Symbiodinium* (Lohr *et al.*, 2007), and have been shown to cause lysis of *Symbiodinium* cells (Wilson *et al.*, 2001). It has also been shown in this thesis that numerous types of

Symbiodinium harbour latent viral infections that can be induced through stress (Chapter 2). Further evidence for a potential viral basis of coral diseases comes from the work of Vega Thurber *et al.* (2008), who found, through the use of metagenomics, that stress induces herpes-like viruses in *Porites compressa*. With these findings in mind, I carried out electron microscopy and PCR-based molecular analyses to identify and enumerate viruses associated with healthy and WPS-infected poritid corals on the Great Barrier Reef.

5.2. Materials and methods

5.2.1. Sample collection

Tissue fragments of *Porites australiensis* were collected with hammer and chisel from colonies at Harry's Bommie, Wistari and Twin Peaks reefs, at ~6 m depth, in July 2010, at Heron Island, GBR. Samples were taken directly from WPS lesions (n = 10), from visibly healthy tissue ~1 cm away from the lesion (n = 10), and from non-diseased colonies (n = 10). The tissue samples were fixed in either 3.7% formaldehyde in seawater (for molecular analysis) or 2.5% glutaraldehyde in seawater (for TEM) within one hour of collection and refrigerated at 4 °C until processing.

5.2.2. Transmission electron microscopy

Glutaraldehyde-fixed tissue samples were decalcified in 0.5 M EDTA and post-fixed in 2% osmium tetroxide. Samples were then dehydrated through an ethanol series (50 – 100%) and propylene oxide, and embedded in Procure 812 resin (Proscitech, Thuringowa, Australia). Ultra-thin sections were cut on an Ultracut T ultramicrotome (Leica Microsystems, Vienna, Austria) and were stained using 2% aqueous uranyl acetate and Reynold's lead citrate. Sections were viewed on a Philips CM-100 transmission electron microscope operated at 80 kV. Five samples of each sample type (healthy, diseased, and 1 cm from lesion) were analysed. In each case 30 fields of view at 24,500 × magnification were examined for the presence of VLPs in *Symbiodinium* cells and coral gastrodermal and epidermal tissues. Observed VLPs were sorted into two morphological groups (icosahedral and filamentous) and four size classes (0-50 nm, 51-100 nm, 101-150 nm, > 150 nm). Statistical analysis was

carried out using PASW Statistics 18 (SPSS Inc., Chicago, IL, USA) to determine differences in virus abundances between samples.

5.2.3. Virus molecular analysis

Five replicates of each tissue sample type (healthy, diseased, 1 cm from disease lesion) were used for molecular analysis. Tissue samples were washed in 0.02 μm -filtered seawater (FSW) and crushed with a sterile mortar and pestle. The resultant slurry (11 mL) was decanted into sterile 15 mL centrifuge tubes. To eliminate large particles, samples were centrifuged at $1,500 \times g$ for 10 min at 4 °C. The supernatant was then transferred to sterile 1.5 mL microcentrifuge tubes and centrifuged at $7,800 \times g$ for 10 min at 4 °C to pellet cells and debris, leaving virus-like particles (VLPs) in suspension. Supernatants from each sample were recombined and RNase I was added to give a final concentration of 10 mg mL⁻¹. Aliquots (200 μL) of supernatant were loaded onto a continuous sucrose gradient (10 – 40%) in TNE buffer in polypropylene centrifuge tubes (Cat no. 331302 Beckman Coulter, Gladesville, Australia) and centrifuged at $78,000 \times g$ for 1.5 h at 4 °C in an Optima™ L-80 XP ultracentrifuge with a SW41Ti rotor (Beckman Coulter, Gladesville, Australia). Fractions of 500 μL volume were sequentially collected from the top of each tube, placed in 1.5 mL microcentrifuge tubes and stored at -20 °C. A 20 μL aliquot of each fraction was spotted onto a pioloform-coated 200 μm mesh copper grid and negatively stained with 0.2 μm -filtered 2% phosphotungstic acid (PTA). Grids were viewed on a Philips CM-100 transmission electron microscope operated at 80 kV to identify the fractions containing VLPs.

Viral DNA was isolated from 400 μL of each fraction showing VLPs. Proteinase K was added to a final concentration of 0.2 mg mL⁻¹ and incubated at 45 °C for 1 h 45 min. Sodium dodecyl sulfate (SDS; 20 μL of 10 % concentration) was added, and the mixture was incubated at 45 °C for a further 1 h. Phenol:chloroform:isoamyl alcohol (440 μL , 25:24:1) was added and thoroughly mixed before being centrifuged at $5,000 \times g$ at room temperature for 5 min. The aqueous layer was transferred to a fresh sterile 1.5 mL microcentrifuge tube and an equal volume of chloroform was added and mixed, before being centrifuged at $5,000 \times g$ at room temperature for 5 min. The aqueous layer was again transferred to a fresh sterile 1.5 mL tube and 1/10 volume of 3 M sodium acetate (pH 5.5), 2 volumes 100% ethanol, and Ambion GlycoBlue™ co-precipitant (Life Technologies, Carlsbad, CA, USA) to a concentration of 50 μg mL⁻¹ were added. The tubes were mixed gently and stored at -20 °C

for 20 min, before being centrifuged at $5,000 \times g$ at 4 °C for 10 min. The supernatant was removed and the pellet was washed with 70% ethanol by spinning at low speed at 4 °C for 2 min. The pellet was left to dry at room temperature, and then dissolved overnight at 4 °C in 100 μ L TE buffer.

A pair of degenerate primers targeting a fragment of the ribonucleotide reductase small sub unit gene was used to amplify viral DNA. These primers were designed using protein sequence information from a number of viruses by Davy (2007), however the ribonucleotide reductase gene is not virus-specific, meaning these primers may also amplify pro- and eukaryotic DNA. The primer sequences were as follows: RR2Forward: GAYGARGGIYTICAY; RR2Reverse: YTCRAARAARTTIGTYTT. A two-stage PCR was carried out, with the product from the first round used as template for the second round. The initial reaction mixture contained 3 μ L DNA, $1.7 \times$ PCR buffer, 5 mM $MgCl_2$, 0.17 mM each deoxynucleoside triphosphate (dNTP), 100 pmol forward primer, 100 pmol reverse primer and 1 unit GoTaq DNA polymerase (Promega, Fitchburg, WI, USA) in a total volume of 30 μ L per reaction. The PCR was performed on a iCycler thermal cycler (Bio Rad, Hercules, CA, USA) using the following conditions: 95 °C for 3 min; 33 cycles of 95 °C for 45 s, 49 °C for 45s, 72 °C for 45 s; and a final extension step of 72 °C for 10 min. Negative controls contained all reagents except template DNA. The positive control was purified genomic DNA from *Emiliana huxleyi* virus 86 (Schroeder *et al.*, 2002). PCR products were visualised on a 2% (w/v) agarose gel in TAE buffer run at 100 V for 30 min. The second round of PCR used 5 μ L of PCR product as the DNA template, but otherwise used the same conditions and controls as above. Replicate samples were pooled and 60 μ L of each PCR reaction were run on a 2% (w/v) agarose gel in TAE buffer at 35 V for 1 min, 50 V for 1 min, and 75 V for 32 min, in order to produce clear bands.

PCR products were cloned using the pGEM-T Easy Vector System (Promega, Fitchburg, WI, USA) following a modified version of the manufacturer's protocol. For the ligation step, 2.5 μ L ligation buffer, 0.5 μ L vector, 1.5 μ L PCR product and 0.5 μ L T4 DNA ligase were incubated at 4 °C overnight. For the transformation step, 2 μ L of ligate were added to 20 μ L of JM109 High Efficiency competent *E. coli* cells (Promega, Fitchburg, WI, USA) and placed on ice for 20 min, then heat shocked at 42 °C for 30 s before being placed back on ice. SOC medium (500 μ L, Promega, Fitchburg, WI, USA) was added to each transformation reaction and incubated at 37 °C in a shaking incubator for 2 h. An aliquot of 300 μ L of each sample

was spread onto LB/ampicillin/X-Gal/IPTG plates and incubated at 37 °C overnight. White colonies were screened for inserts by PCR using the RR2 primers in 10 µL reactions containing 1 × PCR buffer, 1.25 mM MgCl₂, 0.05 mM each dNTP, 10 pmol forward primer, 10 pmol reverse primer, 0.2 units *AmpliTaq* Gold DNA Polymerase, and 2 µL DNA. PCR was performed on a Hybaid PCR Express thermal cycler using the following conditions: 94 °C for 5 min; 33 cycles of 94 °C for 30 s, 49 °C for 30 s, 72 °C for 45 s; and a final extension of 72 °C for 10 min. Negative controls contained all reagents except template DNA. PCR products were run on a 2% (w/v) agarose gel in TAE buffer at 80 V for 20 min to check for inserts. Clones containing inserts were grown overnight in a 37 °C shaking incubator, in 15 mL centrifuge tubes containing 5 mL LB broth and 50 µg mL⁻¹ ampicillin. Following cloning and colony PCR, plasmids containing inserts were isolated using a QIAprep Spin Miniprep kit (Qiagen, Gaithersburg, MD, USA) following the manufacturer's instructions. Plasmid preps were checked by digestion with the enzyme *SacI* (New England Biolabs, Ipswich, MA, USA) and visualisation on a 2% agarose gel in TAE buffer. Restriction digests were performed using the enzymes *HaeIII* and *MspI*. Digest reactions consisted of 10 µL colony PCR product, 1 × digestion buffer and 10 units of each enzyme, and were run at 37 °C for 3 hours, followed by visualisation on a 4% agarose gel in TAE buffer. Plasmids with unique restriction patterns were sequenced at the University of Illinois Core Sequencing Facility (Urbana, IL, USA). Forward and reverse sequences were assembled using the program Geneious (version 5.6.5, Biomatters, Auckland, New Zealand).

Amino acid sequences produced from the RR2 PCR products (three in total) were aligned with BLAST (Altschul *et al.*, 1997) matches from the NCBI non-redundant protein database (<http://www.ncbi.nlm.nih.gov/protein>), six putative viral partial ribonucleotide reductase small subunit (RR) sequences obtained from *Symbiodinium* cultures CCMP421 and PK13, and two putative viral sequences previously obtained from WPS-infected corals (Davy, 2007), using CLUSTALW (Thompson *et al.*, 1994) within the program Geneious (version 5.6.5, Biomatters, Auckland, New Zealand). The six RR sequences from *Symbiodinium* cultures were obtained as part of the latent virus screening carried out in Chapter 2, and the methods used to obtain them can be found in Chapter 2, section 2.2.4. Maximum likelihood analysis was performed using PHYML (Guindon and Gascuel, 2003) in the program Geneious, with bootstrap analysis of 100 replicates.

Translated RR2 PCR products were also searched against newly-generated transcriptomes of three *Symbiodinium* cultures, using the local BLAST function in BioEdit version 7.2.0 (Hall, 1999), with a maximum e-value of 10^{-6} .

The nucleotide sequence accession numbers for the PCR products in the Genbank database are: KC540773 – KC540777 (*Porites australiensis*) and KC540767 – KC540772 (*Symbiodinium*).

Note: In addition to WPS, the coral diseases *Porites* tissue loss (PorTL) and *Porites* growth anomaly (PorGA), affecting *Porites* spp. corals at Kaneohe Bay, Hawaii, were investigated using electron microscopy and a similar sampling regime to that described in this chapter. Brief descriptions of these studies are presented in appendices G and H.

5.3. Results

5.3.1. Transmission electron microscopy

Coral host tissue was found to remain relatively intact within the disease lesion. Although not quantified, necrosis (characterised by chromatin condensation, cell/organelle swelling and vacuolisation of the cytoplasm) and apoptosis (characterised by cell shrinkage, chromatin condensation and formation of apoptotic bodies) of coral and *Symbiodinium* cells appeared to be occurring at similar rates in all samples (see Fig. 5.2A and B for examples). Little cell debris was observed amongst surrounding cells or in the gastric cavity of the host, suggesting that necrosis was not occurring extensively in healthy or diseased tissues. One notable difference among sample types was the presence of ‘holes’ in the gastrodermis of diseased colonies, presumably caused by loss of *Symbiodinium* cells (Fig. 5.2C). Although not quantified, these tissue holes were relatively rare in healthy tissue samples. Numerous bacterial aggregates were seen in both healthy and diseased samples, with no apparent correlation with disease state (Fig. 5.2D), and endolithic microbes were often seen in the calicodermis (the ectodermal cell layer responsible for producing the calcium carbonate skeleton in scleractinian corals; Fig. 5.2E).

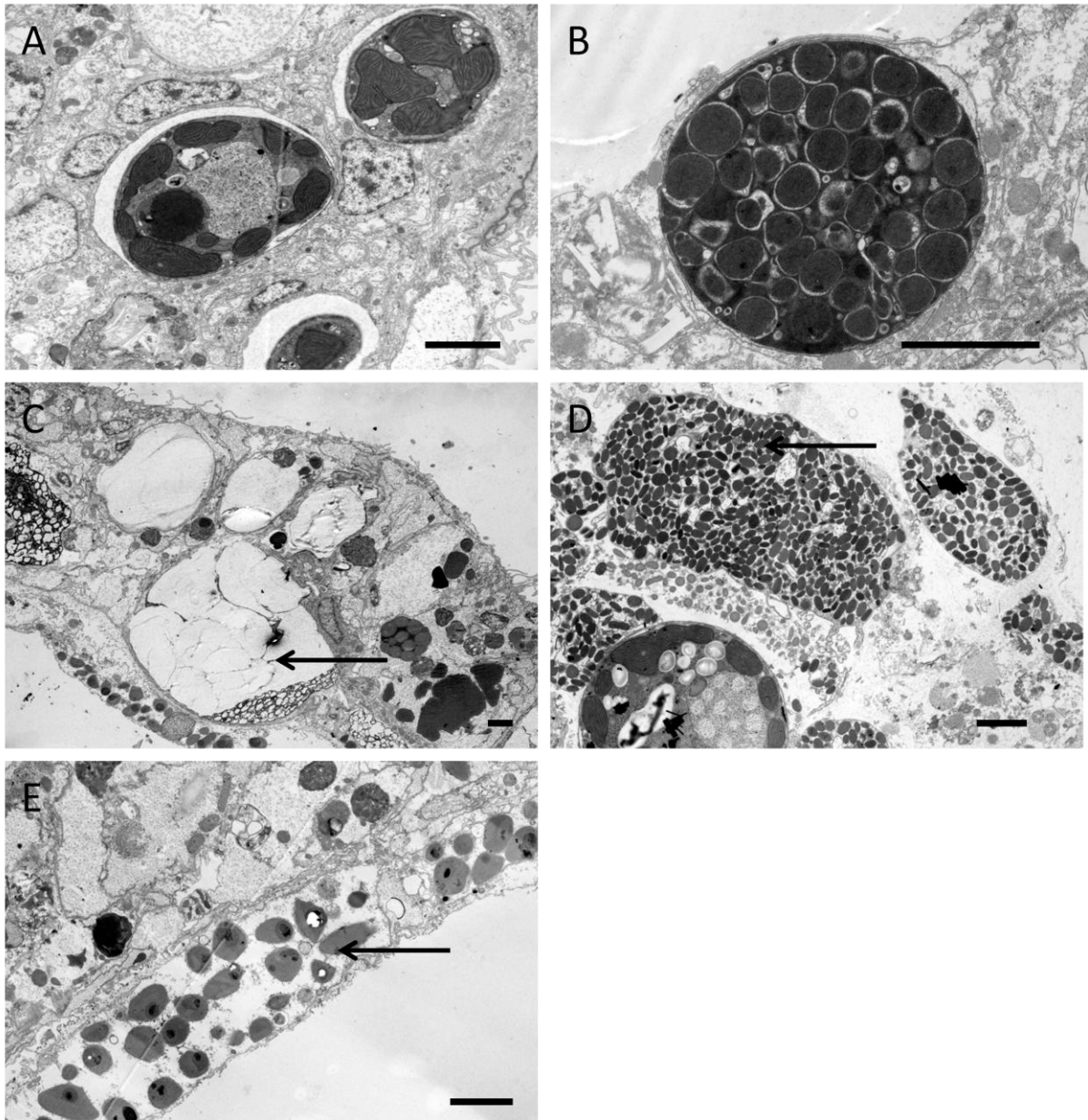


Figure 5.2. Transmission electron micrographs of *Porites australiensis* coral and *Symbiodinium* cells. (A) *Symbiodinium* cells in early stage of apoptosis from tissue 1 cm away from WPS lesion; (B) necrotic *Symbiodinium* cell from lesion tissue; (C) tissue holes (arrow) resulting from *Symbiodinium* loss in coral gastrodermal tissue 1 cm away from lesion; (D) bacterial aggregates (arrow) in the gastrodermis a healthy colony of *P. australiensis*; (E) endolithic bacteria (arrow) in the calicodermis of *P. australiensis*. Scale bars are 2 μ m.

Numerous virus-like particles (VLPs) were observed in all samples and cell types (epidermis, gastrodermis and *Symbiodinium* cells). Virus-like particles often formed large aggregates within the cytoplasm of coral gastrodermis and epidermis cells, as well as being found as

individual particles scattered throughout these tissues (Fig. 5.3). Icosahedral VLPs ranging in size from ~20 nm – 200 nm were seen in coral tissues, while *Symbiodinium* VLPs consisted mostly of filamentous VLPs up to 100 nm in length, with icosahedral VLPs also present in some samples (Fig. 5.4). All VLPs appeared to be non-enveloped, without tails or other appendages (Fig. 5.3). Non-parametric analysis of variance revealed no significant difference in overall VLP abundance among sample types (Kruskal-Wallis, $p = 0.101$). Likewise, at the level of cell type (epidermis, gastrodermis and *Symbiodinium*), there was no significant difference in overall VLP abundance (Kruskal-Wallis, $p = 0.06$) or abundance of individual VLP size/morphology classes among sample types. There was, however, a significant difference in overall abundance of small (< 50 nm diameter) icosahedral VLPs among sample types (Kruskal-Wallis, $p = 0.021$), with ~3 times more seen in tissue collected 1 cm away from disease lesions than in healthy or diseased tissues. There was an apparent increase in filamentous VLPs > 50 nm in length in *Symbiodinium* cells from diseased colonies (lesion: ~400%, 1cm: ~600% increase) (Fig. 5.4), however this difference was not statistically significant (Kruskal-Wallis, $p = 0.218$).

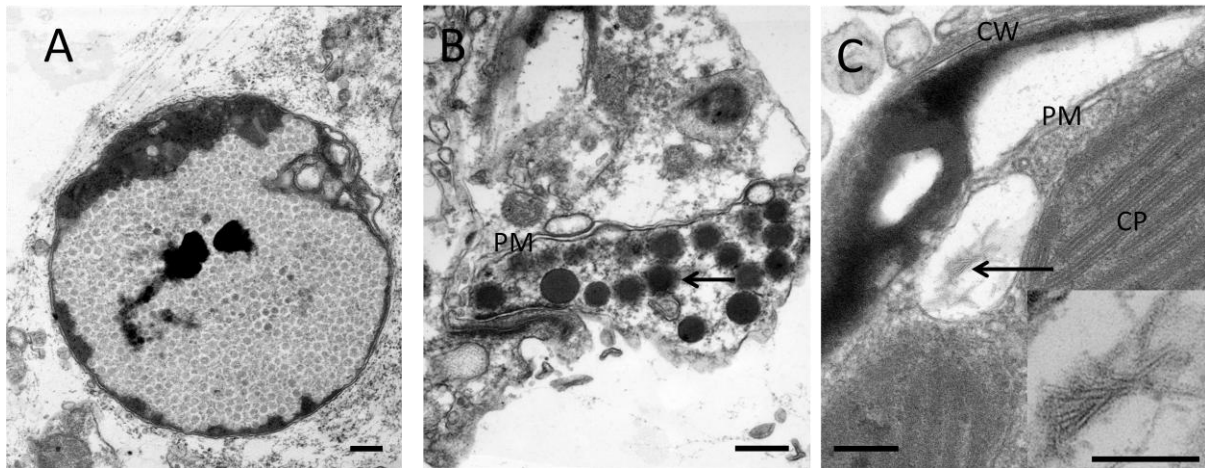


Figure 5.3. Transmission electron micrographs of virus-like particles (VLPs) in *Porites australiensis* colonies. (A) Small (50 – 60 nm diameter), icosahedral VLPs in a *Symbiodinium* cell from a healthy *P. australiensis* colony; (B) large, icosahedral VLPs (arrow) in epidermal tissue collected from a WPS lesion; (C) filamentous VLPs (arrow) in a *Symbiodinium* cell from tissue 1 cm away from WPS lesion (inset: higher magnification image of VLPs). Scale bars are 200 nm. PM: plasma membrane, CW: cell wall, CP: chloroplast.

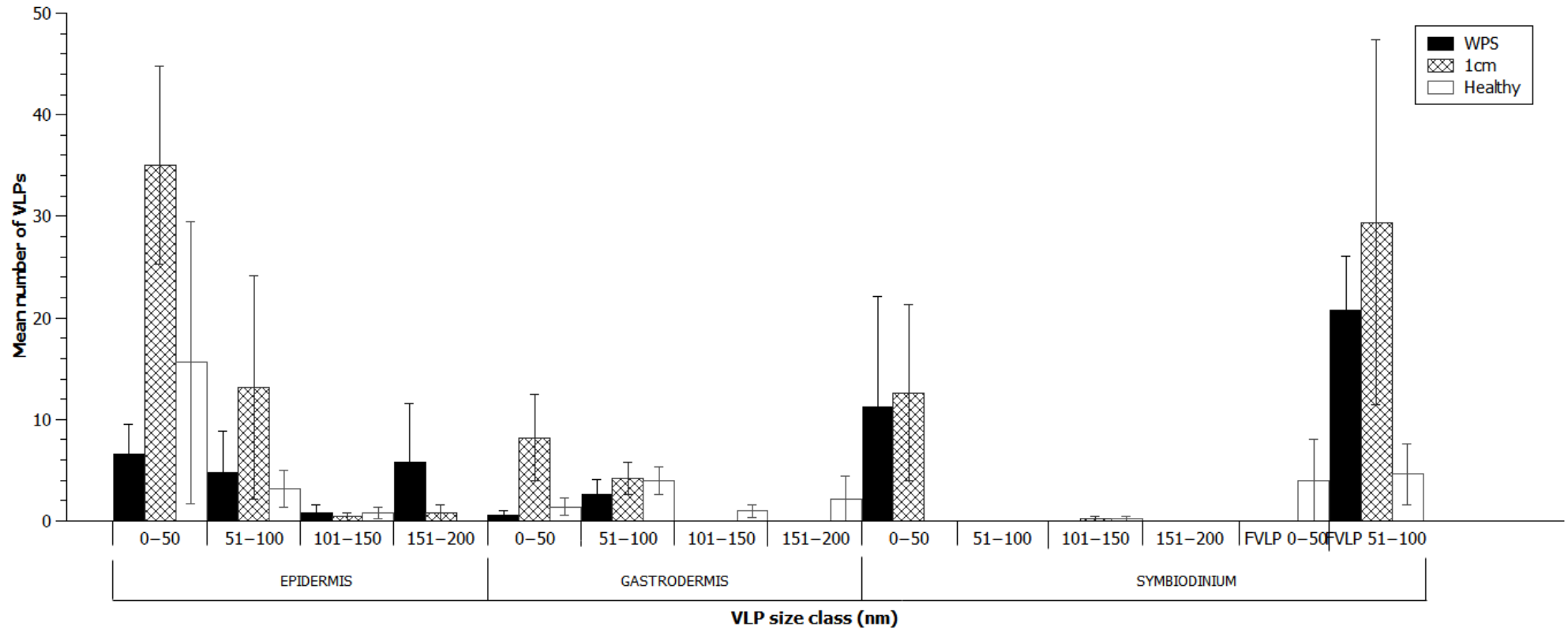


Figure 5.4. Abundance of VLP morphotypes found in *Porites australiensis*. Black bars represent WPS lesion tissue, shaded bars represent tissue 1 cm away from lesion, and white bars represent samples from healthy colonies. Error bars represent standard error.

5.3.2. Virus molecular analysis

Virus-like particles were observed in several fractions of sucrose gradients obtained from *P. australiensis* (see Fig. 5.5 for a representative electron micrograph of a sucrose gradient fraction). Prokaryotic or eukaryotic cells were not seen in any of the sucrose gradient fractions examined with the TEM. Three RR sequences (86 – 95 amino acids (AA) in length) were obtained from three *P. australiensis* samples (all sequences were obtained from tissue samples collected 1 cm away from lesions). BLAST searches showed that these sequences belonged to the RR gene; however the nearest matches were disparate and had fairly low sequence identity (closest matches showed 65 – 85% identity). The RR sequences were also searched against newly-generated transcriptomes of three *Symbiodinium* cultures (see Chapter 3). Significant matches (e-value < 10^{-6}) were found for all RR sequences in the transcriptomes, however the pair-wise sequence identity was < 68% in all cases.

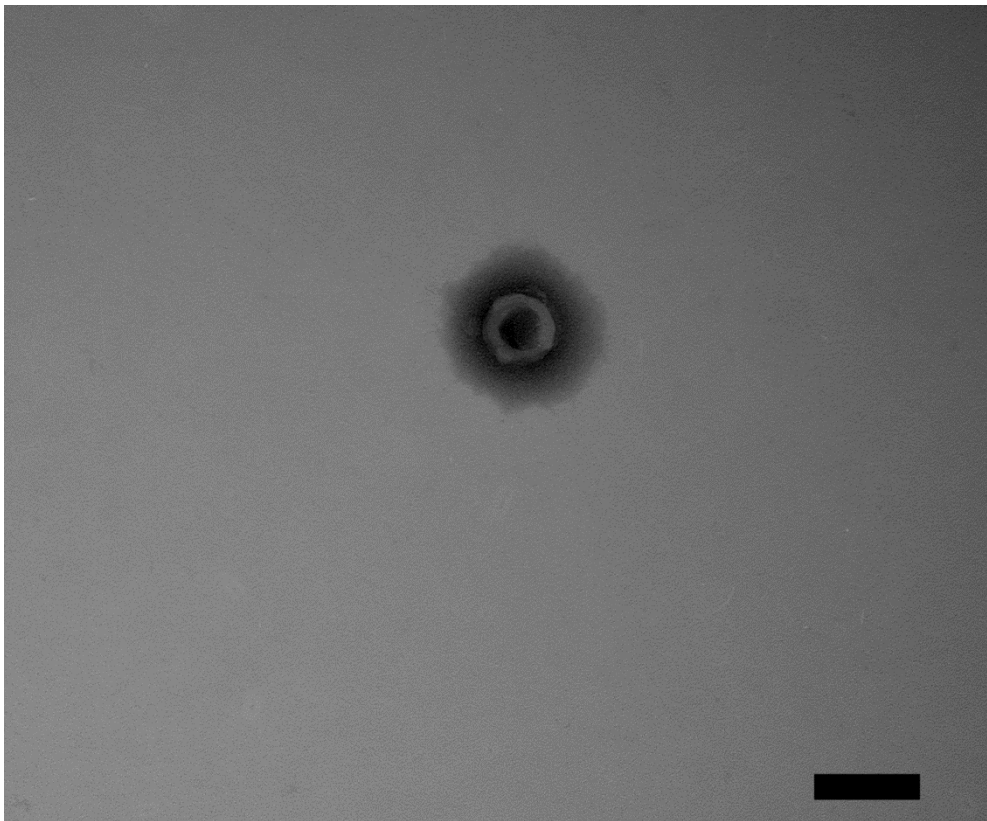


Figure 5.5. Representative transmission electron micrograph of a sucrose gradient fraction obtained from tissue adjacent to a WPS disease lesion in *P. australiensis*. The micrograph shows an icosahedral virus-like particle, approximately 100 nm in diameter. Scale bar represents 100 nm.

The partial RR sequences obtained from putative *Symbiodinium* viruses showed pair-wise identities as low as 50% to the *P. australiensis*-derived sequences, and identity among the coral-derived sequences obtained here and by Davy (2007) was as low as 51%, suggesting that the sequences belong to several different viruses. As can be seen in Fig. 5.6, the coral- and *Symbiodinium*-derived sequences fall on several different branches, among different groups of prokaryotes and eukaryotes. Of note, however, are the three RR sequences obtained from coral tissue adjacent to WPS lesions that show very high identity (up to 97%) to three sequences obtained from UV-stressed *Symbiodinium* cultures (Fig. 5.6).

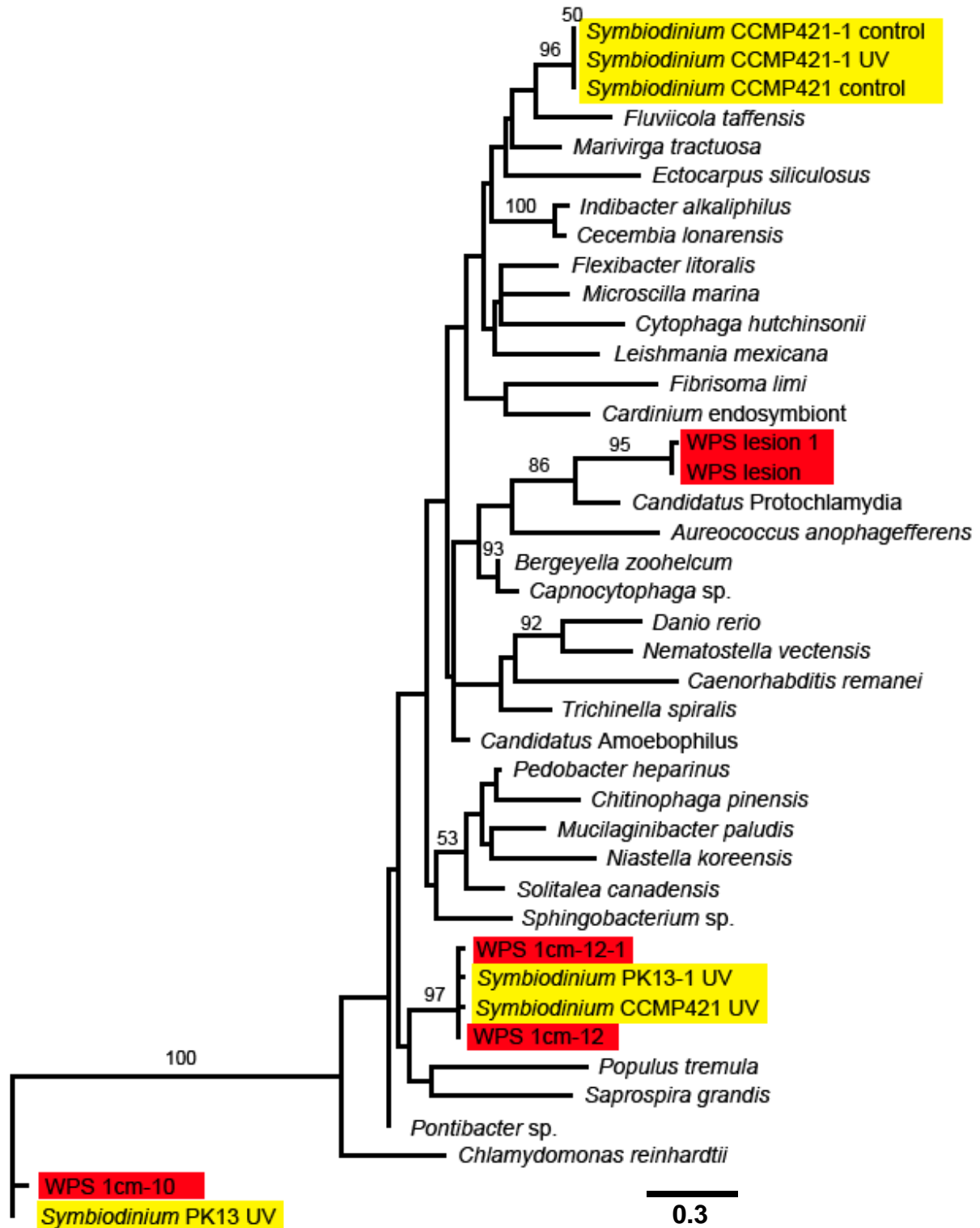


Figure 5.6. Maximum likelihood tree of ribonucleotide reductase small subunit amino acid sequences obtained from *Porites australiensis* corals suffering from the disease white patch syndrome (WPS, red boxes) and from control and UV-irradiated *Symbiodinium* cultures (yellow boxes). WPS lesion – tissue sample taken directly from disease lesion by Davy (2007); WPS 1cm – tissue sample taken 1cm away from the disease lesion. Branch labels show bootstrap support (100 iterations). Branch labels indicate bootstrap support (100 iterations) and the scale bar represents the number of nucleotide substitutions per site. Bootstrap values < 50 are not shown. Note: this figure is reproduced from Chapter 2 (Fig. 2.16).

5.4. Discussion

In this study I examined the microscopic features associated with white patch syndrome (WPS) of *Porites australiensis*, and characterised viruses associated with the disease.

TEM analysis confirmed the findings of Davy (2007), who found evidence that WPS causes *Symbiodinium* cell loss without significant damage to host cells. Host tissues from diseased samples were not visibly different from tissue samples from healthy colonies, but there was evidence of *Symbiodinium* cell loss. This is also in line with the findings of Roff *et al.* (2008), who found decreased photosynthetic health in WPS lesions. The loss of *Symbiodinium* cells seen here is consistent with previous reports of disease-induced symbiont expulsion (Cervino *et al.*, 2004). While the loss of *Symbiodinium* cells is consistent with conventional coral bleaching, the patchy distribution of lesions (Fig. 5.1) and the lack of a correlation between disease prevalence and season or water temperature (Davy, 2007) strongly suggest that WPS is a separate phenomenon. Lesser *et al.* (2007) noted that the majority of infectious coral diseases are opportunistic infections following episodes of stress, but given the apparent lack of environmental stressors found by Davy (2007), the causative agent of WPS may not require a compromised host for infection. Of course, the absence of thermal stress does not mean other stressors were not present; further study is required to rule this out.

Bacterial abundance in the corals studied here was patchy and did not appear to differ with disease state, whereas abundance of small VLPs was significantly higher in tissue samples collected 1 cm away from WPS lesions than in healthy tissues. Although not significantly different, there was also an apparent increase in abundance of filamentous VLPs in *Symbiodinium* cells from diseased colonies, compared to tissue samples from healthy colonies. While the icosahedral VLPs seen in coral tissues are difficult to identify based solely on morphology, the filamentous VLPs seen in *Symbiodinium* resemble those seen in stressed cultured *Symbiodinium* by Lohr *et al.* (2007) and in cultures of *Symbiodinium* following stress in this thesis (Chapter 2). Lohr *et al.* (2007) hypothesised that these filamentous VLPs were members of the *Closteroviridae*, but these VLPs also resemble other virus groups such as the *Inoviridae* and *Flexiviridae*. Without the use of more specific PCR primers or other molecular techniques such as whole-genome amplification, it is not possible to state which family they belong to.

Amino acid sequences obtained here further suggest that viruses are involved in WPS. Very few VLPs were seen in sucrose gradient fractions from healthy colonies compared to those from diseased colonies, and subsequent viral DNA extraction was successful only with samples from diseased colonies. The high level of similarity between sequences from samples taken adjacent to WPS lesions and putative viral sequences from UV-stressed *Symbiodinium* suggests that these viruses may be involved in damage and subsequent loss of the symbionts. The fact that sequences derived from the WPS lesion itself did not group with these sequences may be due to many of the putative disease-causing viruses either being released from lysed cells or being lost simultaneously with the *Symbiodinium* cells; lysis was not seen in electron micrographs however. The sequences obtained from the lesions may therefore belong to another resident virus of the coral, of which there are probably many (Vega Thurber and Correa, 2011).

The PCR primers used here were by necessity non-specific, as primers targeting specific viral groups (*Circoviridae*, *Nanoviridae* and microalgal viruses; see Appendix F) did not successfully amplify DNA. It could therefore be argued that the sequences obtained here represent contamination by host or microbial DNA, rather than being viral in origin. I believe this not to be the case for several reasons. First, the extraction methods used should have removed all host and microbial cells prior to DNA isolation. While this was not confirmed by 16S PCR analysis, no cells were seen in any of the electron micrographs of sucrose gradient fractions (see Fig. 5.5). Second, the NCBI non-redundant protein database contains many thousands of RR sequences, including a vast array for bacteria and several dinoflagellates and cnidarians. If the sequences obtained here were eukaryotic or prokaryotic in origin, one might expect to see a greater degree of similarity between these sequences and BLAST matches (similarly, one would expect a higher degree of similarity between the RR sequences and those detected in the three *Symbiodinium* transcriptomes if they were derived from the *Symbiodinium* genome, rather than latent viruses therein). Finally, assuming based on the above that the sequences do not in fact represent contaminating *Symbiodinium* DNA, the high level of similarity between sequences from tissue adjacent to lesions and sequences from stressed *Symbiodinium* cultures suggests a viral source. These *Symbiodinium* have been in culture for several years, thus ruling out contamination by cnidarian nucleic acid. Taken together, this suggests that the *Symbiodinium* cells in culture and *in hospite* contain latent viral infections which can be induced, through stress or otherwise, to enter the lytic cycle.

Algal viruses are often highly host-specific (Brussaard, 2004b; Dunigan *et al.*, 2006; Bellec *et al.*, 2010), and it would therefore not be surprising to find highly similar viral sequences in different *Symbiodinium* samples. Latent viruses have been found in a range of marine brown algae (Müller *et al.*, 1996; Kapp, 1998) and in *Symbiodinium* (Lohr *et al.*, 2007). These reports are consistent with findings here, where numerous types of *Symbiodinium* may harbour a seemingly harmless latent infection, which can be induced to cause cell lysis through UV stress (Chapter 2).

In summary, I have shown that WPS is a disease affecting, either directly or indirectly, *Symbiodinium* cells in *P. australiensis* on the Great Barrier Reef. *Symbiodinium* cells are lost without any noticeable damage to the surrounding coral tissue, resulting in the bleached appearance of the disease lesion. There is a suggestion that viruses play a role in loss of *Symbiodinium* cells, though the trigger for viral induction has not yet been identified. Furthermore, whether the putative viruses directly infect the *Symbiodinium* cells or cause breakdown of the symbiosis by infecting the coral host's cells remains to be determined. Future work should focus on confirming the viral basis of the disease and determining whether it is a latent or opportunistic infection. If WPS is indeed confirmed as a viral disease, the next step will be to identify the biotic or abiotic factor which induce viral lysis or allow infection. Given the patchy nature of the disease lesions, the cause may either be an environmental stressor causing viral induction, or a vector, such as a fish or invertebrate, transferring the virus to the coral.

Chapter 6: General discussion

6.1. Review of aims

The overall aim of this thesis was to characterise the viruses associated with reef-building corals and dinoflagellates of the genus *Symbiodinium*. The specific objectives of the thesis were to 1) screen a range of *Symbiodinium* cultures for the presence of latent viral infections, and characterise the viruses when found; 2) determine whether similar viruses infect a range of *Symbiodinium* cultures by analysing several *Symbiodinium* transcriptomes; 3) elucidate the host response to induction of latent viral infections in *Symbiodinium* by analysing gene expression; and 4) determine what role, if any, viruses play in several diseases of poritid corals.

A variety of methods were employed to address these objectives. Initial screening of *Symbiodinium* cultures for latent viruses was done using stress experiments and flow-cytometric analysis of cell cultures. This was followed by electron microscope examination of *Symbiodinium* cell sections and phylogenetic analysis of putative viral ribonucleotide reductase small subunit (RR) genes, in an attempt to identify the latent viruses. Several *Symbiodinium* cultures, chosen because they showed evidence of inducible latent viral infections, had their entire transcriptomes sequenced. Differential gene expression was measured for a range of genes involved in response to viral infection, and the transcriptomes were searched for the presence of genes of viral origin. The transcriptomes were also compared with existing *Symbiodinium* EST libraries to identify putative viral genes conserved among different cultures. Electron microscopy and phylogenetic analysis of RR genes were also used to characterise the viruses associated with three coral diseases, with a particular focus on white patch syndrome (WPS) of *Porites australiensis* corals on the Great Barrier Reef (GBR).

6.2. Summary of results

Around 30% of the *Symbiodinium* cultures screened were found to harbour latent or chronic viral infections that could be induced to enter the lytic cycle by stress. Characterisation of the

infections suggested that morphologically diverse viruses can infect *Symbiodinium*, and that they may be unique from other algal viruses, given their lack of sequence identity with known viruses. In the *Symbiodinium* cultures examined here, gene expression was surprisingly similar pre- and post-stress, however several groups of genes known to be involved with viral infection and host response were upregulated following stress. Furthermore, numerous genes believed to be viral in origin had higher expression levels following stress. In addition, several genes apparently belonging to dsDNA viruses were shared between three or more cultures of *Symbiodinium*, suggesting that highly similar viruses can infect a range of *Symbiodinium* types. Finally, microscopic analysis revealed the presence of abundant virus-like particles (VLPs) associated with healthy and diseased poritid corals. Counts of the VLPS and DNA sequence analysis supported the notion that viruses play a role in the development of WPS. Despite higher counts of some VLP types in coral tissues affected by WPS, sequence analysis and microscopic examination of coral tissues suggested that *Symbiodinium*-infecting viruses may play an important role.

The major findings of the thesis will be discussed in more detail in the following sections.

6.3. Viruses of *Symbiodinium*: identities

Following initial screening, electron microscopy was used to examine eleven of the most promising cultures. This revealed the presence of several sizes and morphological types of VLPs. Morphologically, these could be divided into two groups: icosahedral and filamentous. Filamentous VLPs, which were found in eight *Symbiodinium* cultures, varied in length from ~100 – 1,000 nm in length, while icosahedral VLPs were found in seven cultures and ranged from crystalline arrays of ~20 nm diameter particles to giant VLPs > 500 nm in diameter. These findings suggest that *Symbiodinium* cells are susceptible to infection or are already latently infected by a range of viruses, a proposition supported by the fact that several *Symbiodinium* cultures contained more than one type of VLP.

Based on the sizes of the observed icosahedral VLPs, it seems likely that most were dsDNA viruses (Fauquet *et al.*, 2005), i.e. Group I in the Baltimore classification (Baltimore, 1971). Transcriptome analysis produced similar results: with the exception of one transcript in

CCMP421 that matched an RNA virus, the nearest BLAST matches of transcripts identified as ‘viral’ all belonged to dsDNA viruses. It must be stated, however, that > 50% of transcripts in each transcriptome had no significant BLAST hits, so the presence of other types of viruses cannot be ruled out. Approximately 90% of the putative viral genes in each *Symbiodinium* transcriptome belonged to the *Phycodnaviridae*, *Mimiviridae*, or *Mimiviridae*-like (i.e. the *Megaviridae* and *Marseilleviridae*) virus families. These families comprise the “giant viruses” (Claverie *et al.*, 2006; Wilson *et al.*, 2009; Arslan *et al.*, 2011; Colson *et al.*, 2013), so-named because of their large genomes (100,000 – 1,260,000 bp) and particle sizes (100 – 450 nm diameter). Surprisingly, the cultures used for transcriptomic analysis did not contain dsDNA-type VLPs in electron micrographs, despite transcriptome analysis suggesting their presence. There are several possible explanations for this inconsistency. First, only two time points post-stress were chosen for TEM examination, and these did not correspond exactly with the time points at which RNA was extracted for transcriptome analysis. This may have led to the production of VLPs in the cells not being observed. Assuming that these infections are latent, rather than chronic (discussed in section 6.4, below), there would only be a small window of time in which the viral particles could be observed in the cells, prior to lysis. Furthermore, TEM processing involved washing the cells, which removed surrounding culture medium. Thus, most VLPs released from lysed cells would have been lost. Finally, given the low sequence similarity between the ‘viral’ genes in the transcriptomes and their nearest BLAST hits, the genes may have belonged to a different group of viruses. While this is a possibility, given the prevalence of dsDNA viruses in the databases, it seems unlikely due to the large number of ‘dsDNA virus’ genes detected; i.e. one would expect at least a few of them to match with non-dsDNA viruses if they truly belonged to one of these viral groups. It therefore seems probable that the transcriptomic analysis is correct, and that these *Symbiodinium* cultures are infected by dsDNA viruses similar to the phycodnaviruses and mimiviruses, despite not being observed under the microscope.

The tiny VLPs making up the crystalline arrays resembled viruses belonging to the families *Nanoviridae* and *Circoviridae*, however PCR using primers targeting these families failed to amplify DNA (possibly due to unsuitable primers). The identity of these putative viruses therefore remains undetermined. Interestingly, similar VLP arrays were seen in the endolithic bacteria of *Porites australiensis* corals examined in Chapter 5. There was no evidence of bacteria in the *Symbiodinium* cells, however. Similar crystalline virus arrays have been found

in a free-living dinoflagellate (Lawrence *et al.*, 2001), but this is the first report of such viruses in *Symbiodinium*. *Circoviridae*- and *Nanoviridae*-like sequences have been found in coral metagenomes (Wegley *et al.*, 2007; Vega Thurber *et al.*, 2008), however it is unknown whether these were associated with the *Symbiodinium* or coral cells.

The presence of filamentous VLPs in many of the *Symbiodinium* cultures was an interesting finding. While filamentous VLPs have been found previously in *Symbiodinium* (Lohr *et al.*, 2007), viruses with this structure generally infect terrestrial plants, so it is interesting that they are apparently prevalent in several types of *Symbiodinium*. Filamentous viruses almost exclusively contain single-stranded RNA (ssRNA) genomes (Fauquet *et al.*, 2005). Transcriptome analysis revealed only one gene putatively belonging to an RNA virus, though the lack of database matches for > 50% of transcripts may have concealed the presence of other RNA virus genes. Vega Thurber *et al.* (2008) found numerous plant virus-like sequences in metagenomes of the coral *Porites compressa*, so it is entirely possible that similar viruses infect *Symbiodinium*. Correa *et al.* (2012) also found sequence-based evidence of an ssRNA viral infection in *Symbiodinium*, but did not visualise the infection microscopically. It is feasible that the sequence belonged to filamentous VLPs such as those seen here, though further work is required to determine this.

In summary, the results of this thesis suggest that *Symbiodinium* are infected by a variety of viruses. This variety includes viral groups that commonly infect algae, as well as some less-common groups. The *Phycodnaviridae*, for example, are well-known viruses of marine algae (Van Etten *et al.*, 2002). Mimiviruses, on the other hand, were initially isolated from Archaea (La Scola *et al.*, 2003), though they and their relatives have now been found in seawater (Ghedini and Claverie, 2005; Arslan *et al.*, 2011) and in association with corals (Wegley *et al.*, 2007; Vega Thurber *et al.*, 2008). Similarly, the presence of VLPs resembling plant viruses, while unusual in marine algae, is not without precedent in corals (Wegley *et al.*, 2007; Vega Thurber *et al.*, 2008) and *Symbiodinium* (Lohr *et al.*, 2007; Correa *et al.*, 2012). These findings serve to underline the incredible diversity of marine viruses, and how little is currently known about them. With the advances made in viral metagenomics (Edwards and Rohwer, 2005; Kristensen *et al.*, 2009) and the advent of next-generation sequencing technologies (Hall, 2007; Radford *et al.*, 2012), many new and interesting virus-host relationships are likely to be revealed in the near future.

6.4. Viruses of *Symbiodinium*: latent versus chronic infections

One of the objectives of this thesis was to determine whether *Symbiodinium* cells harbour latent viral infections that can be induced, *via* stress, to enter the lytic cycle. Latency is used here to refer to proviral or episomal infections, where the viral genome is maintained in the host cell without the production of virions – i.e. not an active, or lytic, infection. It was initially hypothesised that viral infections in *Symbiodinium* would be latent, based on prior evidence from these algae (Wilson *et al.*, 2001; Lohr *et al.*, 2007). Viruses of other marine algae, however, have been shown to form both latent (Maier *et al.*, 1998; Delaroque *et al.*, 1999; Meints *et al.*, 2008) and chronic infections (Van Etten *et al.*, 1991; Thomas *et al.*, 2011a). A chronic infection is defined here as a productive infection that steadily produces a small number of virions, which are released without cell lysis under normal circumstances.

Examination of thin sections of *Symbiodinium* cells before and after UV stress revealed that, in addition to latent infections, several cultures were apparently chronically infected with viruses. Additionally, some cultures appeared to harbour both chronic and latent infections, as evidenced by the presence of different VLPs pre- and post-stress. This latter finding was particularly interesting, as previous studies have only found one type of virus in the particular *Symbiodinium* culture being examined. That said, the two studies that have demonstrated the presence of latent viruses in *Symbiodinium* found very different VLPs: filamentous VLPs (Lohr *et al.*, 2007) and small, icosahedral VLPs (Wilson *et al.*, 2001). Both of these VLP forms were very similar to those found here, and the possibility exists that secondary viral infections were overlooked in the cited studies.

Based on the TEM examination and flow cytometry analysis, it is hypothesised that three types of viral infection were present in the *Symbiodinium* cultures studied here: 1) dsDNA viruses forming latent infections; 2) filamentous (probably ssRNA) viruses forming latent infections; and 3) chronic infections formed by dsDNA viruses, other icosahedral viruses and filamentous viruses (Fig. 6.1A). This hypothesis is partially supported by the transcriptome data, which showed that genes apparently belonging to dsDNA viruses were expressed in both control and stressed *Symbiodinium* samples. Although the expression of these genes both pre- and post-stress prevents discrimination between latent and chronic infections, it at least rules out a proviral infection, where the viral genes would be hidden in the host genome

and not expressed under normal conditions. Furthermore, when considered alongside the TEM data, these results suggest that the dsDNA viruses form latent episomal infections rather than chronic infections. In the latter scenario, virions would be present in the control *Symbiodinium* cells, but this was not the case in the three cultures whose transcriptomes were analysed. Unfortunately, transcriptome analysis did not reveal any genes belonging to the presumed filamentous viruses, preventing confirmation of their hypothesised infection strategies. This was likely because they belonged to the > 50% of transcripts with no significant BLAST hit, or because they were simply not being expressed at the time of sampling.

6.5. Viruses of *Symbiodinium*: implications for coral health and disease

This thesis has shown that stress can induce viral infections (either latent or chronic) in *Symbiodinium*, resulting in cell lysis. The stressor used here, shortwave (254 nm) UV radiation, was chosen as it most consistently resulted in cell lysis and production of VLPs. As an exploratory study of *Symbiodinium* viruses, this was considered more important than selection of a more ecologically-relevant stressor (UV radiation of this wavelength is not found in the oceans, as it is blocked by atmospheric oxygen). Nevertheless, the results show that stress induction of these viruses is possible, and experiments using the more ecologically-relevant stressor of UV-B radiation (302 nm wavelength) did show evidence of viral induction in some *Symbiodinium* cultures.

Assuming that the viruses discovered here can also be induced in real world situations, this has clear implications for coral functioning and disease. The evidence for anthropogenic global warming is now overwhelming (IPCC, 2007a), and this phenomenon brings with it a suite of potential stressors, including rising ocean temperatures (IPCC, 2007a) and ocean acidification (Orr *et al.*, 2005; Feely *et al.*, 2009). Other threats to corals and their algal symbionts include pollution from terrestrial runoff (ISRS, 2004; Redding *et al.*, 2013), and overfishing (and flow on effects such as increased algal cover) (Mumby *et al.*, 2006; Kennedy *et al.*, 2013). Field experiments have also shown that UV radiation – at naturally-occurring wavelengths – can inhibit coral growth and lead to coral bleaching, both in isolation and in conjunction with thermal stress (reviewed in Banaszak and Lesser, 2009).

Whether any of these stressors are capable of inducing latent infections in corals or *Symbiodinium* cells remains to be seen.

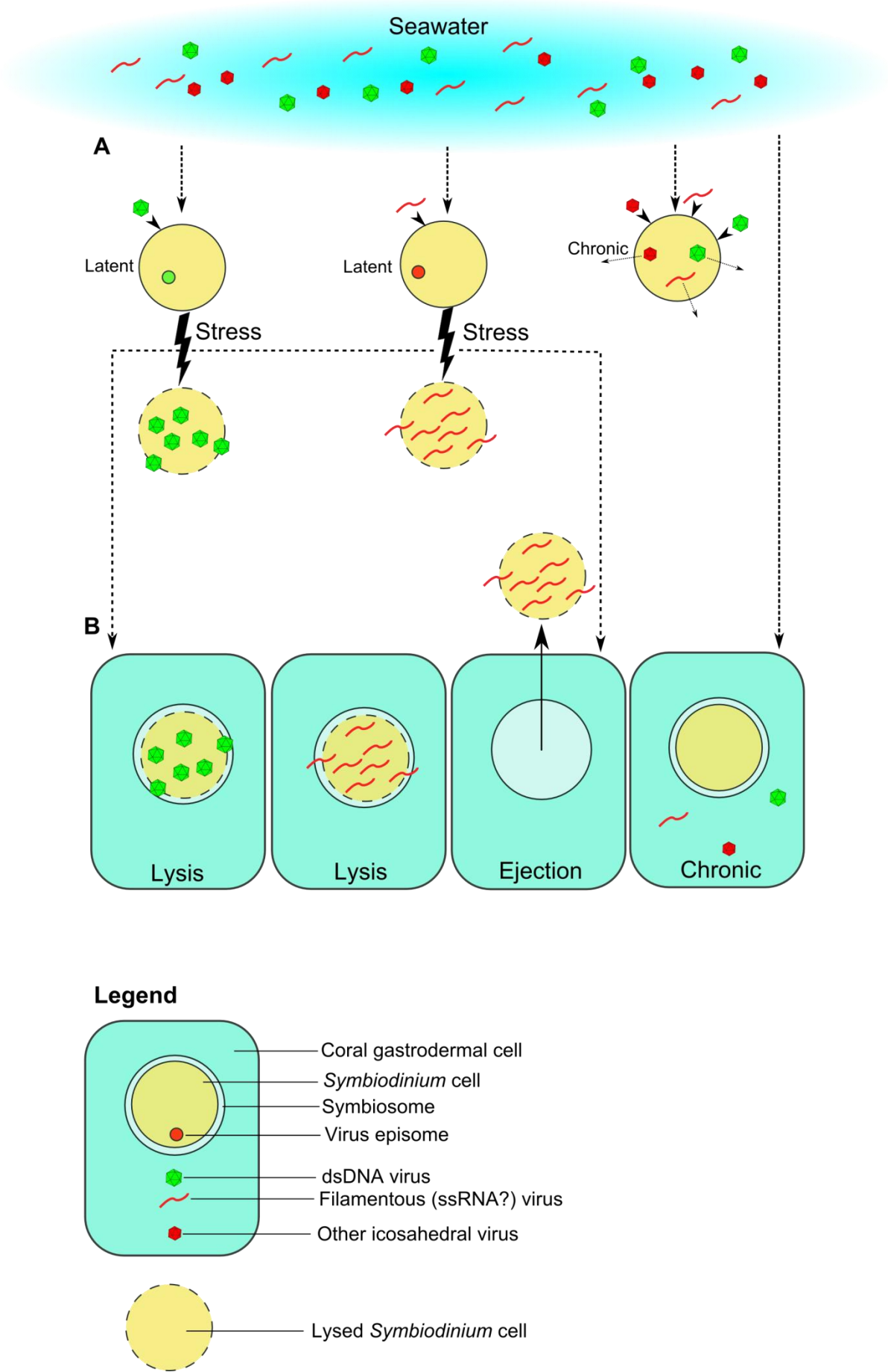
Evidence obtained here from diseased poritid corals suggests that *Symbiodinium* cells *in hospite* may contain latent viral infections that can be induced, resulting in cell lysis. The environmental trigger of induction is unknown; environmental parameters were not recorded during sampling, though there were no obvious stressors, such as temperature anomalies or increased solar irradiation, noted. A theoretical model of latent viral infection in white patch syndrome (WPS) of *Porites* spp. corals is presented in Fig. 6.1B. This model proposes that coral cells are routinely subject to chronic viral infections – evidence for this comes from the finding here and in previous studies (Wilson *et al.*, 2005a; Patten *et al.*, 2008) of abundant VLPs in apparently healthy corals. *Symbiodinium* cells within the coral gastrodermis are proposed to harbour two types of viruses: a chronic or latent filamentous virus, and a small dsDNA virus. This proposition is supported by TEM analysis of WPS, as well as the infection strategies employed by similar viruses in cultured *Symbiodinium*, and the similarity between putative viral ribonucleotide reductase sequences from WPS samples and *Symbiodinium* cultures. Furthermore, this agrees with Correa *et al.* (2012), who found evidence of a dsDNA and an ssRNA virus associated with *Symbiodinium* in the coral *Montastrea cavernosa*. Although the icosahedral VLPs seen in *Symbiodinium* cells *in hospite* were relatively small (~50 nm in diameter) compared to most dsDNA viruses, the families *Caulimoviridae*, *Polyomaviridae* and *Papillomaviridae* contain dsDNA viruses of this size. Papillomavirus- and caulimovirus-like sequences have previously been found in coral metagenomes (Wegley *et al.*, 2007; Vega Thurber *et al.*, 2008). Induction of the putative viruses associated with WPS leads either to lysis of the *Symbiodinium* cell *in hospite*, or breakdown of the symbiosis and ejection of the algal partner prior to lysis. The latter scenario is perhaps the more likely, as *Symbiodinium* cells undergoing lysis were not seen in electron micrographs.

The mode of initial infection of the *Symbiodinium* cells remains unresolved. If, as proposed, the viruses form latent episomal infections, then the virus would be transmitted vertically and the initial infection may have taken place many generations ago. Virus-like genes similar to the ones found here were not found in any of the ancestral alveolate genomes examined, however several of the genes were conserved among different *Symbiodinium* cultures. While not conclusive, these results suggest that an initial infection event may have occurred prior to

the divergence of *Symbiodinium* clades. Alternatively, *Symbiodinium* cells may be infected by viruses resident in seawater or associated with the coral holobiont. As has been shown here (Appendix I) and elsewhere (Davy and Patten, 2007), a diverse range of VLPs is associated with the mucus surrounding corals. Viral abundance is also known to increase with proximity to corals (Seymour *et al.*, 2005), and to be particularly high in the seawater surrounding thermally stressed (Davy *et al.*, 2006) and diseased corals (Patten *et al.*, 2006). There is consequently a vast reservoir available from which *Symbiodinium*-infecting viruses may come.

The potential for latent viral infections to cause *Symbiodinium* cell lysis or loss from the coral host raises the question of whether a similar mechanism is at play in other coral diseases, or in episodes of coral bleaching. The primary cause of bleaching events worldwide is thermal stress, which leads to elevated production of reactive oxygen species (ROS) and dysfunction of photosystem II in *Symbiodinium* cells (Weis, 2008). However, studies have shown that bacteria cause bleaching in the corals *Oculina patagonica* (Kushmaro *et al.*, 1996; Rosenberg and Falkovitz, 2004) and *Pocillopora damicornis* (Ben-Haim *et al.*, 2003a; Ben-Haim *et al.*, 2003b), by producing toxins that block photosynthesis (Ben-Haim *et al.*, 1999). Although there is not yet evidence of a similar role for viruses, in cases where the cause of bleaching is not apparent the possibility of a viral causative agent is certainly worthy of examination.

Figure 6.1 (overleaf). Proposed infection strategies of *Symbiodinium* viruses and their role in white patch syndrome (WPS) of *Porites* spp. corals. A: Two infection strategies – episomal latency and chronic infections – are utilised by viruses infecting *Symbiodinium* cells. In cases of episomal latency, stress can cause induction and cell lysis, whereas in chronic infections, viruses are periodically produced and released without cell lysis. B: Following stress, *Symbiodinium* cells *in hospite* are either lysed or lost from the host's gastrodermal cells, resulting in the bleached appearance of WPS lesions. Coral gastrodermal cells also contain several types of viruses that are apparently chronic in nature. Figures are not to scale.



6.6. Future directions

The results of this thesis open up two avenues of potential future research. First, the evidence presented here of latent viral infections in *Symbiodinium* warrants further investigation and characterisation of these viruses. Second, the transcriptomic data provide a basis for molecular diagnosis of viral infections of *Symbiodinium*, both in culture and *in hospite*.

There is now clear evidence that numerous *Symbiodinium* cultures are infected by viruses. Further, there appear to be several types of viruses infecting *Symbiodinium*, employing several different infection strategies. As this study was largely exploratory in nature, work remains to be done to further characterise these viruses. Several approaches are recommended in order to do so. First, the use of more ecologically-relevant stressors would be helpful in determining whether induction of latent/chronic viruses is likely to be a widespread phenomenon in *Symbiodinium* in nature. Short-term thermal stress experiments were carried out here, but longer-term examinations that more closely mimic conditions found in the ocean would be beneficial. Second, isolation of the putative viruses and reinfection of healthy host cells is necessary for proper virus characterisation and fulfilment of Koch's postulates. In theory this is a straightforward procedure, a description of which can be found in Nagasaki and Bratbak (2010). In practice, however, issues such as loss of infectivity following filtration (Suttle *et al.*, 1991) and the difficulty of creating and maintaining axenic *Symbiodinium* cultures (S. Lawrence, personal observation) pose problems for virus characterisation. Nonetheless, it is worth persisting, as a more thorough characterisation of these viruses will be helpful in understanding their potential role in coral disease.

Perhaps the most useful data to come out of this thesis, in terms of future research, are the *Symbiodinium* transcriptome sequences. The five transcriptomes, from three *Symbiodinium* cultures, comprise the largest transcriptomic resource for *Symbiodinium*, or indeed any dinoflagellate, to date. The wealth of data contained in these sequences offers many opportunities for further research into *Symbiodinium*, in terms of viral infection and the general biology of these organisms. With regard to *Symbiodinium*-infecting viruses, and their potential roles in coral disease, several approaches that make use of the transcriptome sequences and other existing molecular data are proposed.

A potential first step would be validation of the transcriptome data using qPCR. Given the lack of replicates, the estimates of expression levels presented here must be treated with some caution; qPCR analysis of genes of interest (such as putative viral genes) would allow confirmation of gene expression. With the qPCR probes and kits that are now readily available, this should be a relatively rapid and straightforward procedure.

Further confirmation of the presence of viruses in *Symbiodinium* may also be provided by the development of fluorescent probes targeting the genes discovered here. Fluorescence *in situ* hybridisation (FISH) using digoxigenin-labelled probes, for example, allows visualisation of viruses or latent viral nucleic acid within cells, and has been used to identify mimiviruses (Desnues *et al.*, 2012) and herpes-like viruses (Lipart and Renault, 2002) *in situ*. *In situ* hybridisation combining digoxigenin-labelled probes and electron microscopy has also been used to determine the cellular location of viruses (Cantó-Nogués *et al.*, 2001), and could theoretically be applied to the chronic or episomal/proviral infections seen in *Symbiodinium* cells. Similarly, fibre-FISH, a variation on FISH that involves uncoiling chromosomes prior to probe hybridisation, has been used to discriminate episomal infections from proviral infections of Epstein-Barr virus (Reisinger *et al.*, 2006). While this is a fairly specialised method, it may be useful for determining the infection strategy used by viruses infecting *Symbiodinium*, and should be feasible using sequence data obtained in this study. A suggested starting point would be the *Ostreococcus*-virus-like gene identified in four *Symbiodinium* cultures in Chapter 3, as this is perhaps the most promising lead in accurately identifying the latent viruses residing in *Symbiodinium* cells.

Both this study and that of Correa *et al.* (2012) have provided evidence of a dsDNA and an ssRNA virus infecting *Symbiodinium in hospite*, and the sequence data obtained in these studies provide targets for molecular marker development. In order to determine the ubiquity, or otherwise, of these viruses in *Symbiodinium*, PCR primers (including reverse-transcriptase PCR primers to target the putative RNA virus), can now be designed and tested on *Symbiodinium* and coral samples. The development of these PCR primers may provide a useful tool for coral disease diagnosis and management.

6.7. Conclusion

This study has provided evidence that *Symbiodinium* cells are commonly infected by viruses. The data gathered here suggest that the viruses present in *Symbiodinium* are diverse, and employ several different infection strategies. Those that form latent or chronic infections can apparently be induced to enter their lytic cycle *via* environmental stress, leading to lysis of the host cell. Though it cannot be stated conclusively at this point, it appears that viruses infecting *Symbiodinium* play a role in at least one coral disease. As this is the first study to examine such a wide range of *Symbiodinium* types for viral infections, and only the second to use molecular data in an attempt to identify the viruses, much work remains to be done. The sequencing of the complete transcriptomes of three *Symbiodinium* types provides valuable information that can be used to further explore the relationship between viruses and *Symbiodinium*. It is hoped that the data presented here will prove valuable for future research into coral health, especially given the increasing threats to corals from disease, climate change and other sources.

References

- Acevedo, R., Morelock, J., 1988. Effects of terrigenous sediment influx on coral reef zonation in southwestern Puerto Rico. In: Choat, J.H., Barnes, D., Borowitzka, M.A., Coll, J.C., Davies, P.J., Flood, P., Hatcher, B.G., Hopley, D. (Eds.), *Proceedings of the Sixth International Coral Reef Symposium*, Townsville, Australia, pp. 189-194.
- Ackermann, H.-W., Haldal, M., 2010. Basic electron microscopy of aquatic viruses. In: Wilhelm, S.W., Weinbauer, M.G., Suttle, C.A. (Eds.), *Manual of Aquatic Viral Ecology*. ASLO, pp. 182-192.
- Aeby, G.S., 2006. Baseline levels of coral disease in the Northwestern Hawaiian Islands. *Atoll Research Bulletin* 543, 471-488.
- Aeby, G.S., 2007. Spatial and temporal patterns of *Porites* trematodiasis on the reefs of Kaneohe Bay, Oahu, Hawaii. *Bulletin of Marine Science* 80, 209-218.
- Aeby, G.S., Ross, M., Williams, G.J., Lewis, T.D., Work, T.M., 2010. Disease dynamics of *Montipora* white syndrome within Kaneohe Bay, Oahu, Hawaii: Distribution, seasonality, virulence, and transmissibility. *Diseases of Aquatic Organisms* 91, 1-8.
- Aeby, G.S., Williams, G.J., Franklin, E.C., Kenyon, J., Cox, E.F., Coles, S., Work, T.M., 2011. Patterns of coral disease across the Hawaiian archipelago: relating disease to environment. *PLoS One* 6, e20370.
- Allen, L.Z., Ishoey, T., Novotny, M.A., McLean, J.S., Lasken, R.S., Williamson, S.J., 2011. Single virus genomics: a new tool for virus discovery. *PLoS One* 6, e17722.
- Allen, M.J., Howard, J.A., Lilley, K.S., Wilson, W.H., 2008. Proteomic analysis of the EhV-86 virion. *Proteome Science* 6, 11.
- Allen, M.J., Schroeder, D.C., Wilson, W.H., 2006. Preliminary characterisation of repeat families in the genome of EhV-86, a giant algal virus that infects the marine microalga *Emiliania huxleyi*. *Archives of Virology* 151, 525-535.

- Allen, M.J., Wilson, W.H., 2008. Aquatic virus diversity accessed through omic techniques: A route map to function. *Current Opinion in Microbiology* 11, 226-232.
- Altschul, S.F., Madden, T.L., Schaffer, A.A., Zhang, J.H., Zhang, Z., Miller, W., Lipman, D.J., 1997. Gapped BLAST and PSI-BLAST: a new generation of protein database search programs. *Nucleic Acids Research* 25, 3389-3402.
- Anderson, M.J., 2001. A new method for non-parametric multivariate analysis of variance. *Austral Ecology* 26, 32-46.
- Anderson, M.J., 2003. XMATRIX: A FORTRAN computer program for calculating design matrices for terms in ANOVA designs in a linear model. Department of Statistics, University of Auckland, New Zealand.
- Anderson, N.G., Cline, G.B., Harris, W.W., Green, J.G., 1967. Isolation of viral particles from large fluid volumes In: Berg, G. (Ed.), *Transmission of viruses by the water route*. US Public Health Service, pp. 75-88.
- Antonius, A., Lipscomb, D., 2001. First protozoan coral-killer identified in the Indo-Pacific. *Atoll Research Bulletin* 481, 1-21.
- Arlidge, W.N.S., 2011. Coral reef viruses in Kane'ohe Bay, Hawai'i. Abundance, diversity and environmental drivers. School of Biological Sciences. Victoria University of Wellington.
- Arotsker, L., Siboni, N., Ben-Dov, E., Kramarsky-Winter, E., Loya, Y., Kushmaro, A., 2009. *Vibrio* sp. as a potentially important member of the Black Band Disease (BBD) consortium in *Favia* sp. corals. *FEMS Microbiology Ecology* 70, 515-524.
- Arslan, D., Legendre, M., Seltzer, V., Abergel, C., Claverie, J.-M., 2011. Distant Mimivirus relative with a larger genome highlights the fundamental features of Megaviridae. *Proceedings of the National Academy of Sciences of the USA* 108, 17486-17491.
- Baillie, B.K., Belda-Baillie, C.A., Maruyama, T., 2000. Conspecificity and Indo-Pacific distribution of *Symbiodinium* genotypes (Dinophyceae) from giant clams. *Journal of Phycology* 36, 1153-1161.

- Baker, A.C., Glynn, P.W., Riegl, B., 2008. Climate change and coral reef bleaching: An ecological assessment of long-term impacts, recovery trends and future outlook. *Estuarine, Coastal and Shelf Science* 80, 435-471.
- Balinsky, C.A., Delhon, G., Afonso, C.L., Risatti, G.R., Borca, M.V., French, R.A., Tulman, E.R., Geary, S.J., Rock, D.L., 2007. Sheeppox virus kelch-like gene SPPV-019 affects virus virulence. *Journal of Virology* 81, 11392-11401.
- Baltimore, D., 1971. Expression of animal virus genomes. *Microbiology and Molecular Biology Reviews* 35, 235-241.
- Banaszak, A.T., Lesser, M.P., 2009. Effects of solar ultraviolet radiation on coral reef organisms. *Photochemical and Photobiological Sciences* 8, 1276-1294.
- Bayer, T., Aranda, M., Sunagawa, S., Yum, L.K., DeSalvo, M.K., Lindquist, E., Coffroth, M.A., Voolstra, C.R., Medina, M., 2012. *Symbiodinium* transcriptomes: genome insights into the dinoflagellate symbionts of reef-building corals. *PLoS One* 7, e35269.
- Beck, M.A., Handy, J., Levander, O.A., 2000. The role of oxidative stress in viral infections. *Annals of the New York Academy of Sciences* 917, 906-912.
- Belda-Baillie, C.A., Sison, M., Silvestre, V., Villamor, K., Monje, V., Gomez, E.D., Baillie, B.K., 1999. Evidence for changing symbiotic algae in juvenile tridacnids. *Journal of Experimental Marine Biology and Ecology* 241, 207-221.
- Belda, C.A., Lucas, J.S., Yellowlees, D., 1993. Nutrient limitation in the giant clam-zooxanthellae symbiosis: effects of nutrient supplements on growth of the symbiotic partners. *Marine Biology* 117, 655-664.
- Bellec, L., Grimsley, N., Desdevises, Y., 2010. Isolation of prasinoviruses of the green unicellular algae *Ostreococcus* spp. on a worldwide geographical scale. *Applied and Environmental Microbiology* 76, 96-101.

- Ben-Haim, Y., Banin, E., Kushmaro, A., Loya, Y., Rosenberg, E., 1999. Inhibition of photosynthesis and bleaching of zooxanthellae by the coral pathogen *Vibrio shiloi*. *Environmental Microbiology* 1, 223-229.
- Ben-Haim, Y., Thompson, F.L., Thompson, C.C., Cnockaert, M.C., Hoste, B., Swings, J., Rosenberg, E., 2003a. *Vibrio coralliilyticus* sp. nov., a temperature-dependent pathogen of the coral *Pocillopora damicornis*. *International Journal of Systematic and Evolutionary Microbiology* 53, 309-315.
- Ben-Haim, Y., Zicherman-Keren, M., Rosenberg, E., 2003b. Temperature-regulated bleaching and lysis of the coral *Pocillopora damicornis* by the novel pathogen *Vibrio coralliilyticus*. *Applied and Environmental Microbiology* 69, 4236-4242.
- Bench, S.R., Hanson, T.E., Williamson, K.E., Ghosh, D., Radosovich, M., Wang, K., Wommack, K.E., 2007. Metagenomic characterization of Chesapeake Bay viroplankton. *Applied and Environmental Microbiology* 73, 7629-7641.
- Bentis, C.J., Kaufman, L., Golubic, S., 2000. Endolithic fungi in reef-building corals (Order: Scleractinia) are common, cosmopolitan, and potentially pathogenic. *Biological Bulletin* 198, 254-260.
- Bergh, O., Børsheim, K.Y., Bratbak, G., Haldal, M., 1989. High abundance of viruses found in aquatic environments. *Nature* 340, 467-468.
- Berngruber, T.W., Weissing, F.J., Gandon, S., 2010. Inhibition of superinfection and the evolution of viral latency. *Journal of Virology* 84, 10200-10208.
- Bourne, D.G., Garren, M., Work, T.M., Rosenberg, E., Smith, G.W., Harvell, C.D., 2009. Microbial disease and the coral holobiont. *Trends in Microbiology* 17, 554-562.
- Bratbak, G., Egge, J.K., Haldal, M., 1993. Viral mortality of the marine alga *Emiliania huxleyi* (Haptophyceae) and termination of algal blooms. *Marine Ecology Progress Series* 93, 39-48.

- Breitbart, M., 2012. Marine viruses: truth or dare. *Annual Review of Marine Science* 4, 425-448.
- Breitbart, M., Miyake, J.H., Rohwer, F., 2004. Global distribution of nearly identical phage-encoded DNA sequences. *FEMS Microbiology Letters* 236, 249-256.
- Bruno, J.F., Petes, L.E., Harvell, C.D., Hettinger, A., 2003. Nutrient enrichment can increase the severity of coral diseases. *Ecology Letters* 6, 1056-1061.
- Bruno, J.F., Selig, E.R., Casey, K.S., Page, C.A., Willis, B.L., Harvell, C.D., Sweatman, H., Melendy, A.M., 2007. Thermal stress and coral cover as drivers of coral disease outbreaks. *PLoS Biology* 5, e124.
- Brussaard, C.P., Kempers, R.S., Kop, A.J., Riegman, R., Heldal, M., 1996. Virus-like particles in a summer bloom of *Emiliania huxleyi* in the North Sea. *Aquatic Microbial Ecology* 10, 105-113.
- Brussaard, C.P.D., 2004a. Optimization of procedures for counting viruses by flow cytometry. *Applied and Environmental Microbiology* 70, 1506-1513.
- Brussaard, C.P.D., 2004b. Viral control of phytoplankton populations - a review. *The Journal of Eukaryotic Microbiology* 51, 125-138.
- Brussaard, C.P.D., Marie, D., Bratbak, G., 2000. Flow cytometric detection of viruses. *Journal of Virological Methods* 85, 175-182.
- Bythell, J.C., Douglas, A.E., Sharp, V.A., Searle, J.B., Brown, B.E., 1997. Algal genotype and photoacclimatory responses of the symbiotic alga *Symbiodinium* in natural populations of the sea anemone *Anemonia viridis*. *Proceedings of the Royal Society B* 264, 1277-1282.
- Calderwood, M.A., Venkatesan, K., Xing, L., Chase, M.R., Vazquez, A., Holthaus, A.M., Ewence, A.E., Li, N., Hirozane-Kishikawa, T., Hill, D.E., Vidal, M., Kieff, E., Johannsen, E., 2007. Epstein-Barr virus and virus human protein interaction maps. *Proceedings of the National Academy of Sciences of the USA* 104, 7606-7611.

- Cantó-Nogués, C., Hockley, D., Grief, C., Ranjbar, S., Bootman, J., Almond, N., Herrera, I., 2001. Ultrastructural localization of the RNA of immunodeficiency viruses using electron microscopy in situ hybridization and in vitro infected lymphocytes. *Micron* 32, 579-589.
- Carlos, A.A., Baillie, B.K., Kawachi, M., Maruyama, T., 1999. Phylogenetic position of *Symbiodinium* (Dinophyceae) isolates from tridacnids (Bivalvia), cardiids (Bivalvia), a sponge (Porifera), a soft coral (Anthozoa), and a free-living strain. *Journal of Phycology* 35, 1054-1062.
- Cervino, J.M., Hayes, R., Goreau, T.J., Smith, G.W., 2004. Zooxanthellae regulation in Yellow Blotch/Band and other coral diseases contrasted with temperature related bleaching: *in situ* destruction vs expulsion. *Symbiosis* 37, 63-85.
- Chandriani, S., Xu, Y., Ganem, D., 2010. The lytic transcriptome of Kaposi's sarcoma-associated herpesvirus reveals extensive transcription of noncoding regions, including regions antisense to important genes. *Journal of Virology* 84, 7934-7942.
- Chen, F., Lu, J., 2002. Genomic sequence and evolution of marine cyanophage P60: a new insight on lytic and lysogenic phages. *Applied and Environmental Microbiology* 68, 2589-2594.
- Chen, F., Suttle, C.A., 1995. Amplification of DNA polymerase gene fragments from viruses infecting microalgae. *Applied and Environmental Microbiology* 61, 1274-1278.
- Chen, F., Suttle, C.A., Short, S.M., 1996. Genetic diversity in marine algal virus communities as revealed by sequence analysis of DNA polymerase genes. *Applied and Environmental Microbiology* 62, 2869-2874.
- Chevreur, B., Pfisterer, T., Drescher, B., Driesel, A.J., Müller, W.E.G., Wetter, T., Suhai, S., 2004. Using the miraEST assembler for reliable and automated mRNA transcript assembly and SNP detection in sequenced ESTs. *Genome Research* 14, 1147-1159.
- Choi, S., Jeliazkov, I., Jiang, S.C., 2009. Lysogens and free viruses in fresh, brackish, and marine waters: a Bayesian analysis. *FEMS Microbiology Ecology* 69, 243-254.

- Christen, L., Seto, J., Niles, E., 1990. Superinfection exclusion of vaccinia virus in virus-infected cell cultures. *Virology* 174, 35-42.
- Clarke, S.F., Guy, P.L., Burritt, D.J., Jameson, P.E., 2002. Changes in the activities of antioxidant enzymes in response to virus infection and hormone treatment. *Physiologia Plantarum* 114, 157-164.
- Claverie, J.-M., Ogata, H., Audic, S., Abergel, C., Suhre, K., Fournier, P.-E., 2006. Mimivirus and the emerging concept of "giant" virus. *Virus Research* 117, 133-144.
- Claverie, J.M., Grzela, R., Lartigue, A., Bernadec, A., Nitsche, S., Vacelet, J., Ogata, H., Abergel, C., 2009. Mimivirus and Mimiviridae: Giant viruses with an increasing number of potential hosts, including corals and sponges. *Journal of Invertebrate Pathology* 101, 172-180.
- Clokie, M.R.J., Millard, A.D., Wilson, W.H., Mann, N.H., 2003. Encapsidation of host DNA by bacteriophages infecting marine *Synechococcus* strains. *FEMS Microbiology Ecology* 46, 349-352.
- Coles, S.L., Seapy, D.G., 1998. Ultra-violet absorbing compounds and tumorous growths on acroporid corals from Bandar Khayran, Gulf of Oman, Indian Ocean. *Coral Reefs* 17, 195-198.
- Colson, P., Pagnier, I., Yoosuf, N., Fournous, G., La Scola, B., Raoult, D., 2013. "Marseilleviridae", a new family of giant viruses infecting amoebae. *Archives of Virology* 158, 915-920.
- Conesa, A., Götz, S., 2008. Blast2GO: a comprehensive suite for functional analysis in plant genomics. *International Journal of Plant Genomics* 2008, ID 619832.
- Cooney, R.P., Pantos, O., Le Tissier, M.D.A., Barer, M.R., A.G., O.D., Bythell, J.C., 2002. Characterisation of the bacterial consortium associated with black band disease in coral using molecular microbiological techniques. *Environmental Microbiology* 4, 401-413.

- Correa, A.M.S., Welsh, R.M., Vega Thurber, R.L., 2012. Unique nucleocytoplasmic dsDNA and +ssRNA viruses are associated with the dinoflagellate endosymbionts of corals. *The ISME Journal* 7, 13-27.
- Culley, A.I., Lang, A.S., Suttle, C.A., 2003. High diversity of unknown picorna-like viruses in the sea. *Nature* 424, 1054-1057.
- Culley, A.I., Lang, A.S., Suttle, C.A., 2007. The complete genomes of three viruses assembled from shotgun libraries of marine RNA virus communities. *Virology Journal* 4, 69.
- Dalton, S.J., Godwin, S., Smith, S.D.A., Pereg, L., 2010. Australian subtropical white syndrome: a transmissible, temperature-dependent coral disease. *Marine and Freshwater Research* 61, 342-350.
- Danovaro, R., Bongiorno, L., Corinaldesi, C., Giovannelli, D., Damiani, E., Astolfi, P., Greci, L., Pusceddu, A., 2008a. Sunscreens cause coral bleaching by promoting viral infections. *Environmental Health Perspectives* 116, 441-447.
- Danovaro, R., Corinaldesi, C., Filippini, M., Fischer, U.R., Gessner, M.O., Jacquet, S., Magagnini, M., Velimirov, B., 2008b. Viriobenthos in freshwater and marine sediments: a review. *Freshwater Biology* 53, 1186-1213.
- Danovaro, R., Dell'Anno, A., Corinaldesi, C., Magagnini, M., Noble, R., Tamburini, C., Weinbauer, M.G., 2008c. Major viral impact on the functioning of deep-sea ecosystems. *Nature* 454, 1084-1088.
- Davies, P.S., 1984. The role of zooxanthellae in the nutritional energy requirements of *Pocillopora eydouxi*. *Coral Reefs* 2, 181-186.
- Davy, J.E., 2007. Characterisation of White Patch Syndrome, a putative disease affecting corals in the genus *Porites* on the Great Barrier Reef. PhD thesis. Centre for Marine Studies. University of Queensland.
- Davy, J.E., Patten, N.L., 2007. Morphological diversity of virus-like particles within the surface microlayer of scleractinian corals. *Aquatic Microbial Ecology* 47, 37-44.

- Davy, S.K., Allemand, D., Weis, V.M., 2012. Cell biology of cnidarian-dinoflagellate symbiosis. *Microbiology and Molecular Biology Reviews* 76, 229-261.
- Davy, S.K., Burchett, S.G., Dale, A.L., Davies, P., Davy, J.E., Muncke, C., Hoegh-Guldberg, O., Wilson, W.H., 2006. Viruses: agents of coral disease? *Diseases of Aquatic Organisms* 69, 101-110.
- Dawson, M.N., Martin, L.E., Penland, L.K., 2001. Jellyfish swarms, tourists, and the Christ-child. *Hydrobiologia* 451, 131-144.
- Delaroque, N., Maier, I., Knippers, R., Müller, D.G., 1999. Persistent virus integration into the genome of its algal host, *Ectocarpus siliculosus* (Phaeophyceae). *Journal of General Virology* 80, 1367-1370.
- DeLong, E.F., 1992. Archaea in coastal marine environments. *Proceedings of the National Academy of Sciences of the USA* 89, 5685-5689.
- Derelle, E., Ferraz, C., Escande, M.-L., Eychenié, S., Cooke, R., Piganeau, G., Desdevises, Y., Bellec, L., Moreau, H., Grimsley, N., 2008. Life-cycle and genome of OtV5, a large DNA virus of the pelagic marine unicellular green alga *Ostreococcus tauri*. *PLoS One* 3, e2250.
- DeSalvo, M.K., Voolstra, C.R., Sunagawa, S., Schwarz, J.A., Stillman, J.H., Coffroth, M.A., Szmant, A.M., Medina, M., 2008. Differential gene expression during thermal stress and bleaching in the Caribbean coral *Montastrea faveolata*. *Molecular Ecology* 17, 3952-3971.
- Desnues, C., La Scola, B., Yutin, N., Fournous, G., Robert, C., Azza, S., Jardot, P., Monteil, S., Campocasso, A., Koonin, E.V., Raoult, D., 2012. Provirophages and transpovirons as the diverse mobilome of giant viruses. *Proceedings of the National Academy of Sciences of the USA* 109, 18078-18083.
- Dinsdale, E.A., Pantos, O., Smriga, S., Edwards, R.A., Angly, F., Wegley, L., Hatay, M., Hall, D., Brown, E., Haynes, M., Krause, L., Sala, E., Sandin, S.A., Vega Thurber, R., Willis, B.L., Azam, F., Knowlton, N., Rohwer, F., 2008. Microbial ecology of four coral atolls in the Northern Line Islands. *PLoS ONE* 3, e1584.

- Domart-Coulon, I.J., Traylor-Knowles, N., Peters, E., Elbert, D., Downs, C.A., Price, K., Stubbes, J., McLaughlin, S., Cox, E., Aeby, G., Brown, P.R., Ostrander, G.K., 2006. Comprehensive characterization of skeletal tissue growth anomalies of the finger coral *Porites compressa*. *Coral Reefs* 25, 531-543.
- Donaldson, K.A., Griffin, D.W., Paul, J.H., 2002. Detection, quantitation and identification of enteroviruses from surface waters and sponge tissue from the Florida Keys using real-time RT-PCR. *Water Research* 36, 2505-2514.
- Douglas, A.E., 2003. Coral bleaching - how and why? *Marine Pollution Bulletin* 46, 385-392.
- Douglas, A.E., Smith, D.C., 1989. Are endosymbioses mutualistic? *Trends in Ecology and Evolution* 4, 350-352.
- Ducklow, H.W., Mitchell, R., 1979. Composition of mucus released by coral reef coelenterates. *Limnology and Oceanography* 24, 707-714.
- Dunigan, D.D., Fitzgerald, L.A., Van Etten, J.L., 2006. Phycodnaviruses: A peek at genetic diversity. *Virus Research* 117, 119-132.
- Dunn, S.R., Thomason, J.C., Le Tissier, M.D.A., Bythell, J.C., 2004. Heat stress induces different forms of cell death in sea anemones and their endosymbiotic algae depending on temperature and duration. *Cell Death and Differentiation* 11, 1213-1222.
- Edge, S.E., Morgan, M.B., Gleason, D.F., Snell, T.W., 2005. Development of a coral cDNA array to examine gene expression profiles in *Montastrea faveolata* exposed to environmental stress. *Marine Pollution Bulletin* 51, 507-523.
- Edwards, R.A., Rohwer, F.L., 2005. Viral metagenomics. *Nature Reviews Microbiology* 3, 504-510.
- Efrony, R., Atad, I., Rosenberg, E., 2009. Phage therapy of coral white plague disease: properties of phage BA3. *Current Microbiology* 58, 139-145.

- Efrony, R., Loya, Y., Bacharach, E., Rosenberg, E., 2007. Phage therapy of coral disease. *Coral Reefs* 26, 7-13.
- Ekström, J., Forslund, O., Dillner, J., 2010. Three novel papillomaviruses (HPV109, HPV112 and HPV114) and their presence in cutaneous and mucosal samples. *Virology* 397, 331-336.
- Ellenberg, P., Edreira, M., Scolaro, L., 2004. Resistance to superinfection of Vero cells persistently infected with Junin virus. *Archives of Virology* 149, 507-522.
- Elston, R., 1997. Special topic review: bivalve mollusc viruses. *World Journal of Microbiology and Biotechnology* 13, 393-403.
- Essbauer, S., Ahne, W., 2001. Viruses of lower vertebrates. *Journal of Veterinary Medicine, Series B* 48, 403-475.
- Evans, C., Kadner, S.V., Darroch, L.J., Wilson, W.H., Liss, P.S., Malin, G., 2007. The relative significance of viral lysis and microzooplankton grazing as pathways of dimethylsulfoniopropionate (DMSP) cleavage: An *Emiliania huxleyi* culture study. *Limnology and Oceanography* 52, 1036-1045.
- Evans, C., Malin, G., Mills, G.P., 2006. Viral infection of *Emiliania huxleyi* (Prymnesiophyceae) leads to elevated production of reactive oxygen species. *Journal of Phycology* 42, 1040-1047.
- Fabrizius, K.E., 2005. Effects of terrestrial runoff on the ecology of corals and coral reefs: review and synthesis. *Marine Pollution Bulletin* 50, 125-146.
- Falkowski, P.G., Dubinsky, Z., 1981. Light-shade adaptation of *Stylophora pistillata*, a hermatypic coral from the Gulf of Eliat. *Nature* 289, 172-174.
- Fauquet, C.M., Mayo, M.A., Maniloff, J., Desselberger, U., Ball, L.A. (Eds.), 2005. *Virus taxonomy: Eighth report of the International Committee on Taxonomy of Viruses*. Elsevier Academic Press, San Diego.

- Feely, R.A., Doney, S.C., Cooley, S.R., 2009. Ocean acidification: present conditions and future changes in a high-CO₂ world. *Oceanography* 122, 36-47.
- Frada, M., Probert, I., Allen, M.J., Wilson, W.H., de Vargas, C., 2008. The "Cheshire Cat" escape strategy of the coccolithophore *Emiliania huxleyi* in response to viral infection. *Proceedings of the National Academy of Sciences of the USA* 105, 15944-15949.
- Franklin, D.J., Hoegh-Guldberg, O., Jones, R.J., Berges, J.A., 2004. Cell death and degeneration in the symbiotic dinoflagellates of the coral *Stylophora pistillata* during bleaching. *Marine Ecology Progress Series* 272, 117-130.
- Fuhrman, J.A., 1999. Marine viruses and their biogeochemical and ecological effects. *Nature* 399, 541-548.
- Fuller, N.J., Wilson, W.H., Joint, I.R., Mann, N.H., 1998. Occurrence of a sequence in marine cyanophages similar to that of T4 g20 and its application to PCR-based detection and quantification techniques. *Applied and Environmental Microbiology* 64, 2051-2060.
- Garren, M., Raymundo, L., Guest, J., Harvell, C.D., Azam, F., 2009. Resilience of coral-associated bacterial communities exposed to fish farm effluent. *PLoS ONE* 4, e7319.
- Ghedini, E., Claverie, J.-M., 2005. Mimivirus relatives in the Sargasso sea. *Virology Journal* 2, 62.
- Gómez-Anduro, G.A., Barillas-Mury, C.-V., Peregrino-Uriarte, A.B., Gupta, L., Gollas-Galván, T., Hernández-López, J., Yepiz-Plascencia, G., 2006. The cytosolic manganese superoxide dismutase from the shrimp *Litopenaeus vannamei*: Molecular cloning and expression. *Developmental and Comparative Immunology* 30, 893-900.
- Gornik, S.G., Ford, K.L., Mulhern, T.D., Bacic, A., McFadden, G.I., Waller, R.F., 2012. Loss of nucleosomal DNA condensation coincides with appearance of a novel nuclear protein in dinoflagellates. *Current Biology* 22, 2303-2312.

- Götz, S., García-Gómez, J.M., Terol, J., Williams, T.D., Nagaraj, S.H., Nueda, M.J., Robles, M., Talón, M., Dopazo, J., Conesa, A., 2008. High-throughput functional annotation and data mining with the Blast2GO suite. *Nucleic Acids Research* 36, 3420-3435.
- Greiner, T., Frohns, F., Kang, M., Van Etten, J.L., Käsmann, A., Moroni, A., Hertel, B., Thiel, G., 2009. Chlorella viruses prevent multiple infections by depolarizing the host membrane. *Journal of General Virology* 90, 2033-2039.
- Guan, K., Broyles, S.S., Dixon, J.E., 1991. A Tyr/Ser protein phosphatase encoded by vaccinia virus. *Nature* 350, 359-362.
- Guillard, R.R.L., 1975. Culture of phytoplankton for feeding marine invertebrates. In: Smith, W.L., Chantey, M.H. (Eds.), *Culture of Marine Invertebrate Animals*. Plenum Publishers, New York, pp. 29-60.
- Guindon, S., Gascuel, O., 2003. A simple, fast, and accurate algorithm to estimate large phylogenies by maximum likelihood. *Systematic Biology* 52, 696-704.
- Guiry, M.D., 2012. How many species of algae are there? *Journal of Phycology* 48, 1057-1063.
- Hall, N., 2007. Advanced sequencing technologies and their wider impact in microbiology. *The Journal of Experimental Biology* 209, 1518-1525.
- Hall, T.A., 1999. BioEdit: a user-friendly biological sequence alignment editor and analysis program for Windows95/98/NT. *Nucleic Acids Symposium Series* 41, 95-98.
- Harvell, C.D., Jordan-Dahlgren, E., Merkel, S., Rosenberg, E., Raymundo, L., Smith, G., Weil, E., Willis, B., 2007. Coral disease, environmental drivers, and the balance between coral and microbial associates. *Oceanography* 20, 172-195.
- Harvell, C.D., Kim, K., Burkholder, J.M., Colwell, R.R., Epstein, P.R., Grimes, D.J., Hofmann, E.E., Lipp, E.K., Osterhaus, A.D.M.E., Overstreet, R.M., Porter, J.W., Smith, G.W., Vasta, G.R., 1999. Emerging marine diseases - climate links and anthropogenic factors. *Science* 285, 1505-1510.

- Harvell, C.D., Mitchell, C.E., Ward, J.R., Altizer, S., Dobson, A.P., Ostfeld, R.S., Samuel, M.D., 2002. Climate warming and disease risks for terrestrial and marine biota. *Science* 296, 2158-2162.
- Hennes, K.P., Suttle, C.A., 1995. Direct counts of viruses in natural waters and laboratory cultures by epifluorescence microscopy. *Limnology and Oceanography* 40, 1050-1055.
- Hensel, M., Schmidt, H. (Eds.), 2008. Horizontal gene transfer in the evolution of pathogenesis. Cambridge University Press, Cambridge, UK.
- Hewson, I., Winget, D.M., Williamson, K.E., Fuhrman, J.A., Wommack, K.E., 2006. Viral and bacterial assemblage covariance in oligotrophic waters of the West Florida Shelf (Gulf of Mexico). *Journal of the Marine Biological Association of the United Kingdom* 86, 591-603.
- Hill, R., Scott, A., 2012. The influence of irradiance on the severity of thermal bleaching in sea anemones that host anemonefish. *Coral Reefs* 31, 273-284.
- Hingamp, P., Grimsley, N., Acinas, S.G., Clerissi, C., Subirana, L., Poulain, J., Ferrera, I., Sarmiento, H., Villar, E., Lima-Mendez, G., Faust, K., Sunagawa, S., Claverie, J.-M., Moreau, H., Desdevises, Y., Bork, P., Raes, J., de Vargas, C., Karsenti, E., Kandels-Lewis, S., Jaillon, O., Not, F., Pesant, S., Wincker, P., Ogata, H., 2013. Exploring nucleo-cytoplasmic large DNA viruses in Tara Oceans microbial metagenomes. *The ISME Journal*, 1-18.
- Hoegh-Guldberg, O., 1999. Climate change, coral bleaching and the future of the world's coral reefs. *Marine and Freshwater Research* 50, 839-866.
- Hoegh-Guldberg, O., 2004. Coral reefs in a century of rapid environmental change. *Symbiosis* 37, 1-31.
- Hoegh-Guldberg, O., Mumby, P.J., Hooten, A.J., Steneck, R.S., Greenfield, P., Gomez, E., Harvell, C.D., Sale, P.F., Edwards, A.J., Caldeira, K., Knowlton, N., Eakin, C.M., Iglesias-Prieto, R., Muthiga, N., Bradbury, R.H., Dubi, A., Hatziolos, M.E., 2007. Coral reefs under rapid climate change and ocean acidification. *Science* 318, 1737-1742.

- Hoegh-Guldberg, O., Smith, G.J., 1989. The effect of sudden changes in temperature, light and salinity on the population density and export of zooxanthellae from the reef corals *Stylophora pistillata* Esper and *Seriatopora hystrix* Dana. *Journal of Experimental Marine Biology and Ecology* 129, 279-303.
- Horiguchi, T., 1995. *Heterocapsa circularisquama* sp. (Peridiniales, Dinophyceae): a new marine dinoflagellate causing mass mortality of bivalves in Japan. *Phycological Research* 43, 129-136.
- Hou, Y., Lin, S., 2009. Distinct gene number-genome size relationships for eukaryotes and non-eukaryotes: gene content estimation for dinoflagellate genomes. *PLoS Biology* 4, e6978.
- Hubbard, J.A., Pocock, Y.P., 1972. Sediment rejection by recent scleractinian corals: a key to paleoenvironmental reconstruction. *Geologische Rundschau* 61, 598-626.
- Hughes, T.P., Baird, A.H., Bellwood, D.R., Card, M., Connolly, S.R., Folke, C., Grosberg, R., Hoegh-Guldberg, O., Jackson, J.B.C., Kleypas, J., Lough, J.M., Marshall, P., Nyström, M., Palumbi, S.R., Pandolfi, J.M., Rosen, B., Roughgarden, J., 2003. Climate change, human impacts, and the resilience of coral reefs. *Science* 301, 929-933.
- Hunter, S., Jones, P., Mitchell, A., Apweiler, R., Attwood, T.K., Bateman, A., Bernard, T., Binns, D., Bork, P., Burge, S., de Castro, E., Coggill, P., Corbett, M., Das, U., Daugherty, L., Duquenne, L., Finn, R.D., Fraser, M., Gough, J., Haft, D., Hulo, N., Kahn, D., Kelly, E., Letunic, I., Lonsdale, D., Lopez, R., Madera, M., Maslen, J., McAnulla, C., McDowall, J., McMenamin, C., Mi, H., Mutowo-Muellenet, P., Mulder, N., Natale, D., Orengo, C., Pesseat, S., Punta, M., Quinn, A.F., Rivoire, C., Sangrador-Vegas, A., Selengut, J.D., Sigrist, C.J.A., Scheremetjew, M., Tate, J., Thimmajananathan, M., Thomas, P.D., Wu, C.H., Yeats, C., Yong, S.-Y., 2012. InterPro in 2011: new developments in the family and domain prediction database. *Nucleic Acids Research* 40, D306-D312.
- Hutchings, P., Kingsford, M., Hoegh-Guldberg, O., 2009. *The Great Barrier Reef: Biology, environment and management*. CSIRO Publishing, Collingwood.
- Hutchinson, G.E., 1961. The paradox of the plankton. *American Naturalist* 95, 137-145.

International Human Genome Sequencing Consortium, 2004. Finishing the euchromatic sequence of the human genome. *Nature* 431, 931-945.

IPCC, 2007a. Climate change 2007: synthesis report. Contribution of working groups I, II and III to the fourth assessment report of the Intergovernmental Panel on Climate Change. IPCC, Geneva, Switzerland.

IPCC, 2007b. Climate change 2007: The physical science basis. Summary for policy-makers. Contribution of working group I to the fourth assessment report of the Intergovernmental Panel on Climate Change. IPCC, Geneva, Switzerland.

Iseli, C., Jongeneel, C.V., Bucher, P., 1999. ESTScan: a program for detecting, evaluating, and reconstructing potential coding regions in EST sequences. *Proceedings of the International Conference on Intelligent Systems for Molecular Biology*.

Ishikura, M., Adachi, K., Maruyama, T., 1999. Zooxanthellae release glucose in the tissue of a giant clam, *Tridacna crocera*. *Marine Biology* 133, 665-673.

ISRS, 2004. The effects of terrestrial runoff of sediments, nutrients and other pollutants on coral reefs. Briefing Paper 3, International Society for Reef Studies, 18 pp.

Iyer, L.M., Aravind, L., Koonin, E.V., 2001. Common origin of four diverse families of large eukaryotic DNA viruses. *Journal of Virology* 75, 11720-11734.

Jacquet, S., Heldal, M., Iglesias-Rodriguez, D., Larsen, A., Wilson, W., Bratbak, G., 2002. Flow cytometric analysis of an *Emiliani huxleyi* bloom terminated by viral infection. *Aquatic Microbial Ecology* 27, 111-124.

Jiang, S.C., Paul, J.H., 1998. Significance of lysogeny in the marine environment: studies with isolates and a model of lysogenic phage production. *Microbial Ecology* 35, 235-243.

Jones, B.W., Maruyama, A., Ouverney, C.C., Nishiguchi, M.K., 2007. Spatial and temporal distribution of the *Vibrionaceae* in coastal waters of Hawaii, Australia, and France. *Microbial Ecology* 54, 314-323.

- Kaczmarek, L., 2006. Coral disease dynamics in the Central Philippines. *Diseases of Aquatic Organisms* 69, 9-21.
- Kaczmarek, L., Richardson, L.L., 2007. Transmission of growth anomalies between Indo-Pacific *Porites* corals. *Journal of Invertebrate Pathology* 94, 218-221.
- Kanehisa, M., Goto, S., Hattori, M., Aoki-Kinoshita, K.F., Itoh, M., Kawashima, S., Katayama, T., Araki, M., Hirakawa, M., 2006. From genomics to chemical genomics: new developments in KEGG. *Nucleic Acids Research* 34, D354-D357.
- Kang, M., Dunigan, D., Van Etten, J.L., 2005. *Chlorovirus*: a genus of Phycodnaviridae that infects certain chlorella-like green algae. *Molecular Plant Pathology* 6, 213-224.
- Kapp, M., 1998. Viruses infecting marine brown algae. *Virus Genes* 16, 111-117.
- Kayal, M., Vercelloni, J., Lison de Loma, T., Bosserelle, P., Chancerelle, Y., Geoffroy, S., Stievenart, C., Michonneau, F., Penin, L., Planes, S., Adjeroud, M., 2012. Predator Crown-of-Thorns Starfish (*Acanthaster planci*) outbreak, mass mortality of corals, and cascading effects on reef fish and benthic communities. *PLoS One* 7, e47363.
- Kegel, J., Allen, M.J., Metfies, K., Wilson, W.H., Wolf-Gladrow, D., Valentin, K., 2007. Pilot study of an EST approach of the coccolithophorid *Emiliania huxleyi* during a virus infection. *Gene* 406, 209-216.
- Kellogg, C.A., 2004. Tropical Archaea: diversity associated with the surface microlayer of corals. *Marine Ecology Progress Series* 273, 81-88.
- Kennedy, E.V., Perry, C.T., Halloran, P.R., Iglesias-Prieto, R., Schönberg, C.H.L., Wisshak, M., Form, A.U., Carricart-Ganivet, J.P., Fine, M., Eakin, C.M., Mumby, P.J., 2013. Avoiding coral reef functional collapse requires local and global action. *Current Biology* 23, 912-918.
- Kim, K.-H., Chang, H.-W., Nam, Y.-D., Roh, S.W., Kim, M.-S., Sung, Y., Jeon, C.O., Oh, H.-M., Bae, J.-W., 2008. Amplification of uncultured single-stranded DNA viruses from rice paddy soil. *Applied and Environmental Microbiology* 74, 5975-5985.

- Kliem, M., Dreiseikelmann, B., 1989. The superimmunity gene sim of bacteriophage P1 causes superinfection exclusion. *Virology* 171, 350-355.
- Knowlton, N., 2001. The future of coral reefs. *Proceedings of the National Academy of Sciences of the USA* 98, 5419-5425.
- Knowlton, N., Rohwer, F.L., 2003. Multispecies microbial mutualisms on coral reefs: the host as a habitat. *The American Naturalist* 162, S51-S62.
- Koonin, E.V., Senkevich, T.G., Dolja, V.V., 2006. The ancient Virus World and evolution of cells. *Biology Direct* 1, 29.
- Kristensen, D.M., Mushegian, A.R., Dolja, V.V., Koonin, E.V., 2009. New dimensions of the virus world discovered through metagenomics. *Trends in Microbiology* 18, 11-19.
- Kushmaro, A., Loya, Y., Fine, M., Rosenberg, E., 1996. Bacterial infection and coral bleaching. *Nature* 380, 396.
- Kushmaro, A., Rosenberg, E., Fine, M., Ben Haim, Y., Loya, Y., 1998. Effect of temperature on bleaching of the coral *Oculina patagonica* by *Vibrio* AK-1. *Marine Ecology Progress Series* 171, 131-137.
- Kvennefors, E.C.E., Sampayo, E., Ridgway, T., Barnes, A.C., Hoegh-Guldberg, O., 2010. Bacterial communities of two ubiquitous Great Barrier Reef corals reveals both site- and species-specificity of common bacterial associates. *PLoS One* 5, e10401.
- La Scola, B., Audic, S., Robert, C., Jungang, L., de Lamballerie, X., Drancourt, M., Birtles, R., Claverie, J.-M., Raoult, D., 2003. A giant virus in amoebae. *Science* 299, 2033.
- LaJeunesse, T.C., Lambert, G., Andersen, R.A., Coffroth, M.A., Galbraith, D.W., 2005. *Symbiodinium* (Pyrrophyta) genome sizes (DNA content) are smallest among dinoflagellates. *Journal of Phycology* 41, 880-886.

- Lang, A.S., Culley, A.I., Suttle, C.A., 2004. Genome sequence and characterization of a virus (HaRNAV) related to picorna-like viruses that infect the marine toxic bloom-forming alga *Heterosigma akashiwo*. *Virology* 320, 206-217.
- Langer, M.R., Lipps, J.H., 1995. Phylogenetic incongruence between dinoflagellate endosymbionts (*Symbiodinium*) and their host foraminifera (*Sorites*): small-subunit ribosomal RNA gene sequence evidence. *Marine Micropaleontology* 26, 179-186.
- Larsen, J.B., Larsen, A., Bratbak, G., Sandaa, R.-A., 2008. Phylogenetic analysis of members of the *Phycodnaviridae* virus family, using amplified fragments of the major capsid protein gene. *Applied and Environmental Microbiology* 74, 3048-3057.
- Lasken, R.S., 2007. Single-cell genomics sequencing using Multiple Displacement Amplification. *Current Opinion in Microbiology* 10, 510-516.
- Lawrence, J.E., Chan, A.M., Suttle, C.A., 2001. A novel virus (HaNIV) causes lysis of the toxic bloom-forming alga *Heterosigma akashiwo* (Raphidophyceae). *Journal of Phycology* 37, 216-222.
- Leggat, W., Hoegh-Guldberg, O., Dove, S., Yellowlees, D., 2007. Analysis of an EST library from the dinoflagellate (*Symbiodinium* sp.) symbiont of reef-building corals. *Journal of Phycology* 43, 1010-1021.
- Leggat, W., Yellowlees, D., Medina, M., 2011. Recent progress in *Symbiodinium* transcriptomics. *Journal of Experimental Marine Biology and Ecology* 408, 120-125.
- Leruste, A., Bouvier, T., Bettarel, Y., 2012. Enumerating viruses in coral mucus. *Applied and Environmental Microbiology* 78, 6377-6379.
- Lesser, M.P., 1996. Elevated temperatures and ultraviolet radiation cause oxidative stress and inhibit photosynthesis in symbiotic dinoflagellates. *Limnology and Oceanography* 41, 271-283.
- Lesser, M.P., 2004. Experimental biology of coral reef ecosystems. *Journal of Experimental Biology and Ecology* 300, 217-252.

- Lesser, M.P., 2006. Oxidative stress in marine environments: biochemistry and physiological ecology. *Annual Review of Physiology* 68, 253-278.
- Lesser, M.P., 2011. Coral bleaching: causes and mechanisms. In: Dubinsky, Z., Stambler, N. (Eds.), *Coral reefs: An ecosystem in transition*. Springer, Netherlands.
- Lesser, M.P., Bythell, J.C., Gates, R.D., Johnstone, R.W., Hoegh-Guldberg, O., 2007. Are infectious diseases really killing corals? Alternative interpretations of the experimental and ecological data. *Journal of Experimental Marine Biology and Ecology* 346, 36-44.
- Lesser, M.P., Farrell, J.H., 2004. Exposure to solar radiation increases damage to both host tissues and algal symbionts of corals during thermal stress. *Coral Reefs* 23, 367-377.
- Lesser, M.P., Mazel, C.H., Gorbunov, M.Y., Falkowski, P.G., 2004. Discovery of symbiotic nitrogen-fixing cyanobacteria in corals. *Science* 305, 997-1000.
- Lewis, J.B., Price, W.S., 1976. Patterns of ciliary currents in Atlantic reef corals and their functional significance. *Journal of Zoology (London)* 178, 77-89.
- Li, H., Durbin, R., 2009. Fast and accurate short read alignment with Burrows-Wheeler transform. *Bioinformatics* 25, 1754-1760.
- Li, R., Li, Y., Kristiansen, K., Wang, J., 2008. SOAP: Short oligonucleotide alignment program. *Bioinformatics* 25, 713-714.
- Li, W., Jaroszewski, L., Godzik, A., 2001. Clustering of highly homologous sequences to reduce the size of large protein databases. *Bioinformatics* 17, 282-283.
- Li, W., Jaroszewski, L., Godzik, A., 2002. Tolerating some redundancy significantly speeds up clustering of large protein databases. *Bioinformatics* 18, 77-82.
- Lindell, D., Jaffe, J.D., Johnson, Z.I., Church, G.M., Chisholm, S.W., 2005. Photosynthesis genes in marine viruses yield proteins during host infection. *Nature* 438, 86-89.

- Lipart, C., Renault, T., 2002. Herpes-like virus detection in infected *Crassostrea gigas* spat using DIG-labelled probes. *Journal of Virological Methods* 101, 1-10.
- Liu, H., Fu, Y., Jiang, D., Li, G., Xie, J., Cheng, J., Peng, Y., Ghabrial, S.A., Yi, X., 2010. Widespread horizontal gene transfer from double-stranded RNA viruses to eukaryotic nuclear genomes. *Journal of Virology* 84, 11876-11887.
- Liu, S., Vijayendran, D., Bonning, B.C., 2011. Next generation sequencing technologies for insect virus discovery. *Viruses* 3, 1849-1869.
- Llewellyn, C.A., Evans, C., Airs, R.L., Cook, I., Bale, N., Wilson, W.H., 2007. The response of carotenoids and chlorophylls during virus infection of *Emiliana huxleyi* (Prymnesiophyceae). *Journal of Experimental Marine Biology and Ecology* 344, 101-112.
- Lobban, C.S., 2002. Ciliate-*Symbiodinium* symbiosis spotted on reefs. *Coral Reefs* 21, 332.
- Lobban, C.S., Schefter, M., Simpson, A.G.B., Pochon, X., Pawlowski, J., Foissner, W., 2002. *Maristentor dinoferus* n. gen., n. sp., a giant heterotrich ciliate (Spirotrichea: Heterotrichida) with zooxanthellae, from coral reefs on Guam, Mariana Islands. *Marine Biology* 140, 411-423.
- Lohr, J., Munn, C.B., Wilson, W.H., 2007. Characterization of a latent virus-like infection of symbiotic zooxanthellae. *Applied and Environmental Microbiology* 73, 2976-2981.
- Longnecker, R., Kieff, E., 1990. A second Epstein-Barr virus membrane protein (LMP2) is expressed in latent infection and colocalizes with LMP1. *Journal of Virology* 64, 2319-2326.
- Lottaz, C., Iseli, C., Jongeneel, C.V., Bucher, P., 2003. Modeling sequencing errors by combining Hidden Markov models. *Bioinformatics* 19, ii103-ii112.
- Lu, J., Du, Z.-X., Kong, J., Chen, L.-N., Qiu, Y.-H., Li, G.-F., Meng, X.-H., Zhu, F., 2012. Transcriptome analysis of *Nicotiana tabacum* infected by *Cucumber mosaic virus* during systemic symptom development. *PLoS One* 7, e43447.

- Luo, C., Tsementzi, D., Kyrpides, N., Read, T., Konstantinidis, K.T., 2012. Direct comparisons of Illumina vs. Roche 454 sequencing technologies on the same microbial community DNA sample. *PLoS One* 7, e30087.
- Maier, I., Wolf, S., Delaroque, N., Müller, D.G., Kawai, H., 1998. A DNA virus infecting the marine brown alga *Pilayella littoralis* (Ectocarpales, Phaeopyceae) in culture. *European Journal of Phycology* 33, 213-220.
- Malin, G., Wilson, W.H., Bratbak, G., Liss, P.S., Mann, N.H., 1998. Elevated production of dimethylsulfide resulting from viral infection of cultures of *Phaeocystis pouchetii*. *Limnology and Oceanography* 43, 1389-1393.
- Manire, C.A., Stacy, B.A., Kinsel, M.J., Daniel, H.T., Anderson, E.T., Wellehan, J.F.X.J., 2008. Proliferative dermatitis in a loggerhead turtle, *Caretta caretta*, and a green turtle, *Chelonia mydas*, associated with novel papillomaviruses. *Veterinary Microbiology* 130, 227-237.
- Mann, N.H., Cook, A., Millard, A., Bailey, S., Clokie, M., 2003. Bacterial photosynthesis genes in a virus. *Nature* 424, 741.
- Mao-Jones, J., Ritchie, K.B., Jones, L.E., Ellner, S.P., 2010. How microbial community composition regulates coral disease development. *PLoS Biology* 8, e1000345.
- Marhaver, K.L., Edwards, R.A., Rohwer, F., 2008. Viral communities associated with healthy and bleaching corals. *Environmental Microbiology* 10, 2277-2286.
- Marie, D., Brussaard, C.P.D., Thyraug, R., Bratbak, G., Vaulot, D., 1999. Enumeration of marine viruses in culture and natural samples by flow cytometry. *Applied and Environmental Microbiology* 65, 45-52.
- Martínez, J.M., Schroeder, D.C., Larsen, A., Bratbak, G., Wilson, W.H., 2007. Molecular dynamics of *Emiliania huxleyi* and cooccurring viruses during two separate mesocosm studies. *Applied and Environmental Microbiology* 73, 554-562.

- McAllister, W.T., Barrett, C.L., 1977. Superinfection exclusion by bacteriophage T7. *Journal of Virology* 24, 709-711.
- McArdle, B.H., Anderson, M.J., 2001. Fitting multivariate models to community data: A comment on distance-based redundancy analysis. *Ecology* 82, 290-297.
- McCloskey, L.R., Muscatine, L., Wilkerson, F.P., 1994. Daily photosynthesis, respiration, and carbon budgets in a tropical marine jellyfish (*Mastigias* sp.). *Marine Biology* 119, 13-22.
- McGinty, E.S., Pieczonka, J., Mydlarz, L.D., 2012. Variations in reactive oxygen release and antioxidant activity in multiple *Symbiodinium* types in response to elevated temperature. *Microbial Ecology* 64, 1000-1007.
- Mei, M.L., Danovaro, R., 2004. Virus production and life strategies in aquatic sediments. *Limnology and Oceanography* 49, 459-470.
- Meints, R.H., Ivey, R.G., Lee, A.M., Choi, T.-J., 2008. Identification of two virus integration sites in the brown alga *Feldmannia* chromosome. *Journal of Virology* 82, 1407-1413.
- Meints, R.H., Lee, K., Burbank, D.E., Van Etten, J.L., 1984. Infection of a *Chlorella*-like alga with the virus, PBCV-1: Ultrastructural studies. *Virology* 138, 341-346.
- Miller, J., Muller, E., Rogers, C., Waara, R., Atkinson, A., Whelan, K.R.T., Patterson, M., Witcher, B., 2009. Coral disease following massive bleaching in 2005 causes 60% decline in coral cover on reefs in the US Virgin Islands. *Coral Reefs* 28, 925-937.
- Minarovits, J., 2006. Epigenotypes of latent herpesvirus genomes. *Current Topics in Microbiology and Immunology* 310, 61-80.
- Minoche, A.E., Dohm, J.C., Himmelbauer, H., 2011. Evaluation of genomic high-throughput sequencing data generated on Illumina HiSeq and Genome Analyzer systems. *Genome Biology* 12, R112.
- Moberg, F., Folke, C., 1999. Ecological goods and services of coral reef ecosystems. *Ecological Economics* 29, 215-233.

- Mohankumar, K., Ramasamy, P., 2006. White spot syndrome virus infection decreases the activity of antioxidant enzymes in *Fenneropenaeus indicus*. *Virus Research* 115, 69-75.
- Moriarty, D.J.W., Pollard, P.C., Hunt, W.G., 1985. Temporal and spatial variation in bacterial production in the water column over a coral reef. *Marine Biology* 85, 285-292.
- Müller, D.G., Bräutigam, M., Knippers, R., 1996. Virus infection and persistence of foreign DNA in the marine brown alga *Feldmannia simplex* (Ectocarpales, Phaeophyceae). *Phycologia* 35, 61-63.
- Muller, E.M., van Woesik, R., 2012. Caribbean coral diseases: primary transmission or secondary infection? *Global Change Biology* 18, 3529-3535.
- Mumby, P.J., Dahlgren, C.P., Harborne, A.R., Kappel, C.V., Micheli, F., Brumbaugh, D.R., Holmes, K.E., Mendes, J.M., Broad, K., Sanchirico, J.N., Buch, K., Box, S., Stoffle, R.W., Gill, A.B., 2006. Fishing, trophic cascades, and the process of grazing on coral reefs. *Science* 311, 98-101.
- Munn, C.B., 2006. Viruses as pathogens of marine organisms - from bacteria to whales. *Journal of the Marine Biological Association of the United Kingdom* 86, 453-467.
- Muscantine, L., 1967. Glycerol excretion by symbiotic algae from corals and tridacna and its control by the host. *Science* 156, 516-519.
- Muscantine, L., Falkowski, P.G., Porter, J.W., Dubinsky, Z., 1984. Fate of photosynthetic fixed carbon in light- and shade-adapted colonies of the symbiotic coral *Stylophora pistillata*. *Proceedings of the Royal Society B* 222, 181-202.
- Muscantine, L., Pool, R.R., 1979. Regulation of numbers of intracellular algae. *Proceedings of the Royal Society B* 204, 131-139.
- Nagasaki, K., Bratbak, G., 2010. Isolation of viruses infecting photosynthetic and nonphotosynthetic protists. In: Wilhelm, S.W., Weinbauer, M.G., Suttle, C.A. (Eds.), *Manual of Aquatic Viral Ecology*. ASLO, pp. 92-101.

- Nagasaki, K., Shirai, Y., Takao, Y., Mizumoto, H., Nishida, K., Tomaru, Y., 2005. Comparison of genome sequences of single-stranded RNA viruses infecting the bivalve-killing dinoflagellate *Heterocapsa circularisquama*. *Applied and Environmental Microbiology* 71, 8888-8894.
- Nagasaki, K., Tomaru, Y., Shirai, Y., Takao, Y., Mizumoto, H., 2006. Dinoflagellate-infecting viruses. *Journal of the Marine Biological Association of the United Kingdom* 86, 469-474.
- Nagasaki, K., Tomaru, Y., Tarutani, K., Katanozaka, N., Yamanaka, S., Tanabe, H., Yamaguchi, M., 2003. Growth characteristics and intraspecies host specificity of a large virus infecting the dinoflagellate *Heterocapsa circularisquama*. *Applied and Environmental Microbiology* 69, 2580-2586.
- Neudecker, S., 1981. Growth and survival of scleractinian corals exposed to thermal effluents at Guam. In: Gomez, E.D., Birkeland, C.E., Buddemeier, R.W. (Eds.), *Proceedings of the fourth international coral reef symposium*, Manila, pp. 173-180.
- Nissimov, J., Rosenberg, E., Munn, C.B., 2009. Antimicrobial properties of resident coral mucus bacteria of *Oculina patagonica*. *FEMS Microbiology Letters* 292, 210-215.
- Nopadon, P., Aranya, P., Tipaporn, T., Toshihiro, N., Takayuki, K., Masashi, M., Makoto, E., 2009. Nodavirus associated with pathological changes in adult spotted coralgroupers (*Plectropomus maculatus*) in Thailand with viral nervous necrosis. *Research in Veterinary Science* 87, 97-101.
- O'Brien, T.L., Macleod, R., Maclean, M.C., 1984. Absence of lytic virus in 2 species of symbiotic algae within the sea anemone *Anthopleura xanthogrammica* (Coelenterata: Anthozoa). *Transactions of the American Microscopical Society* 103, 228-232.
- Ogata, H., Toyoda, K., Tomaru, Y., Nakayama, N., Shirai, Y., Claverie, J.M., Nagasaki, K., 2009. Remarkable sequence similarity between the dinoflagellate-infecting marine girus and the terrestrial pathogen African swine fever virus. *Virology Journal* 6, 178.

- Oksanen, A.J., Blanchet, F.G., Kindt, R., Legendre, P., O'Hara, R.B., Simpson, G.L., Solymos, P., Henry, M., Stevens, H., Wagner, H., 2010. Package 'vegan'. Available at <http://vegan.r-forge.r-project.org/>. Accessed August 26, 2010.
- Onji, M., Nakano, S., Suzuki, S., 2003. Virus-like particles suppress growth of the red-tide-forming marine dinoflagellate *Gymnodinium mikimotoi*. *Marine Biotechnology* 5, 435-442.
- Orr, J.C., Fabry, V.J., Aumont, O., Bopp, L., Doney, S.C., Feely, R.A., Gnanadesikan, A., Gruber, N., Ishida, A., Joos, F., Key, R.M., Lindsay, K., Maier-Reimer, E., Matear, R., Monfray, P., Mouchet, A., Najjar, R.G., Plattner, G.-K., Rodgers, K.B., Sabine, C.L., Sarmiento, J.L., Schlitzer, R., Slater, R.D., Totterdell, I.J., Weirig, M.-F., Yamanaka, Y., Yool, A., 2005. Anthropogenic ocean acidification over the twenty-first century and its impact on calcifying organisms. *Nature* 437, 681-686.
- Ortmann, A.C., Brumfield, S.K., Walther, J., McInnerney, K., Brouns, S.J.J., van de Werken, H.J.G., Bothner, B., Douglas, T., van de Oost, J., Young, M.J., 2008. Transcriptome analysis of infection of the archaeon *Sulfolobus solfataricus* with *Sulfolobus* turreted icosahedral virus. *Journal of Virology* 82, 4874-4883.
- Pandolfi, J.M., Bradbury, R.H., Sala, E., Hughes, T.P., Bjorndal, K.A., Cooke, R.G., McArdle, D., McClenachan, L., Newman, M.J.H., Paredes, G., Warner, R.R., Jackson, J.B.C., 2003. Global trajectories of the long-term decline of coral reef ecosystems. *Science* 301, 955-958.
- Panek, F.M., 2005. Epizootics and disease of coral reef fish in the Tropical Western Atlantic and Gulf of Mexico. *Reviews in Fisheries Science* 13, 1-21.
- Parrish, S., Resch, W., Moss, B., 2007. Vaccinia virus D10 protein has mRNA decapping activity, providing a mechanism for control of host and viral gene expression. *Proceedings of the National Academy of Sciences of the USA* 104, 2139-2144.
- Patel, A., Noble, R.T., Steele, J.A., Schwalbach, M.S., Hewson, I., Fuhrman, J.A., 2007. Virus and prokaryote enumeration from planktonic aquatic environments by epifluorescence microscopy with SYBR Green I. *Nature Protocols* 2, 269-276.

- Patten, N.L., Harrison, P.L., Mitchell, J.G., 2008. Prevalence of virus-like particles within a staghorn scleractinian coral (*Acropora muricata*) from the Great Barrier Reef. *Coral Reefs* 27, 569-580.
- Patten, N.L., Seymour, J.R., Mitchell, J.G., 2006. Flow cytometric analysis of virus-like particles and heterotrophic bacteria within coral-associated reef water. *Journal of the Marine Biological Association of the United Kingdom* 86, 563-566.
- Patterson, K.L., Porter, J.W., Ritchie, K.B., Polson, S.W., Mueller, E., Peters, E.C., Santavy, D.L., Smith, G.W., 2002. The etiology of white pox, a lethal disease of the Caribbean elkhorn coral, *Acropora palmata*. *Proceedings of the National Academy of Sciences of the USA* 99, 8725-8730.
- Pelley, J., 2004. Untangling the causes of coral reef decline. *Environmental Science & Technology* 38, 286A-287A.
- Pennisi, E., 2012. ENCODE project writes eulogy for junk DNA. *Science* 337, 1159-1161.
- Perna, J.J., Mannix, M.L., Rooney, J.F., Notkins, A.L., Straus, S.E., 1987. Reactivation of latent herpes simplex virus infection by ultraviolet light: a human model. *Journal of the American Academy of Dermatology* 17, 473-478.
- Peters, M.A., Jackson, D.C., Crabb, B.S., Browning, G.F., 2002. Chicken anemia virus VP2 is a novel dual specificity protein phosphatase. *The Journal of Biological Chemistry* 277, 39566-39573.
- Philipp, E., Fabricius, K., 2003. Photophysiological stress in scleractinian corals in response to short-term sedimentation. *Journal of Experimental Marine Biology and Ecology* 287, 57-78.
- Pochon, X., Garcia-Cuetos, L., Baker, A.C., Castella, E., Pawlowski, J., 2007. One-year survey of a single Micronesian reef reveals extraordinarily rich diversity of *Symbiodinium* types in soritid foraminifera. *Coral Reefs* 26, 867-882.

- Pochon, X., Pawlowski, J., 2006. Evolution of the soritids-*Symbiodinium* symbiosis. *Symbiosis* 42, 77-88.
- Prescott, L.M., Harley, J.P., Klein, D.A., 1993. *Microbiology*. WC Brown, Dubuque.
- Proctor, L.M., Fuhrman, J.A., 1990. Viral mortality of marine bacteria and cyanobacteria. *Nature* 343, 60-62.
- R Development Core Team, 2006. *R: A language and environment for statistical computing*. R Foundation for Statistical Computing, Vienna, Austria.
- Radford, A.D., Chapman, D., Dixon, L., Chantrey, J., Darby, A.C., Hall, N., 2012. Application of next-generation sequencing technologies in virology. *Journal of General Virology* 93, 1853-1868.
- Raghunathan, A., Ferguson, H.R.J., Bornarth, C.J., Song, W., Driscoll, M., Lasken, R.S., 2005. Genomic DNA amplification from a single bacterium. *Applied and Environmental Microbiology* 71, 3342-3347.
- Raymundo, L.J., Harvell, C.D., Reynolds, T., 2003. *Porites* ulcerative white spot disease: description, prevalence, and host range of a new coral disease affecting Indo-Pacific Reefs. *Diseases of Aquatic Organisms* 56, 95-104.
- Raymundo, L.J., Rosell, K.B., Reboton, C.T., Kaczmarzsky, L., 2005. Coral diseases on Philippine reefs: genus *Porites* is a dominant host. *Diseases of Aquatic Organisms* 64, 181-191.
- Redding, J.E., Myers-Miller, R.L., Baker, D.M., Fogel, M., Raymundo, L.J., Kim, K., 2013. Link between sewage-derived nitrogen pollution and coral disease severity in Guam. *Marine Pollution Bulletin* <http://dx.doi.org/10.1016/j.marpolbul.2013.06.002>.
- Reisinger, J., Rumpler, S., Lion, T., Ambros, P.F., 2006. Visualization of episomal and integrated Epstein-Barr virus DNA by fiber fluorescence *in situ* hybridization. *International Journal of Cancer* 118, 1603-1608.

- Reshef, L., Koren, O., Loya, Y., Zilber-Rosenberg, I., Rosenberg, E., 2006. The coral probiotic hypothesis. *Environmental Microbiology* 8, 2068-2073.
- Rhodes, C.J., Truscott, J.E., Martin, A.P., 2008. Viral infection as a regulator of oceanic phytoplankton populations. *Journal of Marine Systems* 74, 216-226.
- Richardson, L.L., 1998. Coral diseases: what is really known? *Trends in Ecology and Evolution* 13, 438-443.
- Richier, S., Rodriguez-Lanetty, M., Schnitzler, C.E., Weis, V.M., 2008. Response of the symbiotic cnidarian *Anthopleura elegantissima* transcriptome to temperature and UV stress. *Comparative Biochemistry and Physiology, Part D* 3, 283-289.
- Riedle-Bauer, M., 2000. Role of reactive oxygen species and antioxidant enzymes in systemic virus infections of plants. *Journal of Phytopathology* 148, 297-302.
- Ritchie, K.B., 2006. Regulation of microbial populations by coral surface mucus and mucus-associated bacteria. *Marine Ecology Progress Series* 322, 1-14.
- Ritchie, K.B., Smith, G.W., 1997. Physiological comparison of bacterial communities from various species of scleractinian corals. *Proceedings of the 8th International Coral Reef Symposium* 1, 521-526.
- Ritchie, K.B., Smith, G.W., 2004. Microbial communities of coral surface mucopolysaccharide layers. In: Rosenberg, E., Loya, Y. (Eds.), *Coral health and disease*. Springer-Verlag, New York, pp. 259-264.
- Rodriguez-Lanetty, M., Phillips, W.S., Weis, V.M., 2006. Transcriptome analysis of a cnidarian - dinoflagellate mutualism reveals complex modulation of host gene expression. *BMC Genomics* 7, 23.
- Roff, G., Ulstrup, K.E., Fine, M., Ralph, P.J., Hoegh-Guldberg, O., 2008. Spatial heterogeneity of photosynthetic activity within diseased corals from the Great Barrier Reef. *Journal of Phycology* 44, 526-538.

- Rohwer, F., Breitbart, M., Jara, J., Azam, F., Knowlton, N., 2001. Diversity of bacteria associated with the Caribbean coral *Montastrea franksi*. *Coral Reefs* 20, 85-91.
- Rohwer, F., Seguritan, V., Azam, F., Knowlton, N., 2002. Diversity and distribution of coral-associated bacteria. *Marine Ecology Progress Series* 243, 1-10.
- Rohwer, F., Vega Thurber, R., 2009. Viruses manipulate the marine environment. *Nature* 459, 207-212.
- Roossinck, M.J., 2008. Symbiosis, mutualism and symbiogenesis. In: Roossinck, M.J. (Ed.), *Plant Virus Evolution*. Springer-Verlag, Berlin, pp. 157-164.
- Rosenberg, E., Ben-Haim, Y., 2002. Microbial diseases of corals and global warming. *Environmental Microbiology* 4, 318-326.
- Rosenberg, E., Falkovitz, L., 2004. The *Vibrio shiloi/Oculina patagonica* model system of coral bleaching. *Annual Review of Microbiology* 58, 143-159.
- Rosenberg, E., Koren, O., Reshef, L., Efrony, R., Zilber-Rosenberg, I., 2007. The role of microorganisms in coral health, disease and evolution. *Nature Reviews Microbiology* 5, 355-362.
- Rowan, R., 1998. Diversity and ecology of zooxanthellae on coral reefs. *Journal of Phycology* 34, 407-417.
- Rypien, K.L., Ward, J.R., Azam, F., 2010. Antagonistic interactions among coral-associated bacteria. *Environmental Microbiology* 12, 28-39.
- Sandaa, R.-A., 2008. Burden or benefit? Virus-host interactions in the marine environment. *Research in Microbiology* 159, 374-381.
- Sano, E., Carlson, S., Wegley, L., Rohwer, F., 2004. Movement of viruses between biomes. *Applied and Environmental Microbiology* 70, 5842-5846.

- Schaub, S.A., Sorber, C.A., Taylor, G.W., 1974. The association of enteric viruses with natural turbidity in the aquatic environment. In: Malina, J.F., Sagik, B.P. (Eds.), Virus survival in water and wastewater systems. University of Texas, Austin.
- Schroeder, D.C., Oke, J., Hall, M., Malin, G., Wilson, W.H., 2003. Virus succession observed during an *Emiliania huxleyi* bloom. *Applied and Environmental Microbiology* 69, 2484-2490.
- Schroeder, D.C., Oke, J., Malin, G., Wilson, W.H., 2002. Coccolithovirus (*Phycodnaviridae*): Characterisation of a new large dsDNA algal virus that infects *Emiliania huxleyi*. *Archives of Virology* 147, 1685-1698.
- Schuster, A.M., Girtton, L., Burbank, D.E., Van Etten, J.L., 1986. Infection of a *Chlorella*-like alga with the virus PBCV-1: Transcriptional studies. *Virology* 148, 181-189.
- Schwarz, K.B., 1996. Oxidative stress during viral infection: a review. *Free Radical Biology and Medicine* 21, 641-649.
- Segel, L.A., Ducklow, H.W., 1982. A theoretical investigation into the influence of sublethal stresses on coral-bacterial ecosystem dynamics. *Bulletin of Marine Science* 32, 919-935.
- Seymour, J.R., Patten, N., Bourne, D.G., Mitchell, J.G., 2005. Spatial dynamics of virus-like particles and heterotrophic bacteria within a shallow coral reef system. *Marine Ecology Progress Series* 288, 1-8.
- Sharon, I., Alperovitch, A., Rohwer, F., Haynes, M., Glaser, F., Atamna-Ismaeel, N., Pinter, R.Y., Partensky, F., Koonin, E.V., Wolf, Y.I., Nelson, N., Béjà, O., 2009. Photosystem I gene cassettes are present in marine virus genomes. *Nature* 461, 258-262.
- Shashar, N., 1992. Endolithic algae within corals - Life in an extreme environment. *Journal of Experimental Marine Biology and Ecology* 163, 277-286.
- Short, C.M., Suttle, C.A., 2005. Nearly identical bacteriophage structural gene sequences are widely distributed in both marine and freshwater environments. *Applied and Environmental Microbiology* 71, 480-486.

- Si, X., Gao, G., Wong, J., Wang, Y., Zhang, J., Luo, H., 2008. Ubiquitination is required for effective replication of coxsackievirus B3. *PLoS One* 3, e2585.
- Sicko-Goad, L., Walker, G., 1979. Viroplasm and large virus-like particles in the dinoflagellate *Gymnodinium uberrimum*. *Protoplasma* 99, 203-210.
- Simpson, J.T., Durbin, R., 2012. Efficient de novo assembly of large genomes using compressed data structures. *Genome Research* 22, 549-556.
- Simpson, J.T., Wong, K., Jackman, S.D., Schein, J.E., Jones, S.J.M., Birol, I., 2009. ABySS: A parallel assembler for short read sequence data. *Genome Research* 19, 1117-1123.
- Spencer, R., 1955. A marine bacteriophage. *Nature* 175, 690-691.
- Squires, D.F., 1965. Neoplasia in a coral? *Science* 148, 503-505.
- Stepanauskas, R., 2012. Single cell genomics: an individual look at microbes. *Current Opinion in Microbiology* 15, 613-620.
- Stimson, J., Sakai, K., Sembali, H., 2002. Interspecific comparison of the symbiotic relationship in corals with high and low rates of bleaching-induced mortality. *Coral Reefs* 21, 409-421.
- Streamer, M., Griffiths, D.J., Thinh, L., 1988. The products of photosynthesis by zooxanthellae (*Symbiodinium microadriaticum*) of *Tridacna gigas* and their transfer to the host. *Symbiosis* 6, 237-252.
- Strychar, K.B., Sammarco, P.W., Piva, T.J., 2004. Apoptotic and necrotic stages of *Symbiodinium* (Dinophyceae) cell death activity: bleaching of soft and scleractinian corals. *Phycologia* 43, 768-777.
- Sudek, M., Aeby, G.S., Davy, S.K., 2012a. Localized bleaching in Hawaii causes tissue loss and a reduction in the number of gametes in *Porites compressa*. *Coral Reefs* 31, 351-355.

- Sudek, M., Work, T.M., Aeby, G.S., Davy, S.K., 2012b. Histological observations in the Hawaiian reef coral, *Porites compressa*, affected by *Porites* bleaching with tissue loss. *Journal of Invertebrate Pathology* 111, 121-125.
- Sun, R., Lin, S.-F., Gradoville, L., Yuan, Y., Zhu, F., Miller, G., 1998. A viral gene that activates lytic cycle expression of Kaposi's sarcoma-associated herpesvirus. *Proceedings of the National Academy of Sciences of the USA* 95, 10866-10871.
- Sunagawa, S., Wilson, E.C., Thaler, M., Smith, M.L., Caruso, C., Pringle, J.R., Weis, V.M., Medina, M., Schwarz, J., 2009. Generation and analysis of transcriptomic resources for a model system on the rise: the sea anemone *Aiptasia pallida* and its dinoflagellate endosymbiont. *BMC Genomics* 10, 258.
- Sunda, W.G., Graneli, E., Gobler, C.J., 2006. Positive feedback and the development and persistence of ecosystem disruptive algal blooms. *Journal of Phycology* 42, 963-974.
- Sussman, M., Willis, B.L., Victor, S., Bourne, D.G., 2008. Coral pathogens identified for white syndrome (WS) epizootics in the Indo-Pacific. *PLoS One* 3, e2393.
- Sutherland, K.P., Porter, J.W., Torres, C., 2004. Disease and immunity in Caribbean and Indo-Pacific zooxanthellate corals. *Marine Ecology Progress Series* 266, 273-302.
- Suttle, C.A., 2005. Viruses in the sea. *Nature* 437, 356-361.
- Suttle, C.A., 2007. Marine viruses - major players in the global ecosystem. *Nature Reviews Microbiology* 5, 801-812.
- Suttle, C.A., Chan, A.M., Cottrell, M.T., 1991. Use of ultrafiltration to isolate viruses from seawater which are pathogens of marine phytoplankton. *Applied and Environmental Microbiology* 57, 721-726.
- Suttle, C.A., Chen, F., 1992. Mechanisms and rates of decay of marine viruses in seawater. *Applied and Environmental Microbiology* 58, 3721-3729.

- Suttle, C.A., Fuhrman, J.A., 2010. Enumeration of virus particles in aquatic or sediment samples by epifluorescence microscopy. In: Wilhelm, S.W., Weinbauer, M.G., Suttle, C.A. (Eds.), *Manual of Aquatic Viral Ecology*. ASLO, pp. 145-153.
- Tai, V., Lawrence, J.E., Lang, A.S., Chan, A.M., Culley, A.I., Suttle, C.A., 2003. Characterization of HaRNAV, a single-stranded RNA virus causing lysis of *Heterosigma akashiwo* (Raphidophyceae). *Journal of Phycology* 39, 343-352.
- Tarutani, K., Nagasaki, K., Itakura, S., Yamaguchi, M., 2001. Isolation of a virus infecting the novel shellfish-killing dinoflagellate *Heterocapsa circularisquama*. *Aquatic Microbial Ecology* 23, 103-111.
- Telesnicki, G.J., Goldberg, W.M., 1995. Effects of turbidity on the photosynthesis and respiration of two South Florida reef coral species. *Bulletin of Marine Science* 57, 527-539.
- Temin, H.M., 1985. Reverse transcription in the eukaryotic genome: retroviruses, pararetroviruses, retrotransposons, and retrotranscripts. *Molecular Biology and Evolution* 2, 455-468.
- The Gene Ontology Consortium, 2000. Gene Ontology: tool for the unification of biology. *Nature Genetics* 25, 25-29.
- Thomas, R., Grimsley, N., Escande, M., Subirana, L., Derelle, E., Moreau, H., 2011a. Acquisition and maintenance of resistance to viruses in eukaryotic phytoplankton populations. *Environmental Microbiology* 13, 1412-1420.
- Thomas, V., Bertelli, C., Collyn, F., Casson, N., Telenti, A., Goesmann, A., Croxatto, A., Greub, G., 2011b. Lausannevirus, a giant amoebal virus encoding histone doublets. *Environmental Microbiology* 13, 1454-1466.
- Thompson, J.D., Higgins, D.G., Gibson, T.J., 1994. Clustal-W - Improving the sensitivity of progressive multiple sequence alignment through sequence weighting, position-specific gap penalties and weight matrix choice. *Nucleic Acids Research* 22, 4673-4680.

- Tomaru, Y., Katanozaka, N., Nishida, K., Shirai, Y., Tarutani, K., Yamaguchi, M., Nagasaki, K., 2004. Isolation and characterization of two distinct types of HcRNAV, a single-stranded RNA virus infecting the bivalve-killing microalga *Heterocapsa circularisquama*. *Aquatic Microbial Ecology* 34, 207-218.
- Tomaru, Y., Mizumoto, H., Nagasaki, K., 2009. Virus resistance in the toxic bloom-forming dinoflagellate *Heterocapsa circularisquama* to single-stranded RNA virus infection. *Environmental Microbiology* 11, 2915-2923.
- Tomaru, Y., Shirai, Y., Nagasaki, K., 2008. Ecology, physiology and genetics of a phycodnavirus infecting the noxious boom-forming raphidophyte *Heterosigma akashiwo*. *Fisheries Science* 74, 701-711.
- Trench, R.K., 1987. Dinoflagellates in non-parasitic symbiosis. In: Taylor, F.J.R. (Ed.), *The biology of dinoflagellates*. Blackwell Scientific Publishers, Oxford, pp. 530-570.
- Trench, R.K., Winsor, H., 1987. Symbiosis with dinoflagellates in two pelagic flatworms, *Amphiscolops* sp. and *Haplodiscus* sp. *Symbiosis* 3, 1-21.
- Van Elk, C.E., Van De Bildt, M.W.G., De Jong, A.A.W., Osterhaus, A.D.M.E., Kuiken, T., 2009. Genital herpesvirus in bottlenose dolphins (*Tursiops truncatus*): cultivation, epidemiology, and associated pathology. *Journal of Wildlife Diseases* 45, 895-906.
- Van Etten, J.L., Burbank, D.E., Xia, Y., Meints, R.H., 1983. Growth cycle of a virus, PBCV-1, that infects *Chlorella*-like algae. *Virology* 126, 117-125.
- Van Etten, J.L., Graves, M.V., Müller, D.G., Boland, W., Delaroque, N., 2002. *Phycodnaviridae* - large DNA algal viruses. *Archives of Virology* 147, 1479-1516.
- Van Etten, J.L., Lane, L.C., Meints, R.H., 1991. Viruses and viruslike particles of eukaryotic algae. *Microbiological Reviews* 55, 586-620.
- Van Etten, J.L., Meints, R.H., 1999. Giant viruses infecting algae. *Annual Review of Microbiology* 53, 447-494.

- van Oppen, M.J.H., Leong, J.A., Gates, R.D., 2009. Coral-virus interactions: A double-edged sword? *Symbiosis* 47, 1-8.
- Vega Thurber, R., Correa, A.M.S., 2011. Viruses of reef-building scleractinian corals. *Journal of Experimental Marine Biology and Ecology* 408, 102-113.
- Vega Thurber, R.L., Barott, K.L., Hall, D., Liu, H., Rodriguez-Mueller, B., Desnues, C., Edwards, R.A., Haynes, M., Angly, F.E., Wegley, L., Rohwer, F., 2008. Metagenomic analysis indicates that stressors induce production of herpes-like viruses in the coral *Porites compressa*. *Proceedings of the National Academy of Sciences of the USA* 105, 18413-18418.
- Venn, A.A., Loram, J.E., Douglas, A.E., 2008. Photosynthetic symbioses in animals. *Journal of Experimental Botany* 59, 1069-1080.
- Veron, J.E.N., 2011. Ocean acidification and coral reefs: an emerging big picture. *Diversity* 3, 262-274.
- Villareal, L.P., DeFilippis, V.R., 2000. A hypothesis for DNA viruses as the origin of eukaryotic replication proteins. *Journal of Virology* 74, 7079-7084.
- Voss, J.D., Richardson, L.L., 2006. Nutrient enrichment enhances black band disease progression in corals. *Coral Reefs* 25, 569-576.
- Wagner, G.P., Kin, K., Lynch, V.J., 2012. Measurement of mRNA abundance using RNA-seq data: RPKM measure is inconsistent among samples. *Theory in Biosciences* 131, 281-285.
- Wanders, J.B.W., 1977. The role of benthic algae in the shallow reef of Curacao (Netherlands Antilles) III: The significance of grazing. *Aquatic Botany* 3, 357-390.
- Wang, Y., Kleespies, R.G., Ramle, M.B., Jehle, J.A., 2008. Sequencing of the large dsDNA genome of *Oryctes rhinoceros* nudivirus using multiple displacement amplification of nanogram amounts of virus DNA. *Journal of Virological Methods* 152, 106-108.

- Waters, R.E., Chan, A.T., 1982. *Micromonas pusilla* virus: the virus growth cycle and associated physiological events within the host cells; host range mutation. *Journal of General Virology* 63, 199-206.
- Wegley, L., Edwards, R., Rodriguez-Brito, B., Liu, H., Rohwer, F., 2007. Metagenomic analysis of the microbial community associated with the coral *Porites astreoides*. *Environmental Microbiology* 9, 2707-2719.
- Wegley, L., Yu, Y., Breitbart, M., Casas, V., Kline, D.I., Rohwer, F., 2004. Coral-associated Archaea. *Marine Ecology Progress Series* 273, 89-96.
- Weil, E., Smith, G., Gil-Agudelo, D.L., 2006. Status and progress in coral reef disease research. *Diseases of Aquatic Organisms* 69, 1-7.
- Weinbauer, M.G., 2004. Ecology of prokaryotic viruses. *FEMS Microbiology Reviews* 28, 127-181.
- Weinbauer, M.G., Suttle, C.A., 1997. Comparison of epifluorescence and transmission electron microscopy for counting viruses in natural marine waters. *Aquatic Microbial Ecology* 13, 225-232.
- Weis, V.M., 2008. Cellular mechanisms of Cnidarian bleaching: stress causes the collapse of symbiosis. *The Journal of Experimental Biology* 211, 3059-3066.
- Weis, V.M., Davy, S.K., Hoegh-Guldberg, O., Rodriguez-Lanetty, M., Pringle, J.R., 2008. Cell biology in model systems as the key to understanding corals. *Trends in Ecology and Evolution* 23, 369-376.
- Weynberg, K.D., Allen, M.J., Ashelford, K., Scanlan, D.J., Wilson, W.H., 2009. From small hosts come big viruses: the complete genome of a second *Ostreococcus tauri* virus, OtV-1. *Environmental Microbiology* 11, 2821-2839.
- Wilcox, R.M., Fuhrman, J.A., 1994. Bacterial viruses in coastal seawater: lytic rather than lysogenic production. *Marine Ecology Progress Series* 114, 35-45.

- Wilhelm, S.W., Weinbauer, M.G., Suttle, C.A., Jeffrey, W.H., 1998. The role of sunlight in the removal and repair of viruses in the sea. *Limnology and Oceanography* 43, 586-592.
- Williams, G.J., Aeby, G., Cowie, R.O.M., Davy, S.K., 2010. Predictive modeling of coral disease distribution within a reef system. *PLoS ONE* 5, 9264.
- Wilson, W.H., Chapman, D.M., 2001. Observation of virus-like particles in thin sections of the plumose anemone, *Metridium senile*. *Journal of the Marine Biological Association of the United Kingdom* 81, 879-880.
- Wilson, W.H., Dale, A.L., Davy, J.E., Davy, S.K., 2005a. An enemy within? Observations of virus-like particles in reef corals. *Coral Reefs* 24, 145-148.
- Wilson, W.H., Francis, I., Ryan, K., Davy, S.K., 2001. Temperature induction of viruses in symbiotic dinoflagellates. *Aquatic Microbial Ecology* 25, 99-102.
- Wilson, W.H., Schroeder, D.C., 2010. Sequencing and characterization of virus genomes. In: Wilhelm, S.W., Weinbauer, M.G., Suttle, C.A. (Eds.), *Manual of Aquatic Viral Ecology*. ASLO, pp. 134-144.
- Wilson, W.H., Schroeder, D.C., Allen, M.J., Holden, M.T.G., Parkhill, J., Barrell, B.G., Churcher, C., Hamlin, N., Mungall, K., Norbertczak, H., Quail, M.A., Price, C., Rabinowitsch, E., Walker, D., Craigon, M., Roy, D., Ghazal, P., 2005b. Complete genome sequence and lytic phase transcription profile of a *Coccolithovirus*. *Science* 309, 1090-1092.
- Wilson, W.H., Tarran, G., Zubkov, M.V., 2002. Virus dynamics in a coccolithophore-dominated bloom in the North Sea. *Deep-Sea Research II* 49, 2951-2963.
- Wilson, W.H., Turner, S., Mann, N.H., 1998. Population dynamics of phytoplankton and viruses in a phosphate-limited mesocosm and their effect on DMSP and DMS production. *Estuarine, Coastal and Shelf Science* 46, 49-59.
- Wilson, W.H., Van Etten, J.L., Allen, M.J., 2009. The *Phycodnaviridae*: the story of how tiny giants rule the world. In: Van Etten, J.L. (Ed.), *Lesser known large dsDNA viruses*. *Current Topics in Microbiology and Immunology* 328. Springer-Verlag, Berlin, pp. 1-42.

- Wommack, K.E., Colwell, R.R., 2000. Virioplankton: viruses in aquatic ecosystems. *Microbiology and Molecular Biology Reviews* 64, 69-114.
- Woodhouse, S.D., Narayan, R., Latham, S., Lee, S., Antrobus, R., Gangadharan, B., Luo, S., Schroth, G.P., Klenerman, P., Zitzmann, N., 2010. Transcriptome sequencing, microarray, and proteomic analyses reveal cellular and metabolic impact of hepatitis C virus infection *in vitro*. *Hepatology* 52, 443-453.
- Wu, S., Zhu, Z., Fu, L., Niu, B., Li, W., 2011. WebMGA: a customizable web server for fast metagenomic sequence analysis. *BMC Genomics* 12, 444.
- Yang, Z., Bruno, D.P., Martens, C.A., Porcella, S.F., Moss, B., 2010. Simultaneous high-resolution analysis of vaccinia virus and host cell transcriptomes by deep RNA sequencing. *Proceedings of the National Academy of Sciences of the USA* 107, 11513-11518.
- Ye, J., Zheng, H., Zhang, Y., Chen, J., Zhang, Z., Wang, J., Li, S., Li, R., Bolund, L., Wang, J., 2006. WEGO: a web tool for plotting GO annotations. *Nucleic Acids Research* 34, W293-W297.
- Yoon, H.S., Price, D.C., Stepanauskas, R., Rajah, V.D., Sieracki, M.E., Wilson, W.H., Yang, E.C., Duffy, S., Bhattacharya, D., 2011. Single-cell genomics reveals organismal interactions in uncultivated marine protists. *Science* 332, 714-717.

Appendices

Appendix A: Additional data for Chapter 2.

Table A1. *Symbiodinium* cultures screened for latent viral infections.

Culture ID	Host	Original collection location	Clade
CCMP421	<i>Free-living</i>	Wellington Harbour, NZ	E
CCMP827	<i>Unknown</i>	Unknown	Unknown
CCMP828	<i>Unknown</i>	Florida Keys, USA	Unknown
CCMP829	<i>Tridacna crocera</i>	Great Barrier Reef, Australia	Unknown
CCMP830	<i>Aiptasia pallida</i>	Bermuda	Unknown
CCMP831	<i>Tridacna gigas</i>	Great Barrier Reef, Australia	Unknown
CCMP832	<i>Hippopus hippopus</i>	Great Barrier Reef, Australia	Unknown
CCMP1633	<i>Aiptasia pallida</i>	Hawaii, USA	Unknown
CCMP2428	<i>Leptastrea purpurea</i>	Great Barrier Reef, Australia	Unknown
CCMP2429	<i>Heliofungia actiformis</i>	Great Barrier Reef, Australia	Unknown
CCMP2430	<i>Tridacna maxima</i>	Great Barrier Reef, Australia	A
CCMP2431	<i>Leptastrea purpurea</i>	Great Barrier Reef, Australia	Unknown
CCMP2434	<i>Leptastrea purpurea</i>	Great Barrier Reef, Australia	Unknown
CCMP2456	<i>Plexaura homamalla</i>	Bermuda	Unknown
CCMP2457	<i>Tridacna crocera</i>	Coral Sea, Australia	Unknown
CCMP2458	<i>Cassiopeia andromeda</i>	Gulf of Aqaba, Red Sea	Unknown
CCMP2459	<i>Oculina diffusa</i>	Bermuda	B
CCMP2460	<i>Aiptasia pallida</i>	Florida, USA	Unknown
CCMP2461	<i>Zoanthus sociatus</i>	Jamaica	Unknown
CCMP2464	<i>Cassiopeia xamachana</i>	Florida, USA	Unknown
CCMP2465	<i>Tridacna maxima</i>	Palau	A
CCMP2466	<i>Discosoma sanctithomae</i>	Jamaica	Unknown
CCMP2467	<i>Stylophora pistillata</i>	Gulf of Aqaba, Red Sea	A
CCMP2468	<i>Montipora verrucosa</i>	Hawaii, USA	Unknown
CCMP2469	<i>Condylactis gigantea</i>	Jamaica	A
CCMP2470	<i>Pseudoterogorgia bipinnata</i>	Jamaica	Unknown

Table A1 (continued).

CCMP2548	Unknown	Hawaii, USA	Unknown
CCMP2556	<i>Montastrea faveolata</i>	Florida Keys, USA	Unknown
CCMP2592	<i>Heliofungia actiniformis</i>	Great Barrier Reef, Australia	Unknown
2a	<i>Plexaura kuna</i>	Florida, USA	A
A001	<i>Acropora</i> sp.	Okinawa, Japan	D
Ap1	<i>Aiptasia pulchella</i>	Okinawa, Japan	B
SLClone1	<i>Aiptasia pulchella</i>	Davy Lab, VUW	Unknown
SLClone2	<i>Aiptasia pulchella</i>	Davy Lab, VUW	Unknown
FLAp1	<i>Aiptasia pallida</i>	Florida, USA	A
FLAp2	<i>Aiptasia pallida</i>	Florida, USA	B
Mf7.5T	Unknown	Unknown	C
Mf13.14	Unknown	Unknown	A
Mp	<i>Mastigia papua</i>	Palau	C
Pd	<i>Pocillopora damicornis</i>	Hawaii, USA	B
Pd45a	<i>Porites divaricata</i>	Unknown	C
Pe	<i>Porites evermanni</i>	Hawaii, USA	B
PK13	<i>Plexaura kuna</i>	Florida, USA	B
<i>S. bermudense</i>	Unknown	Unknown	B
<i>S. californium</i>	Unknown	Unknown	E
Sin	<i>Sinularia</i> sp.	Guam	C
Stylo0	<i>Stylophora</i> sp.	Unknown	Unknown
Stylo1	<i>Stylophora</i> sp.	Unknown	Unknown
Zs	<i>Zoanthus sociatus</i>	Jamaica	A

Figures A1 – A12 show the responses of *Symbiodinium*, VLP, bacterium and phage populations in *Symbiodinium* cell cultures exposed 302 nm wavelength UV radiation. Experimental conditions were as described for screening experiments in Chapter 2, except that cultures were exposed to 69 J m⁻² total irradiation provided by an inverted 302 nm wavelength UVP transilluminator. Samples were collected every 24 – 48 h and counts were carried out using flow cytometry as described in Chapter 2.

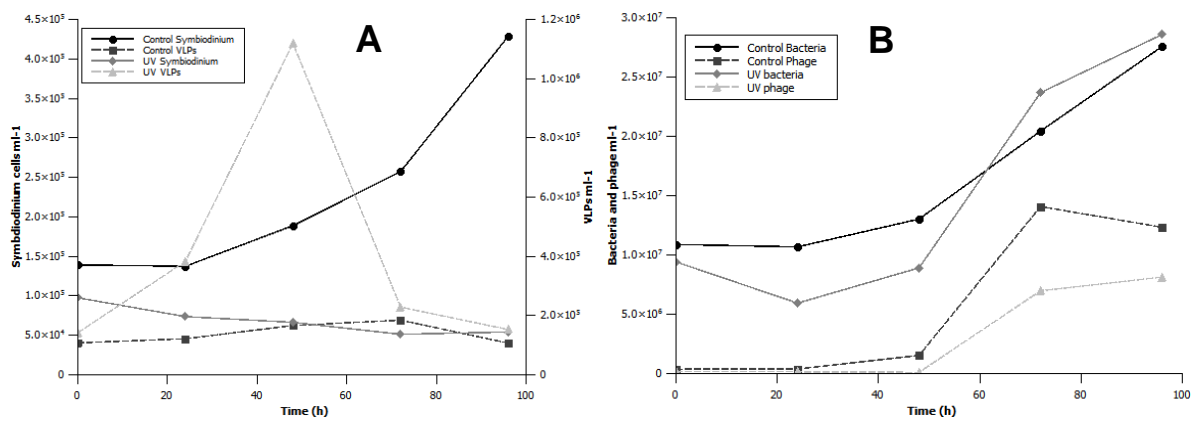


Figure A1. *Symbiodinium* & VLP (A) and bacterium & phage (B) population density in control and 302 nm UV-irradiated cultures of *Symbiodinium* culture CCMP421.

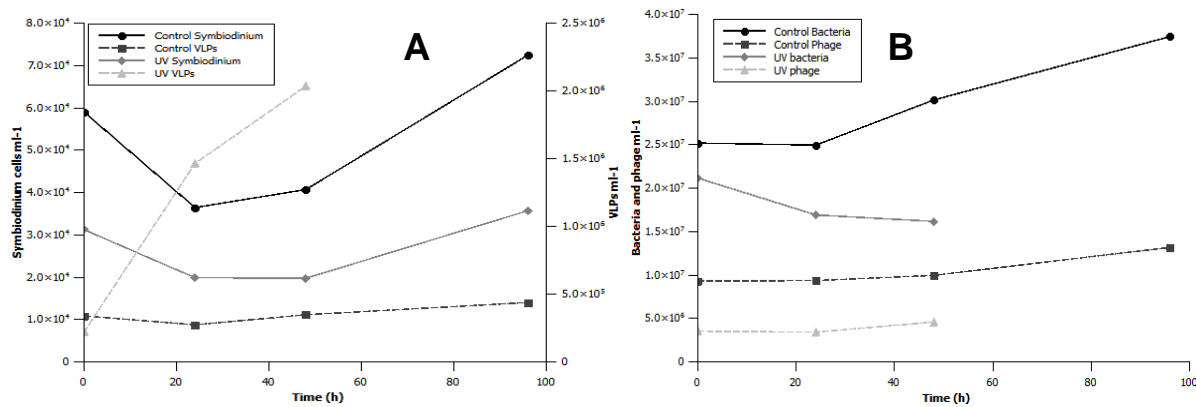


Figure A2. *Symbiodinium* & VLP (A) and bacterium & phage (B) population density in control and 302 nm UV-irradiated cultures of *Symbiodinium* culture CCMP828. Bacteria, phage and VLP samples taken 96 h after UV exposure were lost, therefore the data points for these cultures end at 48 h post-exposure.

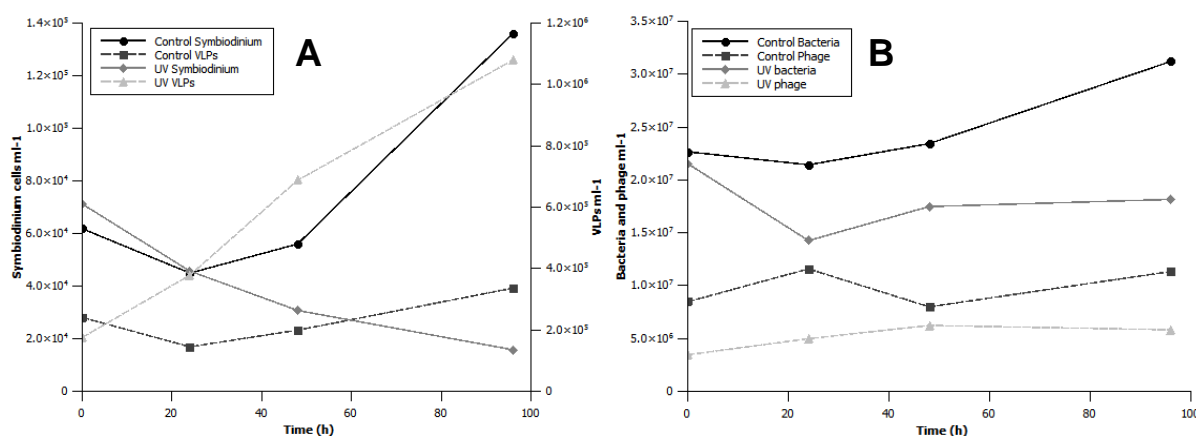


Figure A3. *Symbiodinium* & VLP (A) and bacterium & phage (B) population density in control and 302 nm UV-irradiated cultures of *Symbiodinium* culture CCMP2430.

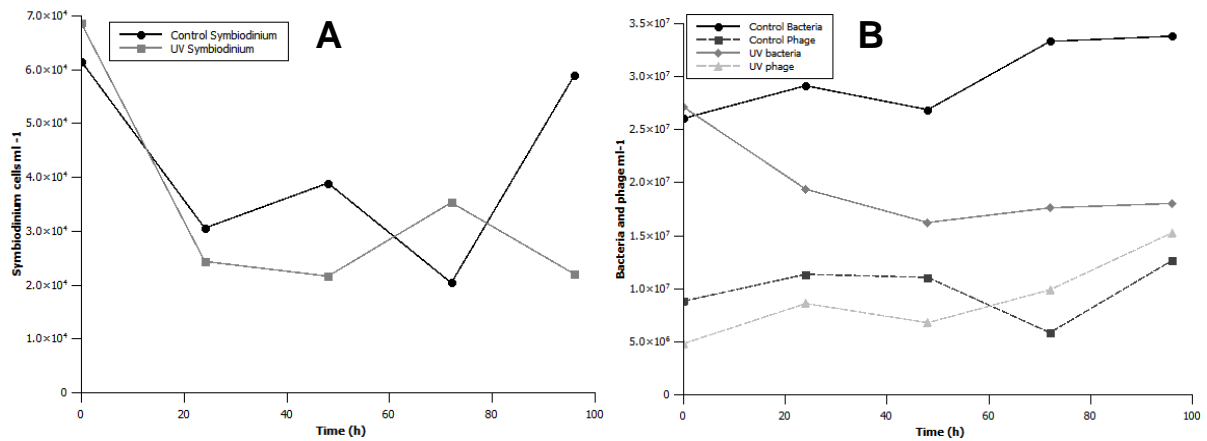


Figure A4. *Symbiodinium* (A) and bacterium & phage (B) population density in control and 302 nm UV-irradiated cultures of *Symbiodinium* culture CCMP2431. No VLPs were seen in control or UV-irradiated samples.

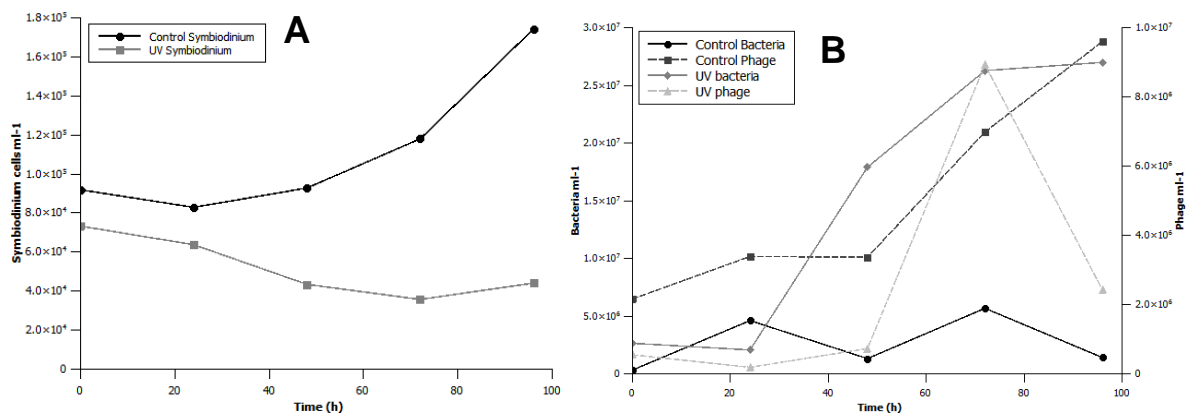


Figure A5. *Symbiodinium* (A) and bacterium & phage (B) population density in control and 302 nm UV-irradiated cultures of *Symbiodinium* culture CCMP2465. No VLPs were seen in control or UV-irradiated samples.

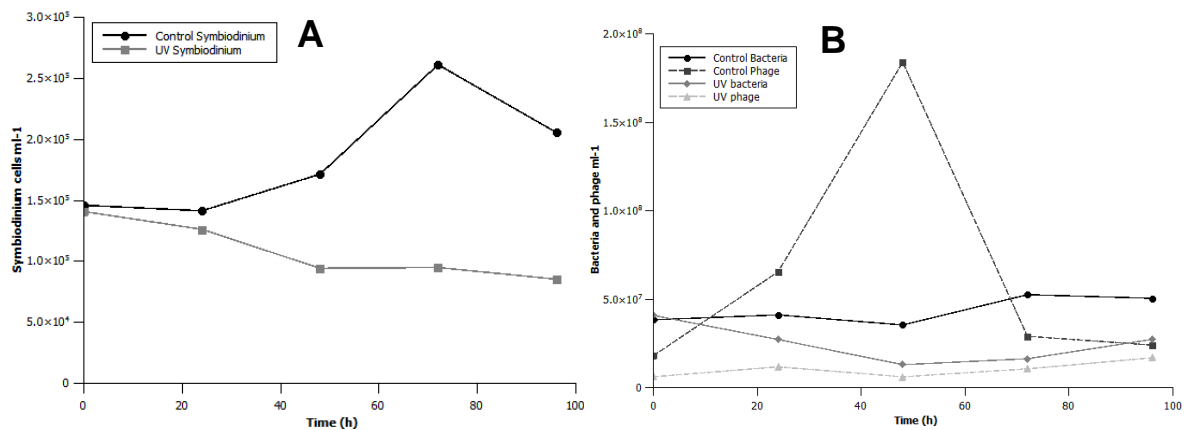


Figure A6. *Symbiodinium* (A) and bacterium & phage (B) population density in control and 302 nm UV-irradiated cultures of *Symbiodinium* culture CCMP2467. No VLPs were seen in control or UV-irradiated samples.

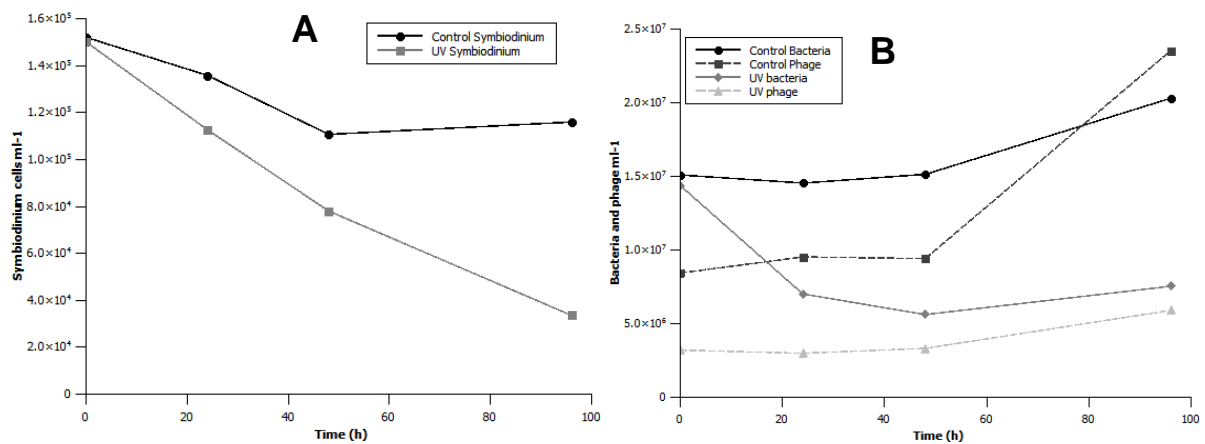


Figure A7. *Symbiodinium* (A) and bacterium & phage (B) population density in control and 302 nm UV-irradiated cultures of *Symbiodinium* culture Ap1. No VLPs were seen in control or UV-irradiated samples.

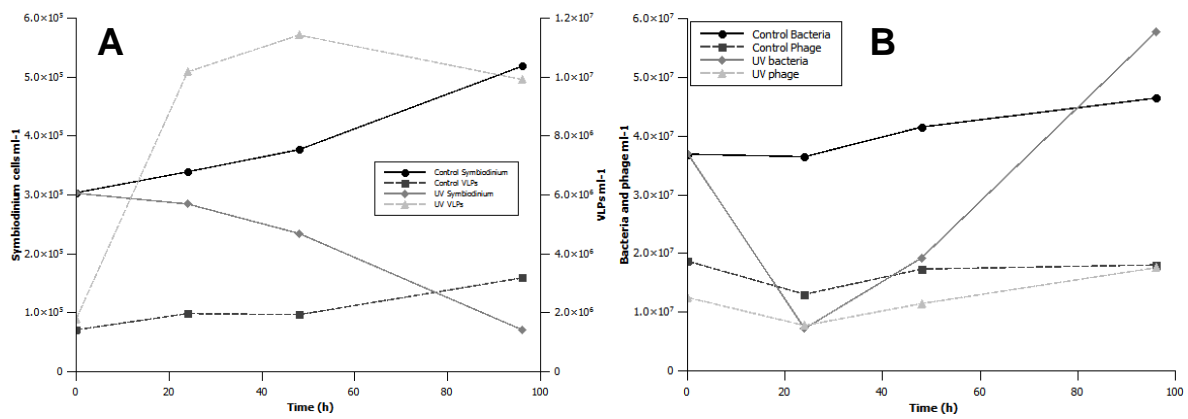


Figure A8. *Symbiodinium* & VLP (A) and bacterium & phage (B) population density in control and 302 nm UV-irradiated cultures of *Symbiodinium* culture FLAp1.

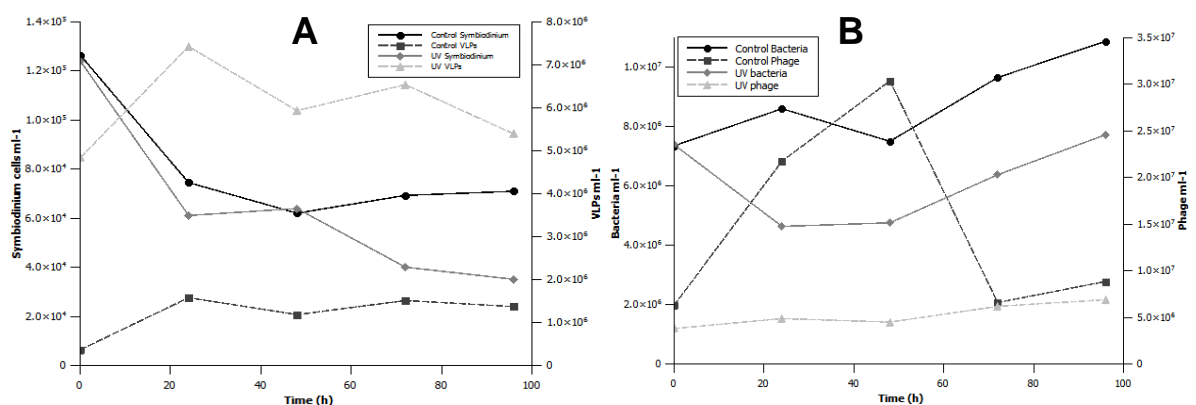


Figure A9. *Symbiodinium* & VLP (A) and bacterium & phage (B) population density in control and 302 nm UV-irradiated cultures of *Symbiodinium* culture Mf13.14.

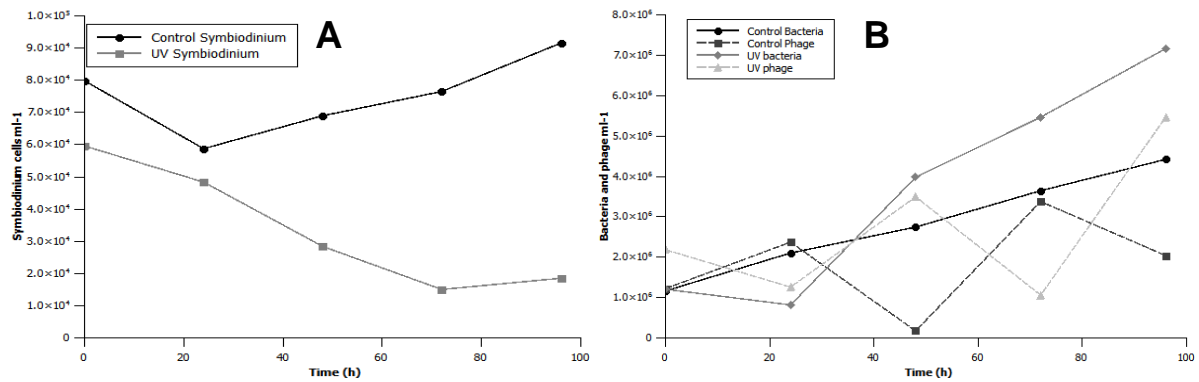


Figure A10. *Symbiodinium* (A) and bacterium & phage (B) population density in control and 302 nm UV-irradiated cultures of *Symbiodinium* culture Mp. No VLPs were seen in control or UV-irradiated samples.

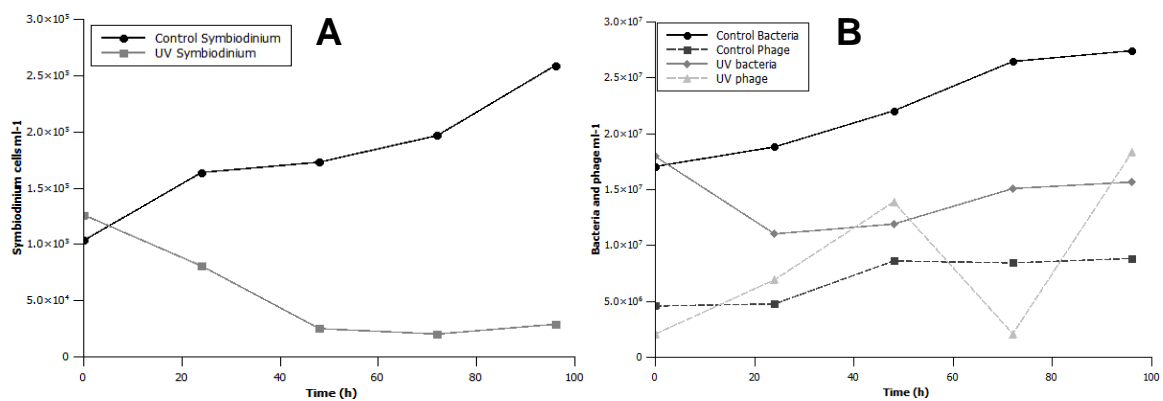


Figure A11. *Symbiodinium* (A) and bacterium & phage (B) population density in control and 302 nm UV-irradiated cultures of *Symbiodinium* culture Pd. No VLPs were seen in control or UV-irradiated samples.

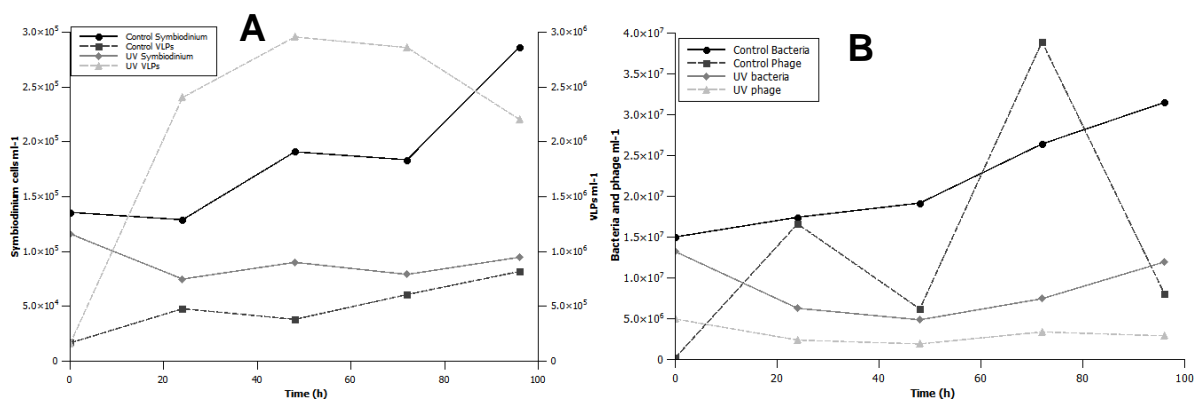


Figure A12. *Symbiodinium* & VLP (A) and bacterium & phage (B) population density in control and 302 nm UV-irradiated cultures of *Symbiodinium* culture PK13.

Figures 13 – 25 show the responses of *Symbiodinium*, VLP, bacterium and phage populations to thermal stress. Culture growth conditions were as for the screening experiments in Chapter 2. *Symbiodinium* cultures (50 mL) were heated to 36 °C for 24 h, and then returned to normal growth conditions. Control samples were subjected to all experimental procedures, but were maintained at the normal growth temperature of 25 °C. Samples were collected every 24 h for 5 days and counts were carried out using flow cytometry as described in Chapter 2. Experiments using temperatures of 30 °C and 33 °C were also carried out, but did not cause *Symbiodinium* cell lysis (data not shown).

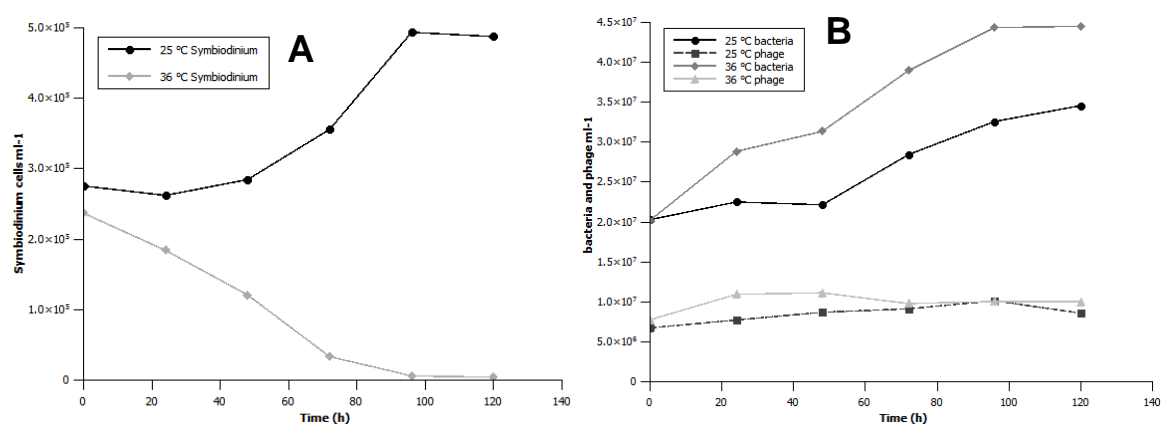


Figure A13. *Symbiodinium* (A) and bacterium & phage (B) population density in control and thermally-stressed cultures of *Symbiodinium* culture CCMP421.

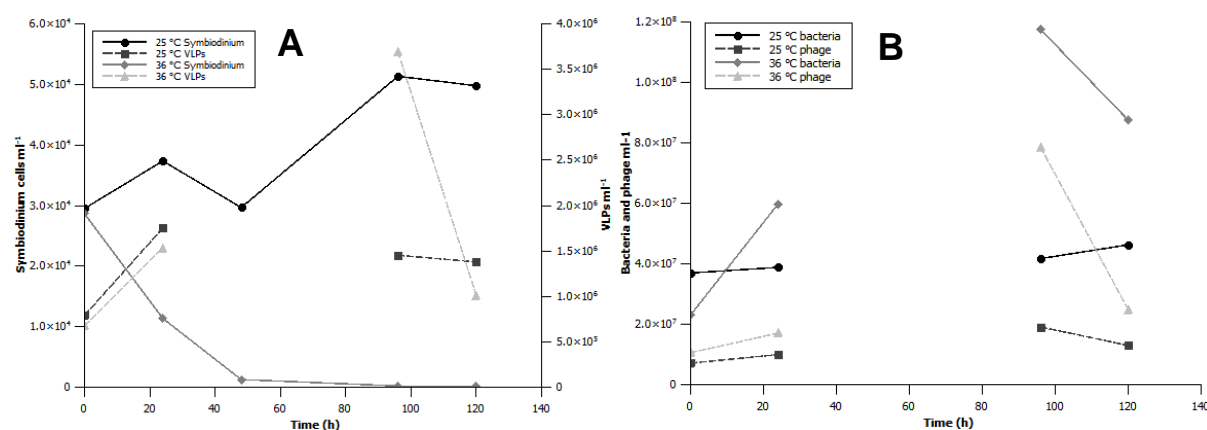


Figure A14. *Symbiodinium* & VLP (A) and bacterium & phage (B) population density in control and thermally-stressed cultures of *Symbiodinium* culture CCMP828. Bacterium, VLP and phage samples collected at T48 (24 h after end of heat stress) were lost, leading to the missing data points in the above graphs.

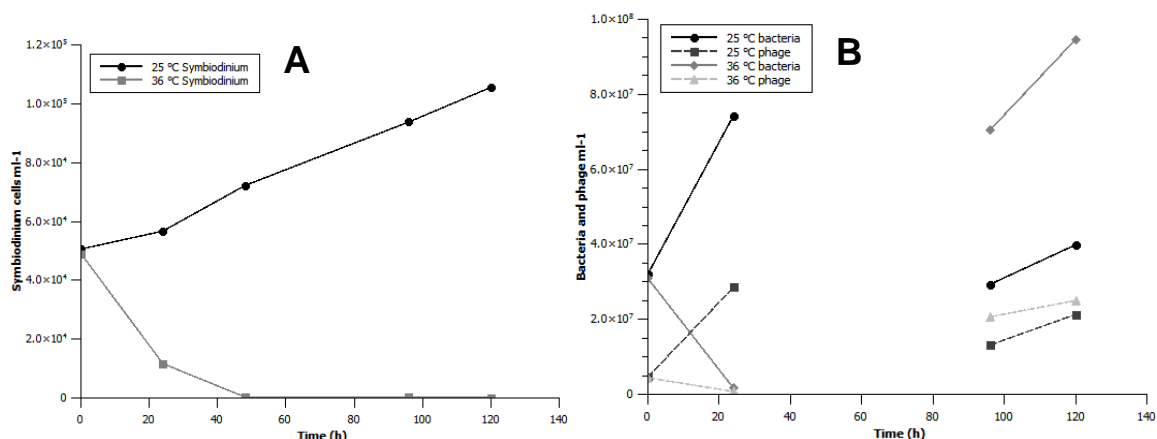


Figure A15. *Symbiodinium* (A) and bacterium & phage (B) population density in control and thermally-stressed cultures of *Symbiodinium* culture CCMP2430. All samples collected at T48 (24 h after end of heat stress) were lost, leading to the missing data points in the above graph.

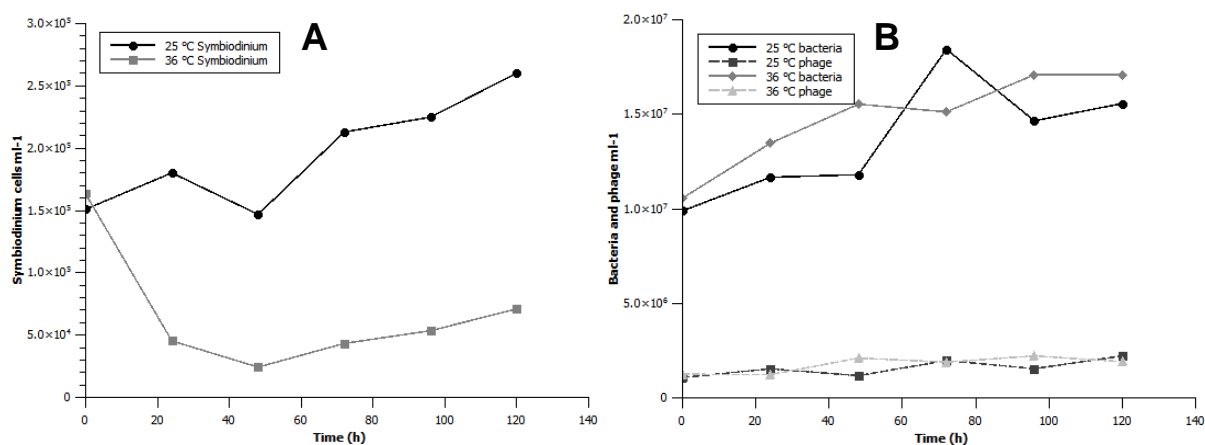


Figure A16. *Symbiodinium* (A) and bacterium & phage (B) population density in control and thermally-stressed cultures of *Symbiodinium* culture CCMP2465.

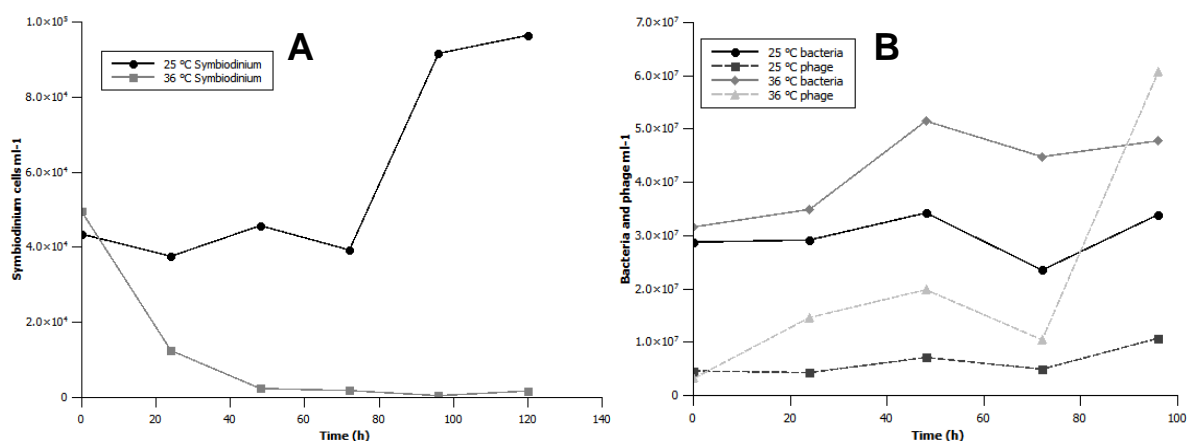


Figure A17. *Symbiodinium* (A) and bacterium & phage (B) population density in control and thermally-stressed cultures of *Symbiodinium* culture CCMP2467.

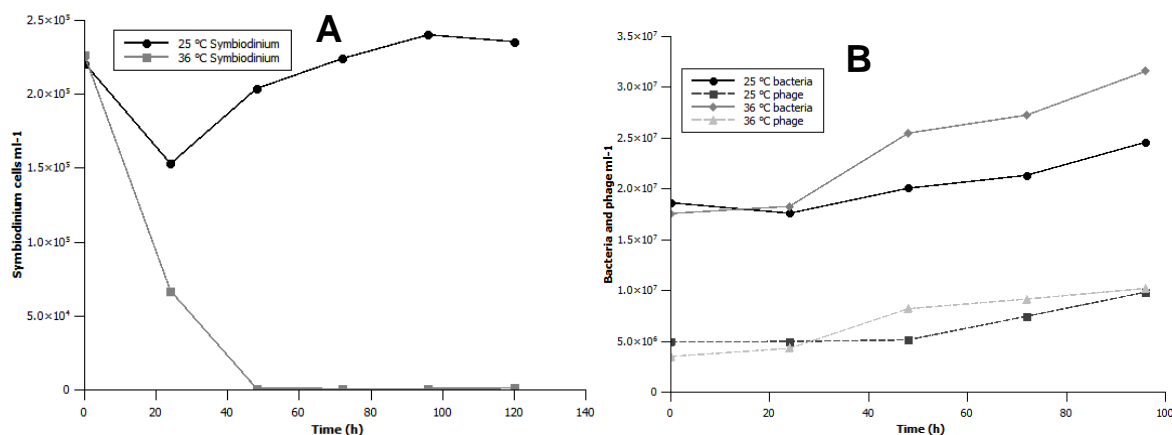


Figure A18. *Symbiodinium* (A) and bacterium & phage (B) population density in control and thermally-stressed cultures of *Symbiodinium* culture Ap1.

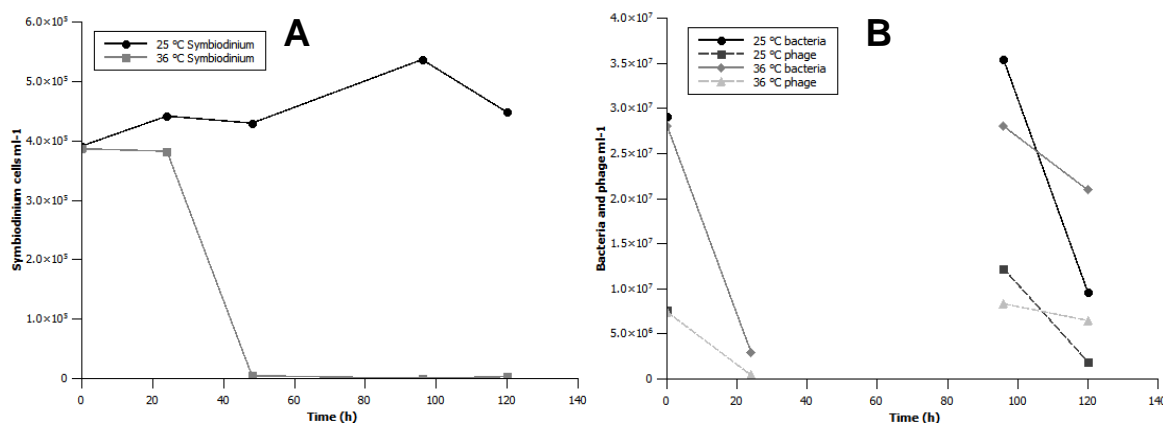


Figure A19. *Symbiodinium* (A) and bacterium & phage (B) population density in control and thermally-stressed cultures of *Symbiodinium* culture SLClone2. All samples collected at T48 (24 h after end of heat stress) were lost, leading to the missing data points in the above graph.

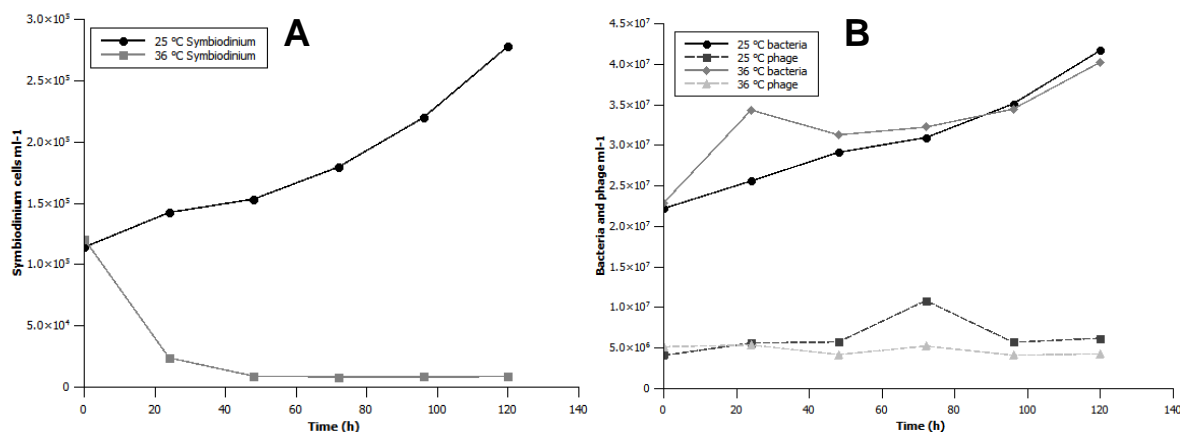


Figure A20. *Symbiodinium* (A) and bacterium & phage (B) population density in control and thermally-stressed cultures of *Symbiodinium* culture FLAp1.

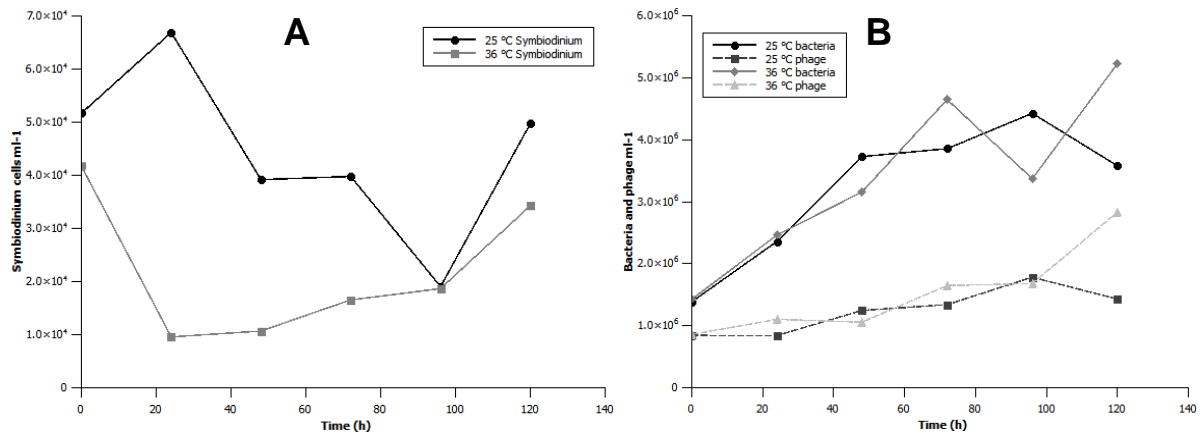


Figure A21. *Symbiodinium* (A) and bacterium & phage (B) population density in control and thermally-stressed cultures of *Symbiodinium* culture Mp.

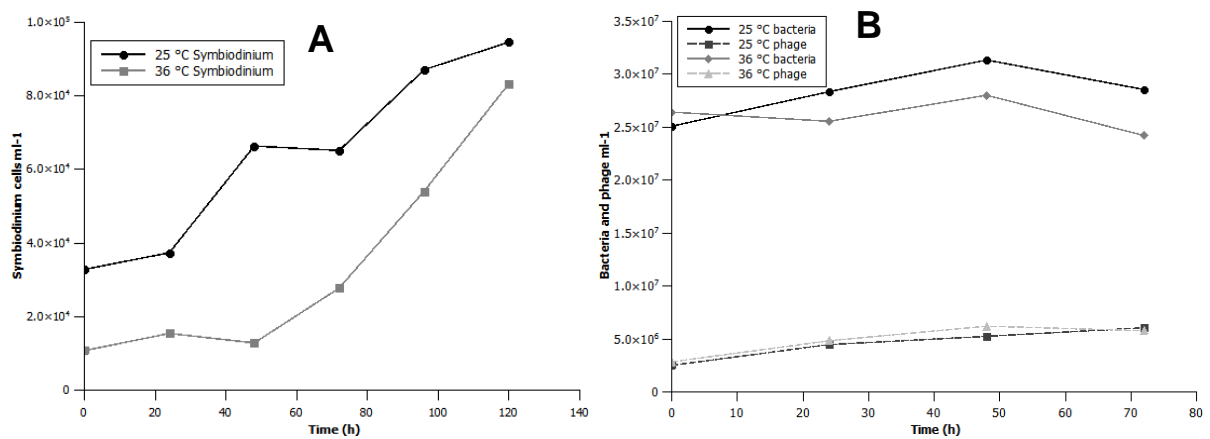


Figure A22. *Symbiodinium* (A) and bacterium & phage (B) population density in control and thermally-stressed cultures of *Symbiodinium* culture Pd.

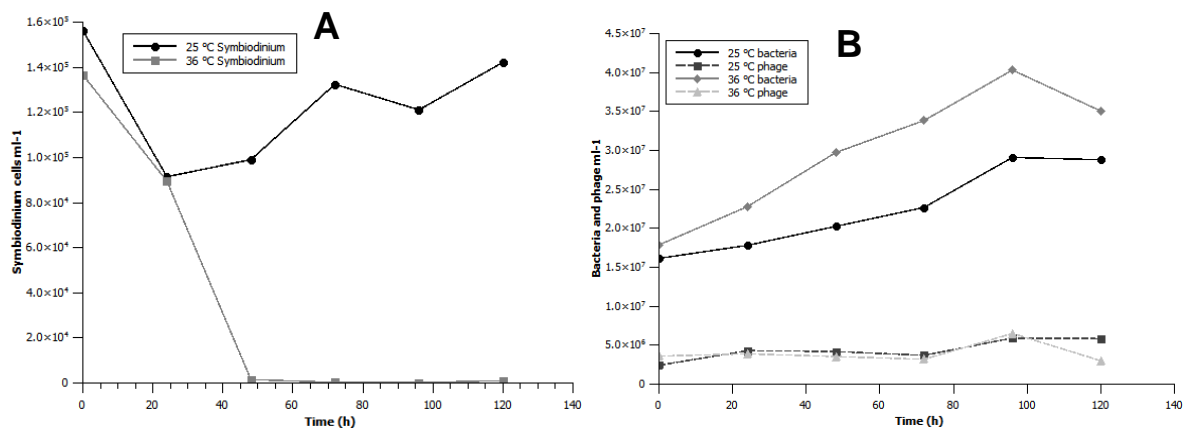


Figure A23. *Symbiodinium* (A) and bacterium & phage (B) population density in control and thermally-stressed cultures of *Symbiodinium* culture PK13.

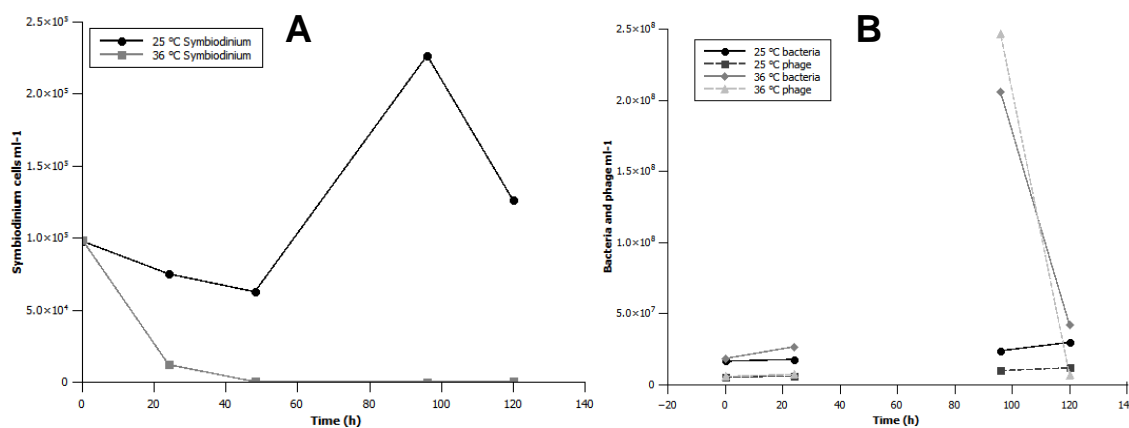


Figure A24. *Symbiodinium* (A) and bacterium & phage (B) population density in control and thermally-stressed cultures of *Symbiodinium* culture *S. bermudense*. All samples collected at T48 (24 h after end of heat stress) were lost, leading to the missing data points in the above graph.

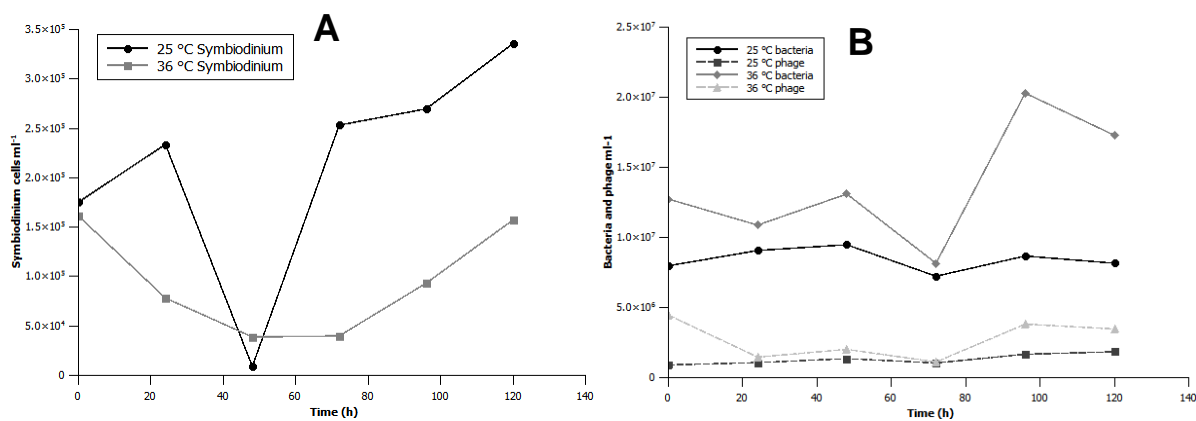


Figure A25. *Symbiodinium* (A) and bacterium & phage (B) population density in control and thermally-stressed cultures of *Symbiodinium* culture Stylo0.

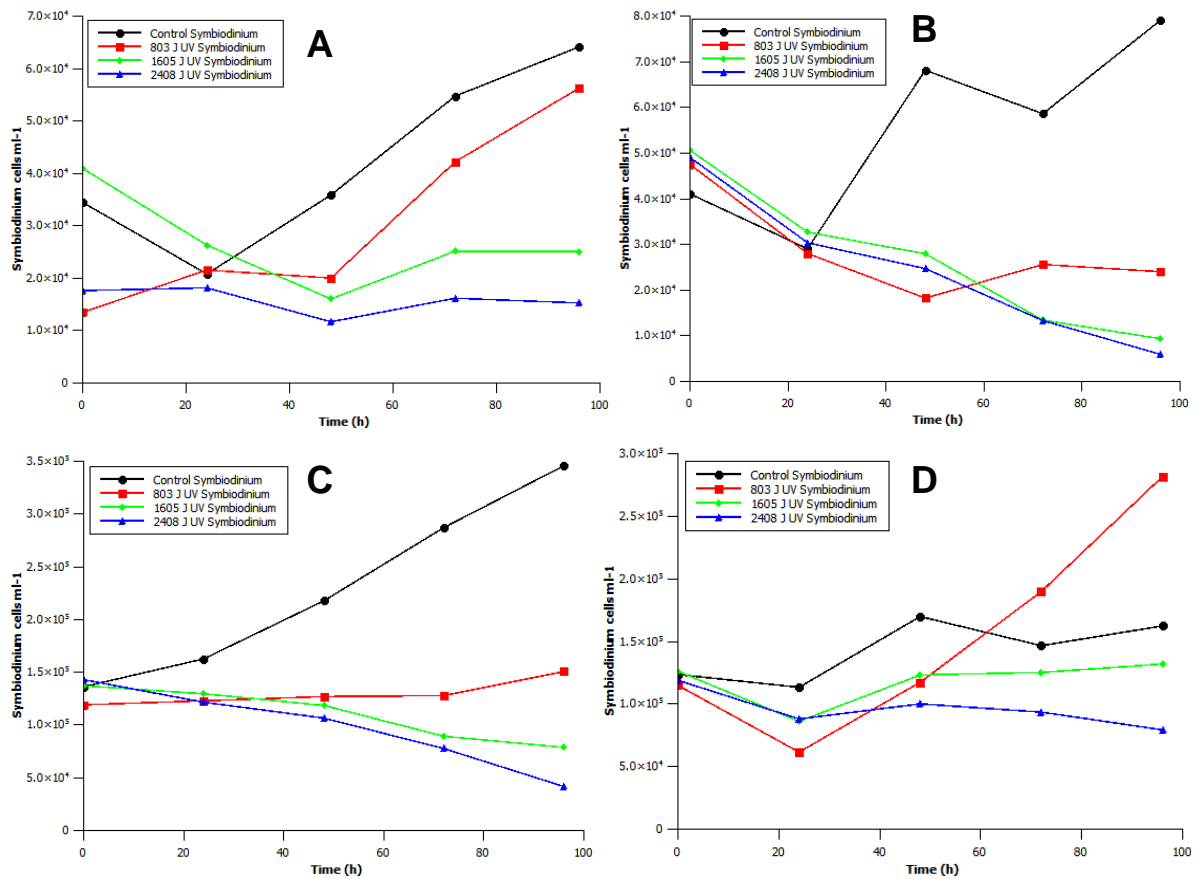


Figure A26. *Symbiodinium* cell densities of four test cultures after exposure to UV radiation. (A) CCMP828; (B) CCMP2430; (C) FLAp1; (D) PK13. Cultures were exposed to 803 J m⁻² (red lines), 1606 J m⁻² (green lines) or 2408 J m⁻² (blue lines) total radiation at 254 nm. Control cultures (black lines) were subjected to all experimental steps except UV exposure.

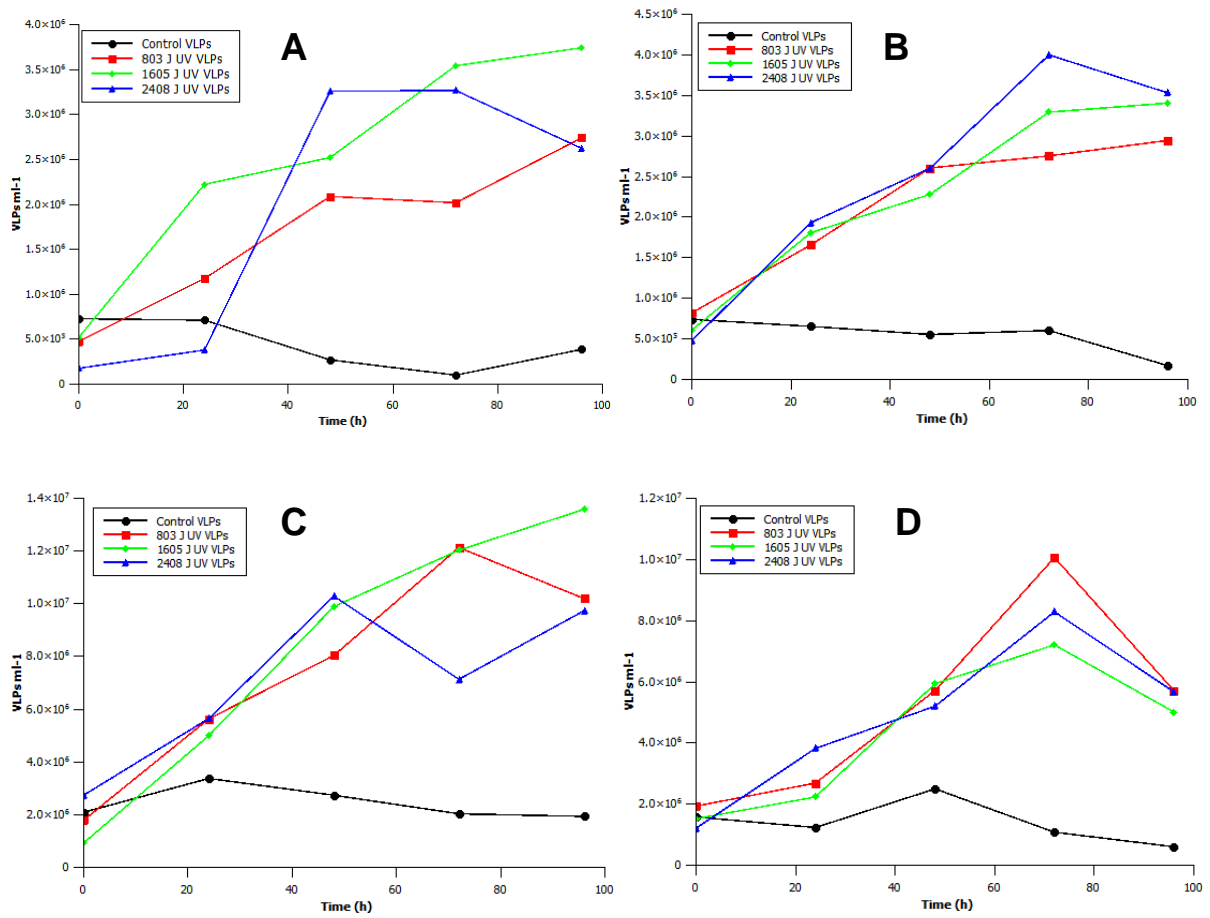


Figure A27. Virus-like particle (VLP) densities of four *Symbiodinium* test cultures after exposure to UV radiation. (A) CCMP828; (B) CCMP2430; (C) FLAp1; (D) PK13. Cultures were exposed to 803 J m^{-2} (red lines), 1606 J m^{-2} (green lines) or 2408 J m^{-2} (blue lines) total radiation at 254 nm. Control cultures (black lines) were subjected to all experimental steps except UV exposure.

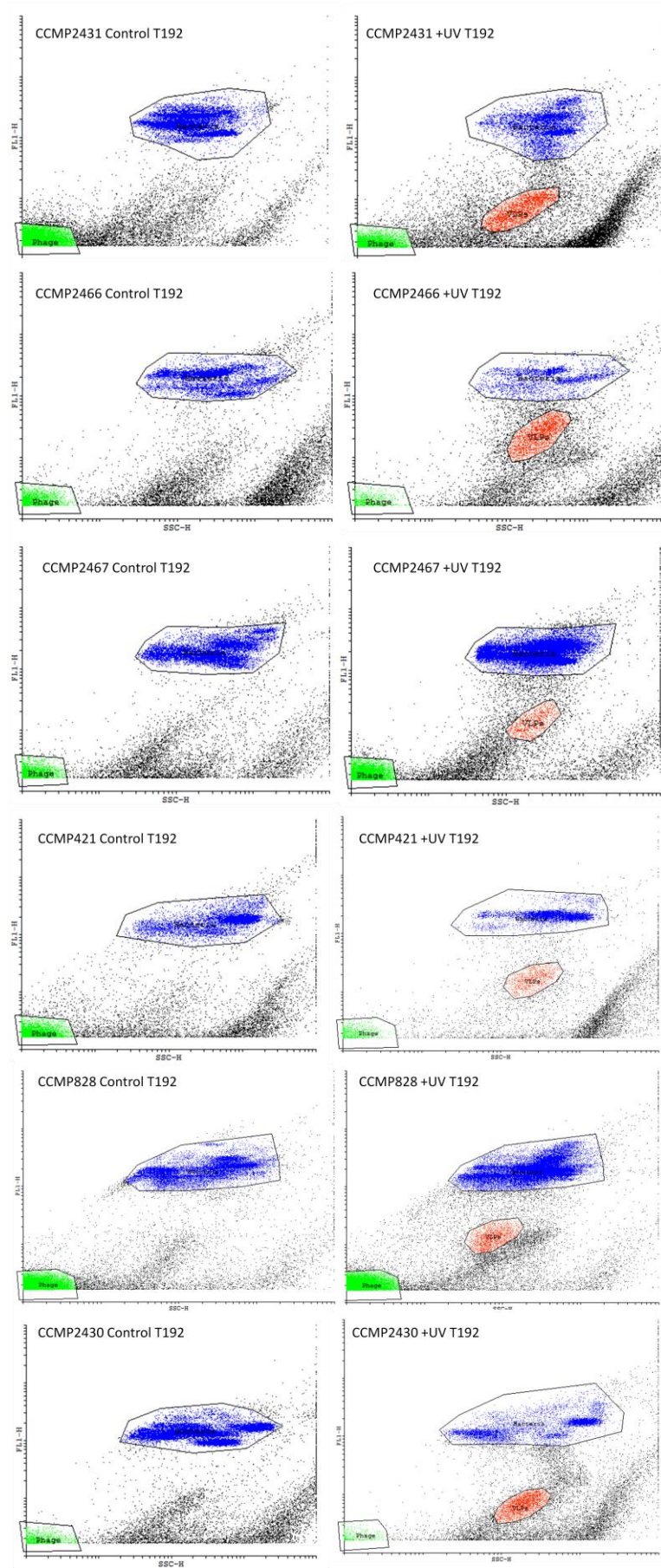


Figure A28. Description on page 198.

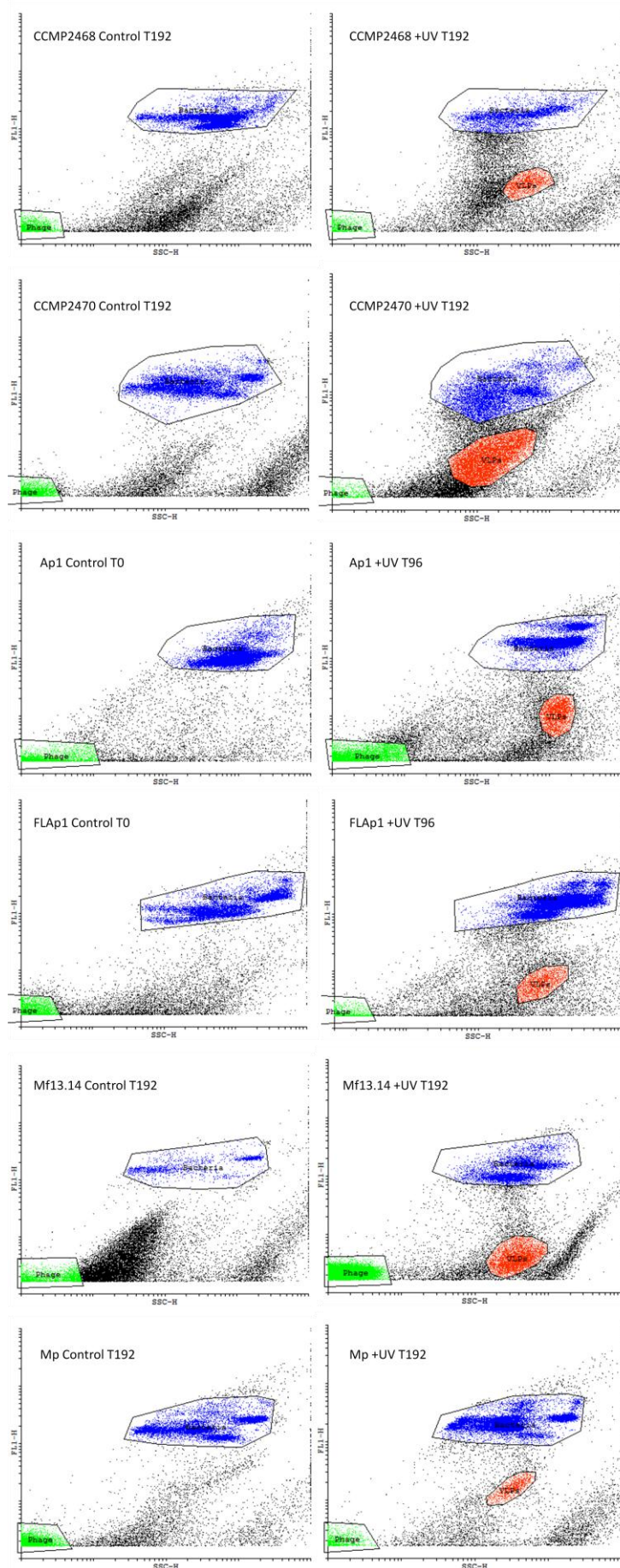


Figure A28. Description overleaf.

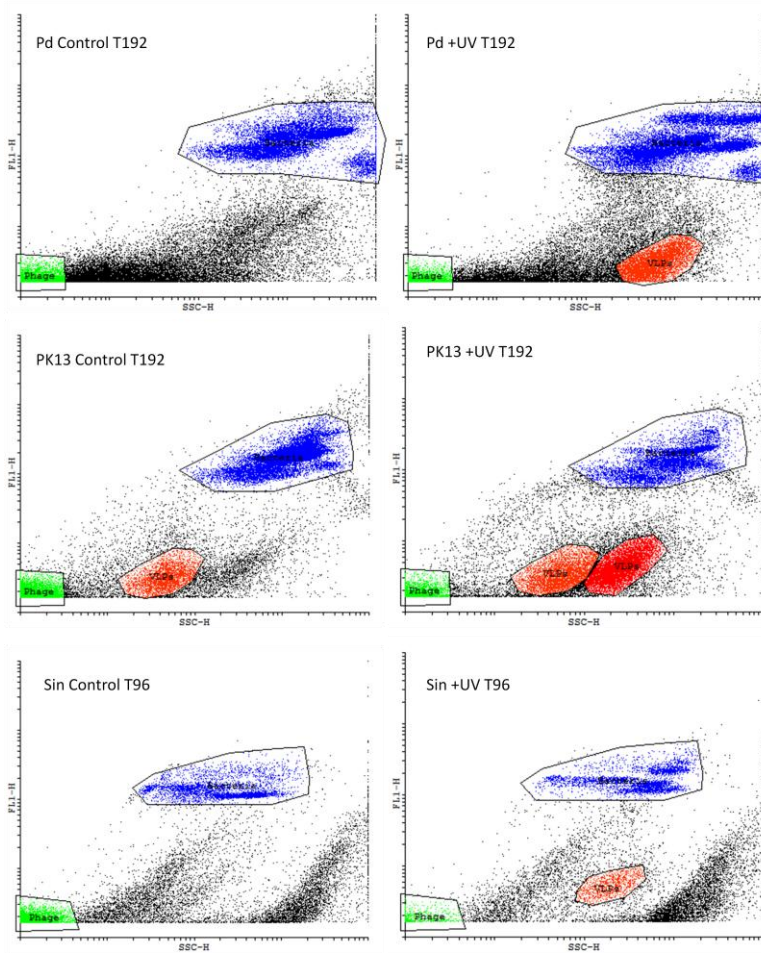


Figure A28. Cytograms of *Symbiodinium* cultures showing putative virus-like particle (VLP) populations following UV irradiation. Axes are side scatter (SSC-H) vs. green fluorescence (FL1-H). Red populations are putative VLPs, blue populations are bacteria and green populations are putative phages and other small particles. All samples were diluted 1:100 with TE buffer except for CCMP2470 Control, which was diluted 1:1,000, and FLAp1, Pd and PK13, which were diluted 1:10.

Table A2. Polymerase chain reaction (PCR) protocols used in this study. Where several annealing temperatures are listed, each temperature was tested in a separate reaction. *Reactions using primer pair RR2F/R were run twice, with the second reaction using 5 µL of product from the first reaction as template DNA. **In addition to the protocol listed in the table, a touchdown PCR was run using Herpes F/R primers, starting with an annealing temperature of 60 °C and decreasing 0.5 °C each cycle.

Primer pair	Initialization	Denaturation	Annealing	Extension	Final extension
RR2F/R*	95 °C – 3 min	95 °C – 45 s	49 °C – 45 s	72 °C – 45 s	72 °C – 10 min
			×33		
CircoRep F1/R1	94 °C – 3 min	94 °C – 30 s	40 °C – 30 s 45 °C – 30 s 50 °C – 30 s 56 °C – 30 s	72 °C – 30 s	72 °C – 10 min
			×30		
<i>Nanoviridae</i> F1/R1	94 °C – 3 min	94 °C – 30 s	42 °C – 30 s 47 °C – 30 s 52 °C – 30 s	72 °C – 30 s	72 °C – 10 min
			×30		
Nanovirus F1/R1	95 °C – 3 min	95 °C – 30 s	40 °C – 30 s 45 °C – 30 s 50 °C – 30 s 55 °C – 30 s 60 °C – 30 s	72 °C – 30 s	72 °C – 10 min
			×30		
Herpes F/R**	95 °C – 3 min	95 °C – 1 min	60 °C – 30 s	72 °C – 1 min	72 °C – 10 min
			×30		
AVS1/AVS2	95 °C – 3 min	95 °C – 30 s	50 °C – 45 s	72 °C – 1 min	72 °C – 10 min
			×30		

Table A3. Results of initial screening for latent *Symbiodinium* viruses, based on cytograms obtained after 254 nm UV irradiation of cultures. Y: yes. N: no.

<i>Symbiodinium</i> culture ID	Population	Population	Complete	VLP group	
	decline vs. control	decline from T0	population lysis	Control	UV
CCMP421	Y	Y	N	N	Y
CCMP827	Y	Y	N	N	N
CCMP828	Y	Y	N	N	Y
CCMP829	Y	Y	N	N	N
CCMP830	Y	Y	Y	N	N
CCMP831	Y	Y	N	N	N
CCMP832	Y	Y	N	N	N
CCMP1633	Y	Y	Y	N	N
CCMP2428	Y	Y	N	N	N
CCMP2429	N	N	N	N	N
CCMP2430	Y	Y	N	N	Y
CCMP2431	Y	N	N	N	Y
CCMP2434	N	N	N	N	N
CCMP2456	Y	Y	N	N	N
CCMP2457	Y	Y	N	N	N
CCMP2458	Y	Y	N	N	N
CCMP2459	Y	Y	N	N	N
CCMP2460	Y	Y	Y	N	N
CCMP2461	Y	N	N	N	N
CCMP2464	Y	Y	N	N	N
CCMP2465	N	N	N	N	N
CCMP2466	Y	Y	N	N	Y
CCMP2467	Y	Y	N	N	Y
CCMP2468	Y	Y	N	N	Y
CCMP2469	Y	Y	N	N	N
CCMP2470	Y	Y	Y	N	Y
CCMP2548	N	Y	N	N	N
CCMP2556	Y	Y	N	N	N

Table A3 (continued).

CCMP2592	N	Y	N	N	N
2a	Y	Y	N	N	N
A001	Y	Y	N	N	N
Ap1	Y	Y	N	N	Y
SLClone1	Y	Y	Y	N	N
SLClone2	Y	Y	N	N	N
FLAp1	Y	Y	Y	N	Y
FLAp2	Y	Y	N	N	N
Mf7.5T	Y	Y	Y	N	N
Mf13.14	Y	Y	N	N	Y
Mp	Y	Y	N	N	Y
Pd	Y	Y	Y	N	Y
Pd45a	Y	Y	N	N	N
Pe	Y	Y	N	N	N
PK13	Y	Y	N	Y	Y
<i>S. bermudense</i>	Y	Y	N	N	N
<i>S. californium</i>	N	N	N	N	N
Sin	Y	Y	Y	N	Y
Stylo0	Y	Y	N	N	N
Stylo1	N	N	N	N	N
Zs	Y	Y	N	N	N

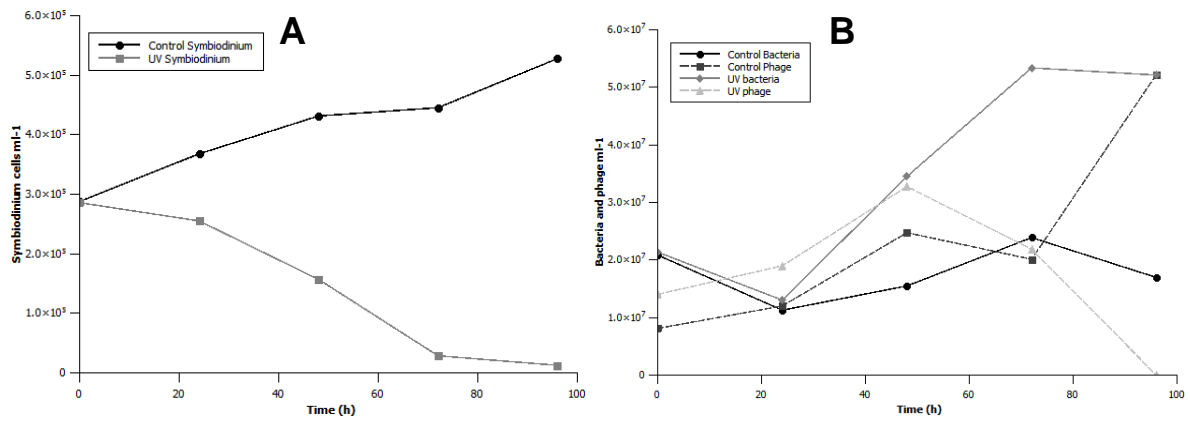


Figure A29. *Symbiodinium* (A) and bacterium and phage (B) population density in control and 254 nm UV-irradiated cultures of *Symbiodinium* culture CCMP421. No VLP group was seen in either control or irradiated samples.

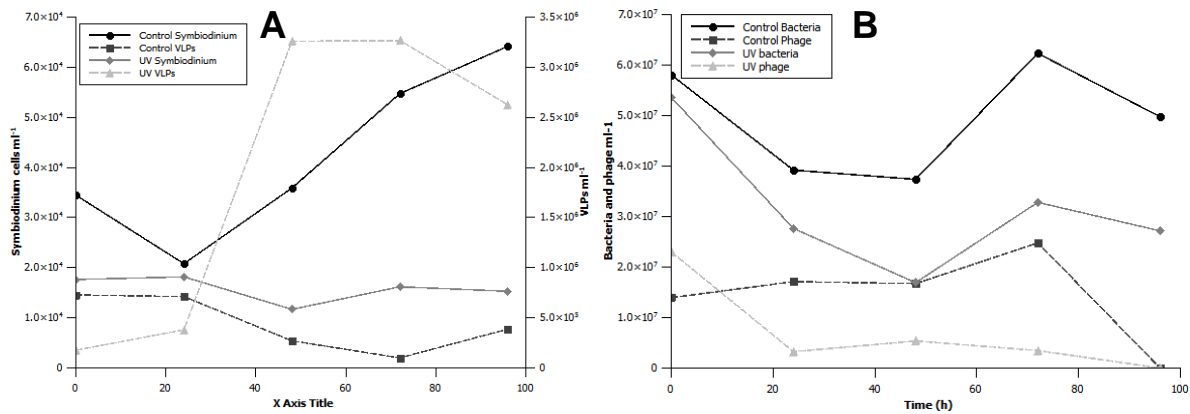


Figure A30. *Symbiodinium* & VLP (A) and bacterium & phage (B) population density in control and 254 nm UV-irradiated cultures of *Symbiodinium* culture CCMP828.

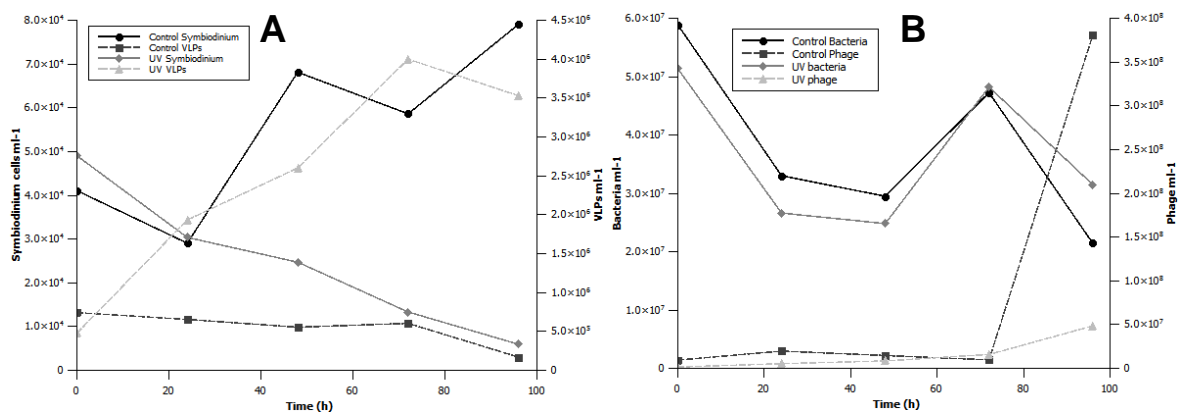


Figure A31. *Symbiodinium* & VLP (A) and bacterium & phage (B) population density in control and 254 nm UV-irradiated cultures of *Symbiodinium* culture CCMP2430.

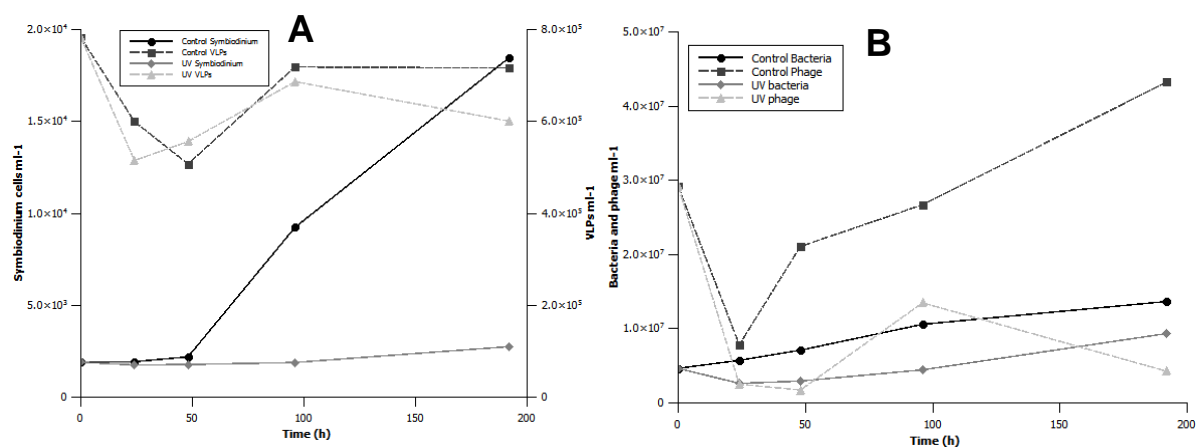


Figure A32. *Symbiodinium* & VLP (A) and bacterium & phage (B) population density in control and 254 nm UV-irradiated cultures of *Symbiodinium* culture CCMP2431.

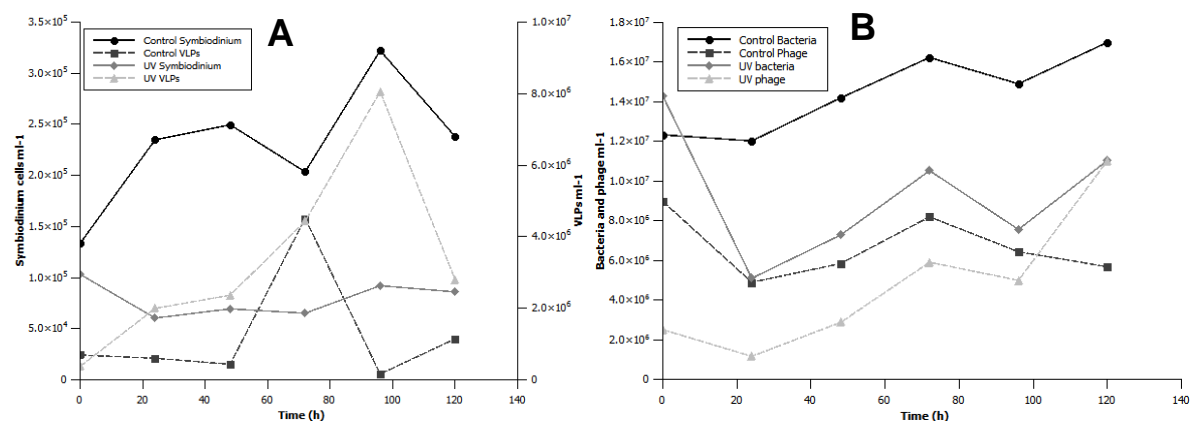


Figure A33. *Symbiodinium* & VLP (A) and bacterium & phage (B) population density in control and 254 nm UV-irradiated cultures of *Symbiodinium* culture CCMP2467.

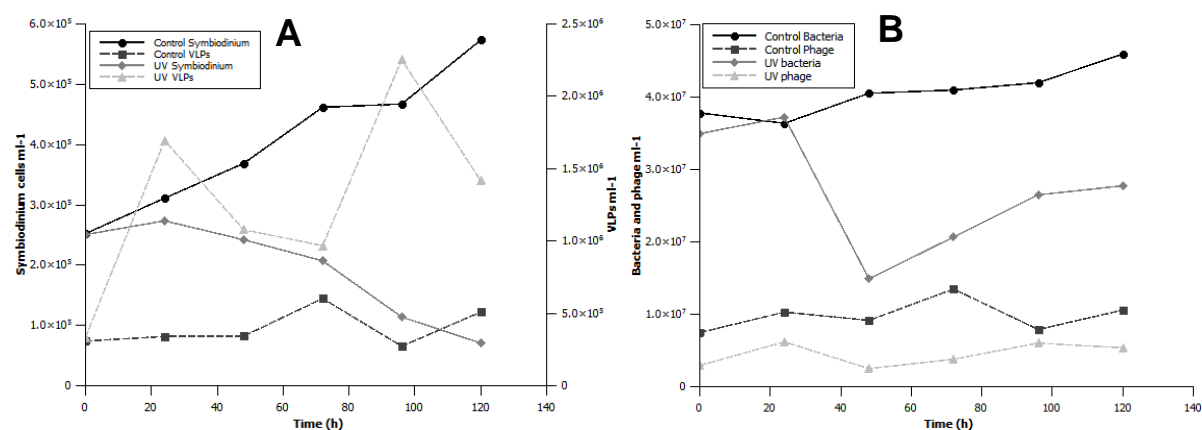


Figure A34. *Symbiodinium* & VLP (A) and bacterium & phage (B) population density in control and 254 nm UV-irradiated cultures of *Symbiodinium* culture Ap1.

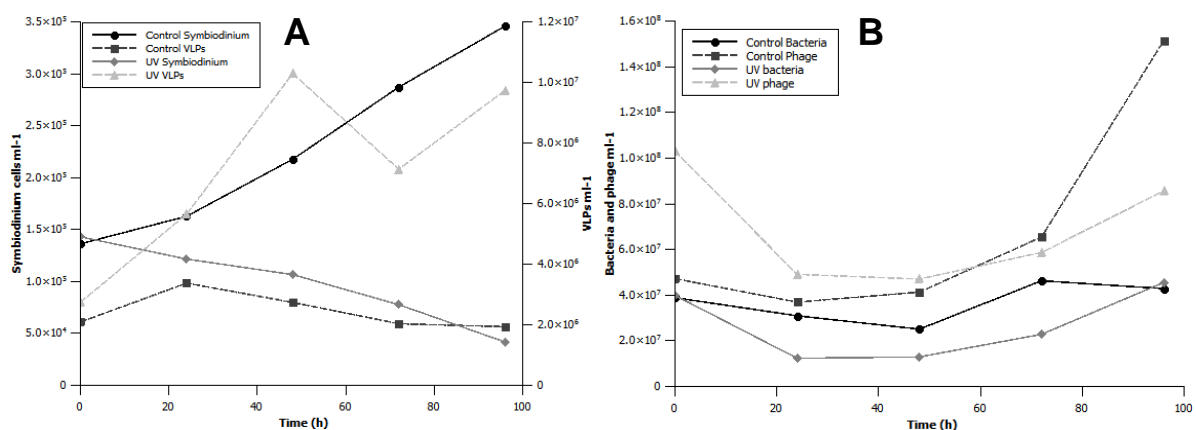


Figure A35. *Symbiodinium* & VLP (A) and bacterium & phage (B) population density in control and 254 nm UV-irradiated cultures of *Symbiodinium* culture FLAp1.

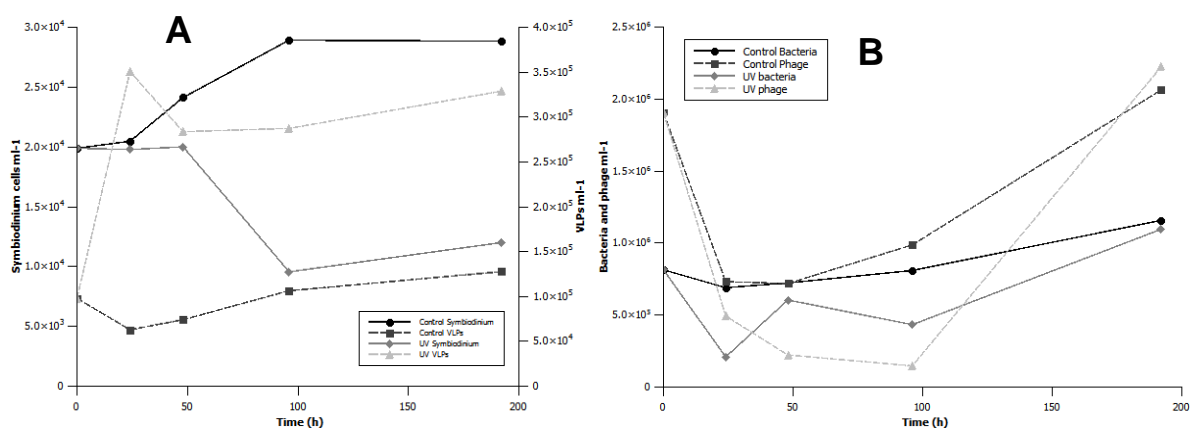


Figure A36. *Symbiodinium* & VLP (A) and bacterium & phage (B) population density in control and 254 nm UV-irradiated cultures of *Symbiodinium* culture Mf13.14.

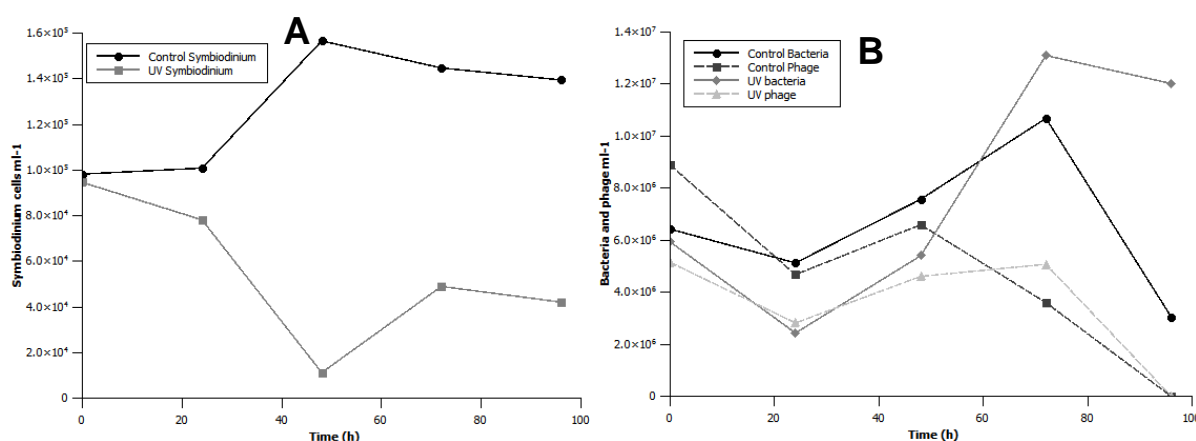


Figure A37. *Symbiodinium* (A) and bacterium & phage (B) population density in control and 254 nm UV-irradiated cultures of *Symbiodinium* culture Mp. No VLPs were seen in control or UV-irradiated samples.

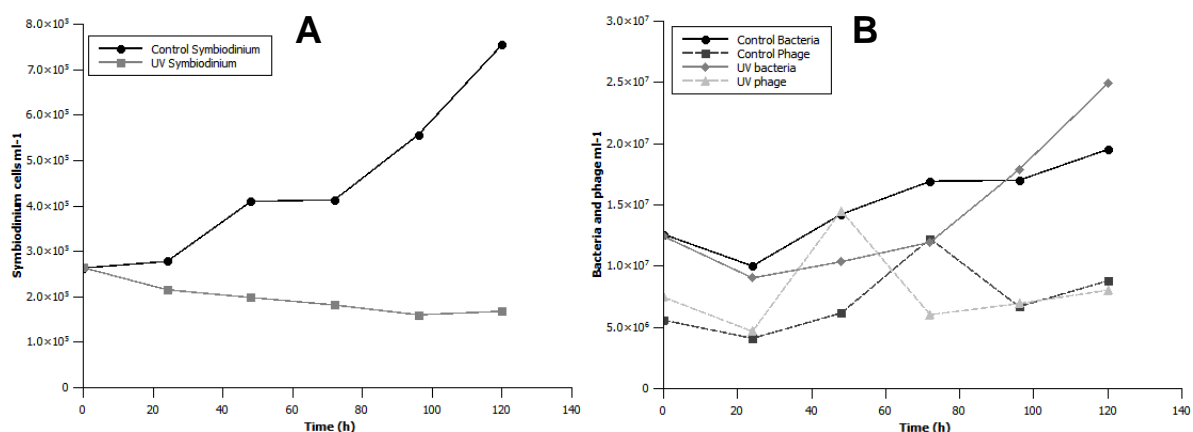


Figure A38. *Symbiodinium* (A) and bacterium & phage (B) population density in control and 254 nm UV-irradiated cultures of *Symbiodinium* culture Pd. No VLPs were seen in control or UV-irradiated samples.

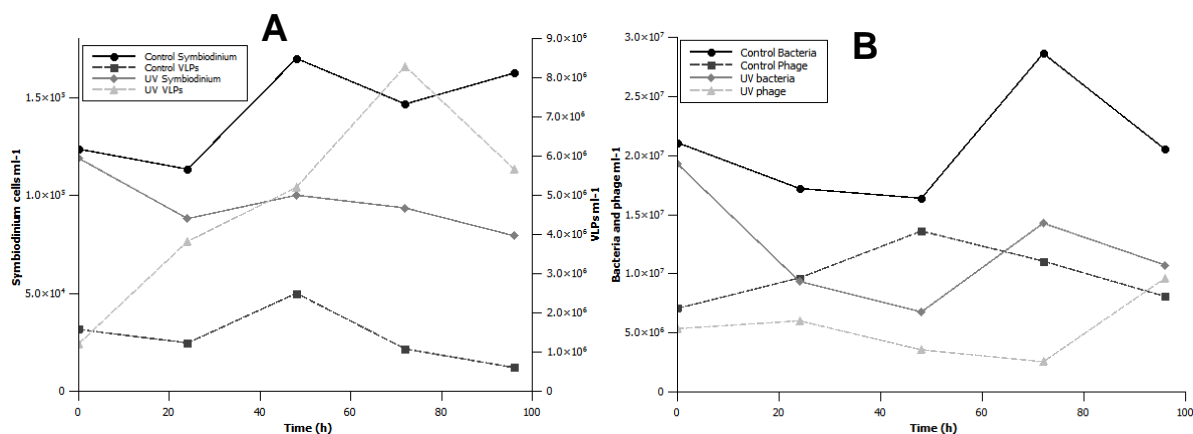


Figure A39. *Symbiodinium* & VLP (A) and bacterium & phage (B) population density in control and 254 nm UV-irradiated cultures of *Symbiodinium* culture PK13.

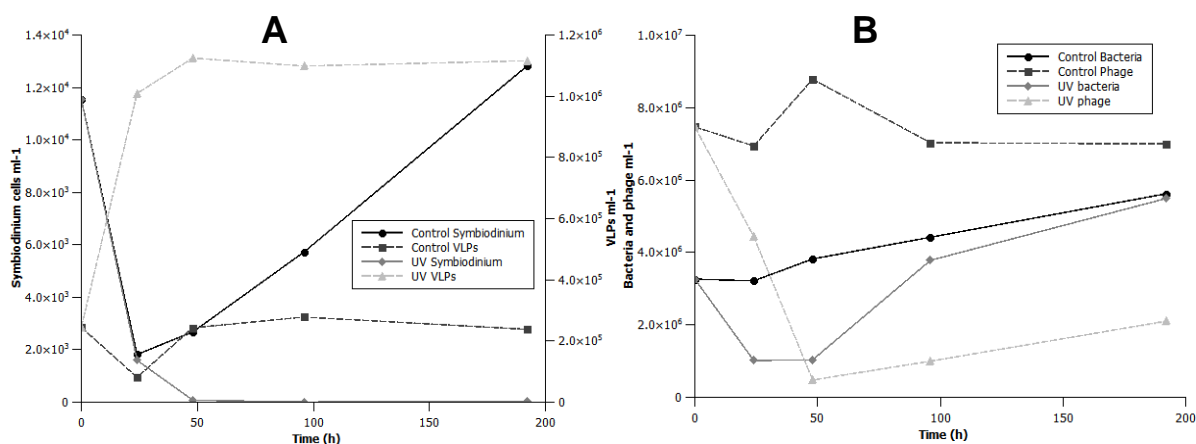


Figure A40. *Symbiodinium* & VLP (A) and bacterium & phage (B) population density in control and 254 nm UV-irradiated cultures of *Symbiodinium* culture Sin

Appendix B: Single virus sorting and whole genome amplification

Materials and methods

In an attempt to better characterise the putative latent viruses associated with *Symbiodinium*, cultures FLAp1 and Mf13.14 were selected for single virus sorting and viral genome amplification. A 50 mL sample of each culture was placed in a sterile Petri dish and exposed for 2 min to 254 nm UV radiation from an inverted Apollo transilluminator placed 12 cm above the dish. After irradiation, samples were placed in sterile culture flasks and returned to normal growth conditions (25 °C on a 12 h light: 12 h dark cycle at 80 $\mu\text{mol quanta m}^{-2} \text{s}^{-1}$). A control sample from each culture was subjected to all steps except UV irradiation. After 96 h, aliquots were taken from each sample and DNase-treated to remove any free DNA: DNase I reaction buffer (New England Biolabs, Ipswich, MA, USA) was added to samples to a final $1 \times$ concentration, then mixed with 2 U DNase I and incubated at 37 °C for 10 min. EDTA was added to a final concentration of 5 mM, and the DNase was deactivated by heating at 75 °C for 10 min. Following DNase treatment, the optimal dilutions, fixation and staining method for virus sorting were determined. Samples were diluted either 1:10, 1:100 or 1:1,000 with sterile 0.2 μm -filtered TE buffer. Samples were fixed in 0.1% glutaraldehyde or were processed fresh (no fixation). Staining was done using SYBR Green as previously described, but the samples were incubated with the stain for 10 min at room temperature, 2 min at 80 °C or 10 min at 80 °C. All staining was done in the dark. For FLAp1, a 1:100 dilution fixed in 0.1% glutaraldehyde and stained for 2 min at 80 °C was found to be optimal for sorting. For Mf13.14, a 1:100 dilution of fresh (no fixative) sample, stained for 10 min at room temperature was optimal. Virus-like particles were gated on a SSC vs GFL plot and sorted into 384 well plates using an Influx fluorescence-activated cell sorter (Becton Dickinson, Franklin Lakes, NJ, USA). Prior to VLP sorting, the Influx and associated consumables were thoroughly cleaned and sterilised to prevent DNA contamination. The sheath fluid used in the Influx was a sterile 7.5 ppt saline solution. Of the 384 wells, 330 were used for single sorted VLPs, 7 received 10 VLPs, 8 received 100 VLPs, and 39 received no droplet (negative controls). The putative viruses sorted from Mf13.14 were lysed and their DNA was denatured using cold (4 °C) potassium hydroxide. DNA amplification was then attempted, using multiple displacement amplification (MDA; Raghunathan *et al.*, 2005; Lasken, 2007), by the

Bigelow Single Cell Genomics Center (SCGC, Bigelow Laboratory for Ocean Sciences, East Boothbay, ME, USA).

In addition to the VLPs sorted into plates for DNA amplification, VLPs from FLAp1 and Mf13.14 were sorted into tubes for transmission electron microscope (TEM) examination. Two tubes were sorted for each culture, one containing 5,000 VLPs and the other 10,000. Samples taken from the tubes containing 10,000 VLPs were placed on to TEM grids, stained with 2% uranyl acetate for 3 min and visualised on a FEI Tecnai BioTwin TEM.

Results and discussion

Virus-like particles from cultures of FLAp1 and Mf13.14 were successfully sorted into 384 well plates (Fig. B1) and into tubes for TEM analysis. Microscopic analysis of the sorted particles failed to show VLPs, however this may have been due to the staining, which appeared patchy and desiccated. Multiple displacement amplification of VLPs from Mf13.14 was not successful (Fig. B1), possibly due to the small amount of nucleic acid that would likely be present in these putative viruses, which would be at the lower limits of sensitivity of the MDA method (R. Stepanauskas, SCGC, pers. comm.). While there was some amplification from several wells, this was most likely caused by contaminants, as evidenced by the fact that wells with 100 VLPs in them failed to amplify.

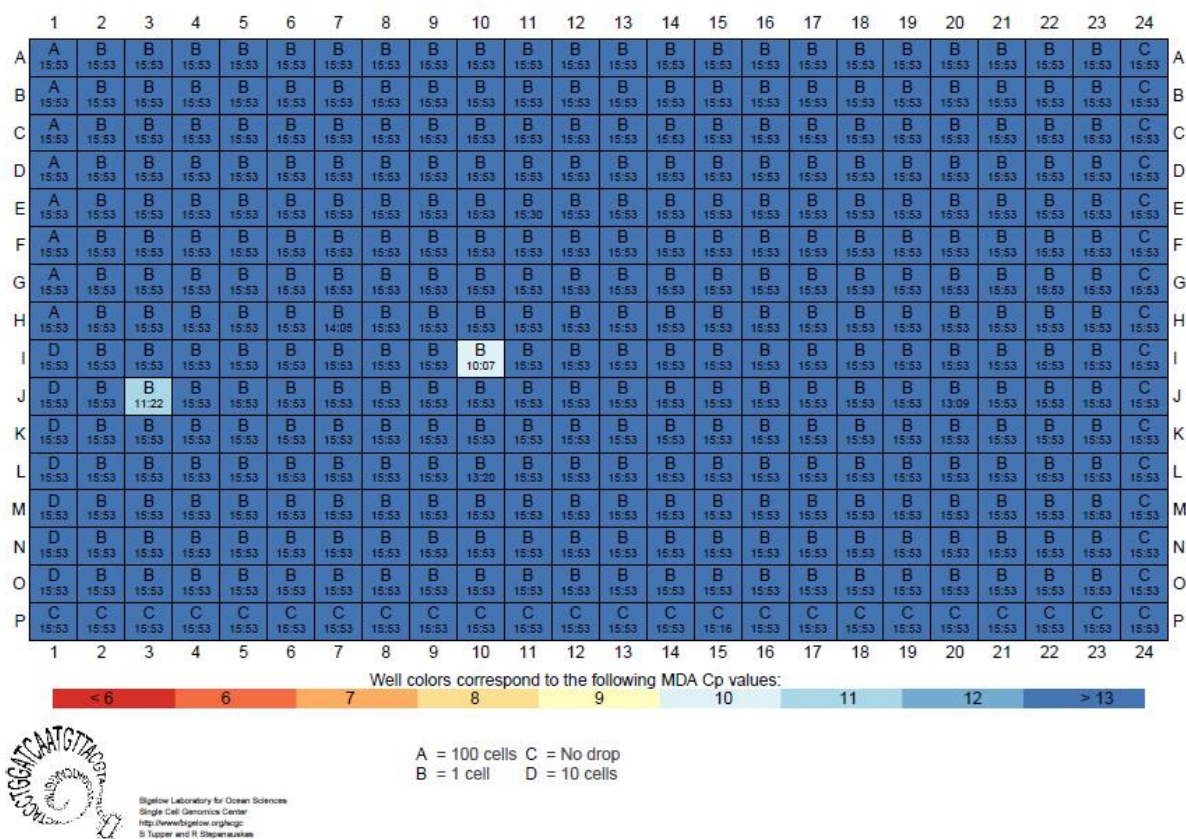


Figure B1. 384 well plate containing sorted VLPs from *Symbiodinium* culture Mf13.14. Key: A – 100 VLPs per well, B – 1 VLP per well, C – No drop in well (negative control), D – 10 VLPs per well. Nucleic acid from wells coloured dark blue failed to amplify (crossing point (Cp) values > 13). Wells with lighter colours had lower Cp values and showed some amplification, but this was likely due to contamination of the wells.

Appendix C: Virus reinfection experiments

Materials and methods

The *Symbiodinium* cultures used for reinfection experiments were: CCMP421, CCMP828, CCMP2430, Ap1, FLAp1, Mf13.14, Mp, Pd, PK13 and Sin. Cultures were grown as in Chapter 2. Triplicate 50 mL samples of each culture were harvested during exponential growth and placed into sterile Petri dishes, which were then exposed to UV radiation (254 nm wavelength, 2,408 J m⁻² total irradiation). Following irradiation, samples were placed in sterile culture flasks and returned to normal growth conditions. Triplicate 50 mL control samples were subjected to all steps except UV irradiation. Samples for *Symbiodinium* and viral/bacterial flow cytometry (1 mL each) were taken from control and irradiated samples at Time 0 (prior to irradiation) and every 24 h thereafter for five days. Flow cytometry and data analysis were carried out as previously described. After five days, 5 mL were removed from each culture flask, passed through a 0.2 µm pore-size polyethersulfone (PES) filter (Axiva, Delhi, India) and added to 50 mL of the corresponding non-stressed, exponentially-growing *Symbiodinium* culture. Cultures were returned to normal growth conditions, and 1 mL samples were taken for *Symbiodinium* and viral/bacterial flow cytometry at Time 0 (immediately after filtrate addition) and every 24 h thereafter, for five days. These experiments were then repeated using the same protocol, but with samples passed through 0.8 µm pore-size PES filters (Membrane Solutions, North Bend, OH, USA) instead of 0.2 µm pore-size filters, to account for large or filamentous viruses that may not have passed through the smaller pore-size filter. In both sets of experiments, flow cytometry and data analysis were carried out as previously described (Chapter 2).

Results

254 nm UV irradiation – 0.2 µm filtration

Following 254 nm wavelength UV irradiation, all ten cultures showed declines in *Symbiodinium* population densities (Figs. C1 – C10). The rate of decline of UV-irradiated *Symbiodinium* varied between cultures, but none except Mf13.14 (Fig. C6A) and Sin (Fig.

C10A) showed any recovery within the study period. Seven of the cultures (CCMP421, CCMP828, CCMP2430, Ap1, FLAp1, Mf13.14 and PK13) showed a concurrent increase in VLP population density. Of the remaining three cultures, Sin contained a VLP population which did not differ between control and irradiated samples over the course of the experiments (Fig. C10), and Mp (Fig. C7A) and Pd (Fig. C8A) showed no VLP group in cytograms of control or irradiated samples. In most cases, the VLP population density in control samples remained constant over the course of the experiment, but in Ap1 (Fig. C4A) there was a concurrent, but smaller, increase in control samples along with the increase in irradiated samples. Where VLP population increases were seen, these generally followed the pattern seen in earlier experiments (Appendix A, Figs. A29 – A40), where a rapid increase in density during the first 24 – 48 h post-UV exposure was followed by a stabilization of the population, and in some cases a subsequent decline. Bacterial and phage populations also generally responded as in the earlier experiments, i.e. bacterial density decreased or remained steady in irradiated samples while control populations increased in density, and the putative phage groups remained unaffected.

Infection of healthy *Symbiodinium* cultures with filtrate from UV-irradiated cultures did not result in *Symbiodinium* population declines in any of the ten cultures examined here. In two cultures (Mf13.14 and Mp; Figs. C6C and C7C, respectively) there was an increase in VLP density, but this increase was seen in both control and UV-irradiated samples. Furthermore, the VLP group seen in reinfected Mf13.14 cultures reached much lower densities ($\sim 1 - 2 \times 10^6$ VLPs mL⁻¹) than the group seen in the original UV-irradiated samples ($\sim 6 - 8 \times 10^6$ VLPs mL⁻¹). These results suggest that the VLP group seen in reinfected cultures of Mf13.14 and Mp may represent a chronic viral infection rather than a new infection or induction caused by the filtrate. No other cultures contained a VLP group after addition of filtrate. Bacterial and phage populations showed no difference between samples containing irradiated or control filtrate in any of the *Symbiodinium* cultures.

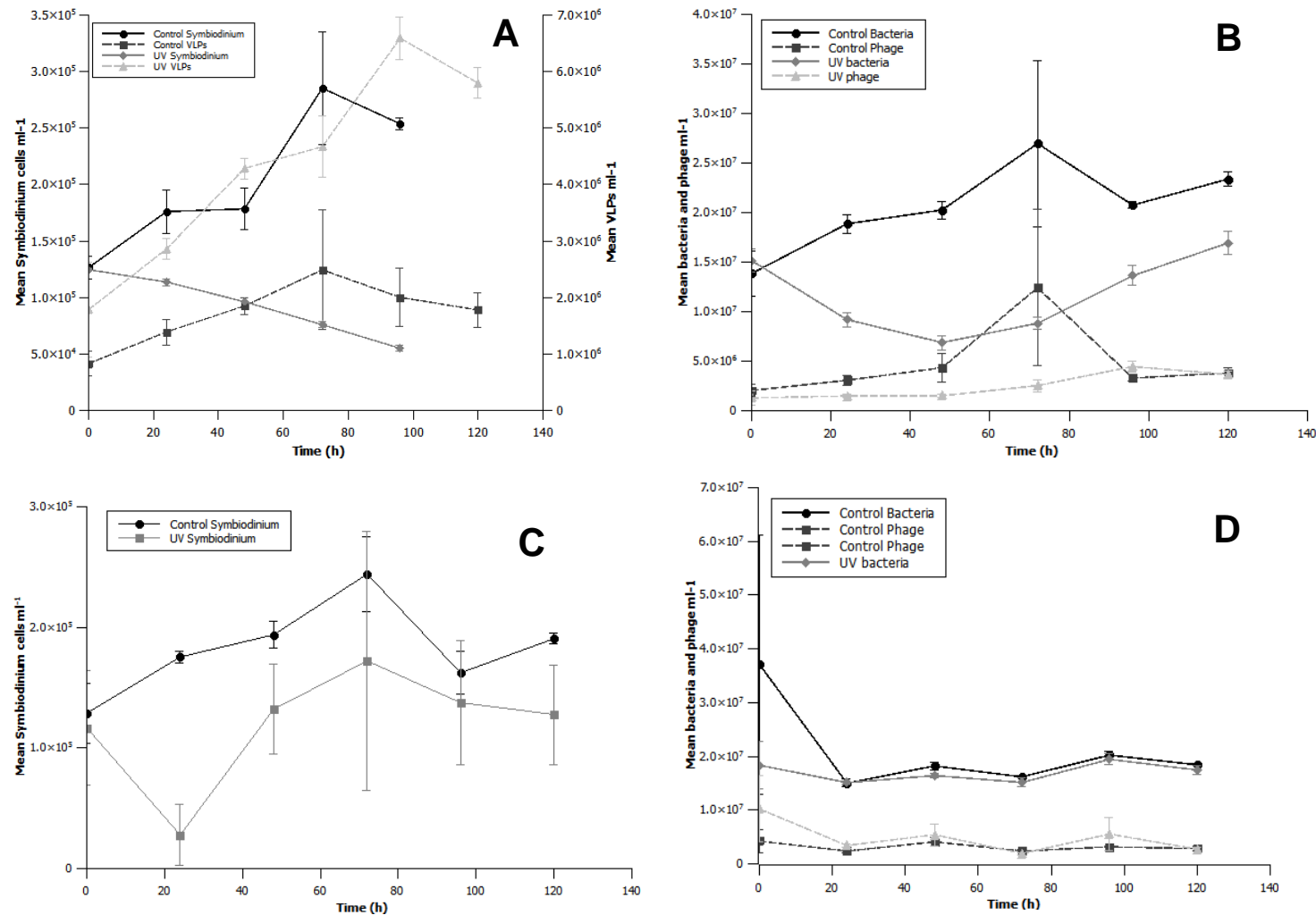


Figure C1. Induction and reinfection experiments, using 0.2 μ m pore-size filters, on *Symbiodinium* culture CCMP421. (A) *Symbiodinium* and VLP densities in UV-irradiated and control samples. (B) Bacterial and putative phage densities in UV-irradiated and control samples. (C) *Symbiodinium* density in healthy cultures infected with filtrate from UV-irradiated and control samples (no VLPs were seen in these samples). (D) Bacterial and putative phage densities in healthy cultures infected with filtrate from UV-irradiated and control samples. Error bars are standard error of triplicate counts.

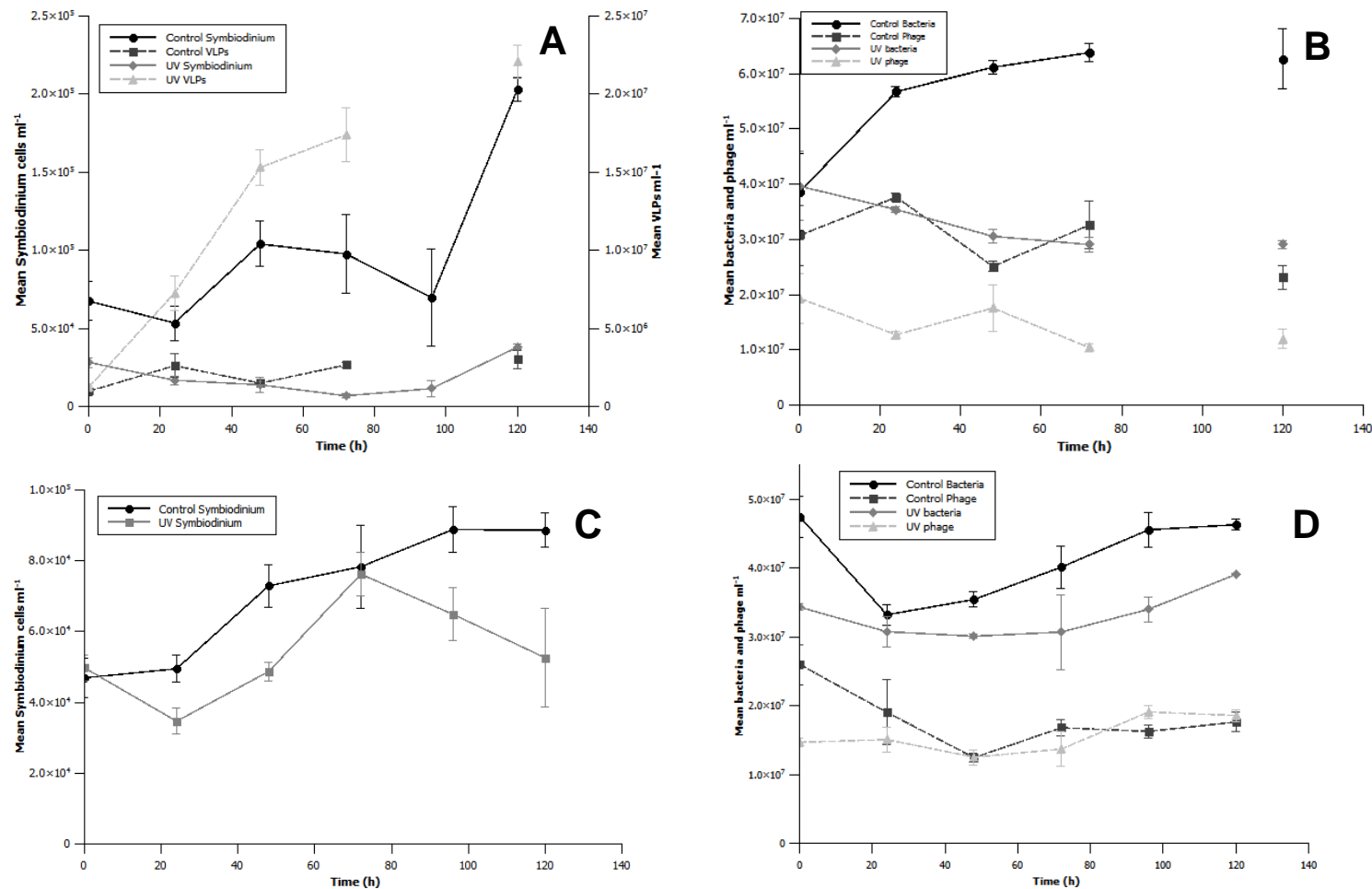


Figure C2. Induction and reinfection experiments, using 0.2 μm pore-size filters, on *Symbiodinium* culture CCMP828. (A) *Symbiodinium* and VLP densities in UV-irradiated and control samples. (B) Bacterial and putative phage densities in UV-irradiated and control samples. (C) *Symbiodinium* density in healthy cultures infected with filtrate from UV-irradiated and control samples (no VLPs were seen in these samples). (D) Bacterial and putative phage densities in healthy cultures infected with filtrate from UV-irradiated and control samples. Error bars are standard error of triplicate counts.

Appendix C

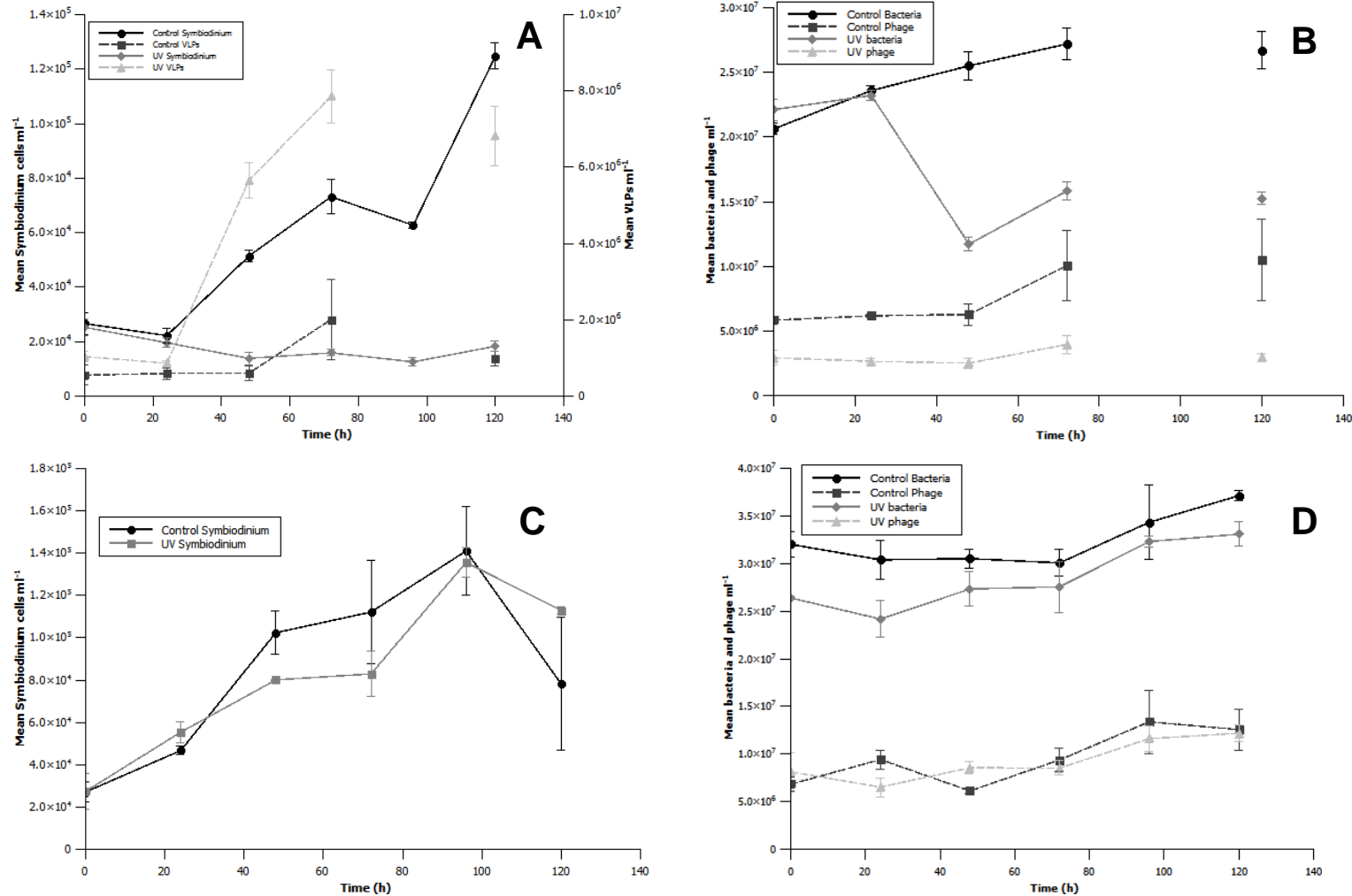


Figure C3. Induction and reinfection experiments, using 0.2 μ m pore-size filters, on *Symbiodinium* culture CCMP2430. (A) *Symbiodinium* and VLP densities in UV-irradiated and control samples. (B) Bacterial and putative phage densities in UV-irradiated and control samples. (C) *Symbiodinium* density in healthy cultures infected with filtrate from UV-irradiated and control samples (no VLPs were seen in these samples). (D) Bacterial and putative phage densities in healthy cultures infected with filtrate from UV-irradiated and control samples. Error bars are standard error of triplicate counts.

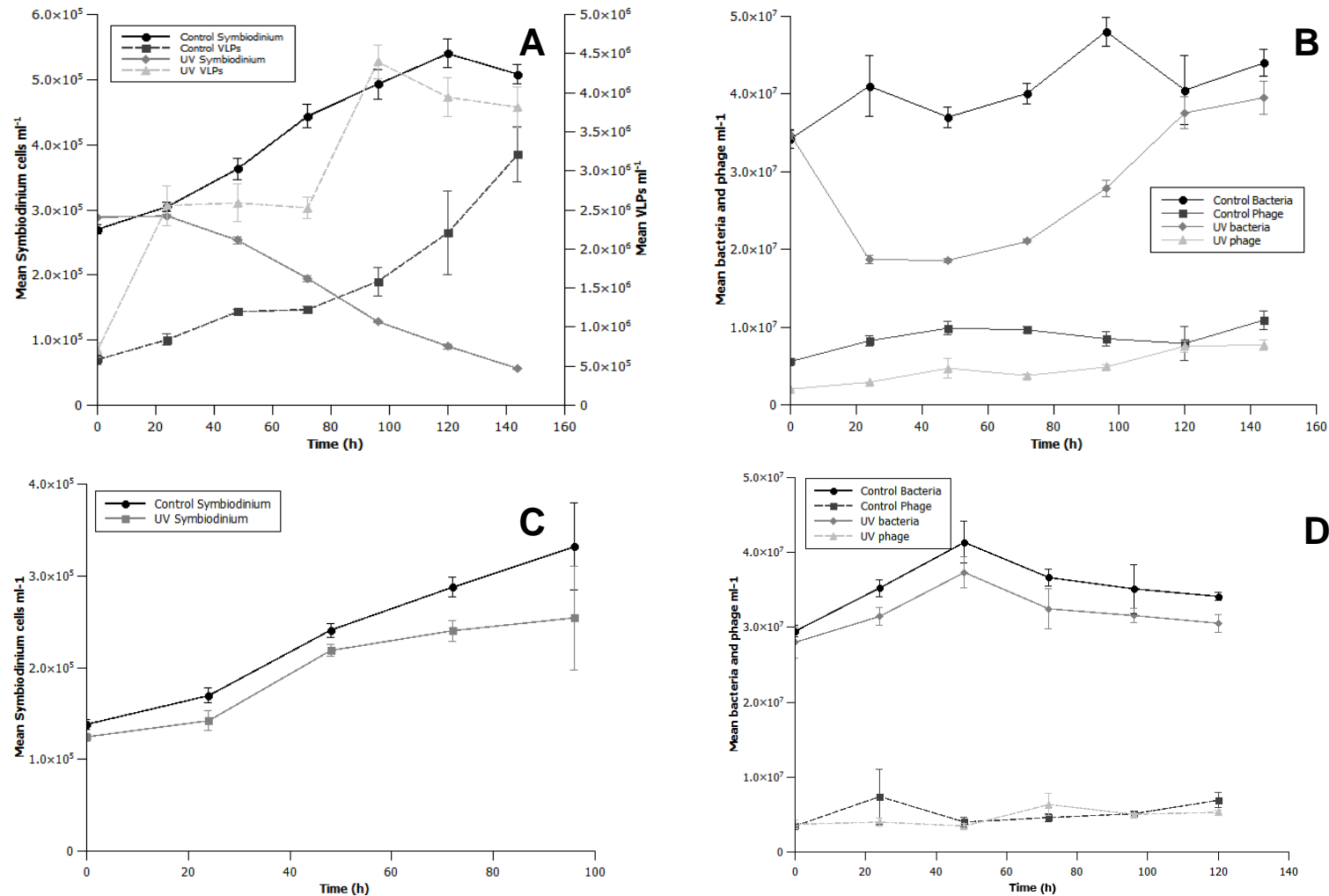


Figure C4. Induction and reinfection experiments, using 0.2 μm pore-size filters, on *Symbiodinium* culture Ap1. (A) *Symbiodinium* and VLP densities in UV-irradiated and control samples. (B) Bacterial and putative phage densities in UV-irradiated and control samples. (C) *Symbiodinium* density in healthy cultures infected with filtrate from UV-irradiated and control samples (no VLPs were seen in these samples). (D) Bacterial and putative phage densities in healthy cultures infected with filtrate from UV-irradiated and control samples. Error bars are standard error of triplicate counts.

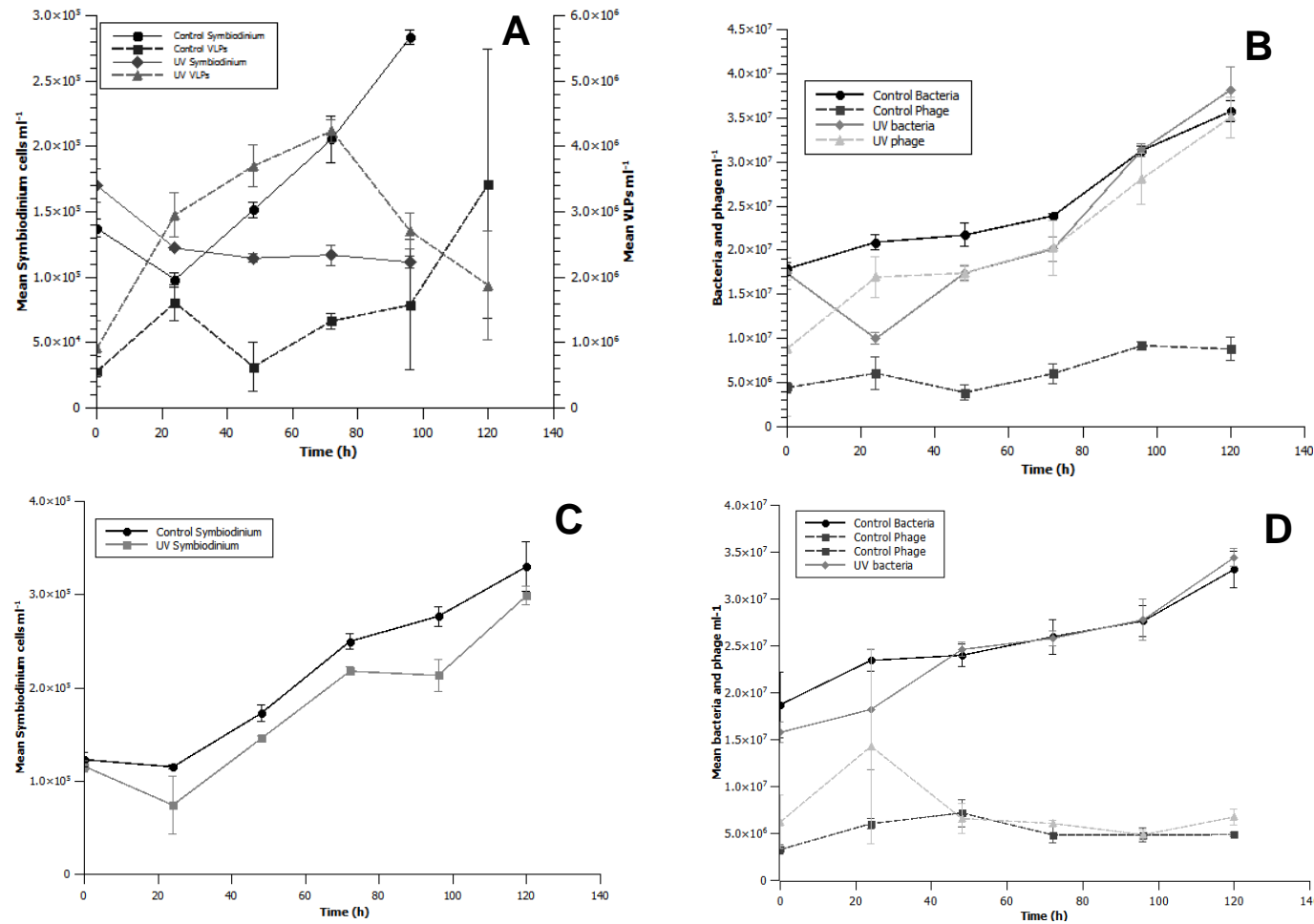


Figure C5. Induction and reinfection experiments, using 0.2 μm pore-size filters, on *Symbiodinium* culture FLAp1. (A) *Symbiodinium* and VLP densities in UV-irradiated and control samples. (B) Bacterial and putative phage densities in UV-irradiated and control samples. (C) *Symbiodinium* density in healthy cultures infected with filtrate from UV-irradiated and control samples (no VLPs were seen in these samples). (D) Bacterial and putative phage densities in healthy cultures infected with filtrate from UV-irradiated and control samples. Error bars are standard error of triplicate counts.

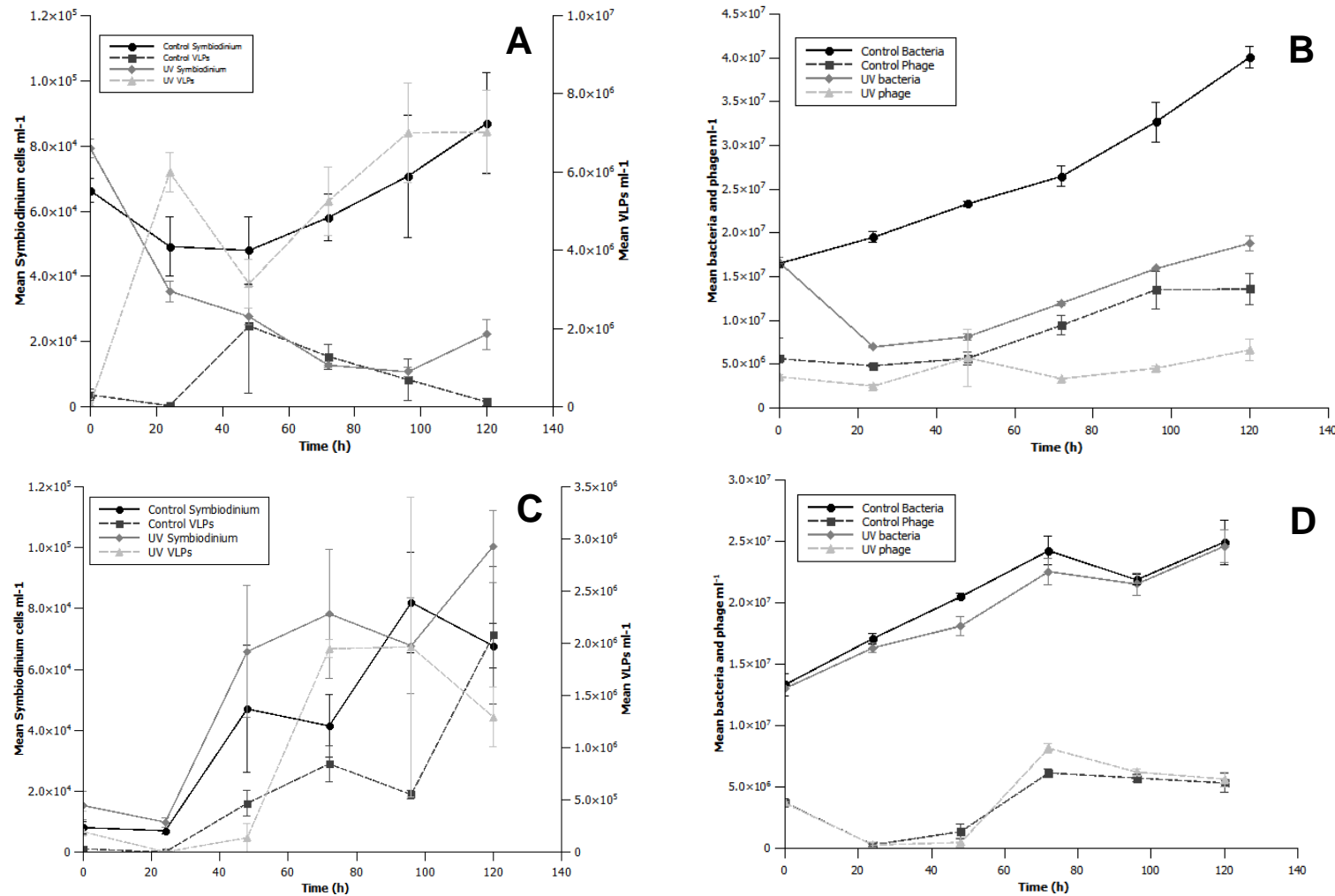


Figure C6. Induction and reinfection experiments, using 0.2 μm pore-size filters, on *Symbiodinium* culture Mf13.14. (A) *Symbiodinium* and VLP densities in UV-irradiated and control samples. (B) Bacterial and putative phage densities in UV-irradiated and control samples. (C) *Symbiodinium* and VLP densities in healthy cultures infected with filtrate from UV-irradiated and control samples. (D) Bacterial and putative phage densities in healthy cultures infected with filtrate from UV-irradiated and control samples. Error bars are standard error of triplicate counts.

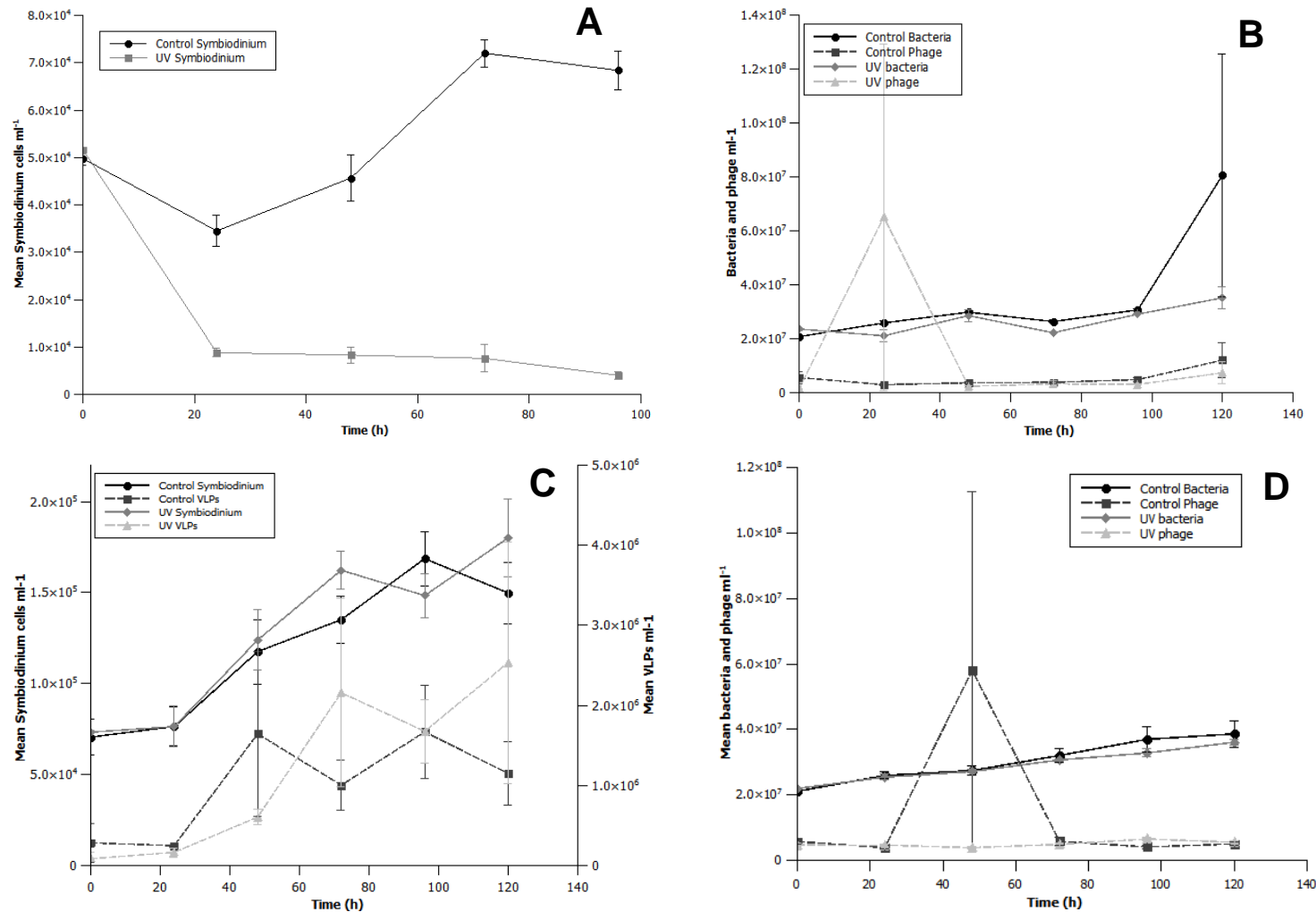


Figure C7. Induction and reinfection experiments, using 0.2 μ m pore-size filters, on *Symbiodinium* culture Mp. (A) *Symbiodinium* density in UV-irradiated and control samples (no VLPs were seen in these samples). (B) Bacterial and putative phage densities in UV-irradiated and control samples. (C) *Symbiodinium* and VLP densities in healthy cultures infected with filtrate from UV-irradiated and control samples. (D) Bacterial and putative phage densities in healthy cultures infected with filtrate from UV-irradiated and control samples. Error bars are standard error of triplicate counts.

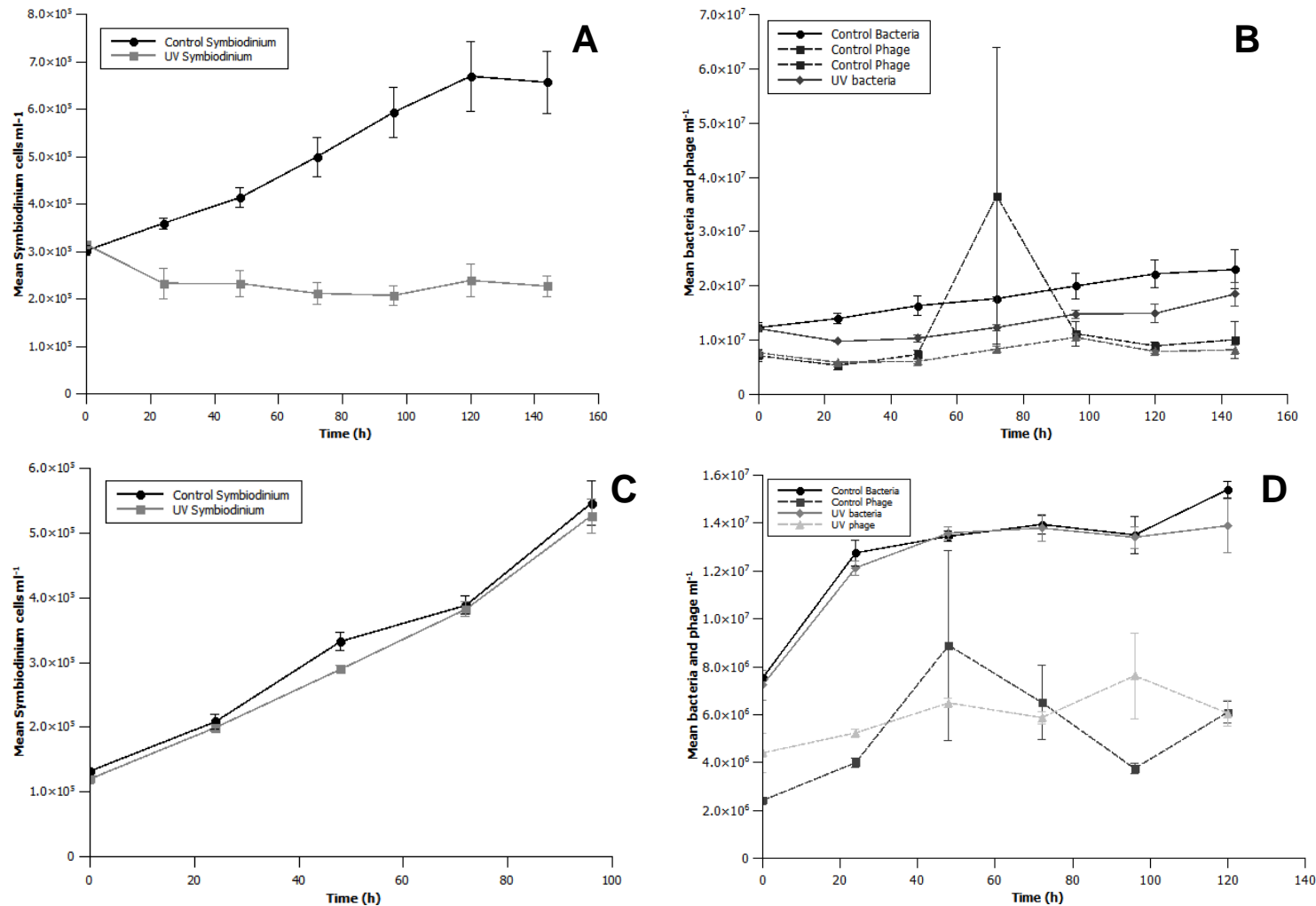


Figure C8. Induction and reinfection experiments, using 0.2 μm pore-size filters, on *Symbiodinium* culture Pd. (A) *Symbiodinium* density in UV-irradiated and control samples (no VLPs were seen in these samples). (B) Bacterial and putative phage densities in UV-irradiated and control samples. (C) *Symbiodinium* density in healthy cultures infected with filtrate from UV-irradiated and control samples (no VLPs were seen in these samples). (D) Bacterial and putative phage densities in healthy cultures infected with filtrate from UV-irradiated and control samples. Error bars are standard error of triplicate counts.

Appendix C

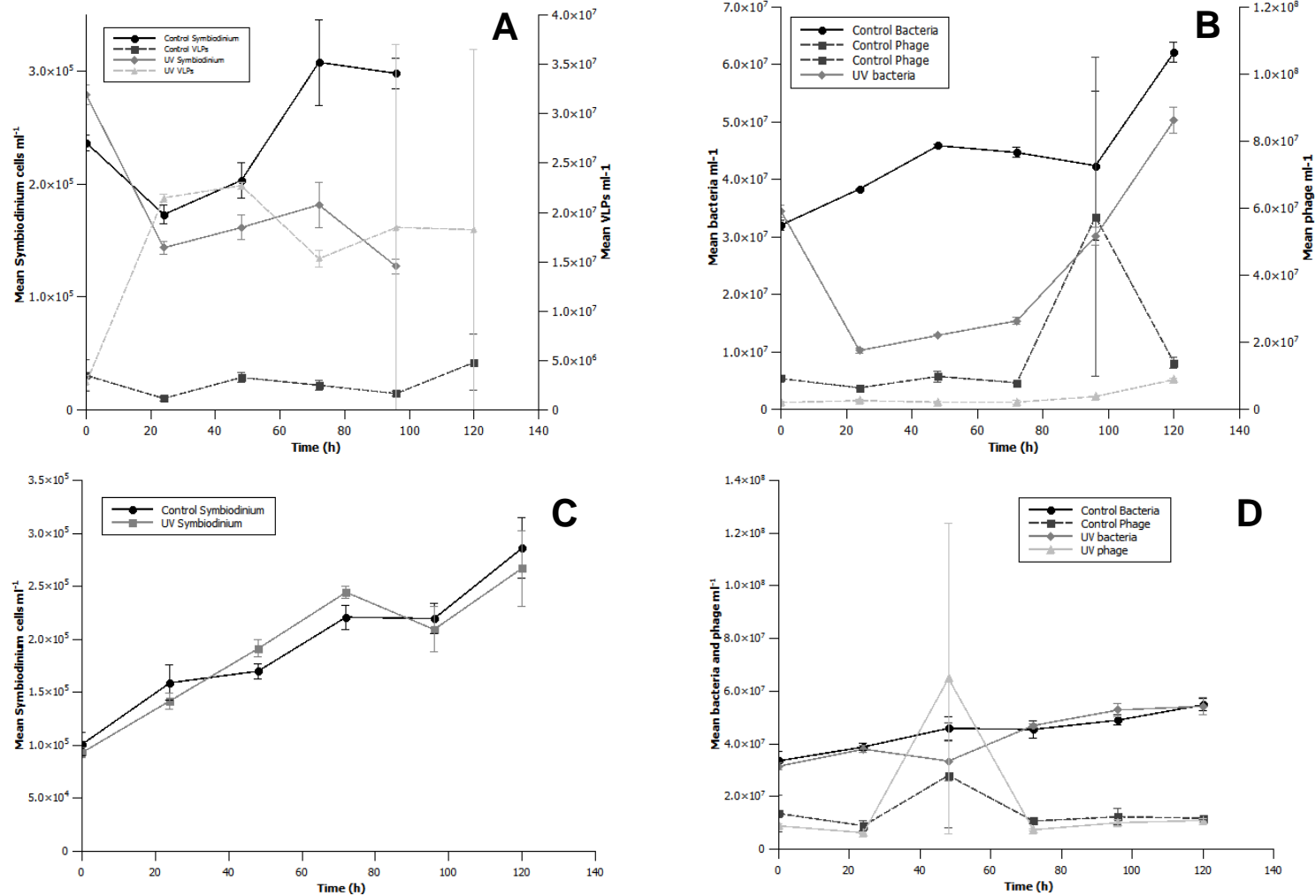


Figure C9. Induction and reinfection experiments, using 0.2 μ m pore-size filters, on *Symbiodinium* culture PK13. (A) *Symbiodinium* and VLP densities in UV-irradiated and control samples. (B) Bacterial and putative phage densities in UV-irradiated and control samples. (C) *Symbiodinium* density in healthy cultures infected with filtrate from UV-irradiated and control samples (no VLPs were seen in these samples). (D) Bacterial and putative phage densities in healthy cultures infected with filtrate from UV-irradiated and control samples. Error bars are standard error of triplicate counts.

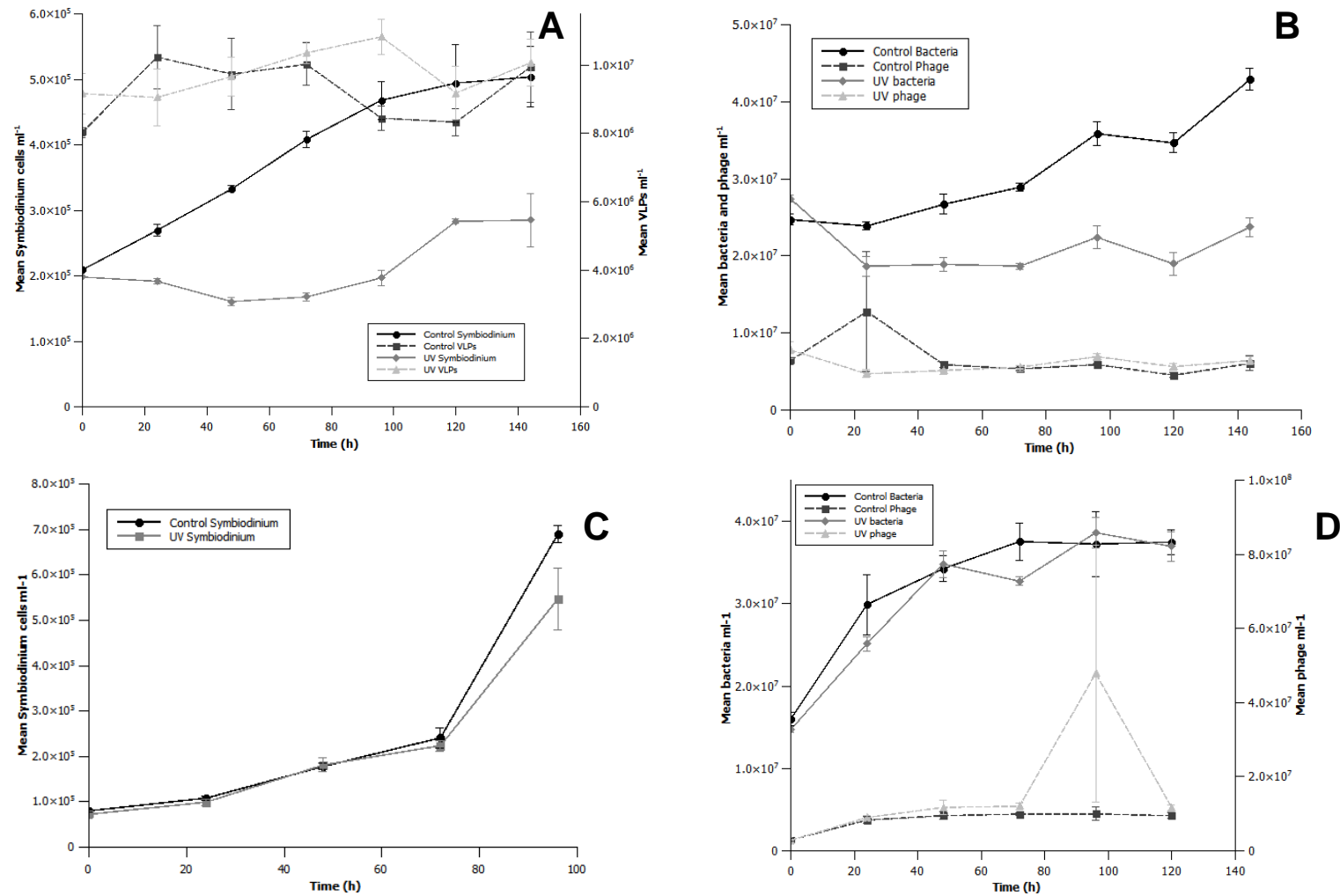


Figure C10. Induction and reinfection experiments, using 0.2 μm pore-size filters, on *Symbiodinium* culture Sin. (A) *Symbiodinium* and VLP densities in UV-irradiated and control samples. (B) Bacterial and putative phage densities in UV-irradiated and control samples. (C) *Symbiodinium* density in healthy cultures infected with filtrate from UV-irradiated and control samples (no VLPs were seen in these samples). (D) Bacterial and putative phage densities in healthy cultures infected with filtrate from UV-irradiated and control samples. Error bars are standard error of triplicate counts.

254 nm UV irradiation – 0.8 µm filtration

The results of this experiment were similar to those of the previous set of experiments (Figs. C11 – C20), which is to be expected, as, apart from a larger filter pore size, the same experimental conditions were used. There were, however, some notable differences. While all ten cultures showed declines in *Symbiodinium* population densities following UV exposure, Apl contained no VLP population in either the control or UV-irradiated samples (Fig. C14A), unlike in the previous experiments, where the VLP population increased after irradiation. Similarly, PK13 showed very little increase in VLP density in comparison to the previous experiments (Fig. C19A). Sin showed similar VLP population dynamics in both control and UV-irradiated samples, namely a rapid increase in density over the first 24 h of the experiment, followed by a series of increases and decreases (Fig. C20A). Bacterial and phage populations in most cultures showed the same responses seen previously: a decrease in bacterial density following UV exposure, and no change in phage population density relative to control samples. Bacterial populations in two cultures (FLApl and Mp; Fig. C15B and Fig. C17B, respectively) showed no response to UV exposure. The phage populations in Mf13.14 (Fig. C16B) and Pd (Fig. C18B) showed an increase in control samples relative to the UV-irradiated samples, which remained constant over the course of the experiment.

The larger filter pore-size of 0.8 µm was used in these experiments to allow the passage of large and/or filamentous viruses, while still excluding the majority of bacteria and other microorganisms. Despite these more liberal experimental conditions, results of infection with the filtrates were much the same as the previous set of experiments, which used a 0.2 µm pore-size filter. In none of the cultures was a decline in *Symbiodinium* population density observed post-infection with the filtrate. Likewise, no increase in VLP population density was seen in samples containing UV-irradiated filtrate, relative to control samples. In CCMP421 (Fig. C11C), CCMP828 (Fig. C12C), FLApl (Fig. C15C), Mf13.14 (Fig. C16C) and Pd (Fig. C18C), there were increases in VLP numbers following infection with UV-irradiated culture filtrate, but this was mirrored by VLP population increases in the corresponding control samples, suggesting an existing chronic viral infection, rather than a new infection or induction by the filtrate. Bacterial and phage populations showed no changes relative to control samples after addition of filtrate from the irradiated samples.

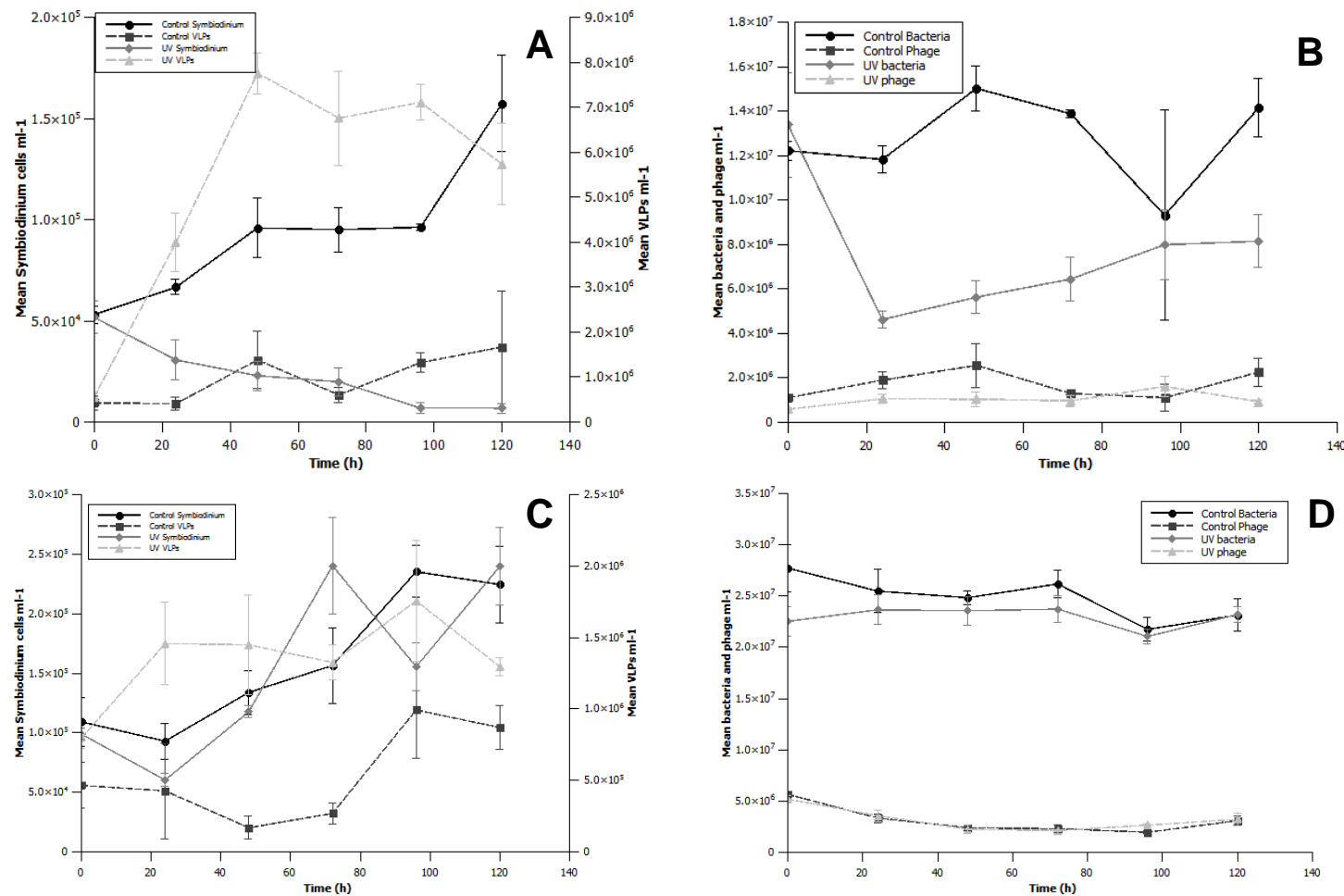


Figure C11. Induction and reinfection experiments, using 0.8 μm pore-size filters, on *Symbiodinium* culture CCMP421. (A) *Symbiodinium* and VLP densities in UV-irradiated and control samples. (B) Bacterial and putative phage densities in UV-irradiated and control samples. (C) *Symbiodinium* and VLP densities in healthy cultures infected with filtrate from UV-irradiated and control samples. (D) Bacterial and putative phage densities in healthy cultures infected with filtrate from UV-irradiated and control samples. Error bars are standard error of triplicate counts.

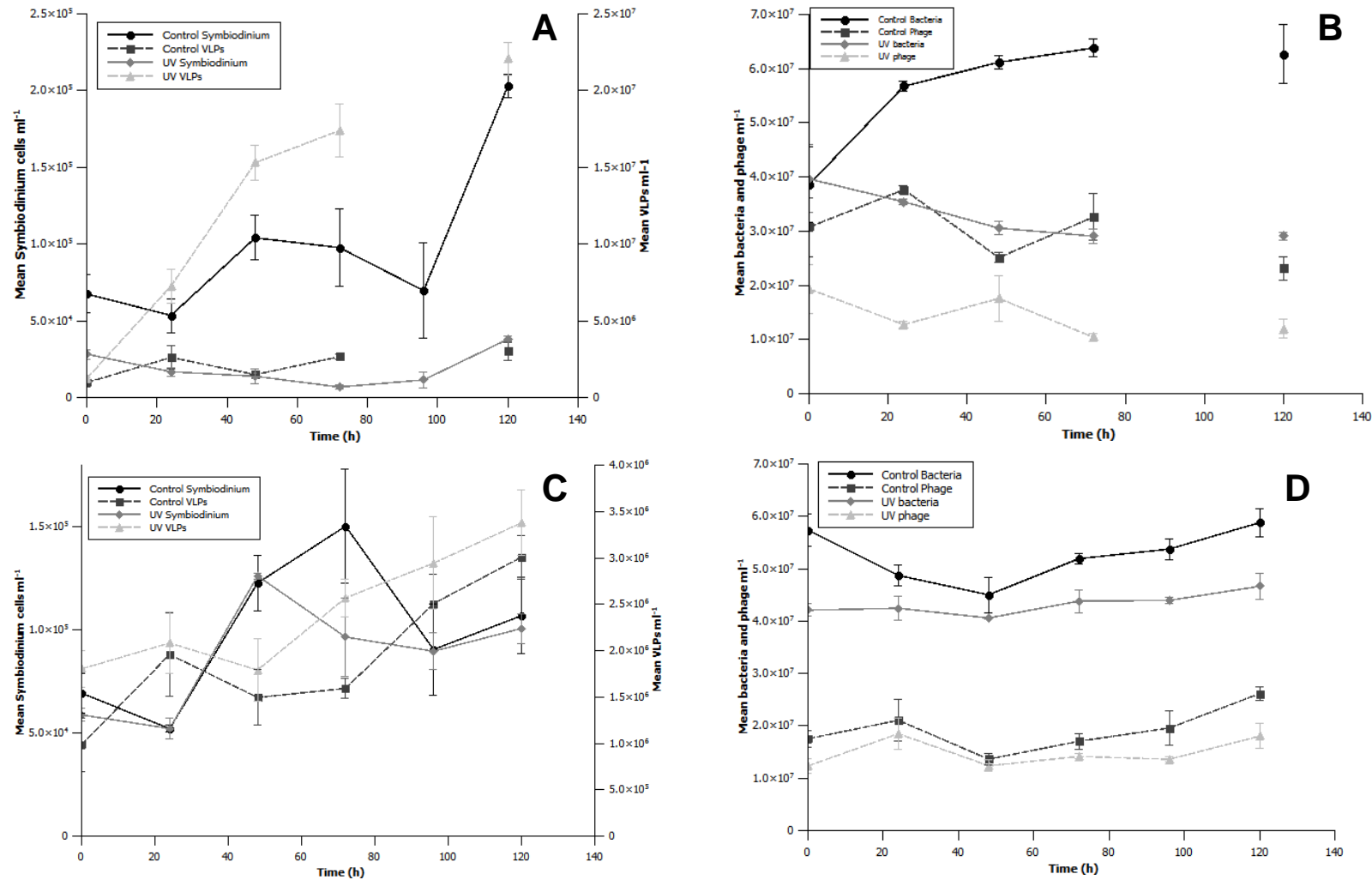


Figure C12. Induction and reinfection experiments, using 0.8 μm pore-size filters, on *Symbiodinium* culture CCMP828. (A) *Symbiodinium* and VLP densities in UV-irradiated and control samples. (B) Bacterial and putative phage densities in UV-irradiated and control samples. (C) *Symbiodinium* and VLP densities in healthy cultures infected with filtrate from UV-irradiated and control samples. (D) Bacterial and putative phage densities in healthy cultures infected with filtrate from UV-irradiated and control samples. Error bars are standard error of triplicate counts.

Appendix C

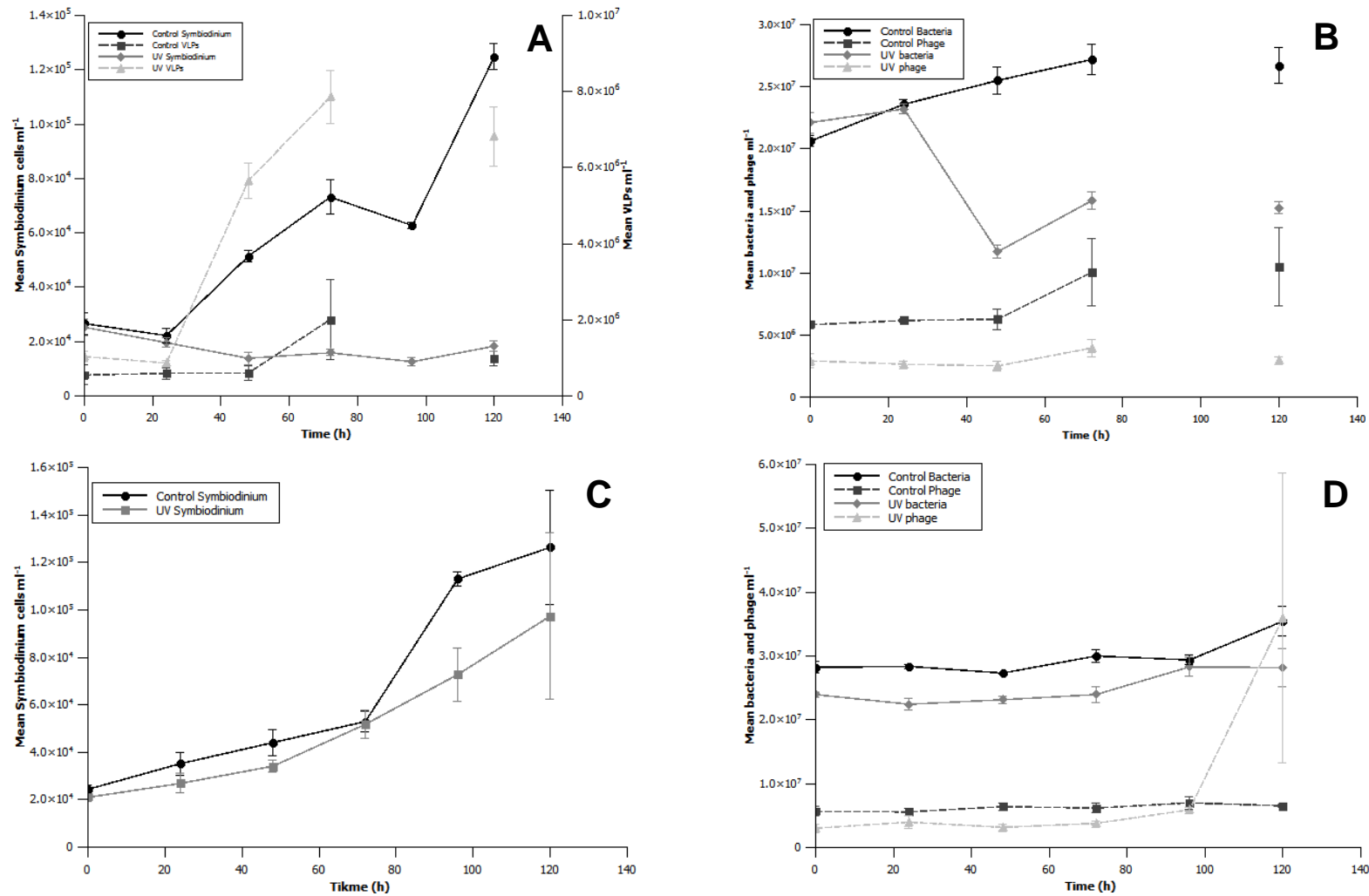


Figure C13. Induction and reinfection experiments, using 0.8 μm pore-size filters, on *Symbiodinium* culture CCMP2430. (A) *Symbiodinium* density in UV-irradiated and control samples (no VLPs were seen in these samples). (B) Bacterial and putative phage densities in UV-irradiated and control samples. (C) *Symbiodinium* density in healthy cultures infected with filtrate from UV-irradiated and control samples (no VLPs were seen in these samples). (D) Bacterial and putative phage densities in healthy cultures infected with filtrate from UV-irradiated and control samples. Error bars are standard error of triplicate counts.

Appendix C

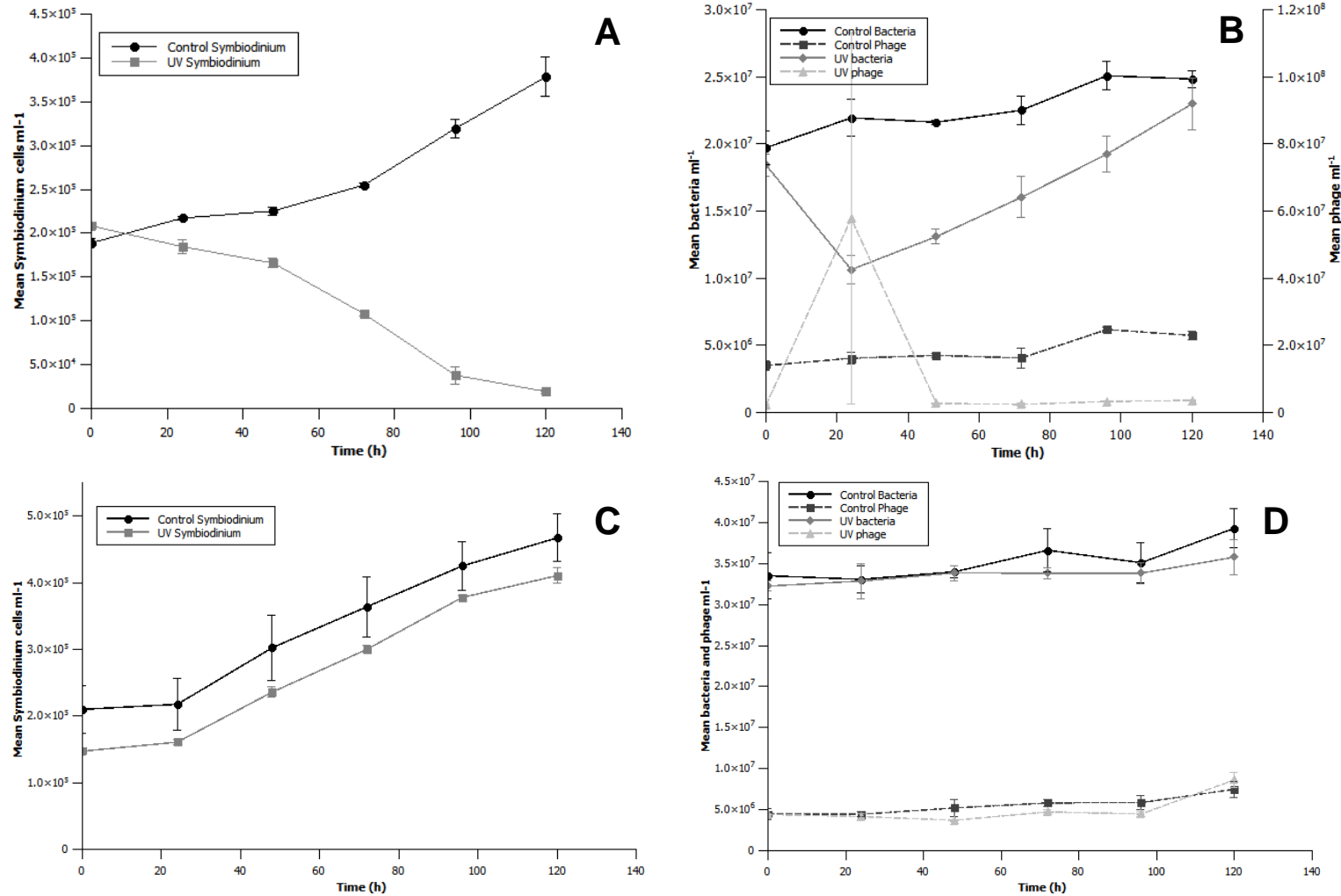


Figure C14. Induction and reinfection experiments, using 0.8 μm pore-size filters, on *Symbiodinium* culture Ap1. (A) *Symbiodinium* density in UV-irradiated and control samples (no VLPs were seen in these samples). (B) Bacterial and putative phage densities in UV-irradiated and control samples. (C) *Symbiodinium* density in healthy cultures infected with filtrate from UV-irradiated and control samples (no VLPs were seen in these samples). (D) Bacterial and putative phage densities in healthy cultures infected with filtrate from UV-irradiated and control samples. Error bars are standard error of triplicate counts.

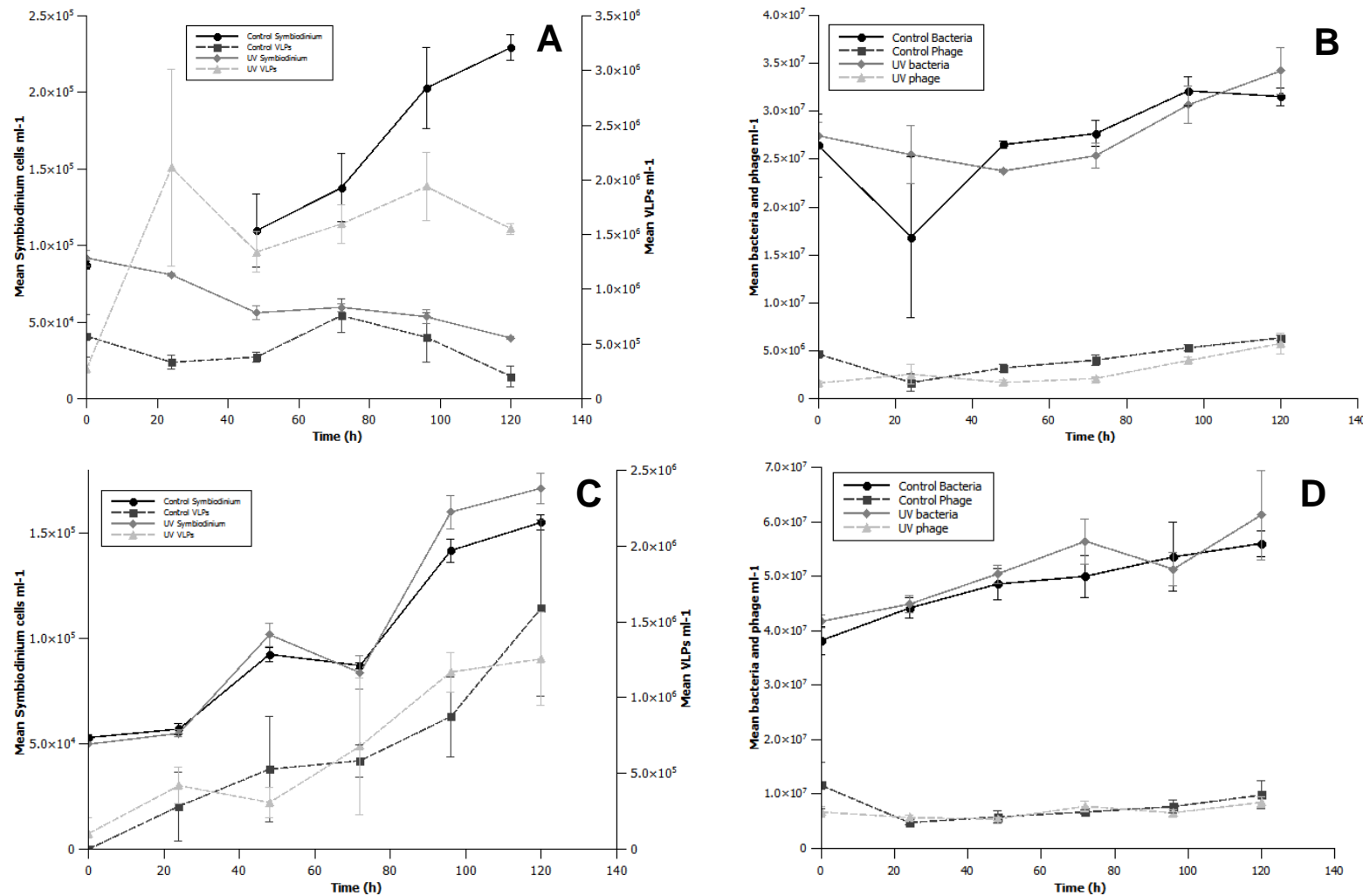


Figure C15. Induction and reinfection experiments, using 0.8 μm pore-size filters, on *Symbiodinium* culture FLAp1. (A) *Symbiodinium* and VLP densities in UV-irradiated and control samples. (B) Bacterial and putative phage densities in UV-irradiated and control samples. (C) *Symbiodinium* and VLP densities in healthy cultures infected with filtrate from UV-irradiated and control samples. (D) Bacterial and putative phage densities in healthy cultures infected with filtrate from UV-irradiated and control samples. Error bars are standard error of triplicate counts.

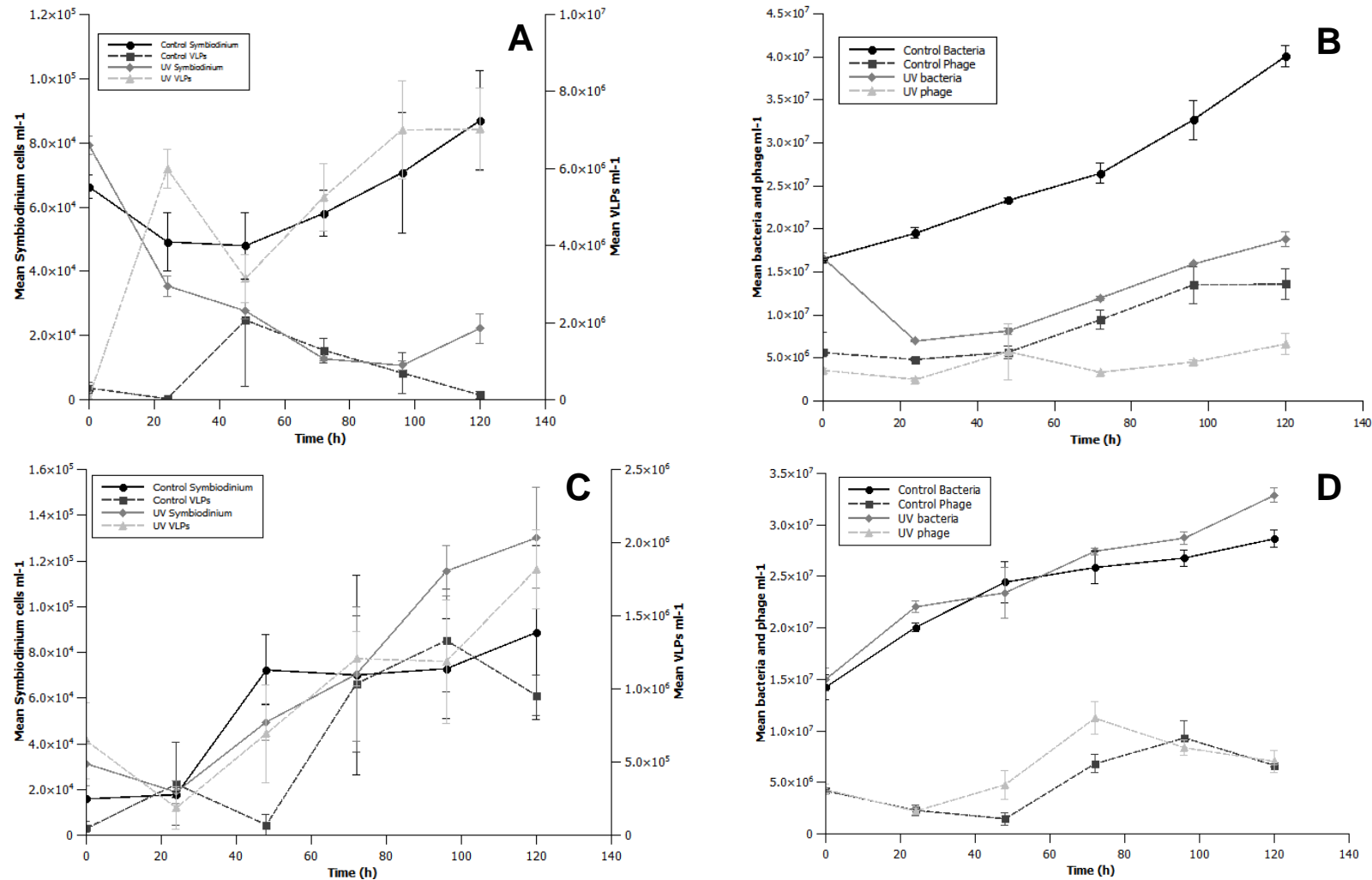


Figure C16. Induction and reinfection experiments, using 0.8 μm pore-size filters, on *Symbiodinium* culture Mf13.14. (A) *Symbiodinium* and VLP densities in UV-irradiated and control samples. (B) Bacterial and putative phage densities in UV-irradiated and control samples. (C) *Symbiodinium* and VLP densities in healthy cultures infected with filtrate from UV-irradiated and control samples. (D) Bacterial and putative phage densities in healthy cultures infected with filtrate from UV-irradiated and control samples. Error bars are standard error of triplicate counts.

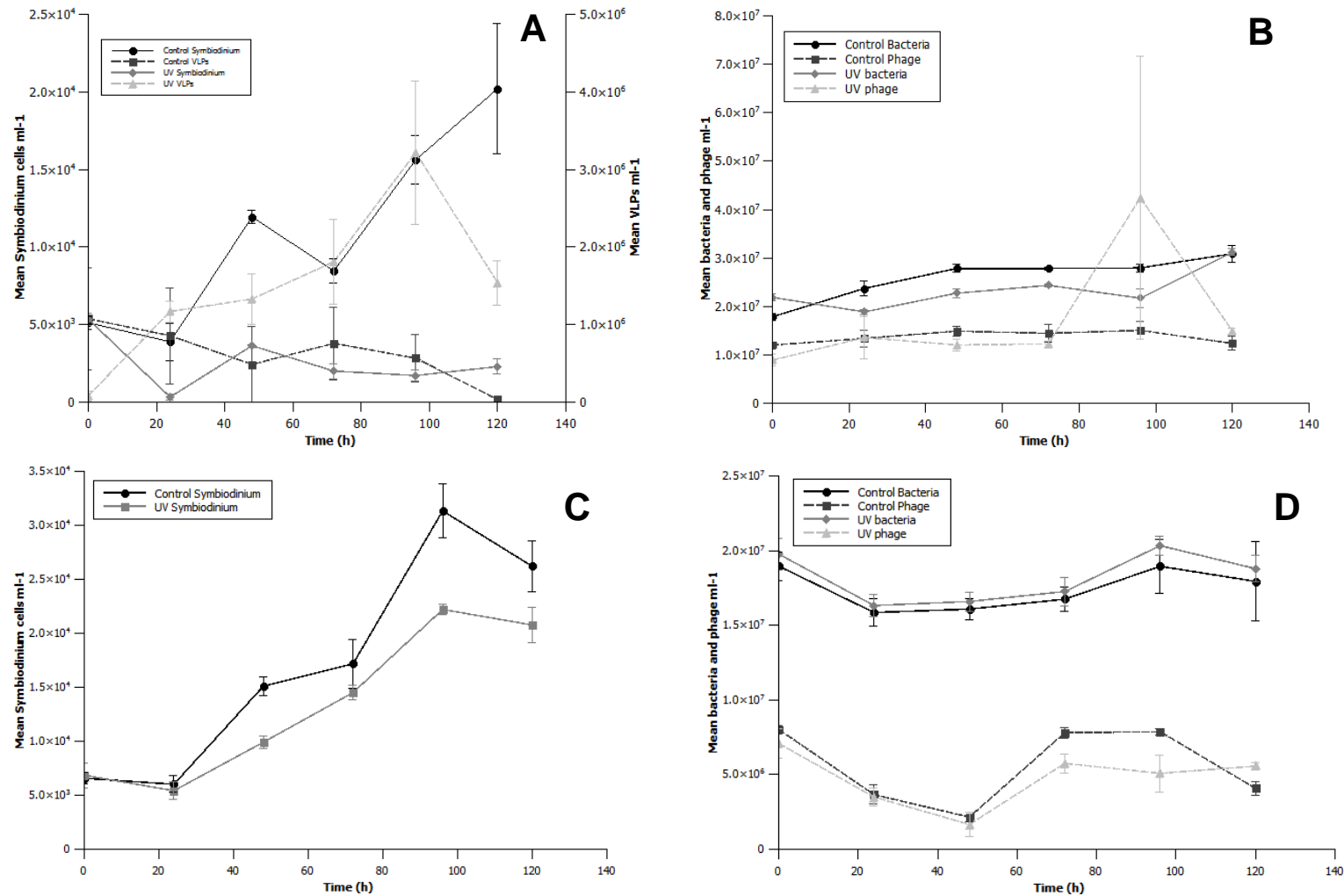


Figure C17. Induction and reinfection experiments, using 0.8 μm pore-size filters, on *Symbiodinium* culture Mp. (A) *Symbiodinium* and VLP densities in UV-irradiated and control samples. (B) Bacterial and putative phage densities in UV-irradiated and control samples. (C) *Symbiodinium* density in healthy cultures infected with filtrate from UV-irradiated and control samples (no VLPs were seen in these samples). (D) Bacterial and putative phage densities in healthy cultures infected with filtrate from UV-irradiated and control samples. Error bars are standard error of triplicate counts.

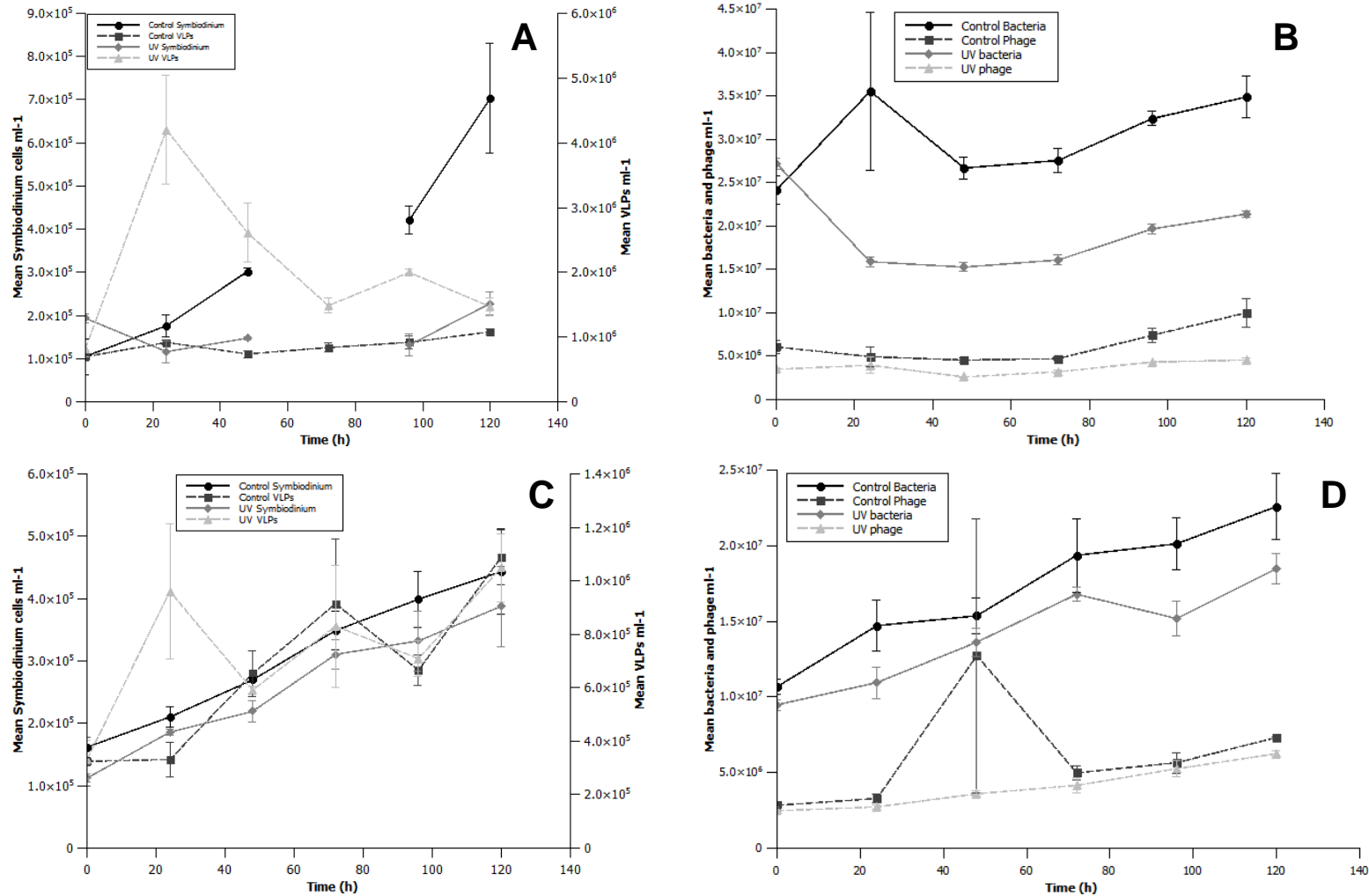


Figure C18. Induction and reinfection experiments, using 0.8 μm pore-size filters, on *Symbiodinium* culture Pd. (A) *Symbiodinium* and VLP densities in UV-irradiated and control samples. (B) Bacterial and putative phage densities in UV-irradiated and control samples. (C) *Symbiodinium* and VLP densities in healthy cultures infected with filtrate from UV-irradiated and control samples. (D) Bacterial and putative phage densities in healthy cultures infected with filtrate from UV-irradiated and control samples. Error bars are standard error of triplicate counts.

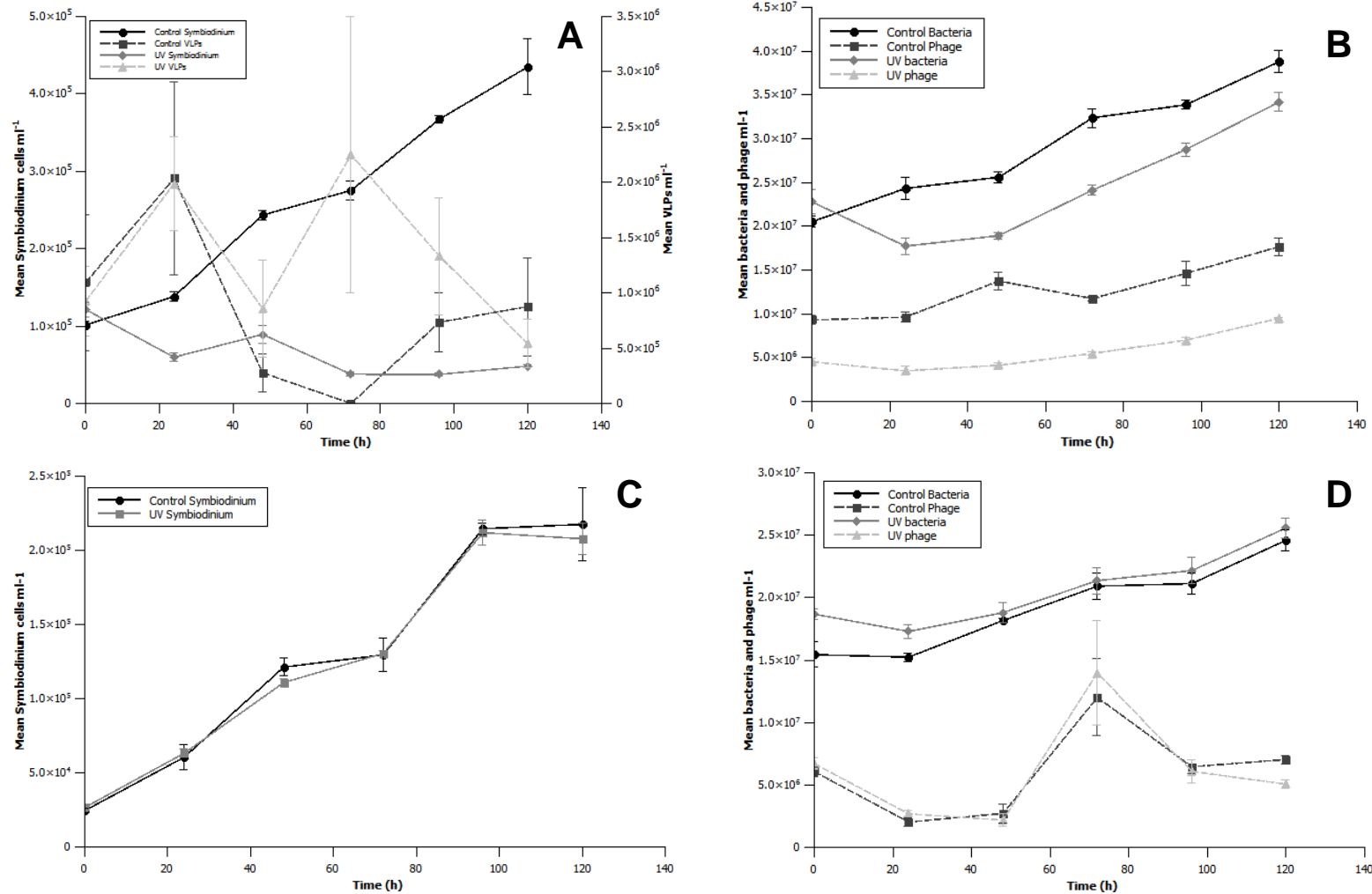


Figure C19. Induction and reinfection experiments, using 0.8 μm pore-size filters, on *Symbiodinium* culture PK13. (A) *Symbiodinium* and VLP densities in UV-irradiated and control samples. (B) Bacterial and putative phage densities in UV-irradiated and control samples. (C) *Symbiodinium* density in healthy cultures infected with filtrate from UV-irradiated and control samples (VLPs were not seen in these samples). (D) Bacterial and putative phage densities in healthy cultures infected with filtrate from UV-irradiated and control samples. Error bars are standard error of triplicate counts.

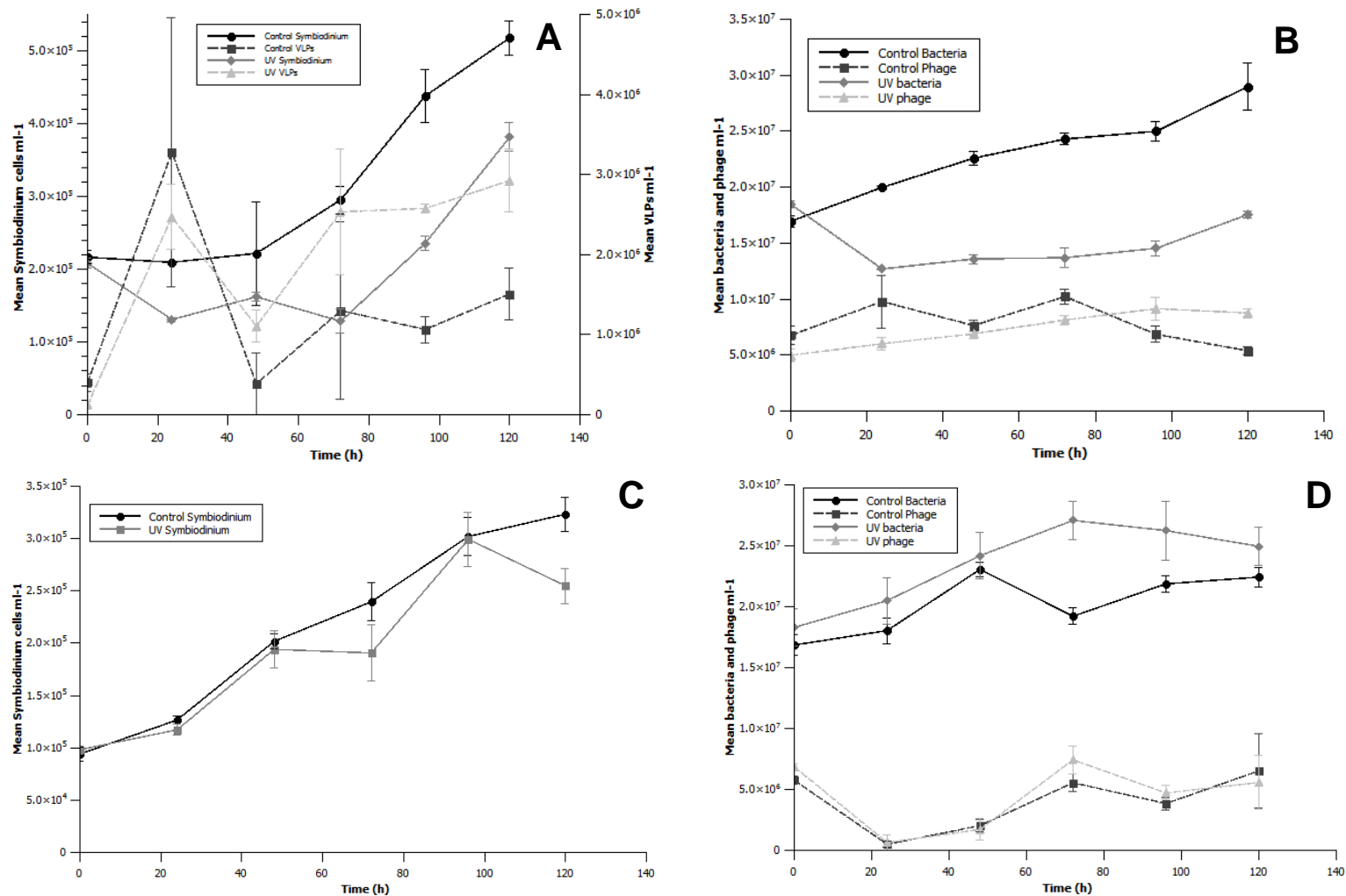


Figure C20. Induction and reinfection experiments, using 0.8 μm pore-size filters, on *Symbiodinium* culture Sin. (A) *Symbiodinium* and VLP densities in UV-irradiated and control samples. (B) Bacterial and putative phage densities in UV-irradiated and control samples. (C) *Symbiodinium* density in healthy cultures infected with filtrate from UV-irradiated and control samples (VLPs were not seen in these samples). (D) Bacterial and putative phage densities in healthy cultures infected with filtrate from UV-irradiated and control samples. Error bars are standard error of triplicate counts.

Discussion

Attempts at infecting healthy *Symbiodinium* cultures with the putative viruses induced by UV irradiation were unsuccessful. In no case did the transfer of irradiated culture lysate result in significant declines in *Symbiodinium* population densities or increases in VLP numbers. This result was somewhat unexpected, given the molecular, microscopic and flow cytometry-based evidence of latent viruses in these cells. Interestingly, Wilson *et al.* (2001) and Davy *et al.* (2006) were able to cause lysis of otherwise healthy *Symbiodinium* cells by addition of filtrate from thermally-stressed *Symbiodinium* cultures. The experimental conditions in these studies were very similar to those used here, except that *Symbiodinium* cells were freshly isolated from their cnidarian hosts. How this difference might have affected the results, however, is unclear. The contrasting result may simply be indicative of different types of viruses present in the *Symbiodinium* cultures studied here.

Assuming, based on the evidence gathered here, that viruses were present following UV exposure, there are three possible explanations for the failure to infect the healthy cultures. First, the putative viruses may have been too large to pass through the 0.2 μm and 0.8 μm pore-size filters, or may have become otherwise trapped in the filter membrane. This seems unlikely, as the VLPs seen in electron micrographs were sufficiently small to pass through such filters, and PES filter membranes generally show a low level of protein binding. Second, the filtration may have resulted in a loss of viral infectivity. This phenomenon has been documented in filtration of algal viruses previously. Suttle *et al.* (1991) tested the infectivity of two algal viruses following filtration through 16 different filters, and found that viruses lost infectivity in 7 of the 32 resulting filtrates, showed variable infectivity in 3, and remained infective in 16 (infectivity was not determined for 6 of the filtrates). PES filters were among those tested, and showed variable results. Given that infectivity was only maintained in ~50% of viral filtrates, it would not be surprising if the lack of infection seen in the present study was due to loss of infectivity. In the study by Suttle *et al.* (1991), glass-fibre filters were the only filter type to consistently result in infective viruses, and these may be an option for future experiments on *Symbiodinium* viruses. However, the variability in post-filtration infectivity seen between two viruses by Suttle *et al.* (1991), even when using the same filter, suggests that even glass-fibre filters would give no guarantee of successful infection in *Symbiodinium*. Finally, infection may have been unsuccessful due to the presence of latent viral infections in the healthy cultures. Superinfection immunity or cross-protection, where

the presence of one virus in a cell prevents infection by another virus of the same or a similar species, is well documented in plants (Roossinck, 2008), animals (Christen *et al.*, 1990; Ellenberg *et al.*, 2004) and bacteria (McAllister and Barrett, 1977; Kliem and Dreiseikelmann, 1989), and has also been shown to occur in a single-celled alga (Greiner *et al.*, 2009). While superinfection immunity often involves productive viral infections, it is also common in latent viral infections, and may in fact be necessary for the maintenance of latent infections (Berngruber *et al.*, 2010) as it ensures survival of the host cell and hence vertical transmission of the latent virus. Given these facts, it is possible that even if the viruses maintained their infectivity after filtration, many or all of them would have been prevented from successfully infecting healthy *Symbiodinium* cells.

Appendix D: Additional data for Chapter 3.

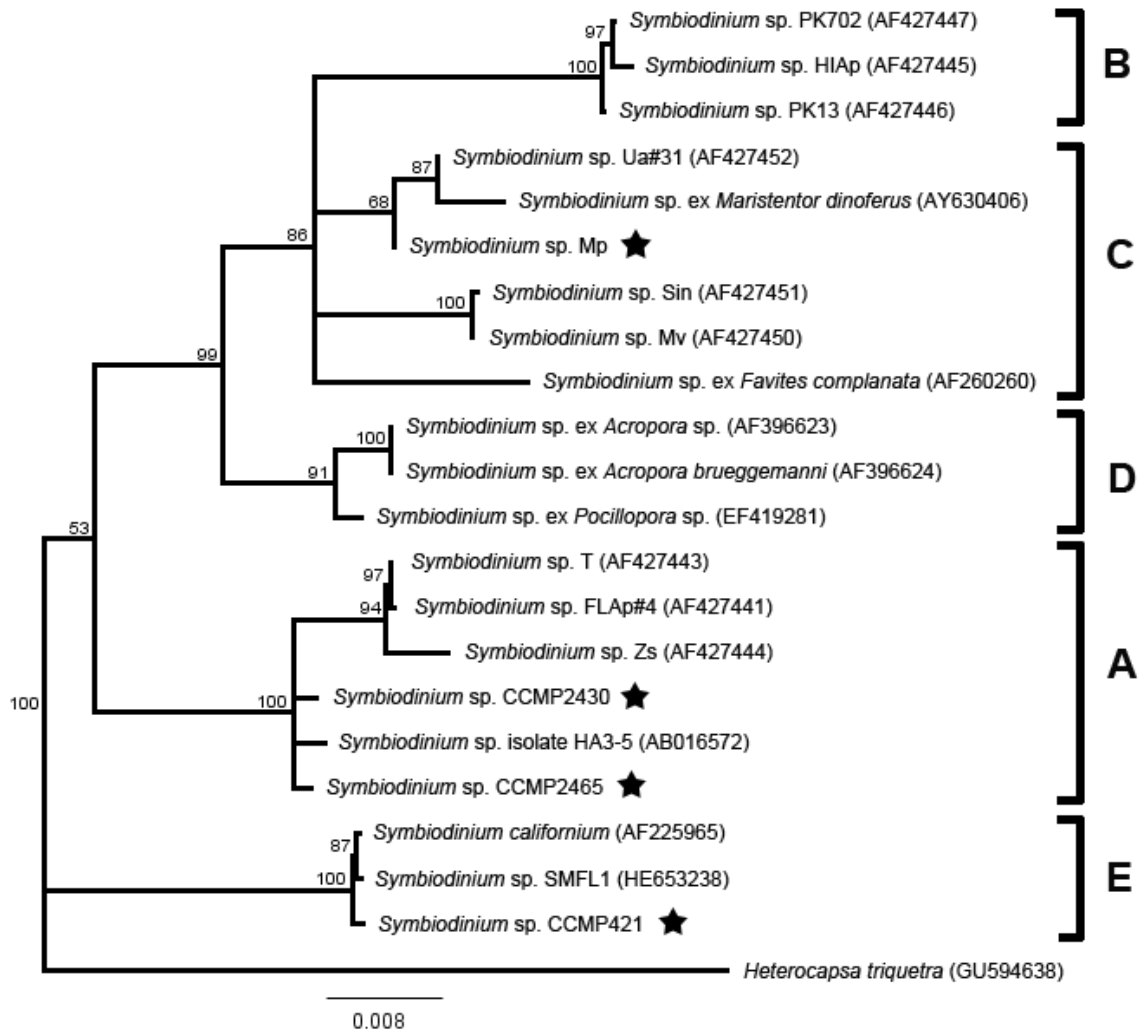


Figure D1. Phylogenetic positions of the *Symbiodinium* cultures (CCMP421, CCMP2430 and Mp) used in this study. The displayed phylogeny is a majority-rule consensus tree of 18S rRNA sequences, based on 100 bootstrap replicates of an initial neighbour-joining tree constructed using a Jukes-Cantor model of evolution. Stars indicate 18S sequences produced in the present study and letters to the right of the tree indicate *Symbiodinium* clades. The scale bar represents the number of nucleotide substitutions per site, and branch numbers indicate the level of bootstrap support (100 iterations).

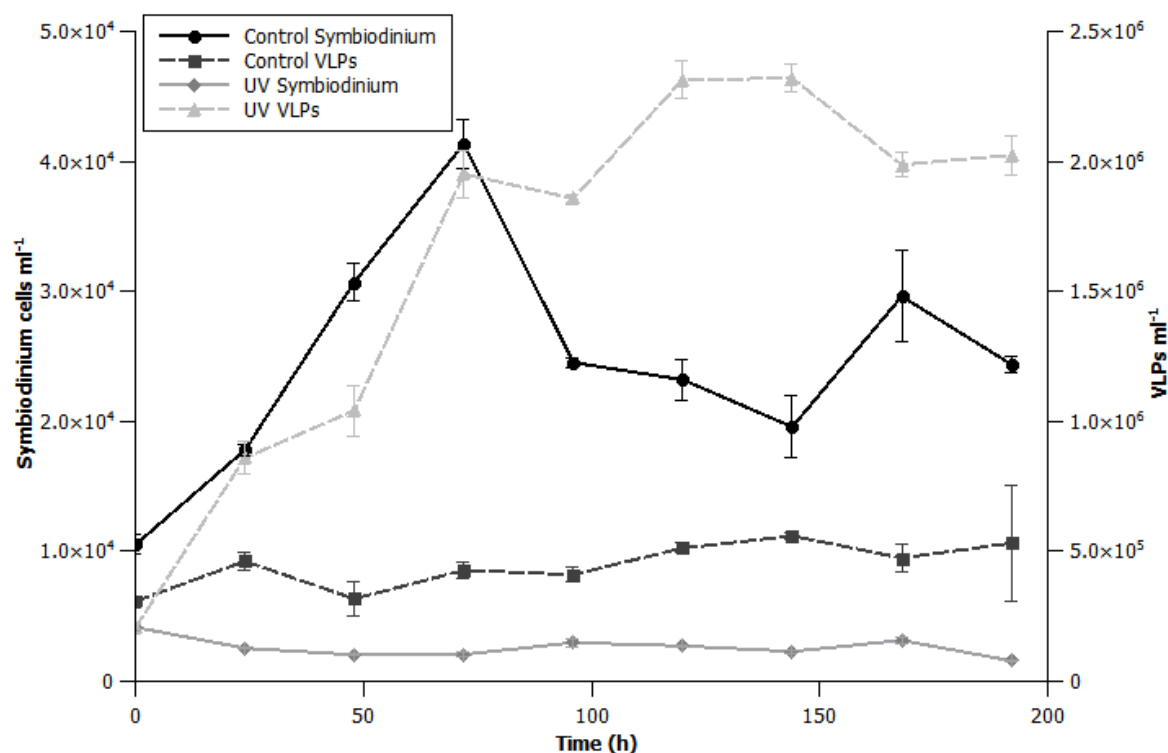


Figure D2. Mean *Symbiodinium* and VLP densities in UV-irradiated and control samples of *Symbiodinium* culture CCMP2430. Error bars are standard error of triplicate counts.

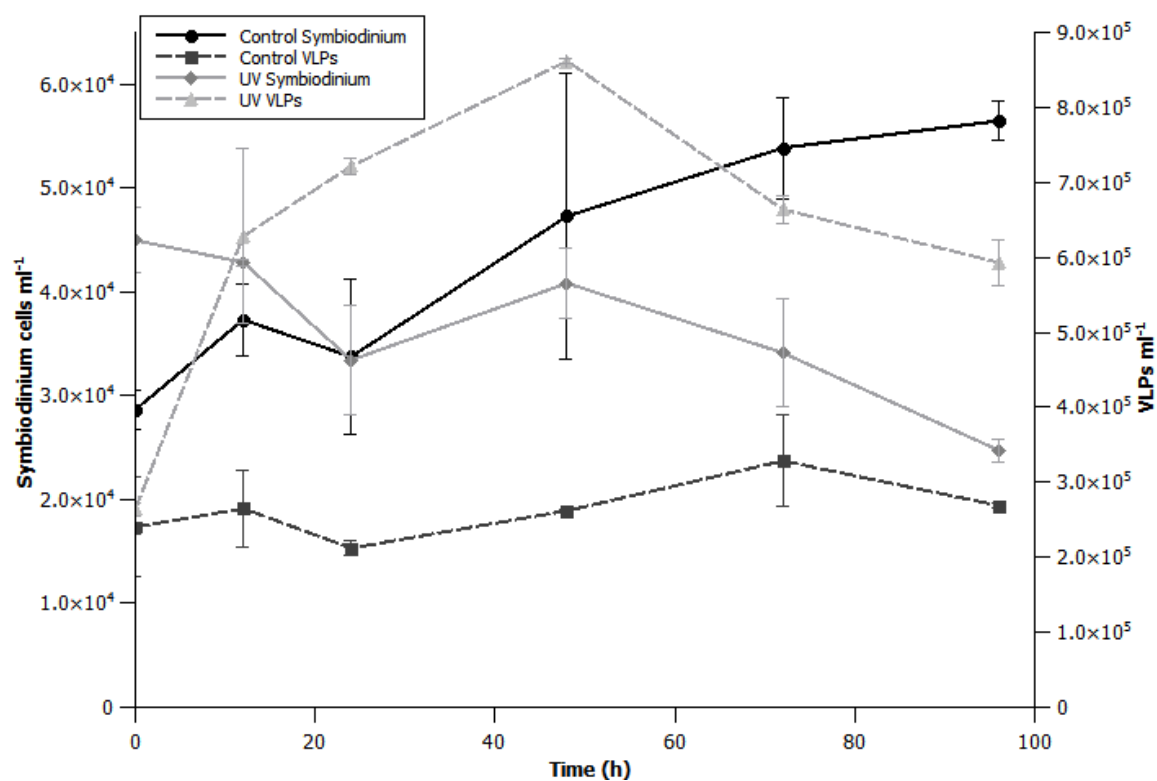


Figure D3. Mean *Symbiodinium* and VLP densities in UV-irradiated and control samples of *Symbiodinium* culture Mp. Error bars are standard error of duplicate counts.

Appendix D

Table D1. Unigenes from the transcriptomes of *Symbiodinium* cultures CCMP421, CCMP2430 and Mp with nearest BLAST matches belonging to members of the *Phycodnaviridae*. Numbers in the *Symbiodinium* culture columns represent the number of different unigenes sharing the same BLAST match. Where several sequences shared the same BLAST match, the range of values for the query length, sequence coverage, similarity and e-value are reported. Table continues overleaf.

Gene product	Accession number	BLAST hit	CCMP421 (Clade E)	CCMP2430 (Clade A)	Mp (Clade C)	Query length (AA)	Query coverage (%)	Sequence similarity (%)	e-value
exported lipoprotein	ADX05786	Organic Lake phycodnavirus	1			214	44.9	57	2.01E-14
elongation factor 2	ADX05812	Organic Lake phycodnavirus	1			589	28.7	59	1.01E-29
hypothetical protein	AEO98022	<i>Emiliana huxleyi</i> virus 203			1	215	74.4	45	3.95E-09
membrane protein	AEO98091	<i>Emiliana huxleyi</i> virus 203	1			668	27.5	42	3.38E-08
hypothetical protein	AEO98286	<i>Emiliana huxleyi</i> virus 203			2	524	42.7	52	5.90E-25
membrane protein	AEP15215	<i>Emiliana huxleyi</i> virus 88			1	243	55.1	49	1.08E-10
membrane protein	AEP15724	<i>Emiliana huxleyi</i> virus 207	1			255	51.4	45	1.02E-10
hypothetical protein	AEP15886	<i>Emiliana huxleyi</i> virus 208		2		209-335	73.6-85.4	54-56	1.32E-42 - 1.27E-12
membrane protein	AET42467	<i>Emiliana huxleyi</i> virus 202			1	785-824	8.1-8.5	56	2.99E-07 - 3.19E-07
hypothetical protein	AET42480	<i>Emiliana huxleyi</i> virus 202	2	1		348-1315	11.9 - 61.2	41-51	1.62E-08 - 4.65E-07
membrane protein	AET42486	<i>Emiliana huxleyi</i> virus 202			1	613	94.4	48	1.94E-64
exonuclease v subunit alpha	AET42504	<i>Emiliana huxleyi</i> virus 202	1	1		222	35.6	62	5.19E-13
hypothetical protein	AET42509	<i>Emiliana huxleyi</i> virus 202	1		1	181-681	13.8-50.3	49-53	1.49E-11 - 2.99E-07
modification methylase	AET73407	<i>Emiliana huxleyi</i> virus PS401	2	1		351-467	73.2-97.1	42-49	1.96E-39 - 2.25E-19
hypothetical protein	AET73509	<i>Emiliana huxleyi</i> virus PS401			1	302	25.8	71	2.19E-14

Appendix D

Table D1 (continued).

hypothetical protein	AET73523	<i>Emiliana huxleyi</i> virus PS401	3	4		242-353	36.8-92.2	39-49	1.27E-11 - 3.88E-07
cytochrome b5	AET84663	<i>Ostreococcus lucimarinus</i> virus OIV4			1	107	63.5	61	1.89E-11
membrane protein	AET98250	<i>Emiliana huxleyi</i> virus 201			1	297	45.1	49	2.79E-10
hypothetical protein	AFC34921	<i>Ostreococcus tauri</i> virus RT-2011	1			325	52.6	46	1.60E-14
NDP-hexose - dehydratase	AFC34947	<i>Ostreococcus tauri</i> virus RT-2011	1	1		352-459	81.5-100	72-75	1.78E-160 - 7.04E-144
ankyrin repeat PH and SEC7 domain containing protein	AGE48310	<i>Paramecium bursaria</i> <i>Chlorella</i> virus AN69C	1			195	43	59	9.77E-23
ankyrin repeat PH and SEC7 domain containing protein	AGE48312	<i>Paramecium bursaria</i> <i>Chlorella</i> virus AN69C		1		799	35.9	44	1.06E-12
ankyrin repeat PH and SEC7 domain containing protein	AGE52194	<i>Paramecium bursaria</i> <i>Chlorella</i> virus CVR-1			1	79	98.7	56	6.44E-07
hypothetical protein	AGE52380	<i>Paramecium bursaria</i> <i>Chlorella</i> virus CvsA1		4		296-845	27.8-97.6	52	5.08E-40 - 1.86E-29
DNA topoisomerase II	AGE58893	<i>Paramecium bursaria</i> <i>Chlorella</i> virus NYs1			1	65	96.9	87	2.26E-24
membrane protein	CAZ69460	<i>Emiliana huxleyi</i> virus 99B1			1	424	42.5	45	7.09E-10
membrane protein	CAZ69519	<i>Emiliana huxleyi</i> virus 99B1			1	169	72.8	56	5.21E-14
ankyrin repeat PH and SEC7 domain containing protein	NP_048353	<i>Paramecium bursaria</i> <i>Chlorella</i> virus 1		1		215-253	45.5-53.5	50	5.48E-09 - 2.33E-08
ankyrin repeat PH and SEC domain containing protein	NP_049038	<i>Paramecium bursaria</i> <i>Chlorella</i> virus 1		2		155-305	92.1-97.4	44-55	4.56E-25 - 2.29E-24
ankyrin repeat protein	YP_001426468	<i>Paramecium bursaria</i> <i>Chlorella</i> virus FR483		1		602	25.9	50	1.14E-13
serine threonine-protein phosphatase/ankyrin repeat	YP_001498097	<i>Paramecium bursaria</i> <i>Chlorella</i> virus AR158			1	576	38.9	45	2.71E-11

Appendix D

Table D1 (continued).

thaumatin pr5-like protein	YP_002154632	<i>Feldmannia species</i> virus			1	68	72.1	67	3.82E-07
membrane protein	YP_002296189	<i>Emiliana huxleyi</i> virus 86	1	1		1337-1451	13.6-14.8	42-44	3.02E-08 - 9.00E-07
membrane protein	YP_002296197	<i>Emiliana huxleyi</i> virus 86	2	1		556-616	88.8-95.7	48	1.93E-64 - 1.81E-62
NDP-hexose - dehydratase	YP_003212865	<i>Ostreococcus tauri</i> virus 1		1	1	60-410	91.0-96.7	73-84	4.65E-165 - 5.93E-21
hypothetical protein	YP_003212936	<i>Ostreococcus tauri</i> virus 1		1	1	259-294	44.2-51.4	47-57	9.24E-18 - 6.18E-14
hypothetical protein	YP_007676259	<i>Micromonas pusilla</i> virus 12T		1		274	58	67	3.72E-44
HNH endonuclease	YP_293937	<i>Emiliana huxleyi</i> virus 86	1			403	91.3	42	8.67E-19
hypothetical protein	YP_294043	<i>Emiliana huxleyi</i> virus 86	2	2	2	233-382	22.1-71.8	43-62	3.72E-144 - 1.27E-07
apolipoprotein	YP_294158	<i>Emiliana huxleyi</i> virus 86			1	218	76.1	54	2.81E-23

Appendix D

Table D2. Unigenes from the transcriptomes of *Symbiodinium* cultures CCMP421, CCMP2430 and Mp with nearest BLAST matches belonging to members of the *Mimiviridae*, *Megaviridae* and *Marseilleviridae*. Numbers in the *Symbiodinium* culture columns represent the number of different unigenes sharing the same BLAST match. Where several sequences shared the same BLAST match, the range of values for the query length, sequence coverage, similarity and e-value are reported. Table continues overleaf.

Gene product	Accession number	BLAST hit	CCMP421 (Clade E)	CCMP2430 (Clade A)	Mp (Clade C)	Query length (AA)	Query coverage (%)	Sequence similarity (%)	e-value
HNH endonuclease	AEX61451	Megavirus Courdo7		1		295	75.3	45	1.74E-11
NUDIX hydrolase	AEX61841	Megavirus Courdo7		1	1	308-314	65.6-66.9	45	4.63-6.37E-07
serine threonine protein kinase receptor	AEX62336	Moumouvirus Monve			1	747	34.7	51	2.10E-25
2OG-FE oxygenase	AEX62373	Moumouvirus Monve			1	126	75.4	50	3.79E-09
helicase	AEX62539	Moumouvirus Monve			1	339	68.1	49	1.00E-23
glycosyl transferase family protein	AEX62595	Moumouvirus Monve		1	1	283-290	65.4-68.0	57-58	1.96E-32 - 6.77E-28
glycosyl transferase	AEX62747	Moumouvirus Monve	1			415	16.1	64	8.03E-07
endonuclease V	AFX92159	Megavirus Courdo11	1	1		166-404	52.0-61.4	58-60	1.80E-38 - 3.21E-12
hypothetical protein	AFX92742	Megavirus Courdo11			1	287	43.9	47	1.22E-08
serine threonine protein kinase receptor	AFX93119	Megavirus Courdo11	1	2		538-640	43.0-51.1	49	7.83E-28 - 2.37E-27
ankyrin repeat protein	AGF84951	Moumouvirus Goulette	1			402	73.9	40	3.40E-09
B cysteine protease	AGF85419	Moumouvirus Goulette		1		82	70	74	5.03E-19
glycosyl transferase	AGF85565	Moumouvirus Goulette	3		2	173-484	36.6-100	44-53	4.98E-27 - 3.50E-08
hypothetical protein	AGF85573	Moumouvirus Goulette	1			294	56.1	53	1.11E-14
hypothetical protein	AGF85712	Moumouvirus Goulette	1			850	32.2	45	2.63E-14
mimivirus encoded protein	ELR14641	<i>Acanthamoeba castellanii</i> str. Neff	2	1	1	137-346	71.1-100	53-62	3.95E-47 - 3.03E-29
ankyrin repeat protein	Q5UPG5	<i>Acanthamoeba polyphaga</i> mimivirus	1		1	192-619	34.9-72.9	47	1.67E-12 - 6.31E-10

Appendix D

Table D2 (continued).

hypothetical protein	YP_003406858	Marseillevirus			1	248-254	59.4-65.3	53-55	8.31E-11 - 1.03E-10
ubiquitin	YP_003406986	Marseillevirus		1		76	59.2	82	2.33E-15
F-box and FNIP repeat-containing protein	YP_003969746	<i>Cafeteria roenbergensis</i> virus BV-PW1	1		4	107-683	46.8-100	56-64	2.50E-103 - 8.15E-22
sulfhydryl oxidase	YP_003969775	<i>Cafeteria roenbergensis</i> virus BV-PW1	1	1		213-235	42.5-46.9	53-56	9.10E-14 - 8.26E-12
hypothetical protein	YP_003969888	<i>Cafeteria roenbergensis</i> virus BV-PW1	1	2		281-397	37.0-50.2	49-52	2.72E-15 - 1.91E-14
DNA repair protein rad8	YP_003970035	<i>Cafeteria roenbergensis</i> virus BV-PW1			1	570	41	44	1.96E-16
hypothetical protein crov406	YP_003970039	<i>Cafeteria roenbergensis</i> virus BV-PW1			1	83	98.8	62	1.34E-18
hypothetical protein	YP_003970042	<i>Cafeteria roenbergensis</i> virus BV-PW1			1	175	35.4	62	5.13E-08
FAD dependent sulfhydryl oxidase Erv1	YP_003970077	<i>Cafeteria roenbergensis</i> virus BV-PW1		1		230	41.7	58	6.48E-12
ubiquitin-conjugating enzyme e2	YP_003970126	<i>Cafeteria roenbergensis</i> virus BV-PW1		1	1	304-341	35.2-39.1	65	3.49E-29 - 3.11E-26
hypothetical protein	YP_003970140	<i>Cafeteria roenbergensis</i> virus BV-PW1			1	84	98.8	73	3.48E-23
proline dehydrogenase	YP_003970160	<i>Cafeteria roenbergensis</i> virus BV-PW1	6	3	14	60-703	40.5-100	48-64	1.81E-154 - 3.05E-09
hypothetical protein	YP_003970163	<i>Cafeteria roenbergensis</i> virus BV-PW1	1	5	41	54-367	31.3-100	54-73	5.79E-52 - 4.10E-7
ankyrin repeat protein	YP_003986584	<i>Acanthamoeba polyphaga</i> mimivirus		1		508	28.9	55	2.80E-14
procollagen-lysine 2-oxoglutarate dioxygenase	YP_003987227	<i>Acanthamoeba polyphaga</i> mimivirus		1		420	52.1	46	1.19E-11
p13-like protein	YP_003987235	<i>Acanthamoeba polyphaga</i> mimivirus		1		477	58.3	44	9.43E-15
dual specificity protein phosphatase	YP_004347041	Lausannevirus	1		1	243-267	36.0-41.6	53	2.02E-13 - 2.76E-11
thiol oxidoreductase	YP_004347288	Lausannevirus		2		155-234	38.0-54.8	58-59	2.29E-13 - 1.14E-10

Appendix D

Table D2 (continued).

p13-like protein	YP_004894309	Megavirus chiliensis	1			404	31.7	52	4.80E-08
FAD-linked sulfhydryl oxidase	YP_004894579	Megavirus chiliensis	1			216	46.8	47	6.35E-12
NUDIX hydrolase	YP_004894702	Megavirus chiliensis			1	306	67.3	45	4.65E-07
JMJC domain protein	YP_004894936	Megavirus chiliensis			1	397	60.2	43	3.39E-11
HNH endonuclease	YP_007354246	<i>Acanthamoeba polyphaga</i> moumouvirus		1		420	64	48	1.01E-16
helicase	YP_007354283	<i>Acanthamoeba polyphaga</i> moumouvirus	1			1334	41.8	43	9.12E-35
protein tyrosine kinase	YP_007354741	<i>Acanthamoeba polyphaga</i> moumouvirus	1		1	553-760	41.6-53.0	47-50	3.94E-24 - 4.88E-22

Appendix D

Table D3. Unigenes from the transcriptomes of *Symbiodinium* cultures CCMP421, CCMP2430 and Mp with nearest BLAST matches belonging to assorted viruses (i.e. those not included in the viral families in Tables D1 and D2). Apart from one sequence from an RNA virus (AAD44044), all BLAST matches belong to dsDNA viruses. Numbers in the *Symbiodinium* culture columns represent the number of different unigenes sharing the same BLAST match. Where several sequences shared the same BLAST match, a range of values for the query length, sequence coverage, similarity and e-value are reported.

Gene product	Accession number	BLAST hit	CCMP421 (Clade E)	CCMP2430 (Clade A)	Mp (Clade C)	Query length (AA)	Query coverage (%)	Sequence similarity (%)	e-value
protein tyrosine phosphatase 1	AAB25579	<i>Autographa californica</i> nuclear polyhedrosis virus			1	257	64.2	58	6.18E-25
polyprotein ubiquitin/peptidase	AAD44044	Bovine viral diarrhea virus 2	1			168	47.6	57	8.28E-07
kelch-like protein	ADZ29770	Cowpox virus	2		1	493-520	27.7-36.5	49-53	2.0E-11 - 1.24E-9
helicase family	CBH29206	African swine fever virus E75			1	1088	10.3	52	4.22E-07
protein tyrosine phosphatase 1	NP_047551	<i>Bombyx mori</i> nucleopolyhedrovirus		1		238-269	63.9-73.1	59	3.31 - 4.83E-30
protein	NP_051895	Rabbit fibroma virus	1			203	50.2	50	9.20E-07
hypothetical protein	NP_078753	Lymphocystis disease virus 1	1			572	66.6	47	2.99E-35
FAD-linked sulfhydryl oxidase	NP_149810	Invertebrate iridescent virus 6			1	146	68.5	54	1.38E-12
transcription termination factor NPH-I	YP_002302437	Deerpox virus W-1170-84	1			957	29	38	5.93E-08
kelch-like protein	YP_002302501	Deerpox virus W-1170-84		1	1	196-224	47.5-52.6	58-59	3.41E-08 - 3.04E-07
kinase protein	YP_004732882	<i>Wiseana</i> iridescent virus	1			608	34.7	50	6.33E-12
protein tyrosine phosphatase 1	YP_007250413	<i>Thysanoplusia orichalcea</i> nucleopolyhedrovirus			1	100	62	69	1.91E-12
ECRF4	YP_068008	Macacine herpesvirus 4			1	199	84.9	48	2.24E-09
transcription termination factor NPH-I	YP_227472	Deerpox virus W-848-83	1			771	11	48	8.07E-07
ubiquitin	YP_874214	<i>Ectropis obliqua</i> nucleopolyhedrovirus		1		142-276	20.3-39.4	71-75	4.47E-14 - 7.84E-10

Appendix D

Table D4. Putative viral genes found in more than one *Symbiodinium* culture. Genes were considered the same if pairwise sequence identity of the protein sequences was > 90% and the sequences shared the same nearest BLAST match in the NCBI non-redundant protein database. The numbers in the table are the identifiers of representative contigs from the assembled transcriptomes. Table continues overleaf.

BLAST match	BLAST accession	CCMP421 (Clade E)	CCMP2430 (Clade A)	Mp (Clade C)	CassKB8 (Clade A)	Mf1.05b (Clade B)
<i>Emiliana huxleyi</i> virus 202	AET42504	66127	1117-715		c28706	
<i>Emiliana huxleyi</i> virus 86	YP_002296197	43418	1116-25469		c2308	
<i>Emiliana huxleyi</i> virus 87	YP_002296197			1122-15575		c23590
<i>Acanthamoeba polyphaga</i> moudouvirus	YP_007354283	1758			c12594	
Megavirus courdo11	AFX93119	31079	1116-9736		c7665	
Cowpox virus	ADZ29770	33985		1125-2463		
Moudouvirus Goulette	AGF85565	72861			c26340	
<i>Ostreococcus tauri</i> virus RT-2011	AFC34921	23427			c2214	
<i>Emiliana huxleyi</i> virus 202	AET42509	72700			c12306	
<i>Emiliana huxleyi</i> virus 86	YP_002296189	16958			c6825	
Moudouvirus Goulette	AGF85712	25848			c27175	
<i>Acanthamoeba castellanii</i> mimivirus encoded	ELR14641	55040	1115-15146		c40745	
<i>Ostreococcus tauri</i> virus RT-2011	AFC34947	50597	1115-4676		c15694	c40461
<i>Acanthamoeba polyphaga</i> mimivirus	Q5UPG5	6549			c37838	
<i>Emiliana huxleyi</i> virus 208	AEP15886		1115-35471		c31047	
<i>Paramecium bursaria Chlorella</i> virus CvsA1	AGE52380		1115-8020		c2099	
Moudouvirus Goulette	AGF85419		1117-18411		c41513	
<i>Paramecium bursaria Chlorella</i> virus 1	NP_049038		1117-234		c15989	
Moudouvirus Monve	AEX62595		1115-6713		c22811	
<i>Bombyx mori</i> nucleopolyhedrovirus	NP_047551		1116-38218		c19044	
Megavirus Courdo7	AEX61841		1116-14462		c3291	
Deerpox virus W-1170-84	YP_002302501		1116-20682		c9327	
<i>Micromonas pusilla</i> virus 12T	YP_007676259		1115-28921		c152	c8654
<i>Cafeteria roenbergensis</i> virus BV-PW1	YP_003969775		1116-8880		c17304	

Appendix D

Table D4 (continued).

<i>Paramecium bursaria</i> <i>Chlorella</i> virus NYs1	AGE58893			1124-28155	c2296	
<i>Feldmannia</i> species virus	YP_002154632			1124-33792	c15256	

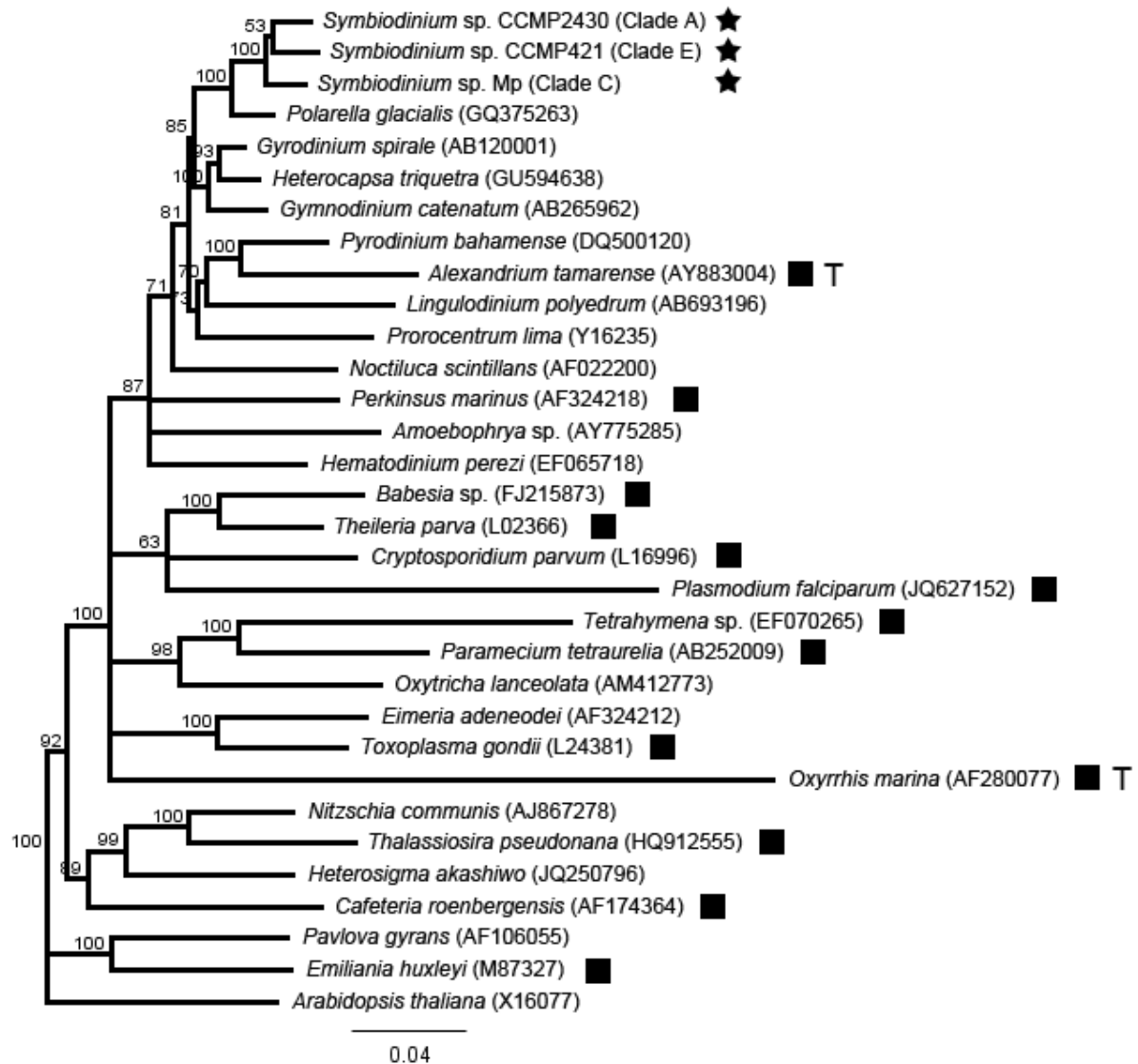


Figure D4. Neighbour-joining tree of chromalveolate 18S rRNA sequences, including the three *Symbiodinium* cultures used in this study (marked with stars). The displayed phylogeny is a majority-rule consensus tree based on 1000 bootstrap replicates of an initial neighbour-joining tree constructed using a Jukes-Cantor model of evolution. Black squares indicate species whose genomes were searched for virus-like sequences, and 'T' indicates that a transcriptome was used in the search because no genome was available. The scale bar represents the number of nucleotide substitutions per site, and branch numbers indicate the level of bootstrap support.

Appendix E: Additional data for Chapter 4.

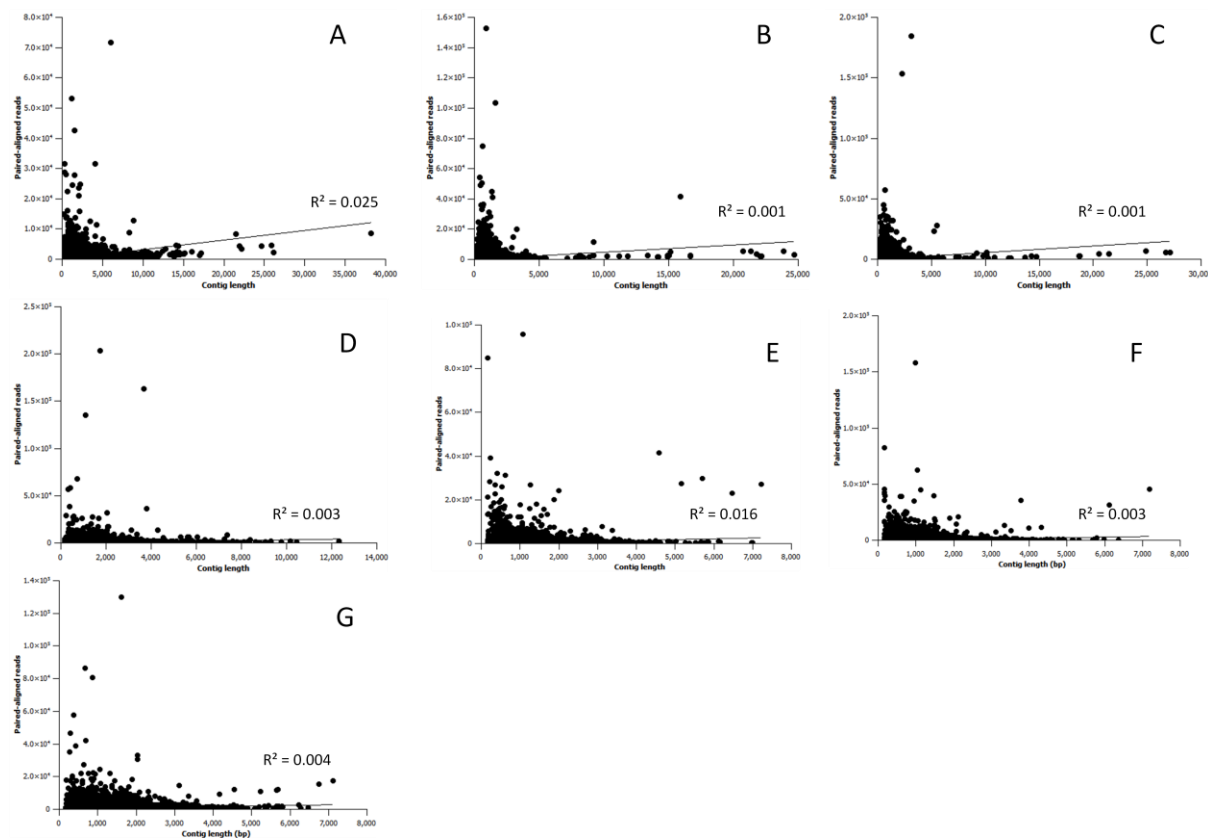


Figure E1. Contig length vs. number of reads mapped to the contig. R^2 values indicate no correlation between contig length and number of reads assigned to each contig. A: CCMP2430 T0, B: CCMP2430 T24, C: CCMP2430 T54, D: Mp T0, E: Mp T24, F: Mp T66, G: Mp T66 control.

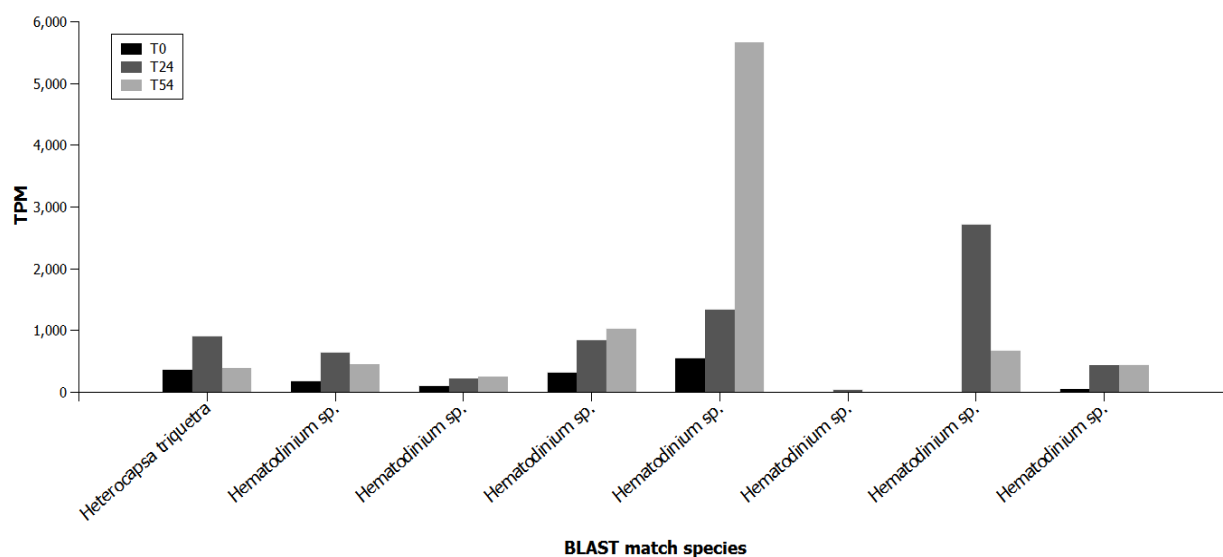


Figure E2. Expression levels (transcripts per million) of dinoflagellate viral nucleoprotein (DVNP) unigenes detected in *Symbiodinium* culture CCMP2430. The x-axis shows the species of the nearest BLAST match for each gene.

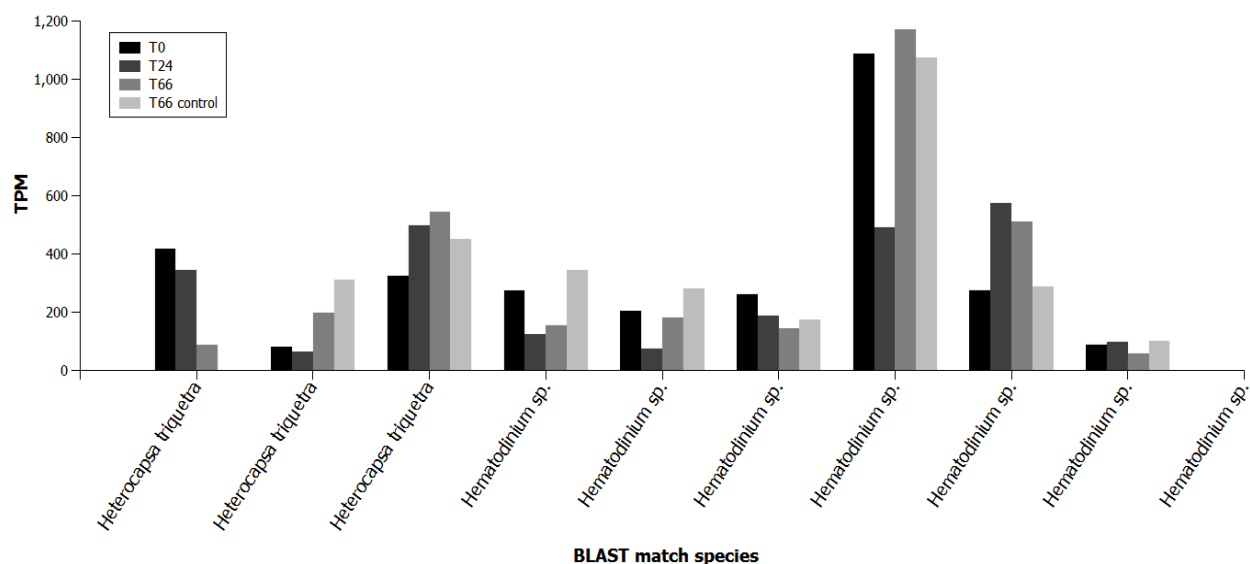


Figure E3. Expression levels (transcripts per million) of dinoflagellate viral nucleoprotein (DVNP) unigenes detected in *Symbiodinium* culture Mp. The x-axis shows the species of the nearest BLAST match for each gene.

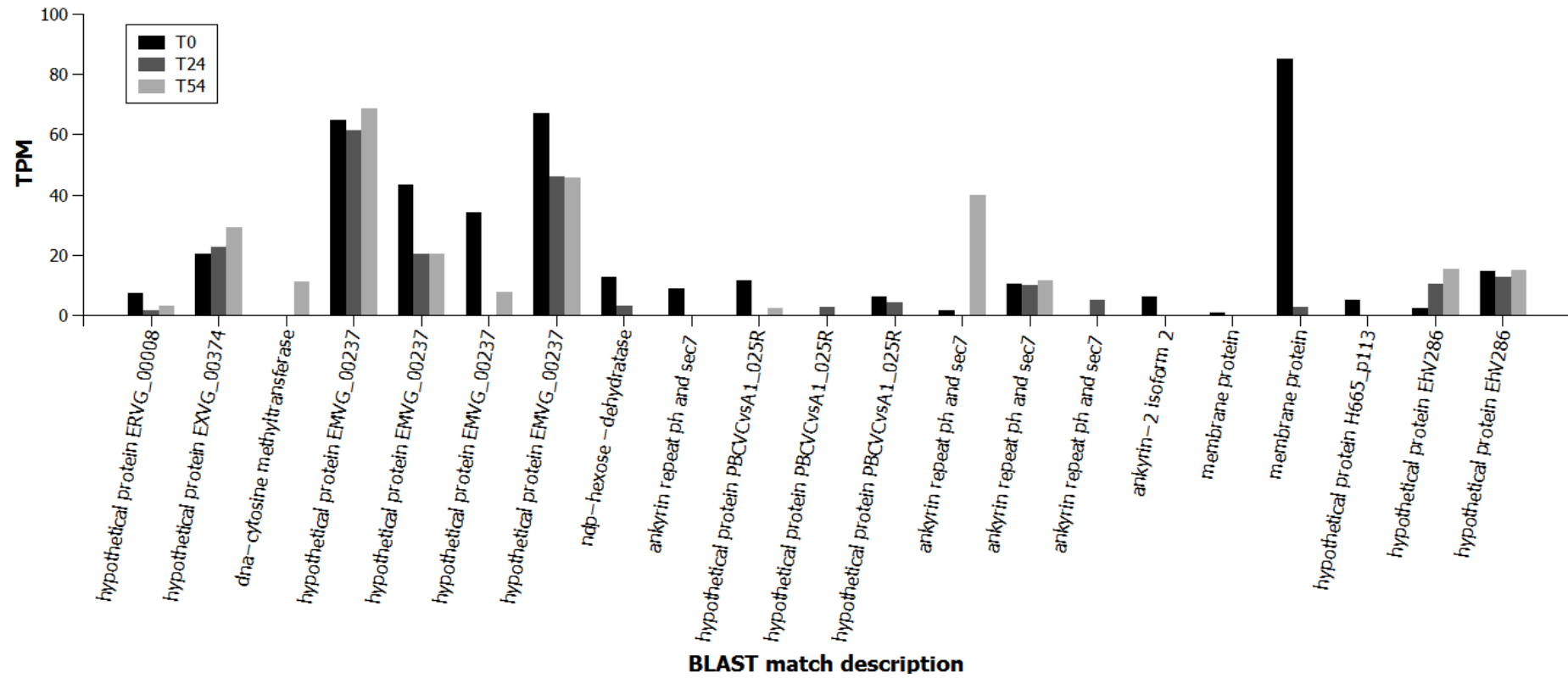


Figure E4. Expression levels (transcripts per million) of *Phycodnaviridae*-like unigenes detected in *Symbiodinium* culture CCMP2430.

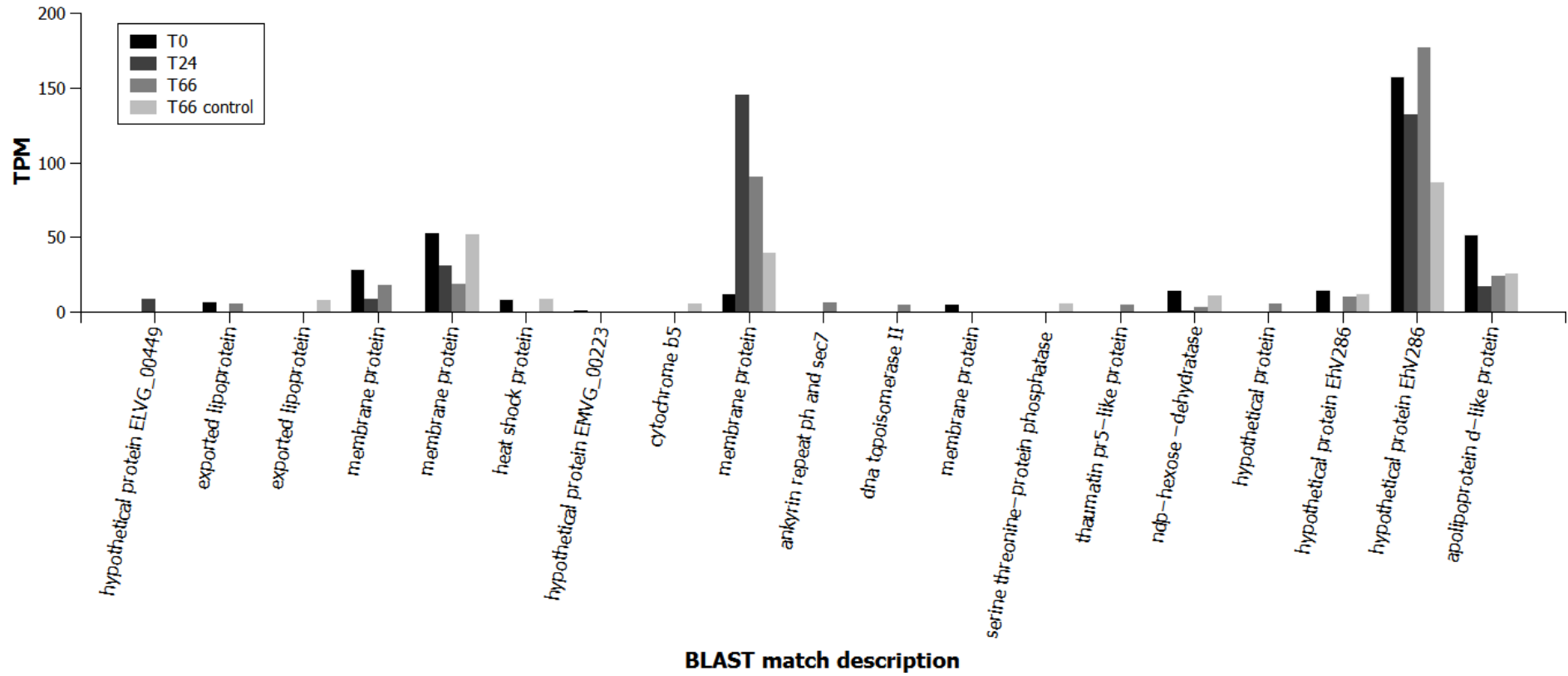


Figure E5. Expression levels (transcripts per million) of *Phycodnaviridae*-like unigenes detected in *Symbiodinium* culture Mp.

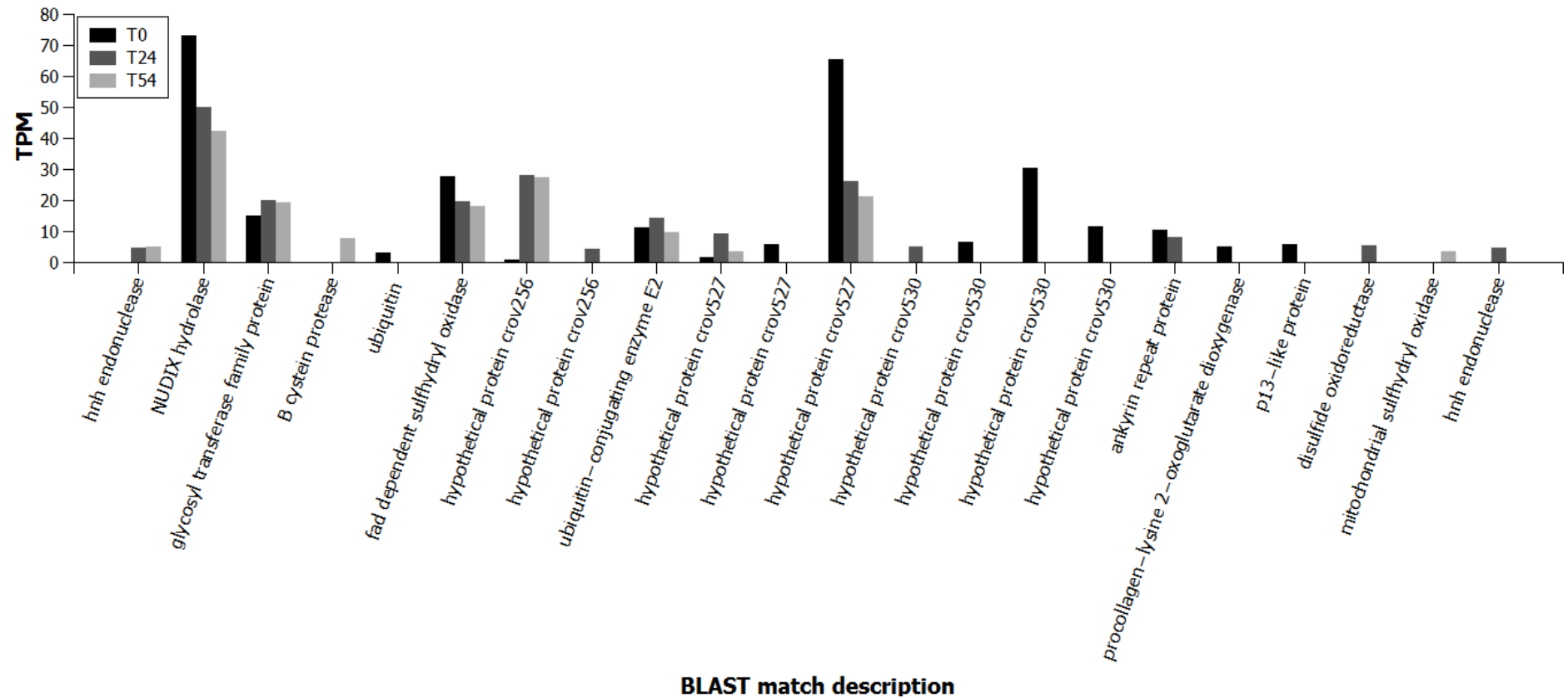


Figure E6. Expression levels (transcripts per million) of *Mimiviridae*-like unigenes detected in *Symbiodinium* culture CCMP2430.

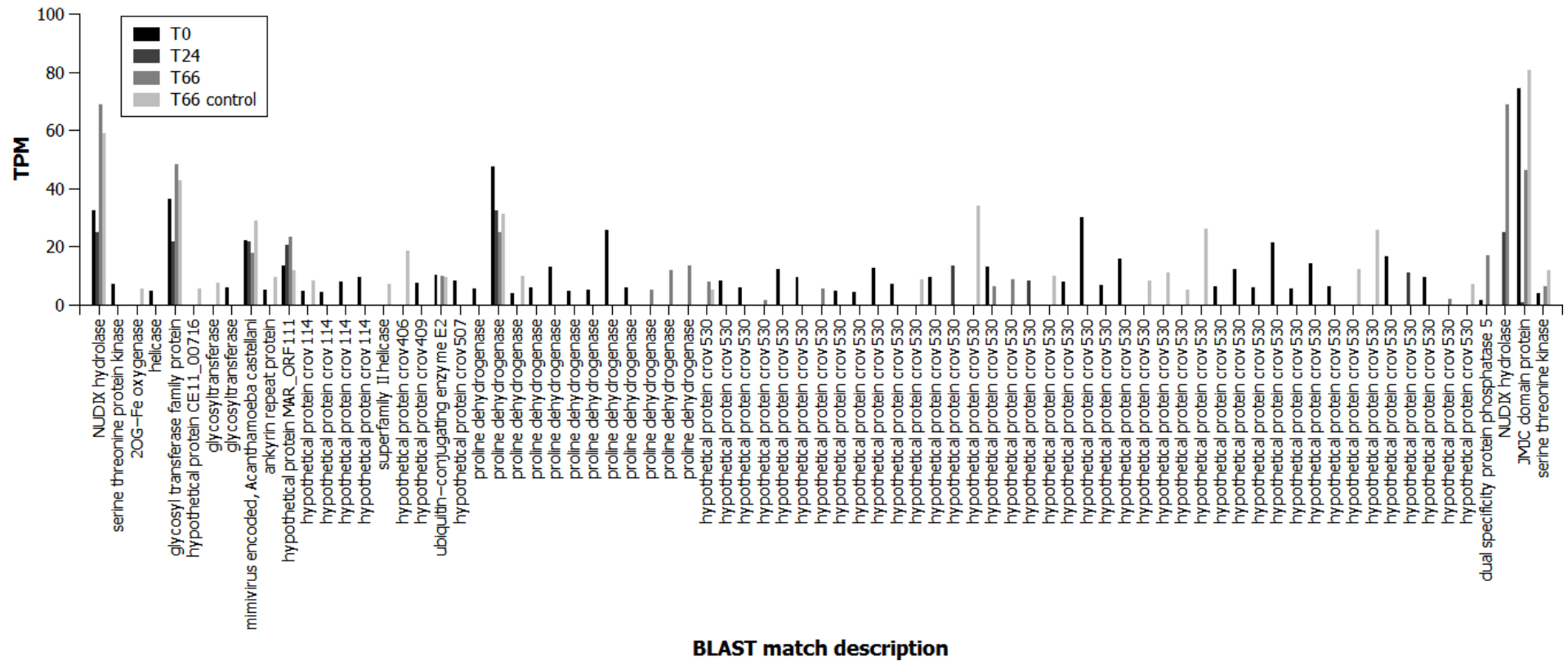


Figure E7. Expression levels (transcripts per million) of *Mimiviridae*-like unigenes detected in *Symbiodinium* culture Mp.

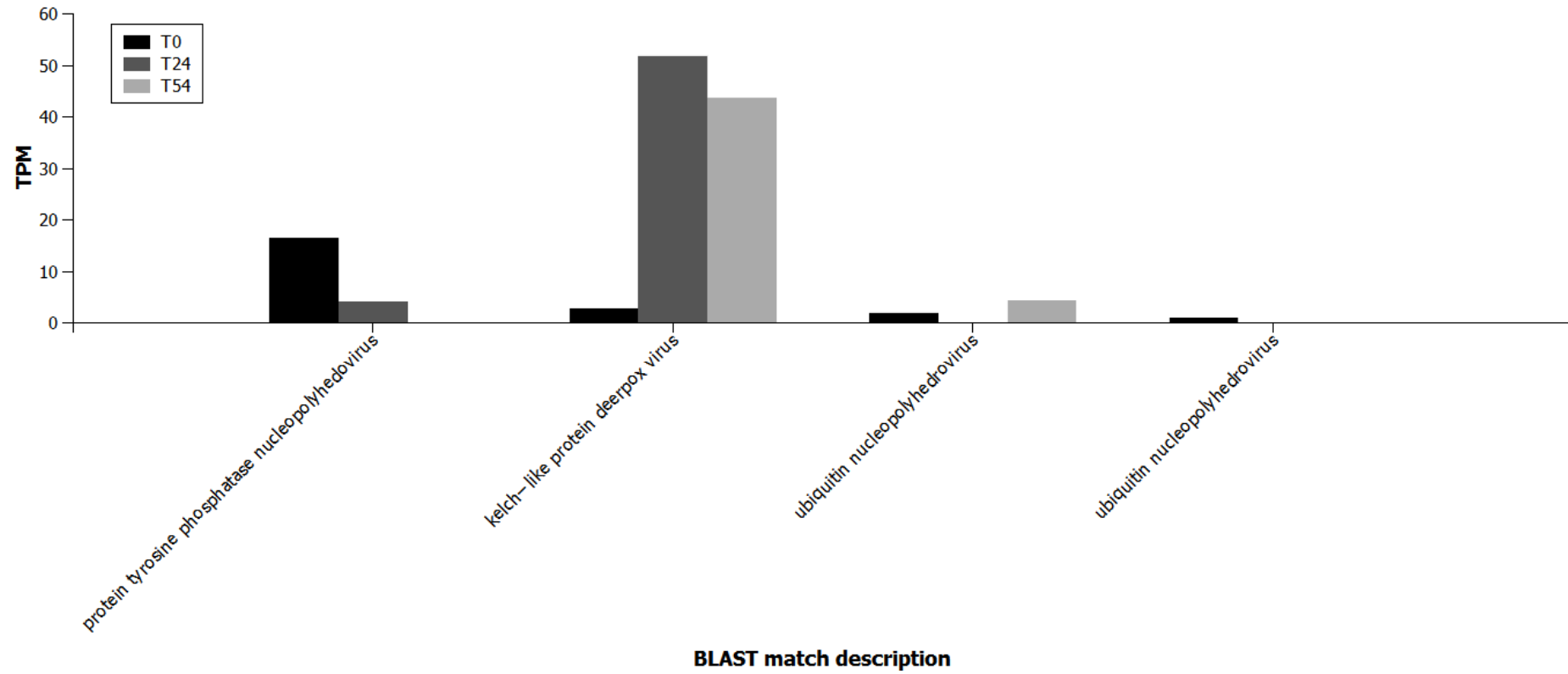


Figure E8. Expression levels (transcripts per million) of other dsDNA virus-like unigenes detected in *Symbiodinium* culture CCMP2430.

Appendix E

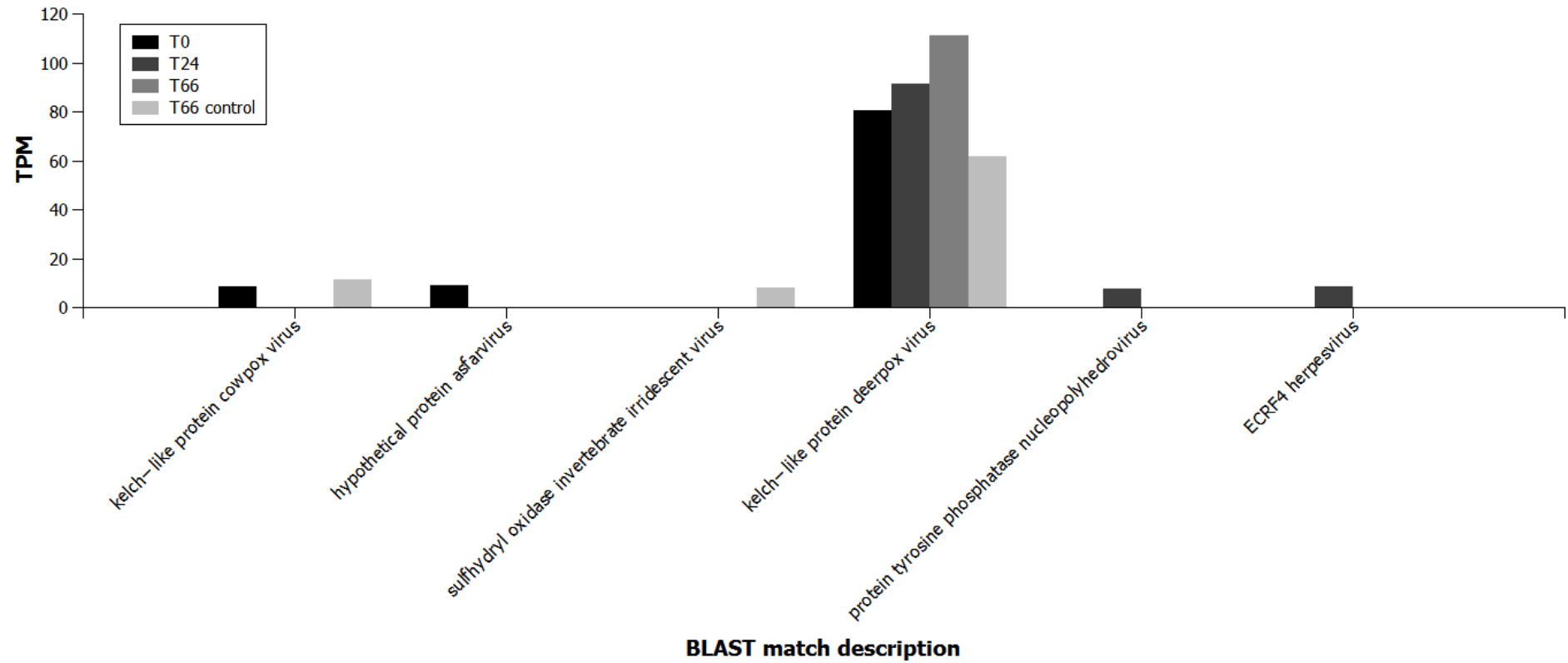


Figure E9. Expression levels (transcripts per million) of other dsDNA virus-like unigenes detected in *Symbiodinium* culture Mp.

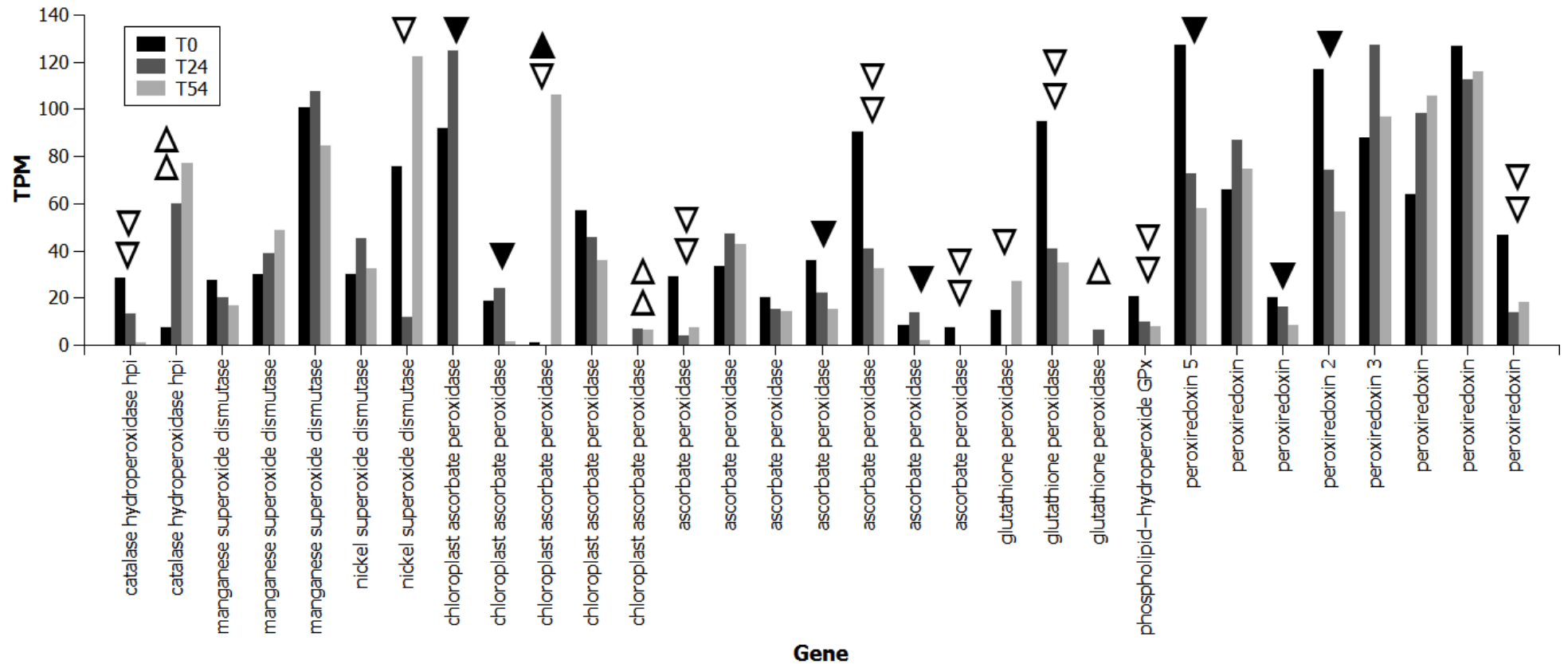


Figure E10. Expression levels (transcripts per million) of unigenes encoding antioxidant enzymes in *Symbiodinium* culture CCMP2430. Single triangles indicate a significant (> 2-fold) change in expression level at T24 (empty triangles) or T54 (filled triangles), relative to T0. Double triangles indicate a significant change in expression level at both T24 and T54, relative to T0. Upward-pointing triangles indicate an increase in expression, downward-pointing triangles indicate a decrease in expression.

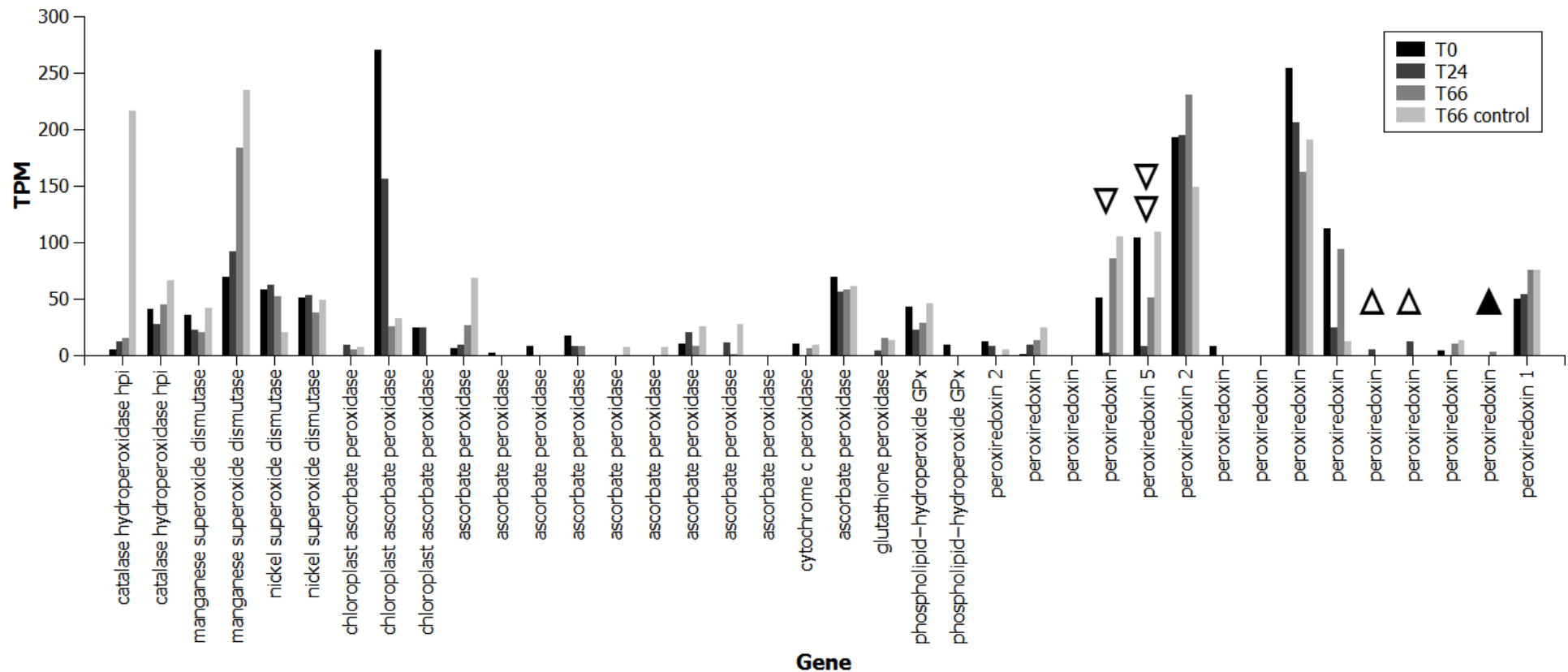


Figure E11. Expression levels (transcripts per million) of unigenes encoding antioxidant enzymes in *Symbiodinium* culture Mp. Single triangles indicate a significant (> 2-fold) change in expression level at T24 (empty triangles) or T66 (filled triangles), relative to T0 and T66 control samples. Double triangles indicate a significant change in expression level at both T24 and T66, relative to T0 and T66 control samples. Upward-pointing triangles indicate an increase in expression, downward-pointing triangles indicate a decrease in expression.

Appendix F: PCR primers used in Chapter 5

Table F1. PCR primers used in Chapter 5.

Primer pair	Sequence	Target group	Target gene
RR2 F/R	GAYGARGGIYTICAY YTCRAARAARTTIGTYTT	Viruses, prokaryotes, eukaryotes	Ribonucleotide reductase small sub-unit
CircoRep F1/R1 (this study)	ACICCICAYYTICARGGI CCAICCRTARAARTCRTC	<i>Circoviridae</i>	Replication- associated (<i>rep</i>) gene
<i>Nanoviridae</i> F1/R1 (this study)	MGIATHATHTGGGTITAYGGICC RTAYTTICCISWYTG DATDATICC	<i>Nanoviridae</i>	Replication- associated (<i>rep</i>) gene
Nanovirus F1/R1 (this study)	CARGTIATHTGYTG GTGYTTYAC SWRAACATICCISWICKIGG	Nanovirus	Replication- associated (<i>rep</i>) gene
Herpes F/R (Vega Thurber <i>et al.</i> , 2008)	AAAATAAGATTGGGAGATCTAGGC TGCCATTTTAGGTAAATCAGAAAC	Herpes-like viruses	Thymidylate synthase gene
AVS1/AVS2 (Chen and Suttle, 1995)	GARGGIGCIACIGTIYTIGAYGC GCIGCRTAICKYTTYTTISWRTA	Green algae viruses	DNA polymerase

Appendix G: Viruses associated with the disease *Porites* tissue loss

Introduction

Porites tissue loss (PorTL) is a disease that affects *Porites compressa*, an abundant coral in Hawaii and one of the dominant species on reefs in Kaneohe Bay (Williams *et al.*, 2010). The disease manifests as irregular patches of tissue loss which are found on central and apical parts of the coral colony (Williams *et al.*, 2010). Disease prevalence varies; some areas show no signs of disease, while infection of up to 36% of colonies is seen in other areas (Williams *et al.*, 2010; Aeby *et al.*, 2011). While no etiological agent has yet been found for PorTL, several biotic and abiotic factors, namely decreased butterflyfish abundance, increased temperature and decreased turbidity, have been shown to be associated with increased disease prevalence (Williams *et al.*, 2010). Studies of PorTL have so far been restricted to macroscopic observation and field surveys, however a similar disease, *Porites* bleaching with tissue loss (PBTL), which also affects *P. compressa*, has recently been examined histologically (Sudek *et al.*, 2012b). *Porites* bleaching with tissue loss is macroscopically similar to PorTL, but the initial stage of the disease involves bleaching of the coenenchyme while polyps remain intact, followed by tissue necrosis and algal overgrowth (Sudek *et al.*, 2012a; Sudek *et al.*, 2012b). Sudek *et al.* (2012b) were unable to find the etiological agent of PBTL, suggesting either an abiotic cause or an infectious agent that was undetectable by light microscopy (e.g. a virus). Although PorTL and PBTL are distinct diseases, their macroscopic similarities, and the apparent lack of a microbial etiological agent in PBTL, raise the possibility that viruses play a role in PorTL.

As a first step towards identification of the etiological agent of PorTL, the aim of the present study was to quantify and morphologically characterise virus-like particles (VLPs) associated with *P. compressa* colonies suffering from the disease.

Materials and methods

Tissue fragments of *Porites compressa* were collected with hammer and chisel from colonies at two sites (designated A and I) at Kaneohe Bay, Hawaii in January 2010. The two sampling

sites differed in depth (Site A: 4 m, site B: 2 m), but otherwise they appeared environmentally similar. Environmental parameters were not measured at the time of sampling, but measurements collected in June 2009 showed that temperature, turbidity, chlorophyll-*a* concentration and salinity did not differ significantly between the sites. Samples were taken directly from disease lesions ($n = 2$ from each site) and from visibly healthy tissues on unaffected colonies ($n = 2$ from each site). Tissue samples were fixed in 2.5% glutaraldehyde and stored at 4 °C until processing.

Glutaraldehyde-fixed tissue samples were decalcified in 0.5 M EDTA and post-fixed in 2% osmium tetroxide. Samples were then dehydrated through an ethanol series (50 – 100%) and propylene oxide and embedded in Procure 812 resin (Proscitech, Thuringowa, Australia). Ultra-thin sections were cut on an Ultracut T ultramicrotome (Leica Microsystems, Vienna, Austria) and stained using 2% aqueous uranyl acetate and Reynold's lead citrate. Sections were viewed on a Philips CM-100 transmission electron microscope operated at 80 kV. Three grids from each tissue sample were analysed. In each case 30 fields of view at $24,500 \times$ magnification were examined for the presence of VLPs in *Symbiodinium* cells and gastrodermal and epidermal tissues. Observed VLPs were sorted into two morphological groups (icosahedral and filamentous) and five size classes (0-50 nm, 51-100 nm, 101-150 nm, 151-200 nm and > 200 nm). Statistical analysis was carried out using PASW Statistics 18 (SPSS Inc., Chicago, IL, USA) to determine any difference in virus abundance between samples.

Results and discussion

As expected, microscopic examination revealed that coral tissue was degraded in samples collected from disease lesions. Both the gastrodermis and epidermis were often lacking normal tissue structure, and many cells, including *Symbiodinium*, were apparently lysed or undergoing cell death (Fig. G1). Apoptotic cells were also seen in healthy tissue samples, but cells and tissues generally appeared more intact (Fig. G1). Due to the extensive degradation of the diseased tissues, it was not possible to characterise the disease progression or determine whether the coral or *Symbiodinium* cells are the primary target of the disease.

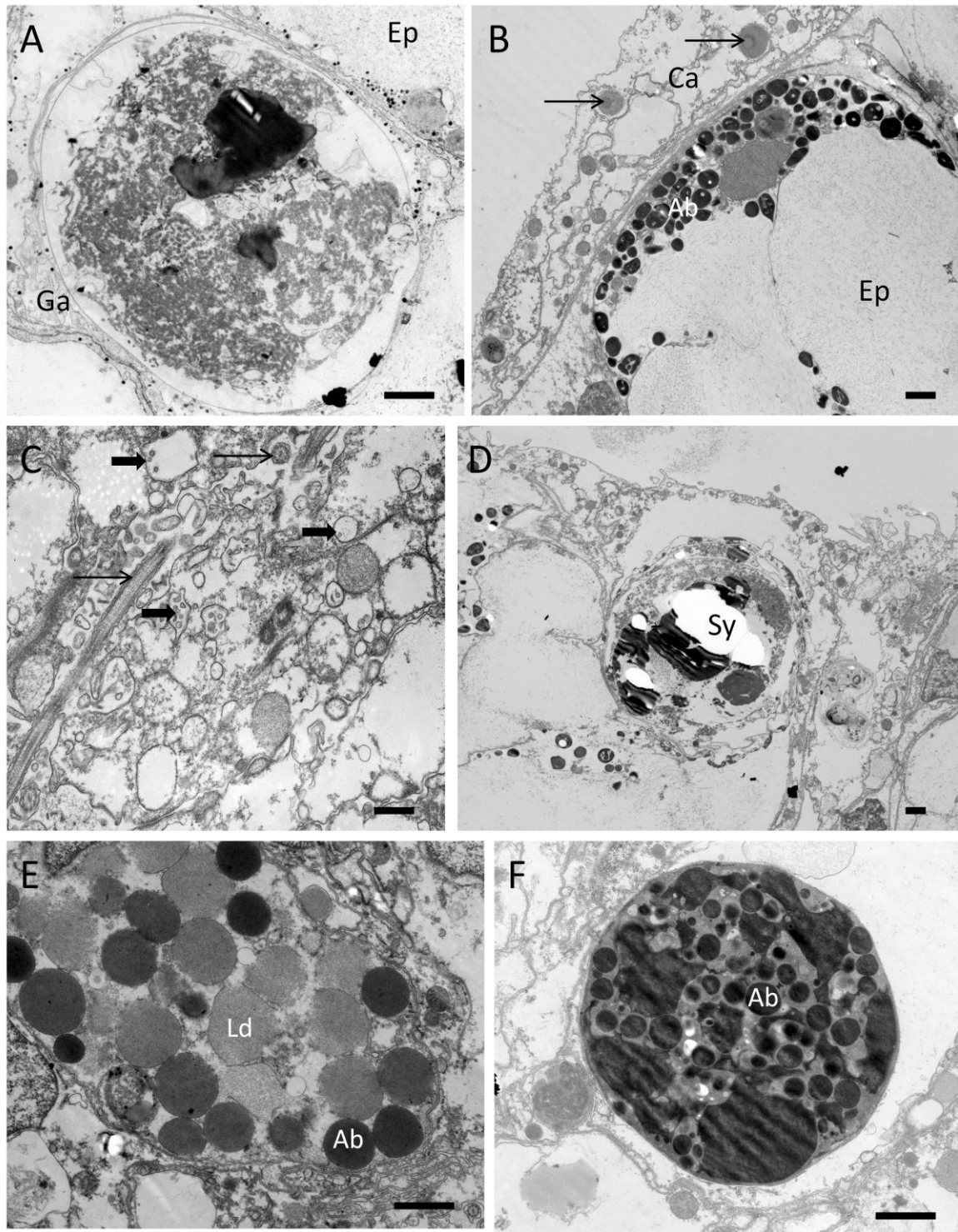


Figure G1. Transmission electron micrographs of coral and *Symbiodinium* cells from healthy and *Porites* tissue loss-affected *Porites compressa* colonies. (A) Necrotic cell in the gastrodermis of diseased colony; (B) degraded tissue and apoptotic bodies in the epidermis of a diseased colony; endolithic microbes (arrows) can also be seen in the calicodermis; (C) degraded tissue in the epidermis of a diseased colony; thin arrows indicate ciliates in the tissue and block arrows indicate vesicles containing cellular debris; (D) apoptotic *Symbiodinium* cell in the gastrodermis of a diseased colony; (E) apoptotic cell in the epidermis of a healthy colony; (F) apoptotic *Symbiodinium* cell in the gastrodermis of a healthy colony. Scale bars represent 1 μm . Ab: apoptotic body, Ca: calicodermis, Ep: epidermis, Ga: gastrodermis, Ld: lipid droplet, Sy: *Symbiodinium* cell.

Bacterial aggregates and ciliates were occasionally seen in gastrodermal and epidermal tissues (Fig. G1), and while these were not quantified, abundance appeared to be similar in healthy and diseased samples. Endolithic bacteria were commonly seen in the coral calicodermis (Figs. G1 and G2), and these also appeared to be equally abundant in healthy and diseased colonies. Microbial organisms were never seen in *Symbiodinium* cells. The most commonly observed biological entities within the tissue samples were virus-like particles (VLPs). In the coral animal cells, VLPs were exclusively icosahedral in shape and non-enveloped, and ranged from < 50 nm to > 200 nm in diameter, with the majority in both healthy and diseased samples belonging to the < 50 nm group (Fig. G4). In *Symbiodinium* cells, the most commonly observed VLPs were filamentous and 50 – 100 nm in length, though icosahedral VLPs of various sizes were also seen (Fig. G4). It is difficult to say, based on morphology alone, which families these putative viruses belonged to, but the presence of filamentous VLPs in *Symbiodinium* cells is an interesting finding, as these VLPs resemble those seen previously in *Symbiodinium* by Lohr *et al.* (2007), which were hypothesised to belong to the *Closteroviridae*, plant-infecting RNA viruses.

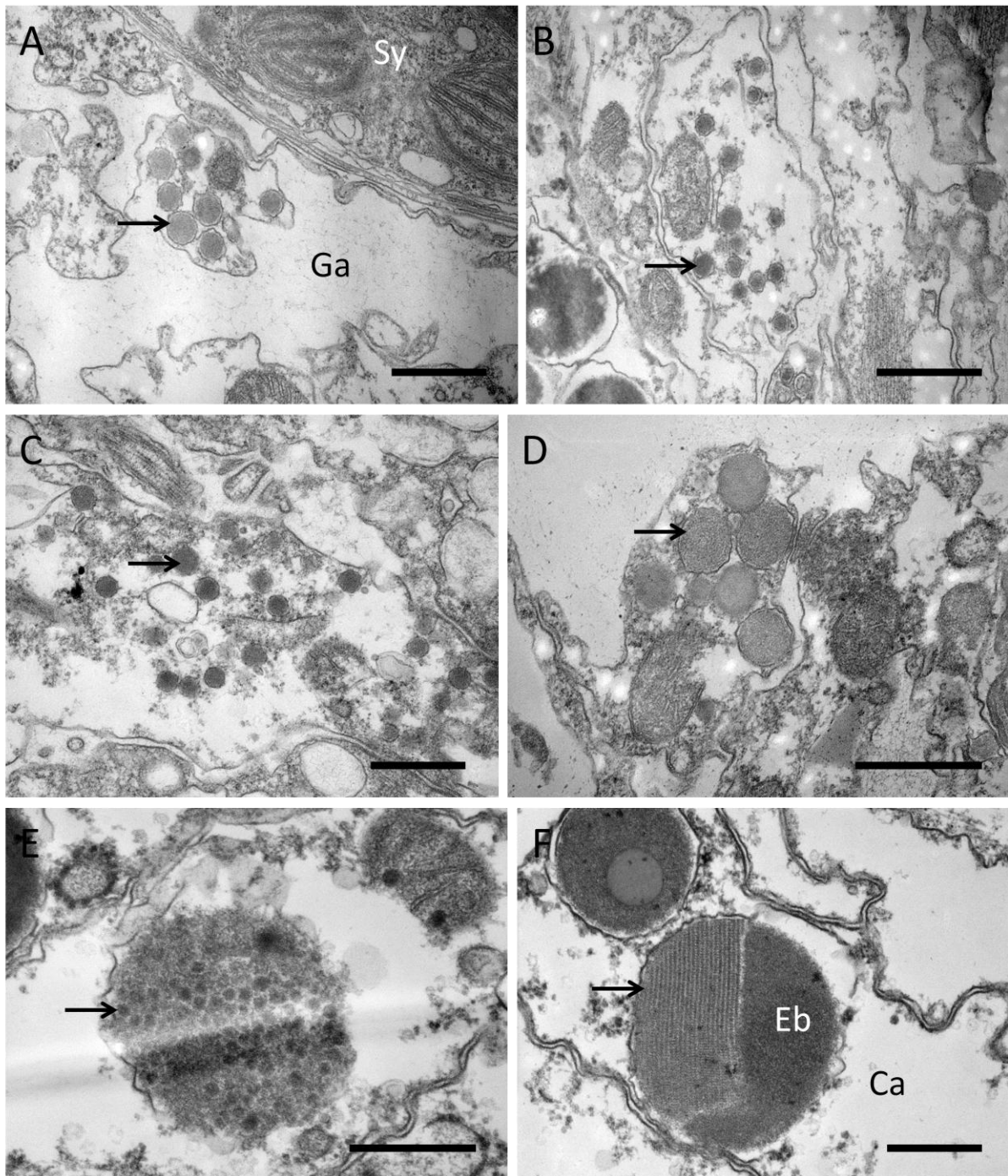


Figure G2. Transmission electron micrographs of virus-like particles (VLPs) in tissues of *Porites compressa* suffering from *Porites* tissue loss (PorTL). (A) ~150 nm diameter icosahedral VLPs in the gastrodermis; (B) ~100 nm diameter VLPs in the gastrodermis; (C) ~100 nm diameter VLPs in the epidermis; (D) ~200 nm diameter VLPs in the epidermis; (E) an inclusion of VLPs, each ~50 nm in diameter; (F) a crystalline array of VLPs, each ~20 nm in diameter. Arrows indicate VLPs. Scale bars represent 500 nm. Eb: endolithic bacterium, Ga: gastrodermis, Sy: *Symbiodinium* cell.

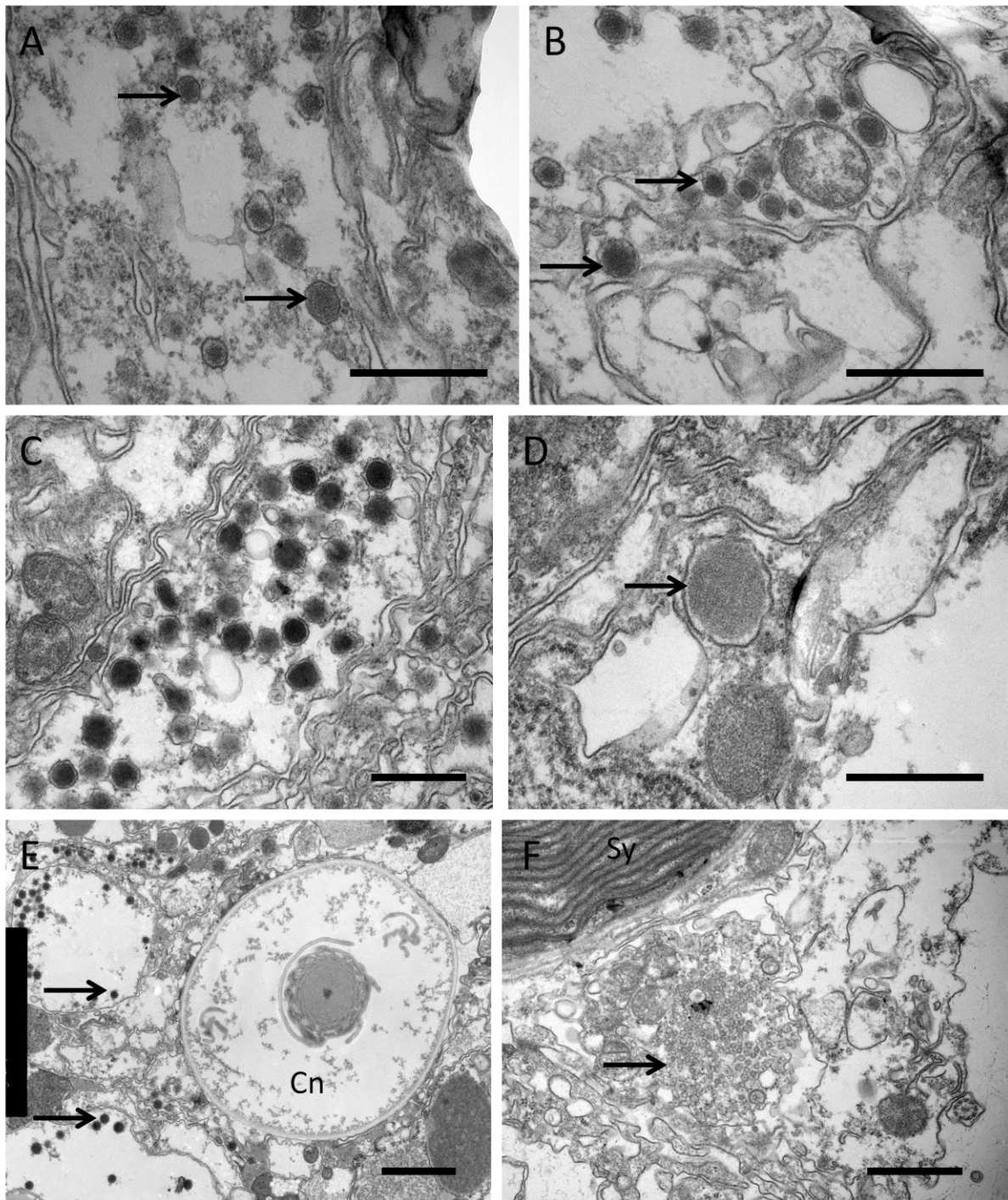


Figure G3. Transmission electron micrographs of virus-like particles (VLPs) in tissues of healthy *Porites compressa* colonies. (A) ~100 nm and ~150 nm diameter icosahedral VLPs (arrows) in the gastrodermis; (B) ~100 nm and ~150 nm diameter icosahedral VLPs (arrows) in the epidermis; (C) an inclusion of ~150 nm diameter icosahedral VLPs in the epidermis; (D) ~250 nm diameter icosahedral VLP in the epidermis; (E) numerous VLPs of ~100 nm diameter in the epidermis; (F) numerous ~50 nm diameter icosahedral VLPs in the gastrodermis. Scale bars represent 500 nm (A – D) and 1 μ m (E – F). Cn: cnidocyte, Sy: *Symbiodinium* cell.

Multivariate analysis of variance (MANOVA) was carried out to determine whether abundances of the various VLP morphotypes differed between diseased and healthy samples, or between sampling sites. The abundance of large (> 200 nm diameter) icosahedral VLPs in the coral gastrodermis differed significantly between sampling sites ($p = 0.04$), however this may be a sampling artefact, as the mean number of VLPs in this category was < 1 per replicate at site A, and 0 at site I. More interestingly, there was a significant difference between healthy and diseased samples ($p = 0.033$) in the abundance of 50 – 100 nm diameter icosahedral VLPs in the gastrodermis. As can be seen in Fig. G4, these VLPs were much more abundant in diseased samples than in healthy samples. Furthermore, this increased abundance does not appear to result from a decrease in VLP numbers within the epidermis, as the abundance of this group was nearly identical in the epidermis of diseased and healthy samples (Fig. G4).

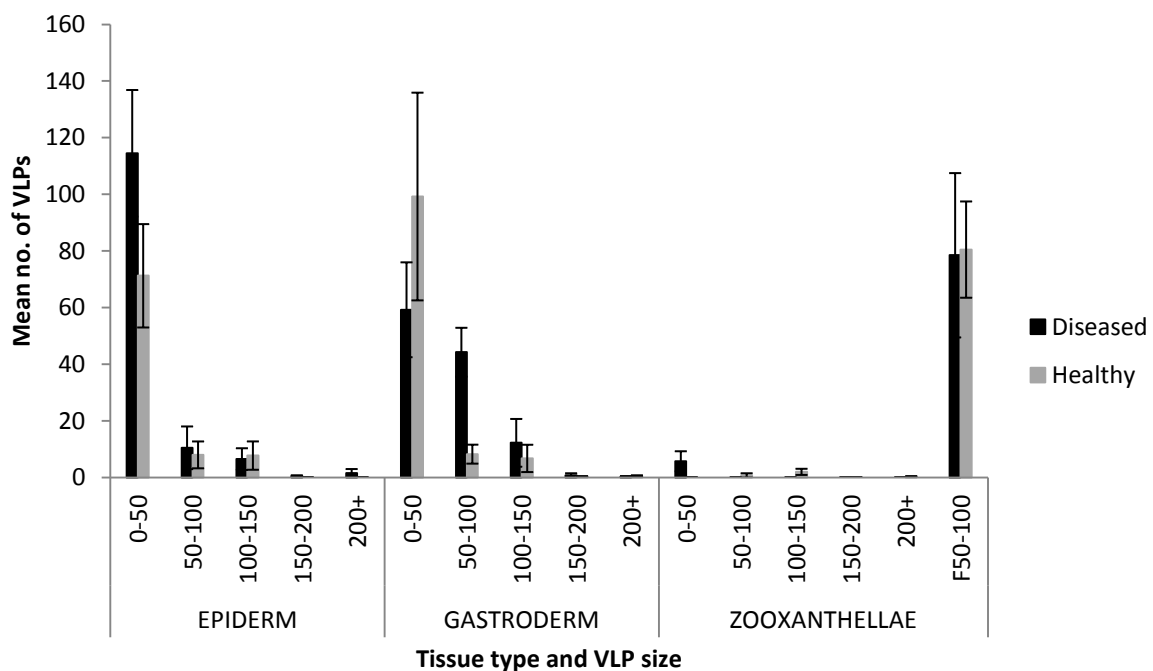


Figure G4. Abundances of VLP size classes in host tissues from diseased and healthy *Porites compressa* colonies. Note: F50-100 refers to filamentous virus-like particles. Error bars are \pm standard error ($n = 4$).

The increased abundance of one putative virus group in diseased colonies is an interesting finding, but does not provide sufficient evidence to suggest a virus as the etiological agent of PorTL for two reasons. First, without molecular characterization, it is not possible to determine the identity of this putative virus group. The resolution obtainable using microscopy is limited, and icosahedral viruses of this size could belong to one of many viral groups. Second, it is often difficult to discern between opportunistic infections and true etiological agents. To do so would require isolation of the putative virus and infection of healthy hosts, or at the least a detailed microscopic/molecular analysis tracking the progression of the disease. Nevertheless, this study has provided preliminary evidence of viral infection in *P. compressa*. Further study of PorTL-associated viruses, along with 16S rRNA analysis and fluorescence *in situ* hybridization to identify bacteria associated with PorTL, should yield interesting insights into the causes of this disease.

Appendix H: Viruses associated with *Porites* growth anomalies

Introduction

The existence of growth anomalies in corals was first noted by Squires (1965), who found evidence of neoplasia and skeletal deformities in the deep-sea coral *Madrepora kauaiensis*. Since this initial study, growth anomalies, or tumours, have been found in at least 20 coral species (Coles and Seapy, 1998; Domart-Coulon *et al.*, 2006; Williams *et al.*, 2010). The genus *Porites* is commonly affected, and the growth anomalies of this group have been relatively well studied (Raymundo *et al.*, 2005; Domart-Coulon *et al.*, 2006; Kaczmarzsky and Richardson, 2007). *Porites* growth anomaly (PorGA) manifests as tumorous, focal to multifocal growths with reduced skeletal density (Williams *et al.*, 2010). These growth anomalies arise as a result of hyperplasia (Domart-Coulon *et al.*, 2006), rather than the neoplasia observed by Squires (1965). The causative agent of PorGA remains to be found, but Kaczmarzsky and Richardson (2007) have shown that an infectious agent may be responsible, rather than a direct environmental cause. These authors demonstrated, through aquarium-based experiments, that healthy colonies sharing the same tank as diseased colonies developed PorGA without the addition of any external stressors. Williams *et al.* (2010) found that the strongest environmental predictors of increased PorGA prevalence at Palmyra atoll were increased turbidity and depth. These findings suggest that solar radiation and/or thermal stress play a role in PorGA development. Combined with the evidence of an infectious etiological agent (Kaczmarzsky and Richardson, 2007), these results raise the possibility of a viral causative agent. The induction of latent viral infections *via* UV irradiation, for example, is well known (e.g. herpes simplex virus in humans; Perna *et al.*, 1987). The induction of latent coral or *Symbiodinium* viruses by increased UV radiation or temperature (both potentially linked to decreased depth and turbidity) has also been demonstrated (Wilson *et al.*, 2001; Wilson *et al.*, 2005a; Lohr *et al.*, 2007).

Given the evidence of an infectious, and possibly viral, causative agent of PorGA, the current study sought to characterise and enumerate virus-like particles associated with corals suffering from the disease, and compare these with healthy coral colonies.

Materials and methods

Tissue fragments of *Porites compressa* were collected with hammer and chisel from colonies at Kaneohe Bay, Hawaii in January 2010. Samples were collected from tissue within the PorGA lesion, ~1 cm away from the lesion, and from visibly healthy colonies (n = 5 for each). Tissue samples were fixed in 2.5% glutaraldehyde and stored at 4 °C until processing.

Glutaraldehyde-fixed tissue samples were decalcified in 0.5 M EDTA and post-fixed in 2% osmium tetroxide. Samples were then dehydrated through an ethanol series (50 – 100%) and propylene oxide and embedded in Procure 812 resin (Proscitech, Thuringowa, Australia). Ultra-thin sections were cut on an Ultracut T ultramicrotome (Leica Microsystems, Vienna, Austria) and stained using 2% aqueous uranyl acetate and Reynold's lead citrate. Sections were viewed on a Philips CM-100 transmission electron microscope operated at 80 kV. Three grids from each tissue sample were analysed. In each case 30 fields of view at 24,500 × magnification were examined for the presence of VLPs in *Symbiodinium* cells and coral gastrodermal and epidermal tissues. Observed VLPs were sorted into two morphological groups (icosahedral and filamentous) and five size classes (0-50 nm, 51-100 nm, 101-150 nm, 151-200 nm and > 200 nm). Statistical analysis was carried out using PASW Statistics 18 (SPSS Inc., Chicago, IL, USA) to determine any difference in virus abundance between samples.

Results and discussion

TEM examination revealed no apparent differences in coral or *Symbiodinium* cell health between diseased and non-diseased samples. Similarly, viral abundance did not differ significantly among sample types (lesion, 1 cm away from lesion, and healthy tissue; MANOVA $p > 0.05$ for all VLP groups). Virus-like particles were abundant in all samples (Fig. H1). In coral tissues, VLPs were all icosahedral and almost exclusively < 100 nm in diameter (Fig. H2), whereas VLPs seen in *Symbiodinium* cells were usually filamentous and 50 – 100 nm in length (Fig. H3).

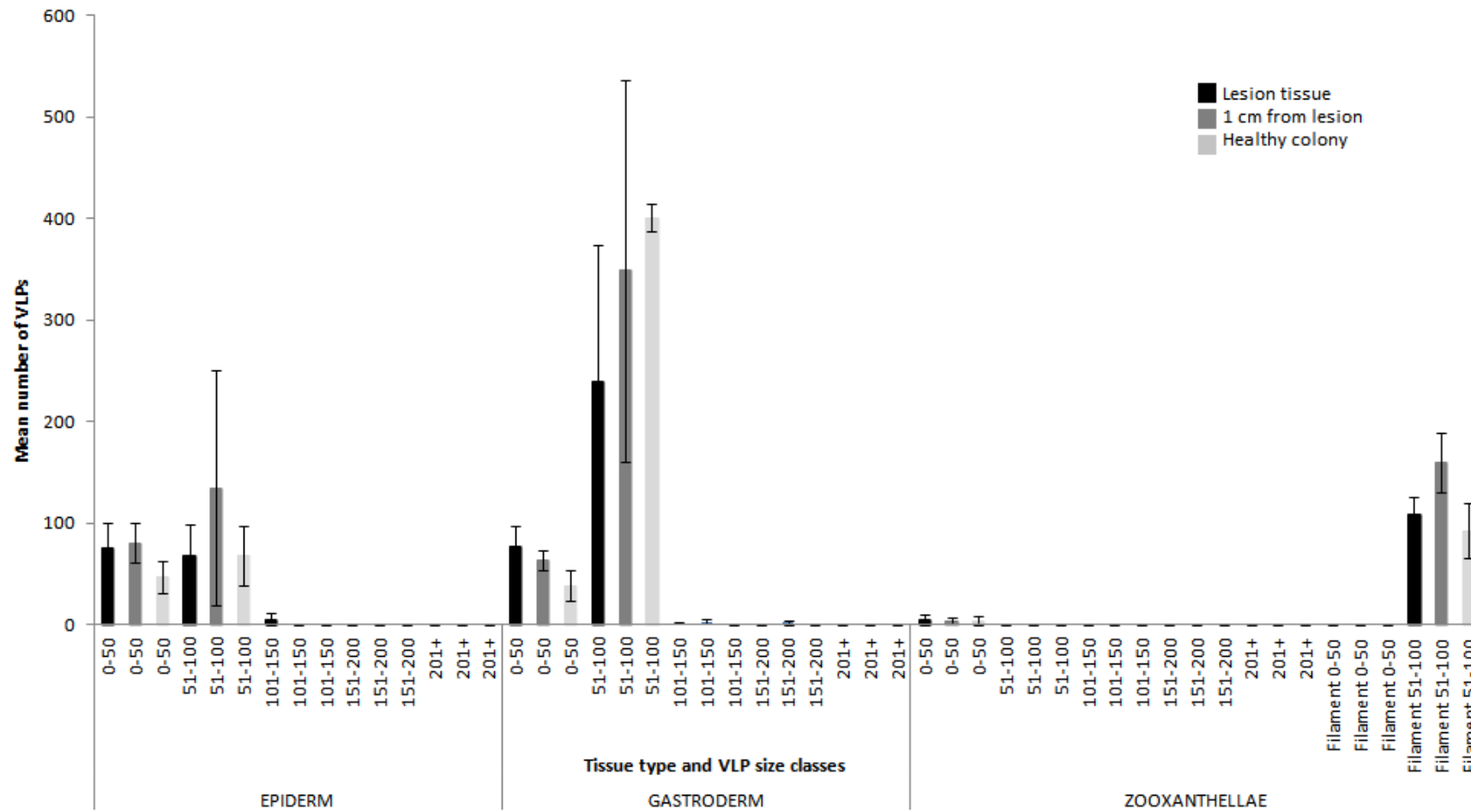


Figure H1. Abundances of VLP size classes in host tissues from diseased and healthy *Porites compressa* colonies. Error bars are \pm SE ($n = 5$ for samples from lesions and from tissue 1 cm away from lesions, $n = 3$ for samples from healthy colonies).

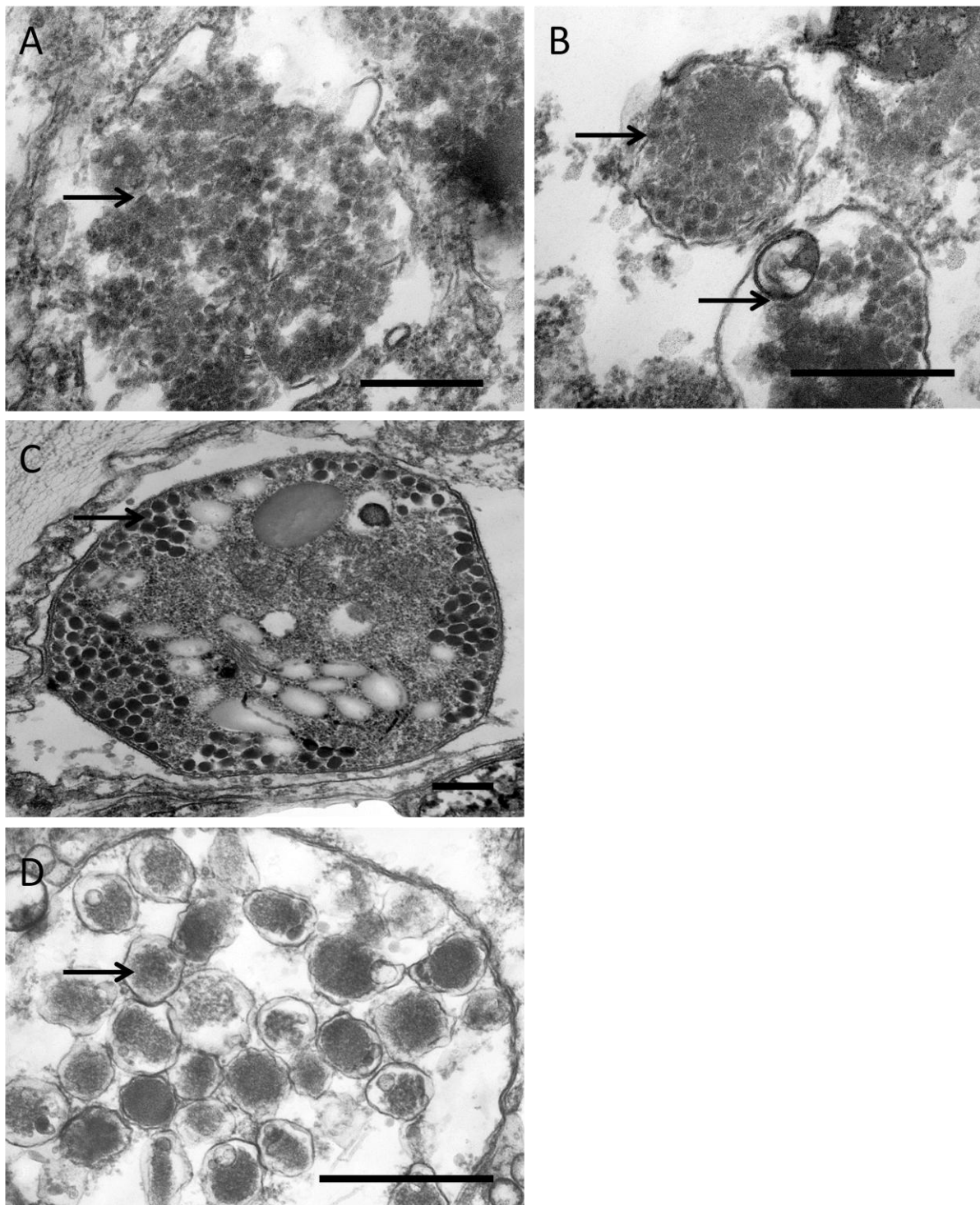


Figure H2. Transmission electron micrographs of virus-like particles (VLPs) in cells of healthy and PorGA-affected *Porites compressa* colonies. (A, B) ~50 nm diameter icosahedral VLPs (arrows) enclosed in vesicles within the gastrodermis of a healthy *P. compressa* colony; (C) ~100 nm diameter VLPs (arrow) in a gastrodermal cell from a healthy *P. compressa* colony; (D) ~200 nm diameter icosahedral VLPs (arrow) in epidermal tissue of a *P. compressa* colony suffering from PorGA. Scale bars represent 500 nm.

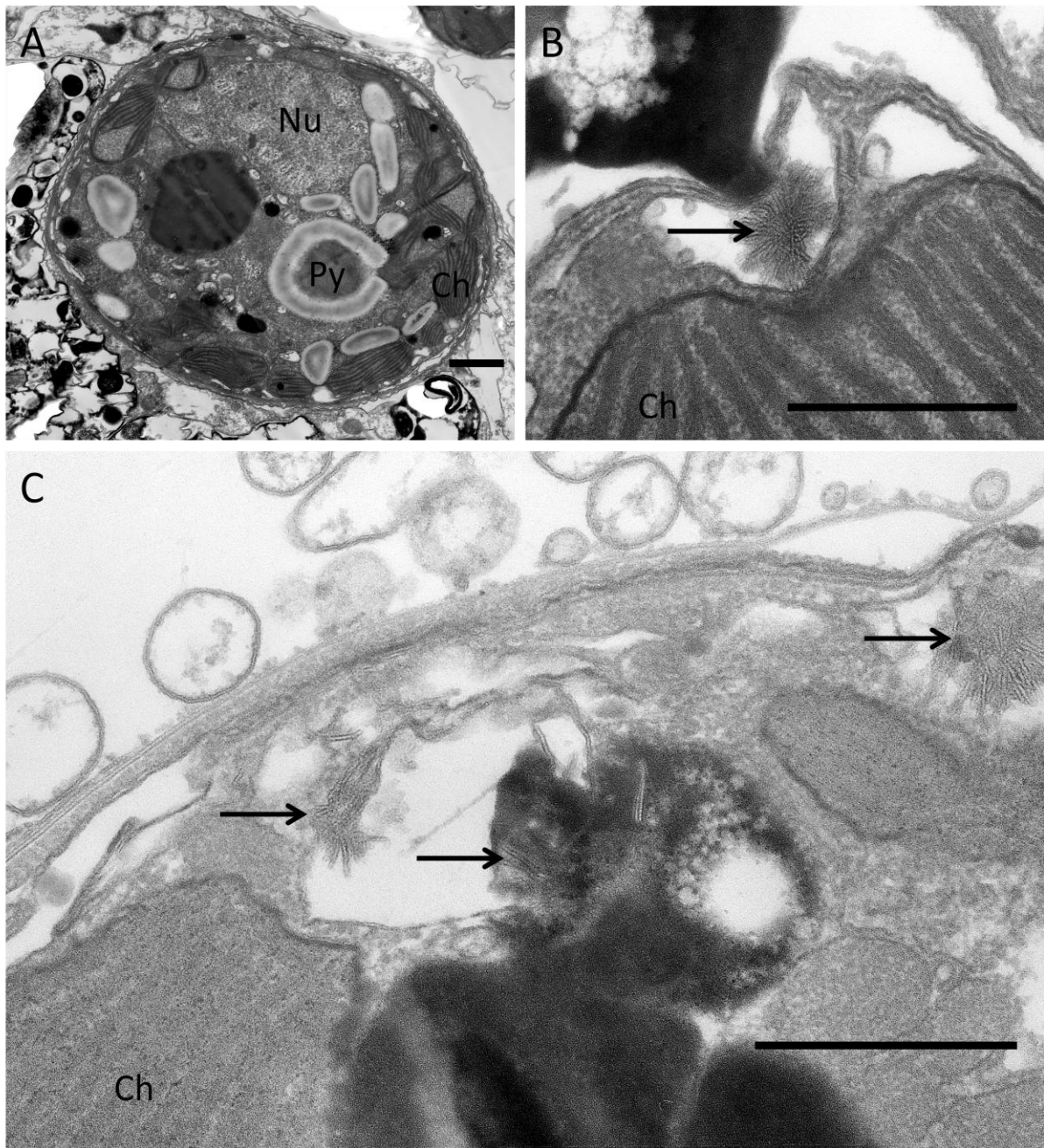


Figure H3. Transmission electron micrographs of *Symbiodinium* cells in healthy and PorGA-affected *Porites compressa* colonies. (A) Healthy *Symbiodinium* cell in a non-diseased *P. compressa* colony; (B) filamentous VLPs (arrow) in a *Symbiodinium* cell in a non-diseased *P. compressa* colony; (C) filamentous VLPs (arrows) in a *Symbiodinium* cell in a tissue sample collected 1 cm away from a PorGA lesion. Scale bars represent 1 μm (A) and 500 nm (B, C). Ch: chloroplast, Nu: nucleus, Py: pyrenoid.

The lack of visible differences between healthy and diseased tissues is not unexpected, given that PorGA is a hyperplastic disease. Hyperplasia involves proliferation of cells in response to a stimulus, and subsequent tissue enlargement, but the cells involved are genetically and physiologically normal. This contrasts with neoplasia, as seen in corals by Squires (1965), which involves unchecked proliferation of genetically abnormal cells. Based on the results of the current study, it is not possible to say what the stimulus for hyperplasia is in PorGA. The finding by Williams *et al.* (2010) that increased PorGA prevalence was correlated with decreased depth and turbidity suggested a possible viral basis to the disease, as both thermal and UV light stress have been shown to promote viral infections in corals and their algal symbionts (Wilson *et al.*, 2001; Davy *et al.*, 2006; Lohr *et al.*, 2007). Furthermore, viral infections have been shown to cause hyperplasia in other marine organisms (Manire *et al.*, 2008; Van Elk *et al.*, 2009) including a coral reef-dwelling fish (Nopadon *et al.*, 2009), suggesting a possible vector. Viral counts carried out here do not support the hypothesis of a viral basis for PorGA, but neither do they refute it, as similar abundances of VLPs in diseased and healthy colonies do not rule out a change in the identity of the viruses present. Further study, utilizing molecular methods to identify the viruses associated with the disease, should be carried out to confirm or deny a viral role.

Appendix I

The following is a manuscript prepared during the course of my PhD for submission to the journal *Aquatic Microbial Ecology*. The work was carried out along with the co-authors listed below. I carried out the majority of the electron microscopy, was involved in data analysis, and wrote the manuscript, with the exception of parts of the Methods and Results, which were written by Shaun P. Wilkinson and William N. S. Arlidge, and Figure 2, which was created by Shaun P. Wilkinson.

Viral communities associated with the coral *Montipora capitata* in Kaneohe Bay: the influence of local environmental variables

Running head: *Montipora capitata* viral communities

Key-words: corals, virus, environmental drivers, turbidity, chlorophyll

Scott A. Lawrence¹, Shaun P. Wilkinson¹, Joanne E. Davy, William N. S. Arlidge, Gareth J. Williams², William H. Wilson³ & Simon K. Davy^{1*}

¹ School of Biological Sciences, Victoria University of Wellington, PO Box 600, Wellington, New Zealand

² Scripps Institution of Oceanography, 8602 La Jolla Shores Drive, La Jolla, California, USA

³ Bigelow Laboratory for Ocean Sciences, PO Box 380, East Boothbay, Maine, USA

*Corresponding author. Mailing address: School of Biological Sciences, Victoria University of Wellington, PO Box 600, Wellington, New Zealand. Phone: +64-4-4635573 Fax: +64-4-4635331 E-mail: simon.davy@vuw.ac.nz

Abstract

Coral-associated viruses are a component of the coral holobiont that have received attention only recently. Given the global increase in coral disease prevalence, and the lack of identified etiological agents for many diseases, these virus communities require increased investigation. In particular, little is known about the viruses that are naturally associated with coral reefs and how they are affected by the local environment. In the present study, a short-term analysis of viral communities associated with the coral *Montipora capitata* in Kaneohe Bay, Hawaii, was carried out to determine the environmental factors influencing their composition. Coral surface microlayer (CSM) and seawater samples collected at four sites across a gradient of anthropogenic impact were analysed using transmission electron microscopy (TEM), and relative abundances of virus-like particle (VLP) morphotypes were correlated with environmental measurements. Within the CSM, water temperature, turbidity and chlorophyll-*a* levels were correlated with changes in relative proportions of several VLP types, including phages and filamentous VLPs. In seawater samples, turbidity and temperature showed the strongest correlation, altering the proportion of *Podoviridae*-like, *Geminiviridae*-like and putative Archaeal viruses, among others. Overall VLP community composition differed significantly between the CSM and seawater only at the more degraded sites, suggesting that human activity is affecting coral-associated virus communities.

Introduction

Coral reefs are the most diverse ecosystems in the ocean, with estimates of diversity ranging from one to nine million species worldwide (Pelley, 2004). A major contributor to this diversity is the vast array of coral-associated microbes, including dinoflagellates of the genus *Symbiodinium* (Douglas and Smith, 1989), endolithic algae (Wanders, 1977; Shashar, 1992), fungi (Bentis *et al.*, 2000), archaea (Kellogg, 2004; Wegley *et al.*, 2004) and both heterotrophic and autotrophic bacteria (Ducklow and Mitchell, 1979; Rohwer *et al.*, 2002; Lesser *et al.*, 2004). One component of this so-called coral holobiont (Rohwer *et al.*, 2002) which has received limited examination until recently is the coral-associated virus community. Viruses are increasingly seen as important members of marine communities that often have significant effects both at the level of the individual host and of the ecosystem and

wider environment (Munn, 2006; Suttle, 2007; Sandaa, 2008; Rohwer and Vega Thurber, 2009). Viruses are known to infect numerous taxa within the coral reef ecosystem, including bacteria, archaea, fungi, algae and fish (Vega Thurber and Correa, 2011). Within the corals themselves, viruses have been found in the gastrodermis, epidermis, coral surface microlayer (CSM, or mucus layer) and intracellular dinoflagellate symbionts (*Symbiodinium*) (Vega Thurber and Correa, 2011). Viruses were first reported from within the tissues of a scleractinian coral in 2005 (Wilson *et al.*, 2005a), but there have only been around 15 subsequent studies of viruses associated with reef-building corals. It is uncertain whether viruses are responsible for any of the ~18 currently recognised coral diseases (Bourne *et al.*, 2009), however there is some evidence that they may play a role in several of them. For example, virus-like particles (VLPs) were observed within tissues of *Porites australiensis* suffering from white patch syndrome, with PCR analysis revealing possible viral sequences from these same samples but not from healthy colonies (Davy, 2007). Similarly, Patten *et al.* (2006) found that virus abundance and virus:bacteria ratio (VBR) increased with proximity to acroporid corals suffering from white syndrome, suggesting an increase in non-phage viruses associated with the diseased corals. Further evidence for viral diseases of the coral holobiont comes from *in vitro* experiments, such as those of Wilson *et al.* (2001) and Davy *et al.* (2006), which showed that thermal stress of otherwise healthy *Symbiodinium* and corals resulted in an increase in viral abundance within *Symbiodinium* cells and possibly corals. In both studies, VLPs induced by heat stress were capable of lysing healthy *Symbiodinium* cells in the absence of stress, providing strong evidence that viruses can indeed cause disease in *Symbiodinium*. Vega Thurber *et al.* (2008) also found that several environmental stressors caused increases in herpes-like virus abundance in *Porites compressa*. It seems likely that, with further research, viruses will be identified as the etiological agents of some coral diseases.

Despite some viruses likely causing disease and disruption of the coral holobiont, it is probable that the majority of coral-associated viruses are in fact a relatively stable and important component of the holobiont. Virus-like particle abundance and VBR in seawater have been shown to increase with proximity to healthy corals (Seymour *et al.*, 2005), albeit not to the same extent seen with diseased corals by Patten *et al.* (2006). Marhaver *et al.* (2008) carried out metagenomic analyses of viral communities associated with the coral *Diploria strigosa* and found that they were highly diverse (healthy colonies were predicted to contain over 28,000 viral types). A diverse viral community is to be expected, given the range

of potential hosts within the coral holobiont. The huge network of interactions arising from this vast assemblage of eukaryotes, prokaryotes and viruses makes determining the roles of individual viruses, and their collective effect on the coral holobiont, all the more difficult. However, in spite of the difficulties involved, the identity and roles of coral-associated viruses deserve investigation, as they represent the least well-known component of an ‘organism’ and ecosystem increasingly at risk of destruction or massive alteration *via* disease (Harvell *et al.*, 2002; Bourne *et al.*, 2009), temperature-induced bleaching (Hoegh-Guldberg, 1999; Baker *et al.*, 2008), ocean acidification (Hughes *et al.*, 2003; Hoegh-Guldberg *et al.*, 2007) and other anthropogenic impacts (Knowlton, 2001; Pandolfi *et al.*, 2003).

In the current study, we examined the VLP communities associated with the CSM of the scleractinian coral *Montipora capitata*. The CSM acts as a selective barrier, keeping the coral free of sediment (Hubbard and Pocock, 1972) while trapping food particles (Lewis and Price, 1976). Additionally, the CSM harbours a diverse microbial community, with bacterial abundance of up to 100 times that of surrounding seawater (Ritchie and Smith, 2004). This bacterial community is thought to be coral species-specific (Ritchie and Smith, 1997; Kvennefors *et al.*, 2010) and there is evidence that these endemic bacteria prevent invasion of the coral by potentially harmful microbes (Reshef *et al.*, 2006; Ritchie, 2006; Nissimov *et al.*, 2009). This community can, however, shift to a predominantly pathogenic state under stress conditions (Mao-Jones *et al.*, 2010; Rypien *et al.*, 2010). Given this fact, and the relatively host-specific nature of viruses, it seems likely that VLP communities differ a) between the CSM and surrounding seawater, and b) between corals subjected to varying levels of environmental stress. With this in mind, the present study used transmission electron microscopy (TEM) to assess the morphological diversity of VLP communities in the CSM of *M. capitata* and in overlying seawater, across a gradient of anthropogenic impact.

Methods

Sampling

Sampling was carried out at four sites on the reef crest of the northern and eastern flanks of Coconut Island, Kaneohe Bay, Oahu, Hawaii (21° 26.000’N, 157° 47.000’W). The distance

from shore was between 50 and 200 m, and the maximum depth at low tide was approximately 4.5 m. Samples were collected by divers using snorkel, and consisted of five mucus samples from the coral surface microlayer (CSM) of separate, healthy *Montipora capitata* colonies, and five seawater samples, from each of the four sites. CSM samples were harvested using sterile 25 mL syringes, with care being taken to ensure that the syringe tip remained in contact with the coral surface at all times. Seawater samples were collected in 50 mL centrifuge tubes 10 cm above the surface of each sampled coral colony. All samples were fixed in 2% glutaraldehyde within two hours of collection and stored in the dark at 4 °C until processing for electron microscopy.

Five environmental variables (temperature, chlorophyll-*a* fluorescence, turbidity, depth and salinity) were measured at each of the four sampling sites over a 48 h period using RBR XR-420 submersible CTD thermistors (RBR Ltd. Ottawa, Canada). The CTDs were set at 1 min sampling intervals from 3 pm on 19 June 2009 until 3 pm on 21 June 2009. Mean values of each parameter measured over this period were used in environmental data analysis.

Virus isolation and microscopy

All samples were centrifuged at $1,500 \times g$ for 10 min at 4 °C to remove coral tissue, bacteria and other non-viral material. Viruses were pelleted from the supernatant by centrifugation at $146,000 \times g$ for 2 h at 4 °C and resuspended in 100 μ L of supernatant. Pioloform-coated 200 μ m-mesh copper grids were carbon coated and rendered hydrophilic by high voltage glow discharge, before being floated on 20 μ L aliquots of the viral suspensions for 1 h. Grids were negative-stained with 3% aqueous uranyl acetate for 30 s and viewed on a Philips CM100 transmission electron microscope (TEM; 80 kV) at $33,000 - 66,000 \times$ magnification. The size (length of filamentous, rod-shaped and beaded VLPs; maximum capsid width of all others) and morphology of the first 100 virus-like particles (VLPs) observed on each grid were determined and assigned to one of 26 subgroups within five major morphological groups (tailed phages, icosahedral/spherical tail-less VLPs, filamentous VLPs (FVLPs), lemon-shaped VLPs, and other miscellaneous VLPs).

Data analysis

To test for differences in virus community structure between sites and between the CSM and surrounding seawater, a two-factor multivariate regression model was applied under permutation of dissimilarities, using the program DISTLM (Anderson, 2001; McArdle and Anderson, 2001). In cases of significant interaction between factors, simple effects tests were carried out using the denominator mean square from the interaction model.

A dissimilarity matrix of the virus morphotype frequencies for each pair of replicate grids was constructed using the semi-metric Bray-Curtis measure. This was done using the `vegdist` function of the `vegan` package in R (R Development Core Team, 2006; Oksanen *et al.*, 2010). The appropriately coded predictor (X_{SITE} , X_{HABITAT} and X_{SXH}) and full (X_{FULL}) matrices were constructed using the program XMATRIX (Anderson, 2003). Orthogonal contrasts were used due to unbalanced replication.

In order to illustrate relative site differences within each habitat type, a non-metric multidimensional scaling (nMDS) ordination of site and species scores was carried out using the `metaMDS` function of the `MASS` package in R (R Development Core Team, 2006; Oksanen *et al.*, 2010), with points representing viral morphotypes and field sites.

To determine how well patterns of virus community composition correlated with measured environmental parameters across the four sites, and in which direction they were correlated, a subset of environmental variables was chosen based on maximum correlation with community dissimilarities. For each habitat type (CSM and seawater), environmental variables were fitted and projected as vectors onto ordination diagrams using the `envfit` procedure in the `vegan` package in R (R Development Core Team, 2006; Oksanen *et al.*, 2010). The goodness of fit for each vector was assessed using the squared correlation coefficient (r^2) test statistic based on 4999 permutations of the environmental variables and a 5% significance level.

Results

Environmental variables

The four reef sites sampled in the present study were chosen to include varying levels of environmental variables. There was a gradient of increasing anthropogenic impact from sites A to D, which was confirmed by elevated turbidity and chlorophyll-*a* concentrations at sites C and D (Table II). This corresponded with observations of reef integrity, with sites A & B displaying a more intact reef structure and sites C & D showing signs of degradation. Temperature and depth varied among sites, while mean salinity remained relatively constant, although site C did experience greater temporal changes in salinity than the other three sites (Table II).

Table II. Mean values (\pm SE) of environmental variables recorded over sampling period.

Site	Chlorophyll- <i>a</i> ($\mu\text{g L}^{-1}$)	Depth (m)	Salinity (ppt)	Temperature ($^{\circ}\text{C}$)	Turbidity (STU)
A	1.55 ± 0.20	4.11 ± 0.10	35.01 ± 0.01	26.83 ± 0.07	1.92 ± 0.21
B	1.06 ± 0.46	2.45 ± 0.05	35.09 ± 0.01	27.23 ± 0.08	1.52 ± 0.32
C	2.32 ± 0.94	1.28 ± 0.11	34.19 ± 1.25	26.57 ± 0.12	4.53 ± 0.97
D	1.73 ± 0.21	1.62 ± 0.07	35.16 ± 0.04	26.02 ± 0.06	8.07 ± 1.67

Viral morphology

3,700 VLPs were counted in this study and sorted into 26 groups, based on morphology and size. These 26 groups were further sorted into five major classes: tailed phages, tail-less icosahedral/spherical VLPs, filamentous VLPs, lemon-shaped VLPs, and miscellaneous VLP types (which made up 4% of the total) (Fig. I1). The numerically dominant VLP class in all samples was the icosahedral/spherical VLPs (56.4%), of which 72.2% were smaller than 50 nm. Large icosahedral/spherical VLPs (> 100 nm), which likely included members of the *Phycodnaviridae* and *Herpesviridae*, constituted 2.9% of the total VLP count. The various tailed phages were present in high numbers in all samples (30.1%), with podoviruses making up 11.1% of the total, myoviruses 12.6%, and siphoviruses 6.4%. Filamentous VLPs, ranging

in size from < 50 nm to over 2 μm in length, comprised 7.2%, while lemon-shaped VLPs (presumably belonging to the archaea-infecting *Fusellovirus* or *Salterprovirus* genera) made up 2.3% of the count. Proportions of each VLP group in both CSM and seawater from the four sites are shown in Table I2.

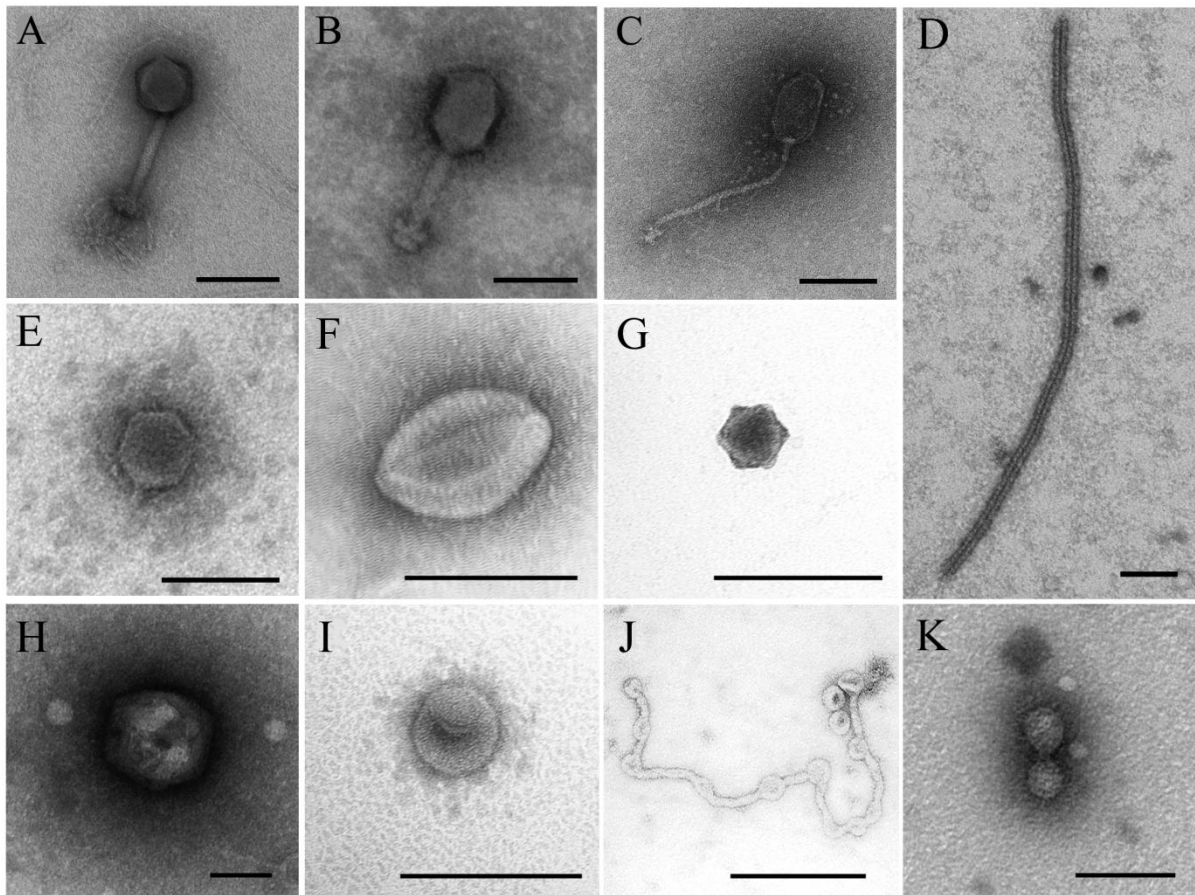


Figure I1. Transmission electron micrographs of VLPs isolated from the CSM of *Montipora capitata* and surrounding seawater. Isometric myovirus (A); elongate myovirus (B); siphovirus (C); filamentous VLP (D); podovirus (E); lemon-shaped VLP (F); small polyhedral VLP (G); large, phycodnavirus-like polyhedral VLP (H); spherical VLP (I); beaded VLP (J); geminivirus-like VLP (K). Scale bars are 100 nm.

Effect of habitat type on VLP communities

Across all four sites, similar levels of VLP diversity were seen in the CSM and surrounding seawater (permutation test, $p > 0.05$; Shannon-Wiener index \pm S.E. = 2.00 ± 0.09 & 1.92 ± 0.05 for CSM and seawater samples, respectively), though hook-shaped VLPs and those classed as ‘other’ (such as mushroom-shaped and polydnavirus-like particles) were found exclusively in the CSM (Table I2).

Table I2. Morphological diversity and proportions (mean \pm SE) of virus-like particles (VLPs) from the coral surface microlayer (CSM) of *Montipora capitata* and in surrounding seawater (SW), from 4 sites in Kaneohe Bay (n = 5 except for Site B CSM, Site C SW and Site D SW, where n = 4).

Viral morphotype	Mean % VLPs							
	Site A		Site B		Site C		Site D	
	CSM	SW	CSM	SW	CSM	SW	CSM	SW
<i>Podoviridae</i> - like								
< 100 nm	13.9 \pm 1.4	12.9 \pm 2.1	11.2 \pm 1.4	13.2 \pm 3.4	6.2 \pm 1.7	7.5 \pm 0.9	5.7 \pm 1.4	8.5 \pm 1.8
> 100 nm	2 \pm 1	0.4 \pm 0.2	0.2 \pm 0.2	1.1 \pm 0.6	1.4 \pm 0.6	0.3 \pm 0.3	0.4 \pm 0.2	3.8 \pm 1.3
Elongate								
<i>Myoviridae</i> - like								
< 100 nm	0.4 \pm 0.4	-	0.7 \pm 0.5	0.8 \pm 0.6	-	-	-	-
100 – 200 nm	0.8 \pm 0.4	0.2 \pm 0.2	1.2 \pm 0.7	1.0 \pm 0.3	0.4 \pm 0.2	0.3 \pm 0.3	1.1 \pm 0.5	1.7 \pm 1.7
> 200 nm	0.8 \pm 0.5	0.4 \pm 0.5	1.3 \pm 0.5	-	-	0.8 \pm 0.5	0.8 \pm 0.8	-
Isometric								
<i>Myoviridae</i> - like								
< 100 nm	5.8 \pm 1.3	6.8 \pm 2.6	9.7 \pm 4.2	3.6 \pm 1.2	2.8 \pm 1.1	2.0 \pm 0.4	1.9 \pm 0.5	2.9 \pm 1
100 – 200 nm	7.6 \pm 2.7	5 \pm 0.8	7 \pm 1.3	4.7 \pm 1.3	3.8 \pm 1.1	8.0 \pm 1.8	5.0 \pm 1.5	6.5 \pm 1.8
> 200 nm	1 \pm 0.5	0.6 \pm 0.4	-	-	0.2 \pm 0.2	2.0 \pm 0.7	0.2 \pm 0.2	0.7 \pm 0.5
<i>Siphoviridae</i> - like								
< 100 nm	3 \pm 1.3	4 \pm 1.4	2.8 \pm 1.5	8.1 \pm 5.5	0.6 \pm 0.2	0.5 \pm 0.3	0.8 \pm 0.4	4.4 \pm 0.5
100 – 200 nm	2.4 \pm 1.2	3.2 \pm 0.8	2.2 \pm 0.5	3.7 \pm 0.9	1.8 \pm 0.7	2.3 \pm 0.6	2.6 \pm 0.6	2.6 \pm 1.7
> 200 nm	0.2 \pm 0.2	0.6 \pm 0.2	0.5 \pm 0.3	0.4 \pm 0.2	0.6 \pm 0.2	2.5 \pm 0.6	0.4 \pm 0.2	0.7 \pm 0.2
Icosahedral/								
Spherical								
< 50 nm	32.0 \pm 3.3	42.4 \pm 2.0	31.9 \pm 6.1	40.9 \pm 6.3	56.4 \pm	51.5 \pm 3.1	38.5 \pm 9.4	32.1 \pm 3.5
50 – 100 nm	12.3 \pm 2.7	6.6 \pm 2.3	14.2 \pm 3.4	6.4 \pm 1.7	11.8 \pm	8.0 \pm 0.9	14.9 \pm 3.7	28.2 \pm 8.4
> 100 nm	1.0 \pm 0.3	0.4 \pm 0.2	1.5 \pm 0.9	6.3 \pm 5.1	2.0 \pm 0.3	0.8 \pm 0.5	8.3 \pm 3.9	2.1 \pm 1.0
Lemon-shaped								
< 100 nm	5.9 \pm 4.0	0.2 \pm 0.2	2.0 \pm 0.4	0.2 \pm 0.2	2.8 \pm 0.9	0.5 \pm 0.5	1.1 \pm 0.6	0.7 \pm 0.5
> 100 nm	1.2 \pm 0.8	-	1.8 \pm 1.4	-	1.0 \pm 0.3	-	0.5 \pm 0.4	0.8 \pm 0.8
Filamentous								
< 100 nm	1.4 \pm 1.0	1.2 \pm 0.4	3.2 \pm 0.5	1.9 \pm 0.9	0.2 \pm 0.2	-	-	1.4 \pm 0.5
100 – 500 nm	3.0 \pm 1.8	2.6 \pm 0.6	3.0 \pm 0.7	2.7 \pm 1.2	1.6 \pm 0.6	1.8 \pm 0.5	3.2 \pm 0.7	1.2 \pm 0.7
500 nm – 1 μ m	0.6 \pm 0.2	3 \pm 1.2	1.7 \pm 0.6	1.5 \pm 0.6	1.6 \pm 0.7	3.8 \pm 1.1	4.0 \pm 0.8	0.3 \pm 0.3
> 1 μ m	1.8 \pm 0.5	2.4 \pm 1.7	0.7 \pm 0.5	1.6 \pm 0.8	0.4 \pm 0.2	2.3 \pm 0.8	3.2 \pm 0.9	-
<i>Geminiviridae</i> - like								
Beaded	1.0 \pm 0.6	2.4 \pm 0.7	1.5 \pm 0.6	0.2 \pm 0.2	1.6 \pm 0.7	-	0.2 \pm 0.2	0.2 \pm 0.2
Rod-shaped	0.8 \pm 0.2	2.2 \pm 0.5	0.5 \pm 0.3	0.2 \pm 0.2	0.8 \pm 0.4	2.3 \pm 0.5	2.6 \pm 1.3	-
Cube-shaped	0.4 \pm 0.2	2 \pm 0.3	1.0 \pm 0.4	0.6 \pm 0.4	-	-	0.5 \pm 0.4	1.0 \pm 0.4
Hook-shaped	-	-	-	-	-	-	0.2 \pm 0.2	-
Other	0.4 \pm 0.4	-	-	-	-	-	0.5 \pm 0.5	-

Non-parametric analysis of variance revealed a significant multivariate interaction between habitat type and site in determining the composition of the VLP assemblage associated with *M. capitata* (permutation $p = 0.007$). Simple effects tests showed a significant difference in VLP community composition between sites in both habitat types (permutation $p = 0.004$ & 0.001 for CSM and seawater samples, respectively). At the two sites with relatively high water quality (A & B), there was no significant difference between the CSM and seawater (permutation $p > 0.05$ for both sites). Community composition did, however, differ significantly between the two habitat types at the more degraded sites (permutation $p = 0.021$ & 0.036 for sites C & D, respectively).

Effect of the environment on VLP communities

The envfit variable selection analysis indicated that the environmental variables that had the most influence on VLP community composition in the CSM of *M. capitata* were temperature, turbidity and chlorophyll-*a* concentration (permutation $p = 0.004$, 0.001 and 0.012 , respectively). Virus-like particle communities in the surrounding seawater were affected by temperature and turbidity (permutation $p = 0.013$ and 0.007 , respectively).

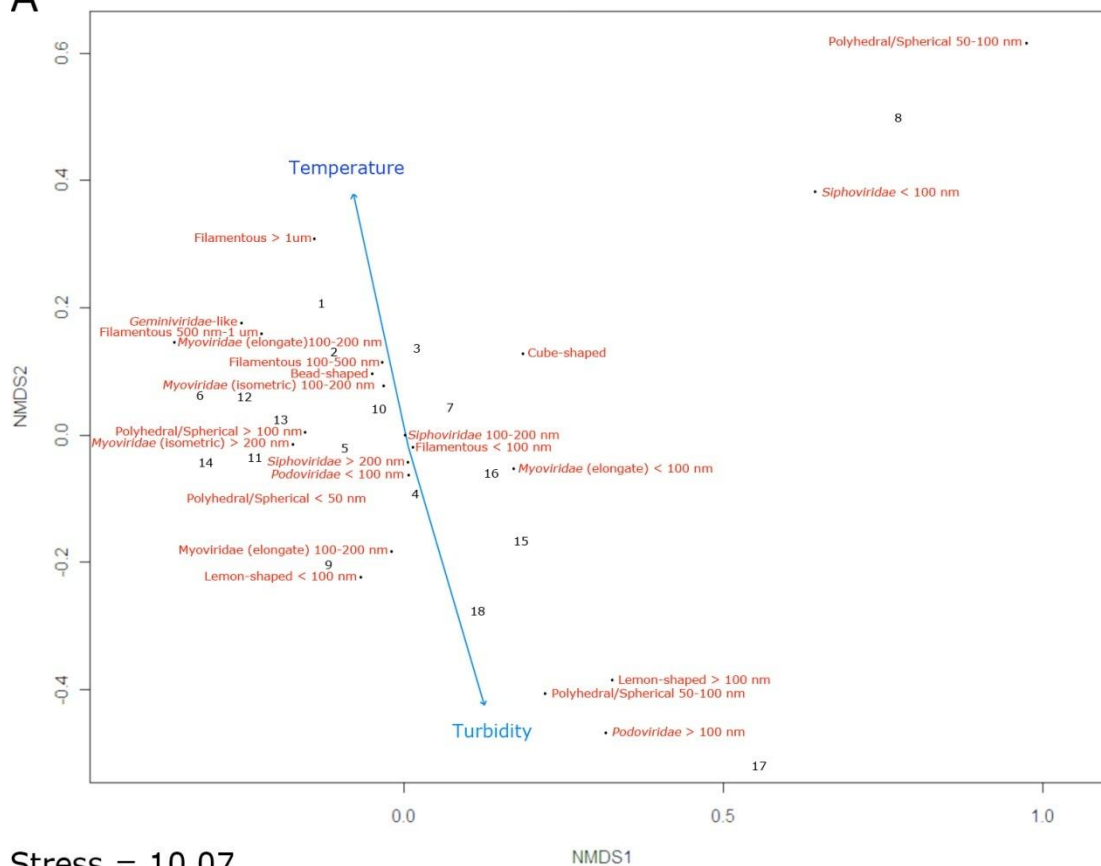
Projection of environmental variables onto nMDS ordinations indicated a negative correlation between turbidity and temperature, as shown by their near-antiparallel vectors (Fig. I2). Subsets of the CSM and seawater VLP communities were distributed along this gradient, with several individual morphotypes having their distribution mode centred in either a positive or negative direction along the axis. In the seawater ordination diagram (Fig. I2B), the near-orthogonal chlorophyll-*a* vector indicated that the concentration of chlorophyll-*a* was not correlated with either temperature or turbidity, i.e. increased turbidity was associated with lower temperature, but chlorophyll-*a* concentration was unrelated to either turbidity or temperature.

Effect of habitat type and environment on individual VLP morphotypes

The ordination diagrams (Fig. I2) revealed several patterns in the association between VLP communities, habitat type and environmental variables at the level of individual virus morphology. In the seawater samples, large (> 100 nm) *Podoviridae*-like VLPs and elongate *Myoviridae*-like VLPs, as well as lemon-shaped VLPs of both size classes, showed a positive

correlation with turbidity. In contrast, the relative abundance of *Geminiviridae*-like, beaded, and rod-shaped VLPs, along with the three largest size classes of FVLPs, showed a positive association with temperature. A different pattern was apparent in the CSM samples, where the relative abundances of all four groups of small (< 100 nm) tailed phages, small lemon-shaped VLPs, FVLPs and beaded VLPs were positively correlated with increased temperature. The abundance of the numerically dominant, small (< 50 nm) polyhedral/spherical VLPs in the CSM samples appeared to be positively correlated with chlorophyll-*a* concentration.

A



B

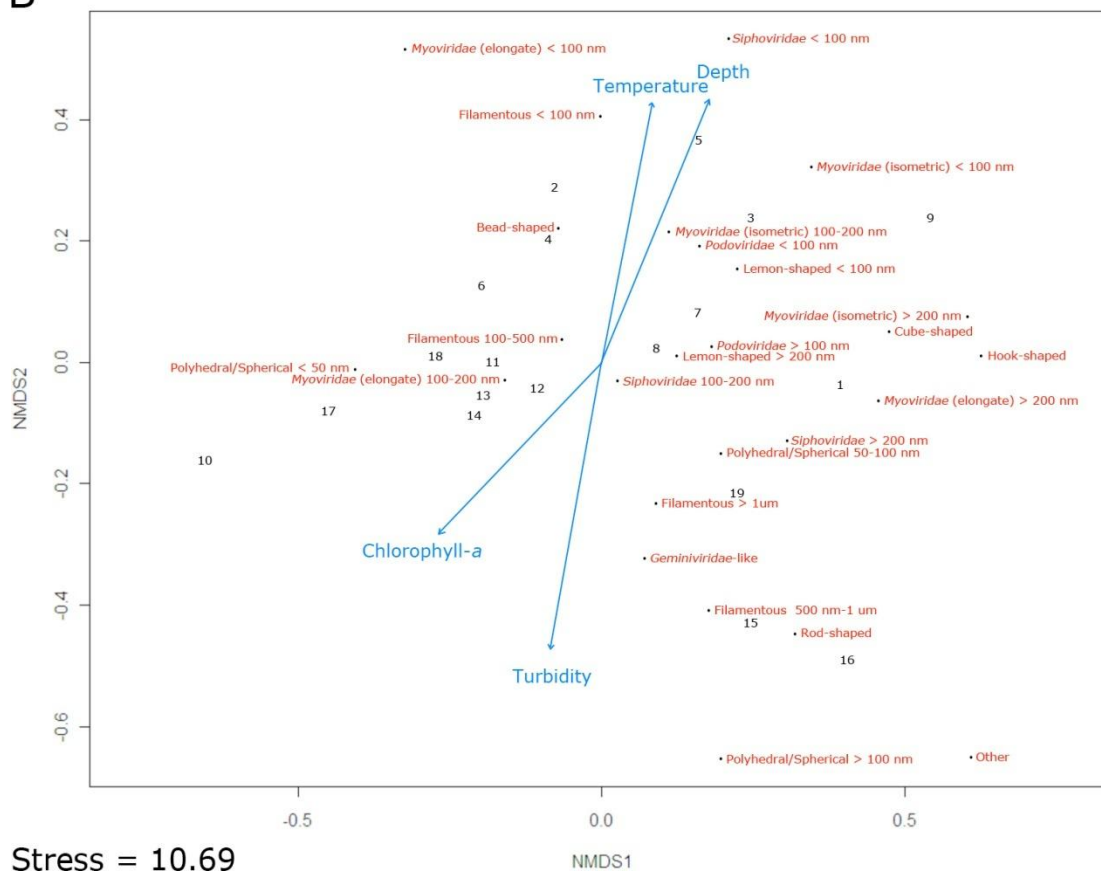


Figure I2 (previous page). Ordination diagrams of the VLP communities of seawater (A) and the CSM of *M. capitata* (B), showing the patterns of variation in community composition explained by environmental variables. Red labels are approximate relative centres of VLP morphotype distributions, black labels represent the approximate positions of each sampling unit (TEM grid) from each of the four field sites, and blue arrows represent the relative size and direction of fitted environmental gradients.

Discussion

In this study, we examined the virus communities associated with the surface microlayer (CSM) of the coral *Montipora capitata* and with the surrounding seawater, across an environmental gradient. Virus-like particle (VLP) diversity was high across all sites and habitats (CSM and seawater), in agreement with previous reports from coral reefs and other oligotrophic waters (Hewson *et al.*, 2006). Interestingly, however, similar levels of VLP diversity were seen in both the CSM and seawater, in contrast to the findings of Davy and Patten (2007), who observed significantly higher diversity in the CSM of *Porites* spp. than in the surrounding seawater on the Great Barrier Reef (GBR). Similar sampling methods were used in both studies, suggesting that either Kaneohe Bay hosts richer planktonic viral communities than those found on the GBR or that coupling between the CSM and the overlying water (e.g. through mucus sloughing) is more prevalent in Kaneohe Bay. Both explanations are conceivable, given that Kaneohe Bay is generally a far more human-impacted site (and hence likely to have higher bacterial counts and more stressed corals) than are the offshore regions of the GBR (Hutchings *et al.*, 2009). There may also be a seasonal component involved; sampling by Davy & Patten was undertaken during autumn, whereas the samples in this study were collected during the summer, when rates of photosynthesis and thermal stress (and hence mucus production) are generally higher (Neudecker, 1981).

All habitats and sites in the present study were dominated by tailed phages and small (< 100 nm) icosahedral VLPs (many of which were likely also phages). Phages are the most prevalent viruses in the marine environment (Danovaro *et al.*, 2008c; Choi *et al.*, 2009), and tend to exist in the lytic rather than lysogenic form in shallow waters (Wilcox and Fuhrman, 1994), which would explain the prevalence seen here. In addition to these dominant groups, numerous other viral morphotypes were present at relatively low proportions. While the specific hosts of these VLP groups cannot be positively identified without further research,

several resembled viruses known to infect Archaea, plants, fungi and animals. Viral abundance was not measured in the present study, but recent data from the same sites and host species indicate that virus numbers are approximately twice as high in the surrounding seawater as they are in the CSM (Arlidge *et al.*, in prep.).

Similar levels of viral diversity were seen across the environmental gradient sampled here. This may, in part, be due to the limited resolution of electron microscopy in terms of viral identification (highlighted by the fact that in the present study, virus-like particles were sorted into just 26 morphological/size groups); molecular analysis would be required to determine the true diversity of these samples. Despite this limitation, several patterns at the level of individual viral morphotypes were observed in relation to environmental variables. Furthermore, the observed patterns were different in the CSM and seawater samples, indicating that there is an interaction between habitat type and environment in structuring viral communities. Such an interaction makes sense, as environmental stressors are known to affect coral mucus production and the abundance and diversity of microbes within the CSM (Segel and Ducklow, 1982).

Within the CSM, temperature, turbidity and chlorophyll-*a* concentration affected viral community composition. Small phages and filamentous VLPs (< 100 nm) were positively correlated with temperature; small polyhedral/spherical VLPs were positively correlated with chlorophyll-*a* concentration; and geminivirus-like, large filamentous and rod-shaped VLPs were positively correlated with turbidity. The correlation between phages and increased temperature is to be expected, as thermal stress can increase coral mucus production (Neudecker, 1981). Stress-induced mucus production also results in increased bacterial abundance (Segel and Ducklow, 1982), thus presenting more potential hosts for phages. Furthermore, the CSM has been shown to contain a bacterial community which is distinct from that of the surrounding seawater (Cooney *et al.*, 2002), which further explains the differing response between the CSM and seawater phage communities to increased temperature. It is more difficult to explain the positive correlation between small filamentous VLPs and temperature, but such viruses are primarily known from plants (Fauquet *et al.*, 2005), suggesting that algae of some sort may be the hosts within the CSM. Slightly larger (~200 nm length) filamentous VLPs have previously been found in stressed *Symbiodinium* cells (Lohr *et al.*, 2007), again hinting that these smaller filamentous VLPs may have algal hosts. Certainly there is no shortage of potential hosts within the CSM and the outer layers of

the coral, including the *Symbiodinium*, endolithic algae, and phytoplankton that have been trapped by the mucus layer. Lohr *et al.* (2007) provided evidence that these larger filamentous VLPs were in fact latent viruses, induced to enter the lytic cycle *via* stress to the host, and this may also be the case here, in response to increased temperature. It must be emphasized, however, that the mean temperatures differed among sites in the present study by only 1.2 °C (26.02 – 27.23 °C), and whether these measurements are representative of long term temperature trends is currently unknown.

Without more precise identification, it is difficult to determine what the small polyhedral/spherical VLPs in the CSM are infecting; this morphological/size group includes viruses of bacteria, plants, invertebrates and vertebrates (Fauquet *et al.*, 2005). The positive correlation with chlorophyll-*a* concentration suggests that they may be infecting algae or cyanobacteria within the mucus. Given that algal viruses tend to be much larger, cyanobacteria seem the likely hosts, though further investigation would be needed to confirm this. Moreover, it is important to note that several studies have documented the effects of eutrophication (for which chlorophyll-*a* is often used as a proxy) on the general health of the coral holobiont (Bruno *et al.*, 2003; Voss and Richardson, 2006), and it is likely that a substantial increase in nutrient (and hence chlorophyll-*a*) levels would have an indirect effect on the dynamics of coral-associated VLP communities.

The increased prevalence of large filamentous and rod-shaped VLPs at the more turbid sites is an interesting finding, as such viruses normally infect plants (Fauquet *et al.*, 2005), and resemble VLPs found in experimentally-stressed *Symbiodinium* cells, which were hypothesized to belong to the *Closteroviridae* (Lohr *et al.*, 2007). Similar levels of turbidity to those seen here have been shown to increase mucus production and reduce net photosynthesis in other coral species (Telesnicki and Goldberg, 1995), while sedimentation (linked to turbidity) has resulted in bleaching (Acevedo and Morelock, 1988) and loss of *Symbiodinium* cells from corals (Philipp and Fabricius, 2003). It is therefore possible that turbidity-related stress is causing induction of latent viruses in *Symbiodinium* or other algae within the CSM. This is further supported by the fact that seawater chlorophyll-*a* concentrations were not closely correlated with turbidity, i.e. the increase in putative algal viruses was not simply due to an increase in planktonic algae. The increased proportion of *Geminiviridae*-like VLPs at the more turbid sites is also of interest. These viruses normally infect plants, but geminivirus-like DNA sequences have been found in association with corals

(Vega Thurber *et al.*, 2008). This may also be a case of stress-related viral induction, but further investigation is again required for confirmation.

Temperature and turbidity appear to be the predominant environmental factors affecting seawater virus communities on Kaneohe Bay reefs, with large (> 100 nm) *Podoviridae*-like, 50 – 100 nm sized polyhedral/spherical and large (> 100 nm) lemon-shaped VLPs positively correlated with turbidity, and geminivirus-like and intermediate and large-sized filamentous VLPs positively associated with temperature. The increase in *Podoviridae*-like and polyhedral VLPs (many of which are likely also phages) may simply be due to an increase in bacterial abundance at the more turbid sites. Likewise, the increased proportion of lemon-shaped VLPs (presumably belonging to the Archaea-infecting *Fuselloviridae* or *Salterproviridae*) at the turbid sites is probably due to an increase in Archaea abundance at these sites. Although Archaea are typically thought of as extremophiles, they are known to be relatively abundant in the plankton (DeLong, 1992) and the CSM (Kellogg, 2004; Wegley *et al.*, 2004), and putative archaeal viruses have previously been observed in the CSM (Davy and Patten, 2007). The increase in geminivirus-like and large filamentous VLPs at sites with higher temperatures may be due to induction of latent algal viruses, as was suggested in the CSM virus communities. Although it is questionable whether an increase of ~1 °C would cause sufficient stress for viral induction, this would explain the response of these virus groups to temperature and not to chlorophyll-*a* concentration (i.e. the viruses are being produced from within the existing algal population, rather than increasing in prevalence due to increased host abundance).

More generally speaking, solar radiation (which is attenuated by turbid water) is known to be responsible for viral decay in surface waters (Suttle and Chen, 1992; Wilhelm *et al.*, 1998), and several studies have shown that distributions of microbial hosts are influenced by both temperature and turbidity (Schaub *et al.*, 1974; Moriarty *et al.*, 1985; Jones *et al.*, 2007). Clearly there is a complex interaction between viruses, their hosts and these environmental variables, and further investigation is warranted.

Conclusions

Given the well-documented global decline of coral reefs in recent decades (Weil *et al.*, 2006; Harvell *et al.*, 2007), a greater understanding of the biological and physical drivers of coral

health and disease is necessary. Although no virus has yet been identified as the etiological agent of a coral disease, there remain numerous coral diseases/syndromes for which causative agents remain to be found (Bourne *et al.*, 2009). Furthermore, evidence is beginning to emerge that viruses may play a role in some coral diseases. For example, Cervino *et al.* (2004) found viruses in *Montastrea* spp. suffering from yellow blotch/band disease, and (Wilson *et al.*, 2001) fulfilled Koch's postulates for a virus causing disease in *Symbiodinium* from a cnidarian host. Likewise, while environmental drivers of most coral diseases remain unknown, recent work has identified environmental predictors of several diseases, including turbidity, temperature and chlorophyll-*a* (Williams *et al.*, 2010), factors which also played a role in structuring VLP communities in the present study.

The majority of coral-associated viruses are likely not harmful to the coral or its symbionts, and in many cases may indeed have a net benefit on the holobiont where they infect potential pathogens (van Oppen *et al.*, 2009). This complex web of interactions means that higher resolution identification *via* molecular means would be necessary to discern pathogenic viruses from relatively harmless ones. Nevertheless, this study clearly shows that environmental variables, including proxies for anthropogenic impact, such as turbidity and chlorophyll-*a*, play a role in structuring these highly dynamic virus communities. Whether these changes represent a negative feedback loop, where an increase in coral pathogens is met by an increase in those viruses which infect them, or a direct increase in pathogenic groups of viruses, remains unknown, and is an interesting avenue of further research.